Exploiting catalytic chain transfer polymerisation and applications for the synthesis of diblock and multi-block co-polymers via sulphur free RAFT polymerisation

by

Ataulla Shegiwal

A thesis submitted in partial fulfilment of the requirements of the degree of Doctor of Philosophy in Chemistry

July 2020

Table of Contents

List of Figures

Chapter 1

Chapter 2

Chapter 3

Chapter 4

Chapter 5

List of Table

Chapter 1

Chapter 2

Chapter 3

Chapter 4

Chapter 5

Schemes

Chapter 1

Chapter 2

Chapter 3

Chapter 4

Chapter 5

Acknowledgements

First and foremost, I would like to thank Professor Dave Haddleton, for allowing me the opportunity to pursue a PhD in his group and for his continued supervision and support throughout. If someone were to ask me what my idea of perfect supervisor would be, I would not even have to hesitate or blink twice before Dave's image would pop up in my head in a Ralph Lauren shirt with a Cuban cigar looking into the horizon (i.e. staring at the end section of floor 2). What I admire most about Professor Haddleton is that he is a great scientist, full of enthusiasm, charismatic and very pragmatic individual. I remember one day, he was very excited about a project we were working on, and by the fourth time that he entered the lab to discuss the project, he politely said "I promise this would be the last time I bother you today". My response was that as students we get a bit of a kick seeing our General, so Professor Haddleton, in his response demonstrated a kick by kicking the door in an enthusiastic manner, which resulted him slightly hurting himself but nevertheless still smiling.

Also I like to thank all the wonderful people and great friends I have made over the years with great memoires to cherish for many years to come. Bingzhen Li my partner in legal crime and I can proudly say I am a godfather to his son; TomTom (i.e. when they named the baby they did not know it was a famous brand of satellite navigation systems) which I met for the first time when I went to spend 3 months with Professor Lei Tao at Tsinghua, Beijing. Lei was Dave's first ever Chinese student and was exceptionally accommodating and I had some wonderful experiences and met some delightful people including: Guoqiang Liu, Yuan Zeng, Yanjin Yao, Na Ren and Ruihao Pan: who took me out to many enjoyable dinners, played many sports activities actively and on consoles (PS4) and showed me around China.

I would also like to thank, the flying Scotsman Alan Wemyss; the gentlemen has a heart of gold, for always being on standby if anyone needed any help/ support and as always offering us with a wealth of entertainment. He has been tremendous help to everyone both in and out of labs. Also special thanks to the people I started my PhD with and shared the journey: Evelina, Pawel and none other than the Doncaster King (a.k.a the MALDI king) James Town the second best thing to have come out of Doncaster after MC Devvo. James has been a great office buddy and incredibly helpful

when it comes to MALDI's: from experience have seen him talk 3 hours none stop with just two sips from his diet coke (true passion)!

I would also like to give special thanks to Cobalt squadron as Chris likes to call it: which includes my good friends George, Chris and Arkadios. It has been a bundle of joy to work together and share many morning water pints, whiles discussing kamasutra as seen through Chris's eyes / imagination before starting the day.

Furthermore, I would like to thanks past and present members including Richard my sauna buddy and political rival, Paul for his suggestion/contribution to group meetings, Dan for all the help with RTP and financing me through interesting and fun projects, David Hammond, Steve, Ahmed Eissa, Linhua, Spyros, Alex, Athina, Vasiliki, Despina, Lucas, Congkai, Glen, Nikos, 2 x Sam, Maria, Fehaid, Ellis, Jamie, Gavin, Jack, Nutepol, Cansu, Mohammed, Samantha, Niamh, Jack, Yujing, Ruitainny, and Yongguang. Apologies if I have missed any names and the names are in non-sequential order. I would also like to thank the wonderful staff and people I have met over the years in the chemistry department that have enhanced, my Warwick experience over the last 8 years! Next I have to thank DSM and my industrial supervisors Dr, Mike AJ Schellekens and Jens de Bont for funding my PhD and having positive inputs on my projects and giving me in depth tour of DSM Waalwijk and introducing me their team. There was always a very chilled and positive ambience with mutual understandings in our meetings.

I would also like to thank my close friends outside our group for their constant love, support and care throughout the years which includes: Abenezer, Joseph, David, Neil, Luca, Jeya, Katharine, Semi, Khawer, Papitos (Italian and Spanish Marco's), Steve, Sank, and Nick. Finally, I would also like to give a special thanks to my parents and siblings for their constant love, financial support, guidance and care. I like to specially thank my parents for encouraging me to pursue my future career freely and independently.

Declaration

The work performed in this thesis was carried out in the Department of Chemistry, University of Warwick between October 2016 and September 2020. Unless otherwise stated, it is the work of the author and has not been submitted in whole or in part for any degree at this or any other university.

The content has not previously been published, except as detailed in the publications listed below:

1. Shegiwal, A. M. Wemyss, M. A. J. Schellekens, J. de Bont, J. Town, E. Liarou, G. Patias, C. J. Atkins and D. M. Haddleton, Journal of Polymer Science Part A: Polymer Chemistry, 2019, 57, E1-E9

2. Shegiwal, A. M. Wemyss, E. Liarou, J. Town, G. Patias, C. J. Atkins, A. Marathianos, D. W. Lester, S. Efstathiou and D. M. Haddleton, European Polymer Journal, 2020,

DOI: https://doi.org/10.1016/j.eurpolymj.2020.109491, 109491.

Symbols and Abbreviations

°C	Degrees Celsius
Đ	Dispersity
ACN	Acetonitrile
AIBN	a,a'-Azoisobutyronitrile
ATRP	Atom transfer radical polymerisation
BA	Butyl acrylate
BMA	Butyl methacrylate
BzMA	Benzyl methacrylate
CHMA	Cyclohexyl methacrylate
CCTP	Catalytic chain transfer polymerisation
$CDCl_3$	Deuterated chloroform
$CHCl_3$	Chloroform
CLRP	Controlled living radical polymerisation
CMC	Critical micelle concentration
CoBF	Bis[difluoroboryldimethylglyoximato] cobalt(II)
CTA	Chain transfer agent
ACVA	4,4′-Azobis(4-cyanovaleric acid)
DLS	Dynamic light scattering
DMSO	Dimethyl sulfoxide
DMA	Dynamic mechanical analysis
DNA	Deoxyribonucleic acid
DOSY	Diffusion-ordered spectroscopy
DP_n	Degree of polymerisation
MAA	Methacrylic acid
2EHMA	2-Ethyl hexyl methacrylate
EMA	Ethyl methacrylate
FA	Fumaric Acid
FL	Fluorescence
FRP	Free radical polymerisation
GLY	Glycerol
HY-3G	Hostasol yellow 3G™
HR-5B	Hostasol red 5B

HR-GG	Hostasol red GG
H	Hours
IPA	Isopropanol
IA	Itaconic Acid
IUPAC	International union of pure and applied chemistry
k_d	Rate constant of initiator decomposition
k_i	Rate constant of initiation
k_p	Rate constant of propagation
KPS	Potassium Persulfate
k_t	Rate constant of termination
MA	Methyl acrylate
MALDI-TOF	Matrix assisted laser desorption ionisation-time of flight
mCTA	Macro chain transfer agent
Me6TREN	*N,N,N',N'',N''*-Hexamethyl-[tris(aminoethyl)amine]
MMA Methyl methacrylate	Methyl methacrylate
M_n	Number-average molecular weight
M_w	Weight-average molecular weight
MWt	Molecular weight
NMP	Nitroxide mediated polymerisation
NMR	Nuclear magnetic resonance spectroscopy
PBMA	Poly(butyl methacrylate)
PBzMA	Poly(benzyl methacrylate)
PEMA	Poly(ethyl methacrylate)
PMMA	Poly(methyl methacrylate)
PS	Poly(styrene)
PCHMA	Poly(cyclohexyl methacrylate)
PDi	Polydispersity Index
PSD	Particle size distribution
P-xylene	Para-xylene
RI	Refractive Index
PVC	Poly(vinyl chloride)

RAFT	Reversible addition fragmentation chain transfer
RDRP	Reversible deactivation radical polymerisation
SEM	Scanning electron microscopy
SEC	Size exclusion chromatography
SET-LRP	Single electron transfer living radical polymerisation
SF-RAFT	Sulphur free reversible addition fragmentation chain transfer
TEMPO	(2,2,6,6-Tetramethyl-piperidin-1-yl)oxyl
T_g	Glass transition temperature
VM	Viscosity modifier
VOC	Volatile organic content

Chapter 1: Introduction

1.1 Polymers

Polymers are generally categorised into two main categories: natural or synthetic. Natural polymers occur in nature and are can be extracted, studied and replicated for global use for diverse application: from pharmaceuticals to cosmetic industries.[1-4] Nature has, through billions of years of evolution, assembled a vast number of polymeric macromolecules capable of exquisite molecular recognition. These functionalities within naturally occurring polymers, arise from the precise control exerted over their biosynthesis that results in key residues being anchored in the appropriate positions to interact with target substrates.[2, 3, 5-9] Examples of common and widely studied natural polymers are silk, wool, DNA, cellulose and proteins. Nucleic acids, such as DNA and RNA, display ordered sequences based on four-nucleotide monomer units, whilst in proteins, 20 amino acids (monomers) are used to form precisely controlled monomer sequences.[2, 3, 6, 9-14] Such precise positioning of monomer units (or functionalities) has an important influence on polymer structure and results in unique properties, such as molecular recognition which spans functions as diverse as the transport of oxygen by haemoglobin, the detection of pathogens by our immune system and the control of metabolic pathways by enzyme catalysts of enviable specificities.[2, 3, 5-7, 10, 11, 13-16]

Conversely, Synthetic polymers are usually derived from petroleum oil and are synthesised to generally mimic nature initially as replacements for natural materials. Synthetic chemistry can be used to prepare sequence-controlled macromolecules with diverse chemical structures. Moreover, in comparison with DNA technologies, chemical procedures may enable larger-scale production of simpler and cheaper sequence-defined materials. The most common synthetic polymers are usually homopolymers, made of the same monomer unit, or copolymers with simple chain microstructures, such as random or block copolymers.[1-3, 5-8, 10, 13-17] Examples of some commonly used and well established synthetic polymers include nylon, polyethylene, polyester, Teflon, and epoxy. These polymers are used in many areas but do not have the structural and functional complexity of sequence-defined biopolymers, such as nucleic acids or proteins.[1, 3, 5, 7-9, 11-13, 16]

Therefore, supplementary mechanisms for monomer sequence control polymerisations have been studied and investigated. For instance, the development of living polymerisation methods such as ionic polymerisations, controlled radical polymerisations, catalytic chain transfer polymerisation and ring opening metathesis polymerisation has all aided progress in the field of polymer science, and it is now possible to form multi-block copolymers with complex microstructures in methods that were inconceivable a few decades ago.[1-20]

1.2 Free Radical polymerisation

Free radical polymerisation a commonly used technique in industry with vast quantities of bulk polymer products being manufactured worldwide by this method every day. Furthermore, free radical polymerisation can be used to synthesise a wide range of different polymer products: such as polystyrene, poly(methyl methacrylate), poly(vinyl acetate), polyethene etc, etc.[21-26] The tolerance of the system to trace impurities and oxygen in the system and the range of polymerisation methods such as bulk, solution, emulsion and suspension makes the reaction commercially appealing.
The polymerisation is divided into four key steps: initiation, propagation, chain transfer, and termination. These steps will be described in turn in more detail. [21-28]

1.2.1 Initiation

The initiation step involves the formation of radicals using precursors such as peroxides, e.g. dibenzoyl peroxide (BPO) and diazo compounds, e.g. 4,4'-azobis-4-cyanovaleric acid (ACVA) are often used for the initiation as they form radicals easily (*figure 1.1*)[23-27, 29]. Both peroxides and azo initiators undergo homolytic bond cleavage in the formation of radicals. Radicals can be formed by a range of methods including thermal decomposition or photochemical reactions. Peroxides generally dissociate by thermal reactions, whilst, diazo initiators can dissociate by either mechanism. Redox initiators are also common, such as hydrogen peroxide /iron(II).[23-28]

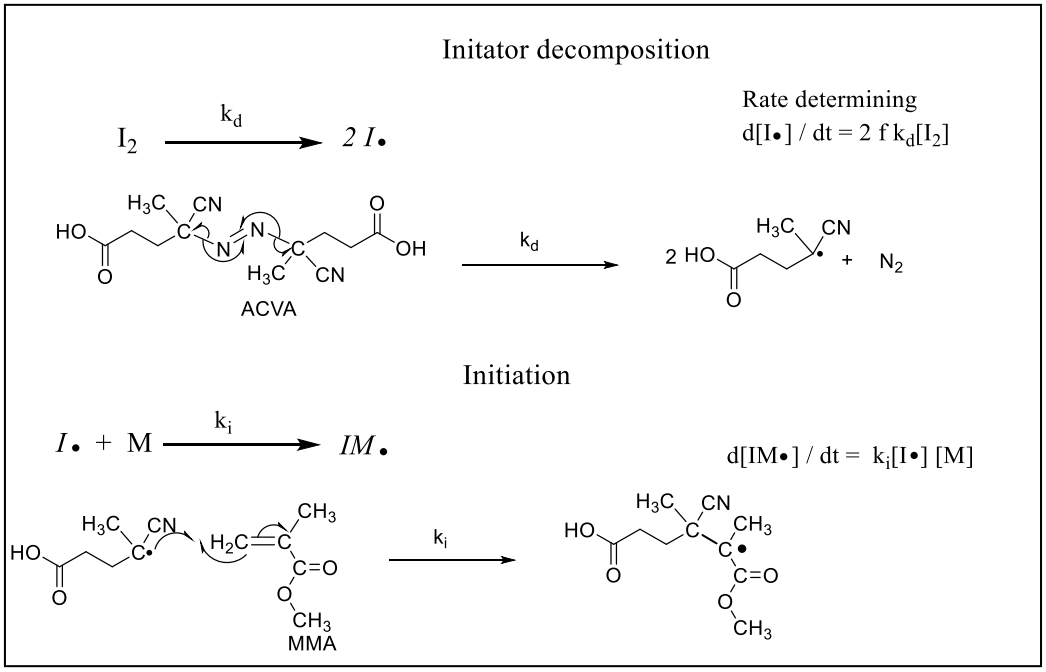

Figure 1.1: Initiation and rate equations, where I_2 is the initiator, I• represents a free radical capable of initiating polymerisation, M represents a molecule of monomer, k_d and k_i are the rate constants of initiator decomposition and initiation, respectively and f is the initiator efficiency.[27, 28]

The suitability of an initiator for a particular reaction is dependent on various factors such as half-life, reaction temperature, solubility in the different reaction media, reactivity towards other than monomer species and sometimes specific end group functionality requirement.[23-27, 30]

1.2.2 Propagation

Propagation is the main chain growth part of free radical polymerisation. The radical formed reacts with the vinyl bond of an unsaturated compound usually a monomer, initiating chain growth. Therefore radicals are formed propagation ensues, and the polymerisation proceeds. The rate of propagation is contingent on concentration of radicals, monomer and the rate constant for propagation, k_p, which will depend on the type of monomer. [23-27, 30]

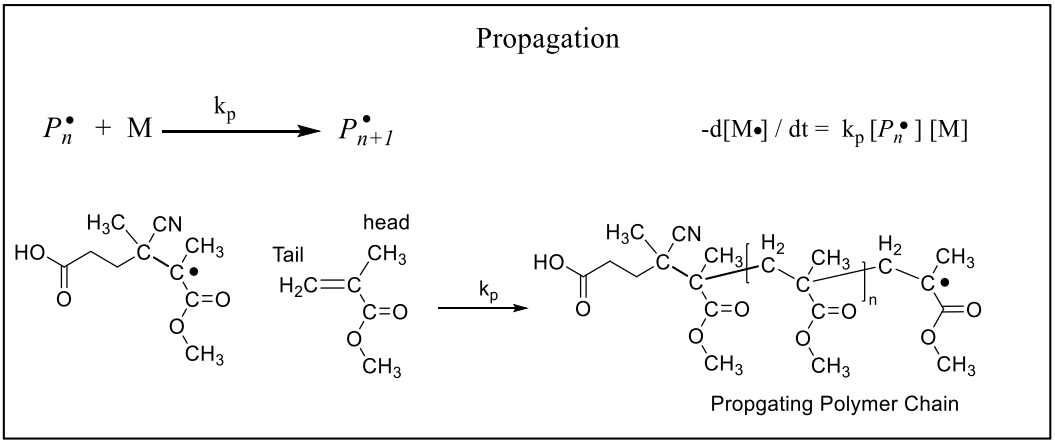

Figure 1.2: Propagation and rate equation, where P_n• refers to propagating radical chain with degrees of polymerisation of n units and k_p is the rate constant of propagation. [24, 26-28]

Assigning k_p to the reaction equation (*figure 1.2*) assumes all the chains react at an identical rate with monomeric units, thus the rate of propagation is chain length independent. Furthermore, evidence in current literature suggest that short-chained radicals propagate much faster than long chain counterparts.

1.2.3 Chain transfer

Chain transfer is chain stopping event which takes place from propagating chains to abstract a hydrogen atom from any other substrate in the reaction. It involves abstraction of a hydrogen or other atoms from monomer, initiator, solvent or other species within the polymerisation medium.

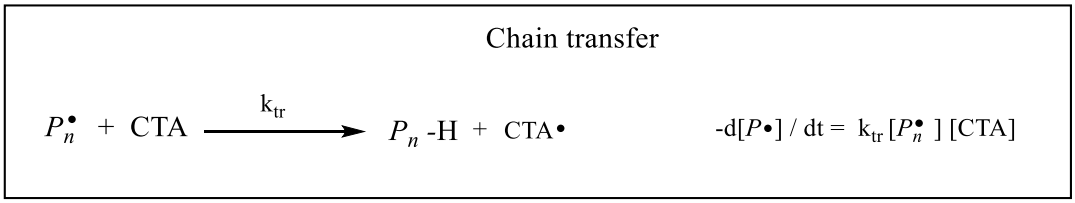

Figure 1.3: Chain transfer and rate equation, where P_n• refers to propagating radical chain with degrees of polymerisation of n units, Pn-H is a polymer chain of n units terminated by H, CTA is a chain transfer agent (whether monomer, solvent, polymer or an added species), k_{tr} is the rate constant of the chain transfer. [27, 28]

The chain transfer event or the deliberate addition of a chain transfer agent (CTA) shortens the polymer chains during polymerisation by directly impacting the degree of polymerisation (DP_n). For a typical CTA, the CTAs should not affect the rate of polymerisation since the reaction with the chain transfer does not change the concentration of radicals within the system. The presence of chain transfer reduces the

DP_n by lowering the number of polymer molecules produced per kinetic chain length, although cases exist in which the relative rates of propagation, chain transfer and re-initiation lead to a decreased rate of polymerisation (*table 1*).[28]

Table 1: Influence of chain transfer on rate of polymerisation, R_p, and DP_n of resulting polymers based on the relative rates of propagation k_p,, k_{tr} the rate constant of the chain transfer, and, k_a the rate constant for reinitiation of polymerization from the CTA fragment. The outcomes of various ratios in free radical polymerisation is represented by $k_p : k_{tr}$ and $k_a : k_p$. [28]

$k_p : k_t$	$k_a : k_p$	Resulting chain transfer	Effect on R_p	Effect on DP_n
$k_p >> k_{tr}$	$k_a \approx k_p$	Normal chain transfer	None	Decrease
$k_p << k_{tr}$	$k_a = k_p$	Telomerisation	None	Large decrease
$k_p >> k_{tr}$	$k_a < k_p$	Retardation	Decrease	Decrease
$k_p << k_{tr}$	$k_a > k_p$	Degradative chain transfer	Large decrease	Large decrease

In some cases in FRP, chain transfer can be an undesirable side reaction. However, it does provide significant control of the average DP_n , reducing the cost of producing lower MW products (as large amounts of initiator are not required).[28, 31] The most widely exploited CTAs in radical polymerisations are thiols (with a C_s of 1-10, the highest value among conventional CTAs), as they readily transfer hydrogen to propagating species, yielding a hydrogen terminated polymer chain end and a thiyl radical.[28] The thiyl radical formed capable of initiating further polymerisation. The adverse result of this type of chain transfer is, the inclusion of additional functionality which may not always be perceived to be desirable.[28, 32]

Stoichiometric levels of thiol have been used to delay or diminish Norrish-Trommsdorff, or gelation in the free radical copolymerisation of vinyl monomers with relatively low levels of divinyl monomers, in what is commonly referred to as the "Strathclyde methology" [33-37]

1.2.4 Termination

Termination leads to 'dead' polymer chains as a chain growth stopping event and can occur either by combination or disproportionation. The occurrence of each process will depend on the monomer and solvents used, as well as the reaction temperature. Combination is the direct joining of two propagating radicals, it usually generates species of higher than average molecular weight (MW) for the system. Since, the process involves the combining of MW of the two terminated radicals.[23-27, 38]

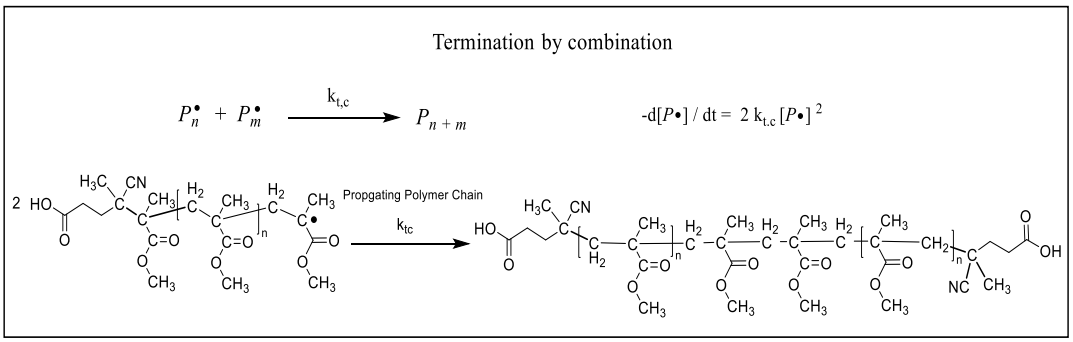

Figure 1.4: Chain transfer and rate equation, where $P_m\bullet$ is a polymer chain consisting of m monomer units, Pn+m is a terminated polymer chain of n + m monomer units and $k_{t,c}$ rate constants of termination by combination.

Alternatively two polymer radicals may terminate by disproportionation via the transfer of a hydrogen atom from one polymeric radical to another, forming terminal unsaturation at the end group of one polymer and a terminal hydrogen on the saturated polymer. [23-27, 38]

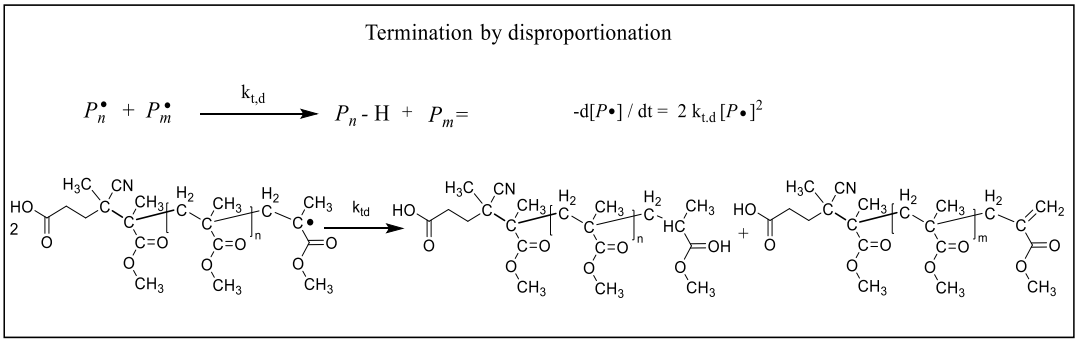

Figure 1.5: Chain transfer and rate equation, where $P_m\bullet$ is a polymer chain consisting of m monomer units, P_n-H is a polymer chain of n units terminated by H, P_m= is a polymer chain of m units terminated by a double bond, and $k_{t,d}$ rate constants of termination by disproportionation.[39]

Commonly in a polymerisation system there is a mixture of both combination and disproportionation occurring. The degree of each termination type is monomer dependent, with mono substituted olefins, acrylates and styrenics, occurs

predominantly via combination. Whereas with polymerisation concerning of monomers containing α–methyl substituents higher amounts of termination by disproportionation is observed. The extent of termination by combination tends to increase as the ability of the substituent to stabilise the radical increases. [3, 23-27, 38]

Temperature also plays a significant role on the relative ratios of combination to disproportionation. Since, disproportionation involves a bond-breaking step and consequently has a greater activation energy than combination. As a result, if temperature is increased the difference in activation energy becomes less significant and disproportionation becomes more competitive. In the case of methyl methacrylate termination by disproportionation at 25 °C is 67% whereas at 80 °C it is 80%.[23-28, 38]

1.2.5 Trommsdorf or gel effect

In bulk or concentrated solution polymerisation the Trommsdorf or gel effect is a common phenomenon. The Trommsdorf or gel effect occurs when the conversion increases (*i.e. around 20%*), the medium viscosity increases the chain mobility deceases so much that the active chain ends cannot find each other to terminate polymerisation.[40-43] This in turn lowers the k_t and increases [P•] are observed. Nevertheless, small molecules such as monomer are still able to diffuse to the reactive chain end causing increase in rate of polymerisation.[28, 43] However, there is no change in k_d and k_p since they are small molecules. Furthermore, as addition polymerisation is an exothermic process generating heat, which cannot dissipate normally this in turn leads to further increase in rate. Under conditions such these that are isothermal the process leads to auto-acceleration which is undesirable and in industry such occurrence are called runaway reactions.[40-44]

1.3 Types of polymerisation process

The synthesis of free radical polymerisation are implemented using four distinguished polymerisation systems: bulk or mass, solution, suspension and emulsion. The type of system used for polymerisation is reliant on nature of the final product required and careful consideration should be taken on the drawbacks and benefits of the polymerisation techniques used.[27, 28]

1.3.1 Bulk polymerisation

Bulk or mass polymerisations is the simplest form of free radical polymerisations, since it usually only involves monomer in a liquid form, an initiator and a chain transfer agent (if necessary). The reaction mixture is exposed to heating or UV-light in order for initiation to pursue. The system becomes homogenous and has to be kept under constant stirring in order to maintain constant heat and mass transfer.[27, 28] The advantages of bulk polymerisation include products that can be used directly, reduced material, processing and expenditure cost since there is no need for tedious removal of residual solvents (assuming full monomer conversion).[27, 28, 45 44]

Nevertheless, bulk polymerisation are challenging to control as a result of their highly exothermic nature, the high activation energies involved, and the affinity toward the Trommsdorf effect combine with reduced heat transfer at high conversions.[44] Therefore, bulk polymerisation requires careful temperature control, need for robust and elaborate stirring equipment as the viscosity of the reaction system increases rapidly at relatively low conversion. In rare cases, uncontrolled acceleration of the polymerisation rate can lead to catastrophic ‘‘runaway’’ reactions.[28, 41, 44]

1.3.2 Solution polymerisation

Solution polymerisation is similar to bulk polymerisation with the inclusion of suitable inert solvent. The presence of inert solvents within the reaction medium reduces the occurrence of Trommsdorf effect significantly since the solvent acts as diluent which in turn enhances the heat capacity, thereby reducing the viscosity and facilitating heat transfer.[44] Conversely, sometimes the presence of solvents may present new waves of problems.[41, 42, 44] Therefore, careful consideration has to be taken in order to avoid chain transfer to solvent occurring or poisoning of the catalyst by solvent impurities. Furthermore, the purity of the polymer may be affected if there are difficulties in removing the solvent.[27, 28, 44]

1.3.3 Suspension polymerisation

Suspension polymerisation (occasionally referred to as bead or pearl polymerisation) is carried out by mechanically suspending the monomer (the discontinuous phase) as droplets (50–500 mm in diameter) in water (the continuous phase) or inert organic

liquids provided the monomer and polymer is insoluble in it, usually water is the medium utilised.[46] Heat transfer occurs from the droplets to the water resulting in low viscosity and large heat capacity. Cooling jackets are implemented to enable heat removal from the reaction system.[28, 44] Therefore, auto-acceleration as a result of Trommsdorf effect can be eliminated since the system is highly efficient at removal of heat from very exothermic reactions.[44] Agitators are also used alongside with suspending agents in the aqueous phase in order to maintain a precise droplet size and dispersion. The polymers produced via suspension polymerisation are small, uniform polymer spheres in the form of granules.[41-43]

1.3.4 Emulsion polymerisation

Emulsion polymerisation processes is responsible for the production of most of the polymeric materials synthesised worldwide industrially. Especially, the production of polymer lattices produced free radically by emulsion polymerisation for the various applications; such as adhesives, paints and coatings, paper and paperboard coating, carpet backing, and textiles.[47-52] Reaction may be carried out via various operating modes such as batch, semi-batch, or continuous system; in the simplest system, the reagents comprise of water, initiators that are usually water soluble (e.g. persulfate like KPS), monomers of low water solubility (e.g. styrene) and amphiphilic surfactant molecules (e.g. sodium dodecyl sulfate) that are dissolved in water until the critical micelle concentration (CMC) is reached (latexes are known to be synthesised without added surfactant and/or initiator, but these are very uncommon).[49-54]

The results of these reagents are the formation of colloidally stable polymeric latex particle, dispersed in a continuous aqueous phase, virtually all the polymerisation occurs within these particles. By the end of the reaction these polymer particles are typically ~10^2 nm in size, each containing numerous polymer chains. The utilisation of water as the dispersion medium has the advantage of being environmentally friendly (compared to using volatile organic solvents VOCs) and allows efficient heat dissipation throughout the course of the reaction. Furthermore, the low viscosity of the emulsion enables polymer chemist to acquire high weight fractions of polymers which are challenging to obtain through solution or bulk polymerisation reactions.[47-50, 52]

Furthermore, from a mechanistic perspective, the advantage of emulsion polymerisation compared to other methods polymerisation methods is: that the radicals are compartmentalized within the particles meaning that the radicals are distributed among different particles and hence the radicals from different particles cannot terminate between them. Therefore, these circumstances, allows simultaneous achievement of high polymerisation rate and high molecular weights which are both dependent on number of radicals per particle.[47-53]

The average number of radicals per particle is dependent upon the relative rates of radical entry from the aqueous phase, radical exit from the polymer particles, and lastly the bimolecular termination within the polymer particles. When water soluble initiators like KPS are utilised, the radical are generated within the aqueous phase, and usually are too hydrophilic to be able to enter polymer particles. Consequently, the hydrophilic water soluble initiators starts propagation within the aqueous phase, with monomeric units until it reaches a critical chain length (z) becomes hydrophobic enough to be able to enter the polymer particles by diffusion through the stagnant liquid film, surfactant hairy layer, and the polymer particle.[50, 53, 55] This model is known, as the propagation entry model and suggests that the entry of radicals of length (z) is instantaneous, and as a result the rate of entry is the rate of formation of radicals of length (z). This model uses a rational approach to estimate the radical entry for homopolymerisation in an emulsion system.[50]

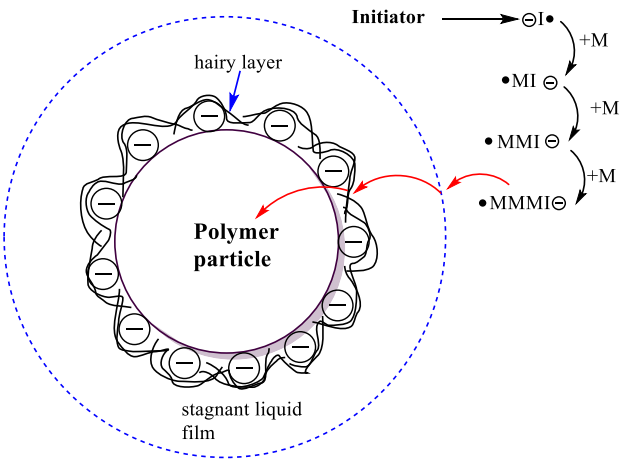

Figure 1.6: Mechanisms for radical entry in emulsion polymerisation

For more complicated systems such as copolymerisation in an emulsion system, the choice of critical chain length (z) for entry into the particle may be challenging to distinguish. This is due to the water solubility of oligomers depend on the composition of the oligomers and especially for short-chain oligomers may differ considerably from chain to chain. Furthermore, the propagation model does not take into account decrease in entry of radicals into particles due to either electrostatic repulsion when highly charged lattices are utilised or the thick layers of the electrostatic stabilisers.[50, 56-58]

Therefore the significance of radical desorption in an emulsion system is an important factor to take into account; desorption usually occurs upon formation of single radical unit by chain transfer to monomeric unit or chain transfer agent (CTAs), subsequently diffusion of newly formed radicals to the aqueous phase follows. At this stage the desorbed radical may either react in aqueous phase via propagation and termination or may re-enter the polymer particle as depicted in *figure 1.7*. Radical desorption is frequently taken into account by using the desorption rate coefficient (k_d), where (k_d) is the overall net rate of radical desorption for a population, (N_p) polymer particles and ($\bar{n}$) is indicative of average number of radicals per particle; $R_{exit} = k_d \bar{n} N_p$.[59]

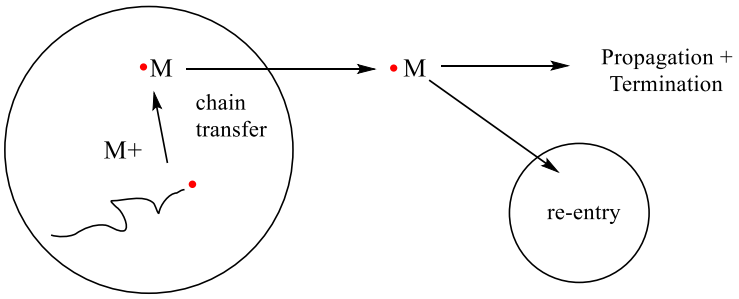

Figure 1.7: Mechanisms of radical exit

Desorption rate equations have been available for some time, however, they usually uphold some discrepancies depending on the type of system and reagents used in the emulsion polymerisation. Therefore, new models have constantly been proposed and developed which closely takes into account the various operational variables affecting k_d.[60] For instance, k_d decreases with increase in the number of particles within a system (namely solid content, for constant particle radius), this is due to the fact that when N_p

increases, the likeliness of desorbed radical re-entering the particle increases, and consequently the net exit rate decreases.[60]

Furthermore, k_d also increases with an increase in the concentration of radicals within the aqueous phases, specifically with an increase in the initiator concentration or redox system. However, when the solid content is kept constant k_d is not affected significantly by particle size due to the counteracting effect of decreasing particle size and increasing number of particles. Nonetheless, for a constant number of particles (N_p), k_d decreases as the particle size increases. Furthermore, this model takes into account the reduction of radical desorption rate coefficient caused by dense hairy layers.[57, 58]

Significant efforts have been taken to understand experimentally radical entry and exit rate coefficients; however these studies have proven to be inconclusive due to the lack of mechanistic understanding of radical exit due to the assumptions that k_d is independent of operational variables such as initiator concentration and number of particles. As a result, desorption rate coefficient is determined under a given set of experimental conditions and cannot be directly utilised to predict the activity of the emulsion system under different conditions.[61-64]

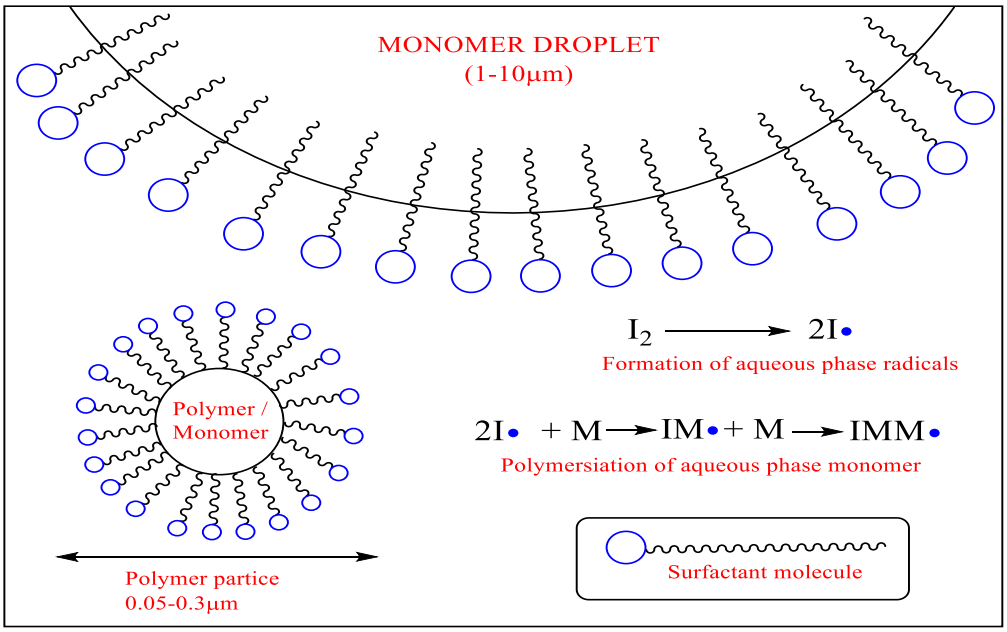

Figure 1.8: Emulsion polymerisation

Interval I

A typical batch ab initio emulsion polymerisation reaction comprises of three distinct intervals, labelled Intervals I, II and III. During Interval I, of emulsion polymerisation, new particles are nucleated by radical entry into micelles or by homogeneous nucleation (*i.e. explained in section 1.3.5*). Normally this takes part in the first 10-20% of monomer conversion. Since the particles are still forming, there is an excess of surfactant in this period and so micelles are present during this interval.[47-52] The number of particles and the rate of polymerisation both increase as new particles are formed. As a surfactant is used to stabilise new particles, the free surfactant concentration falls below the critical micelle concentration (cmc), the micelles are exhausted and nucleation ends. It is estimated that on average, approximately one out of every 10^2 –10^3 micelles can be effectively converted into latex particles. The number of particles remains fairly constant after this point.[47-52, 55]

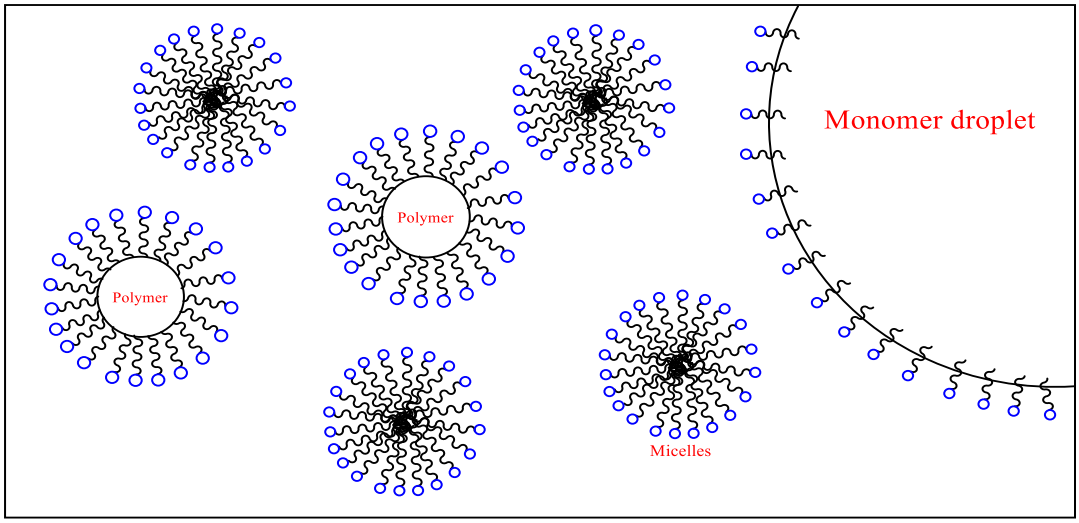

Figure 1.9: Interval I of emulsion polymerisation

Particle nucleation process is significantly affected by surfactant concentration, which in turn affects particle size and particle size distribution of latex. Smith [49, 51] and Ewart [51] devised a quantitative description of the mechanism, under the assumption that once a radical enters a micelle, it stays inside and polymerises effortlessly to from the polymer particle. Number of polymer particles nucleated per unit volume of water [N_p]; is proportional to the micellar surfactants [S] and initiator [I] concentration as depicted in the equation below;

$$N_p \propto [S_{micelles}]^{\frac{3}{5}} \times [I]^{\frac{2}{5}}$$

Furthermore, the proposition of the above equation by Smith and Ewart, eliminated the likeness of nucleation occurring anywhere other than the core locus of the micelles. As a result, the mechanism is not applicable for system where the surfactant concentration are below CMC or in emulsifier-free polymerisation.[47-52]

Using a low concentration of surfactants at the particle nucleation period, usually results in larger latex particles with narrow particle size distribution. This can be attributed to the simple fact that the shorter the particle nucleation period (i.e. the lower the surfactant concentration), the narrower the resultant particle size distribution. Inadequate stabilisation of colloidal system can occur during polymerisation which in turn, adversely affect the control the of particle size and particle size distribution of latex polymer. Another, important implication to consider is total solid content which is closely related to relatively mean free path length (H/r) between two interactive particles as a function of the total solid content. Where, (H) represents the average interparticle distance and (r) the particle radius. The value of H/r decreases with increasing total solid content.

Therefore, the higher the solid content, the more crowded the colloidal system and therefore the more significant the interaction between two approaching particles. In addition, larger particles display higher values of H for a system consisting of stationary packing. Therefore, at a constant total solid content for larger particles the system is believed to be less "crowded". This enables the formation of a high solid content with excellent rheological properties which are desirable in industrial applications. [47-52]

Interval II

During Interval II, the number of particles becomes constant and the existing particles continue to polymerise and consume the monomer contained in the large monomer droplets known as monomer reservoirs. This is the particle growth part of the emulsion polymerisation and it is frequently in the range 10-20 to 60% monomer conversion. The monomer is transported through the aqueous phase, as the consequence of a

concentration gradient, to the site of polymerisation (i.e. the growing polymer particles). At the end of Interval II, the monomer in the droplets is exhausted, and no monomer droplets are present subsequently.[47-52]

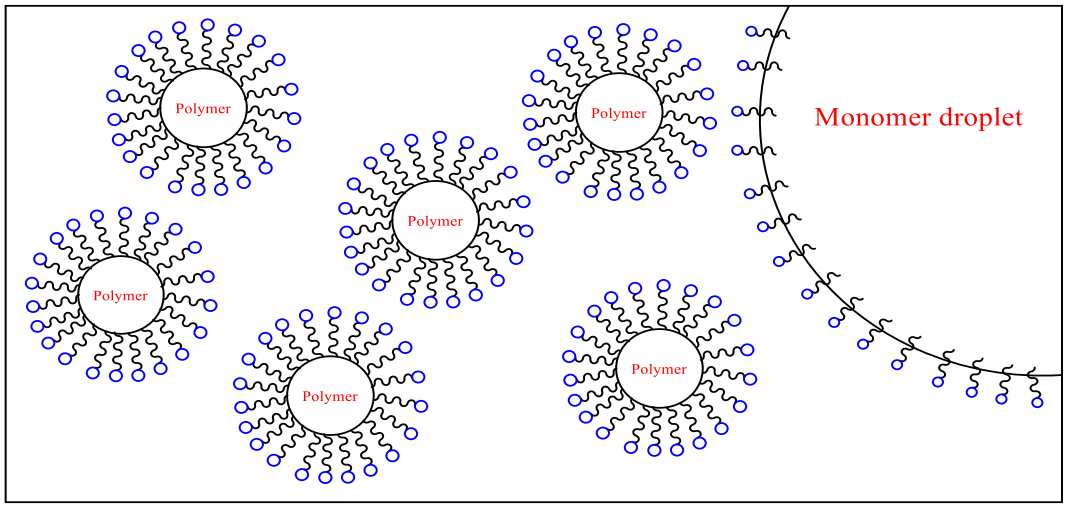

Figure 1.10: Interval II of emulsion polymerisation

Smith–Ewart case 2 kinetics has been extensively utilised to calculate the rate of polymerisation (R_p): where k_p is the propagation rate constant, $[M]_p$ the concentration of monomer in the particles, n the average number of free radicals per particle, and N_A the Avogadro number. [47-52]

$$R_P = k_p[M]_p\left(\frac{nN_p}{N_A}\right)$$

This Smith–Ewart case 2 kinetics model was established on the following assumptions:

(1) Nucleation and coagulation of particles do not occur and the number of particles per unit volume of water remains constant throughout polymerisation.

(2) The particle size distribution is somewhat monodisperse.

(3) Desorption of free radicals out of the particles does not occur.

(4) Bimolecular termination of the polymeric radical within the particle upon the entry of an oligomeric radical from the aqueous phase is instantaneous.

Following from the assumptions for Smith–Ewart case 2 kinetics model, a scenario is developed; where upon any given moment, monomer-swollen particles contain either only one free radical (active) or zero free radical (idle). Therefore, under these conditions a value of n equals 0.5 is obtained for the polymerisation system.[49-51]

Furthermore, when monomer droplets are present the concentration of monomer within the particles does not change to any extent. As a result a steady state polymerisation rate is maintained during Interval II. [47-52] Therefore, polymerisation kinetics is strictly controlled by the number of particles available for consuming monomers. As stated above once all the monomer droplets disappear we proceed from Interval II to III. [47-52]

Interval III

During Interval III, no more monomer droplets are left except the monomer already contained in the polymer particles which polymerises until it is fully converted to polymer. At this stage, the latex particles become monomer starved and the concentration of monomer in the particle continues to decrease, towards the end of polymerisation to principally zero. As a result of the steady state polymerisation rate that was obtained during interval II cannot be retained any longer.

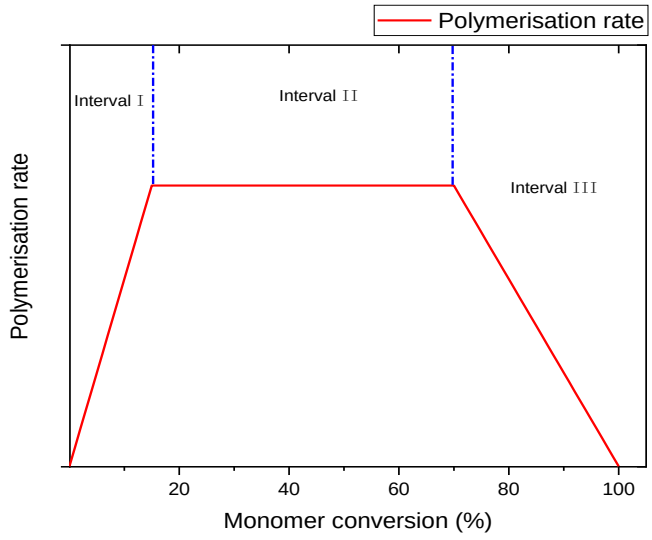

Figure 1.11: Typical rate of polymerisation as a function of the monomer conversion. The three distinct intervals of the polymerization process are also indicated in the plot

Therefore the polymerisation rate decreases at interval III. Nevertheless, the polymerisation rate may increase with increasing monomer conversion close to the end of the polymerisation. As a result of auto acceleration occurring due to the Trommsdorf effect (mention in *section 1.2.5 Trommsdorf or gel effect*)[41, 42]. Where, the significant reduction of bimolecular termination reaction between two polymeric

radicals occur within extremely viscous particles, provided the polymerisation temperature is below the glass transition temperature of the monomer-starved polymer solution. [47-52]

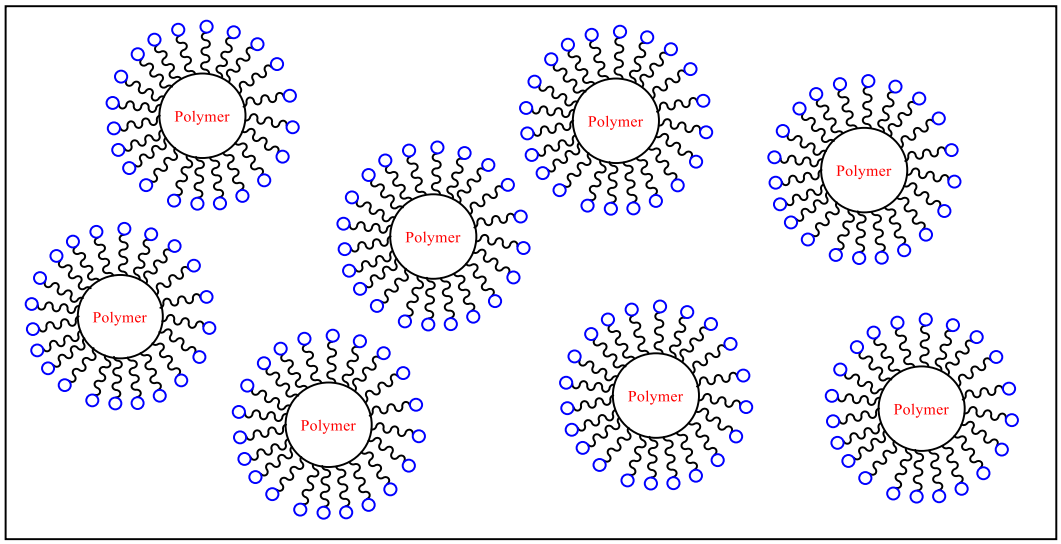

Figure 1.12: Interval III of emulsion polymerisation

1.3.5 Types of particle nucleation in emulsion polymerisation

Emulsion polymerisation is complicated phenomenon as emphasised earlier and in order to get an in depth understanding of the system it is crucial to take into account the types of nucleation occurring at the start of the polymerisation. Therefore, the three major mechanisms for particle nucleation in emulsion polymerization has been proposed to date are: *Micellar Nucleation Theory*, originally proposed by Harkins[40, 53, 65-67] in 1947 Smith[66, 68] and Ewart[40, 69, 70] and modified by Gardon[49, 51, 54, 65, 68-70], submicron latex particles (0.05–1 μm in diameter) are produced through the capture of free radicals by micelles.

The waterborne primary free radicals formed by dissociation of the initiator in the continuous aqueous phase polymerases with monomer molecules dissolved in the aqueous phase. This process results in the increased hydrophobicity of oligomeric radicals. When a critical chain length is achieved, these oligomeric radicals become hydrophobic at which point phase separation occurs, i.e. the chain comes out of the solution and forms a primary particle which exhibit a strong tendency to enter the monomer swollen surfactant-micelles. Continuing the polymerization by propagating with those monomer molecules inside the micelles, monomer-swollen polymer

particles are formed. The growing particles have larger interface which are in turn stabilized by the adsorption of extra surfactants from un-entered micelles.

Instantly after the disappearance of the micelles, the nucleation ceases. At this point, the newly-formed radicals are absorbed by the growing polymer particles. The polymer particles are the main loci of the polymerisation and grow in size. The concentration of monomer inside the polymer particle is kept constant by diffusion of monomer from the monomer reservoir (monomer droplets) through the aqueous phase into the polymer particles. After a certain conversion, the monomer reservoirs are consumed and deplete, resulting in a decreasing rate of polymerization. Furthermore, micellar nucleation is usually understood to be the main nucleation mechanism for the monomers with relatively low water solubilities (**[M]aq** < 15 mmol dm^{-3}).[40, 51, 53, 65-69, 71-73]

Homogeneous nucleation models, proposed by Fitch[40, 53, 67] and Tsai[53, 65, 68], Priest[40, 49, 53, 65, 67-69] and Roe[40, 53, 67-70, 74] for the for the formation of particle nuclei in the continuous aqueous phase, the water soluble initiator radicals are initially formed by the thermal decomposition of the initiator and in turn grows in size by propagation reaction with monomer molecules dissolved in aqueous phase. When the water soluble oligomer radical, j, has reached a critical chain length, j'_{crit} (value of $j > j_{cnt}$) leads to precipitation of insoluble oligomeric chains. The insoluble hydrophobic oligomeric chain can coils up excluding water to form a coil-to-globule transition particle or precursor particle in the aqueous phase. The precursor particle can be swollen with monomer and grow via propagation or coagulation with other precursor particles to form stable particles. Homogeneous nucleation, is considered the primary mechanism for formation of particles in systems with surfactant concertation below the critical micelle concentration CMC, surfactant free polymerisation and formation for the monomers with relatively high water solubilities ($\mathbf{[M]_{aq}}$ > 170 mmol dm^{-3}).[40, 49, 51, 53, 54, 65-71, 73, 75-77]

The third nucleation theory which is significantly less common than the aforementioned, is called monomer droplets nucleation mechanism proposed by Hansen[40, 53, 66-68] and Ugelstad,[66, 67] Durlin[40, 51, 53, 65-70]. Historically this was the novel foundation for producing an emulsion polymerisation. However, it occurs very rarely: the cases are in some systems such as chlorobutadiene which have extremely large

spontaneous initiation component, the unique systems of miniemulsion and microemulsion polymerisation, and some controlled radical systems. As the monomer droplets have comparatively large size (2–10 μm) with small total surface area.[78-80] Monomer droplets implies the presence of separated monomer phase which is enhanced by intense mixing resulting in increase of the total surface area of monomer droplets.[40, 49, 51, 53, 66-70, 72, 74] Furthermore, droplet nucleation is the origin of the high molecular weight products.[81]

1.3.6 Partitioning coefficient

Another fundamental factor to consider in emulsion polymerisation is the partitioning coefficient. It has been widely reported that the observed chain transfer activity in emulsion polymerisation is significantly lower than its counterparts, bulk and solution polymerisation. Furthermore, the reduction in molecular weight comes at an expense of reduction in the rates of polymerisation. Both, these results can be explained due to the fact that the catalyst can be present in both the aqueous phase and/ or the dispersed phases depending of the structure, hydrophobicity of the catalyst and the type of monomer used in the emulsion polymerisation process.

Therefore, the solubility of the cobaloximes catalysts can be modified by changing the size of substituents on the equatorial ligands. It has been reported that the distribution coefficient for water/MMA drops significantly from 0.4 to 0.05 once the substituents in the equatorial ligand are changed from methyl to ethyl ligands within the cobaloxime catalysts.

The partition coefficient (m_{Co}) is given by the following equation:

$$m_{Co} = \frac{[Co]_{disp}}{[Co]_{aq}}$$

where $[Co]_{disp}$ is the catalyst concentrations in the dispersed phase (i.e. monomer droplets, monomer swollen micelles and/or polymer particles) and $[Co]_{aq}$ is the catalyst concentrations aqueous phase. As a rule of thumb, as the hydrophobicity of the equatorial ligand (R-group) increases on the cobaloximes catalysts or the hydrophilicity of the monomer increases the partition coefficient also increases.

Table 1.2: Relation between the catalyst structures and partitioning behaviour with various monomers ($m_{Co}{}^{a}$ is the partition coefficient)

Complex	R	Monomer	$m_{Co}{}^{a}$	References
COBF	Me	MMA	0.31–0.72	[82-84]
		BMA	0.035	[85]
		STY	0.052	[86]
COEtBF	Et	MMA	19–60	[87]
		BMA	8.4	[84, 87]
COPhBF	Ph	MMA	∞	[82, 87]

1.4 Catalytic chain transfer polymerisation (CCTP)

1.4.1 Introduction & history

Catalytic chain transfer polymerisation (CCTP) is a highly effective method at utilising cobalt (II) macrocycles as catalytic chain transfer (CCT) agents in free radical polymerisation for formation of low molecular weight macromonomer.[29, 87-91] The robustness of this technique include; its simplicity (as established by its industrial uptake), uncommonly high (for FRP) level of vinyl end-functionality due to significant number of chains predominantly terminating by disproportionation (near to 100 % end group fidelity), exploitation of the end group functionality and post-polymerisation, and due to high chain transfer constant Co(II) complex, usually only very small amounts of the benign CTA are required (ppm levels) for formation of low molecular weight macromonomers.[92-94]

1.4.2 Initial development

Co(II) porphyrins and related compounds were promoted by Schrauzer, Pattenden, and many other researchers finding several isomerization reactions of these organocobaloximes during these 3 decades as its chemical structure and behaviour exhibited some resemblance to vitamin B_{12}.[95-97] The observation that Co(II) porphyrins appeared to inhibit the FRP of methyl methacrylate (MMA) encouraged further investigation, resulting to a series of papers and patents in the Russian literature in the late 1970s, which went largely unnoticed by the general scientific community in the west.[29, 87, 96-98] Co(II) porphyrins were found to be very efficient at controlling and reducing the molecular weight of poly(methyl methacrylate) and polystyrene polymers by free radical polymerisation via catalytic chain transfer.[29, 87, 90, 91, 95, 96]

CCTP was first discovered in 1975 by Boris Smirnov, Alexander Marchenko, and Nikolai Enikolopyan, with later work by Alexei Gridnev as a method in which they could control the molecular weight in a methacrylate polymerisation by introducing certain low-spin cobalt(II) complexes, in particular cobalt(II) porphyrins (1) which could catalyse and greatly enhance the process of chain transfer to monomer reaction.[29, 87, 90, 91, 99-104] While cobalt porphyrins were somewhat effective as CCTAs, they suffered from the disadvantages of cost, limited solubility in polar media, and strong colour; all of which were adversely affecting its commercial exploitation.[29, 87, 90, 99, 101-104]

Further studies and development by Gridnev, DuPont, ICI/ Zeneca and Glidden Paint Company established significant improvement and insight into number of other cobalt(II) compounds, invariably low spin, have since been shown to be active in CCTP. The most notable among these were cobaloximes and its derivatives (**2, 3**) are depicted in (*figure 1.13)*.[29, 87, 90] These compounds have significant advantages over the porphyrins as they are relatively inexpensive, much less coloured, much more active, and also possess a wide range of solubilities that can be varied. [87, 90, 99-101, 105, 106]

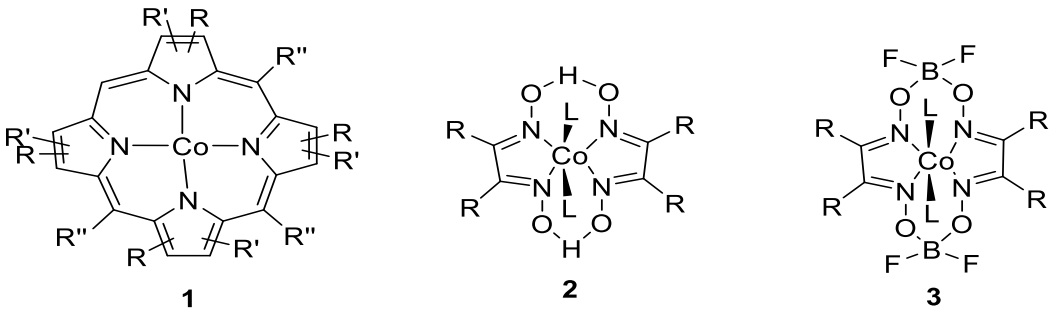

Figure 1.13: A selection of cobalt catalyst

It has been found that cobaloximes (**2**) are very sensitive to hydrolysis and oxidation yet show very higher chain transfer constants (often with $C_s > 2 \times 10^4$). However, stability is significantly increased by the introduction of BF_2 bridges. The catalysts formed as a result (**3**) is typically handled as solid even in aerobic conditions and it is useful as it is water soluble and once again this increases the chain transfer constant further to (C_s 4 x 10^4).[87, 90, 96, 99, 101, 106, 107] However, in solution these BF_2-bridged catalysts are still sensitive to acid hydrolysis or oxidation by peroxides and other

oxygen-centred radicals, but significantly less than catalyst (**2**). The sensitivity to oxidation can be further enhanced by introduction of alkylated Co(III) derivative of (**3**) (Co(III)-alkyl) which will dissociate into the active Co(II) catalyst and an alkyl radical.[29, 87, 101, 103, 108]

Therefore, the most common used catalyst at present are the derivatives of catalyst (**3**), where the substitute **R** can be tailored based on desired solubility and activity. This work will mostly focus on bis[(difluoroboryl)dimethylglyoximato]cobalt(II) often, denoted as CoBF, where the four **R** ¼ substituents are methyl groups. The CoBF catalyst is exceptionally stable due to the boron-bridging groups that impart hydrolytic stability, allowing its use at low pHs and at elevated temperatures.[29, 48, 87, 90, 99, 101, 103, 104]

The development of catalyst (**3**) has resulted in utilisation of the catalyst in CCTP for a wide range of applications such as: fine chemicals (rheology modifiers, macromonomers as hair care additives, paint, adhesives and coatings, ink-jet inks, automotive refinish, contact lenses and in industrial applications (thermoformed sheets of MMA for sinks and aeroplane windows, baths and shower trays), in cosmetic surgeries (breast and gluteus maximus implants).[29, 87, 94, 109-111]

1.4.3 Active catalysts

Functioning catalytic chain transfer agents are derivatives of low-spin Co(II) complexes with octahedral geometry (O_h), derived from a macrocyclic tetra chelate ligand with square planar geometry, leaving two axial coordination sites available for catalysis.[29, 90, 112] Co(II) d^7 complexes can exist either as low or high-spin complexes (i.e. one or three unpaired electrons – (*figure 1.14*), depending upon the type of ligands attached at the coordination sites. However, no conclusive empirical reasoning has been found for why certain macrocycle with nitrogen or oxygen atoms bonding will give high- or low-spin complexes.[29, 87]

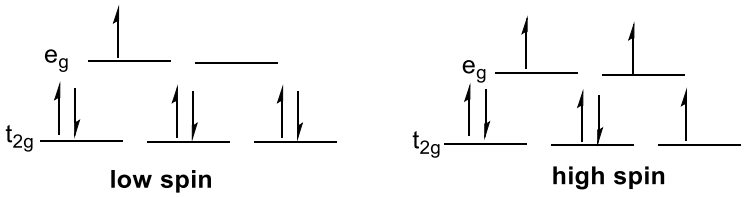

d-electron configurations of d^7 Co(II) in low spin (left) and high spin (right) configurations

Figure 1.14: Spins states and d-configuration of Co(II)

1.4.4 Measuring catalyst activity

The activity of a CTA for any given system (monomer, solvent, temperature, CTA) is given by the chain transfer constant (Cs) – defined as the ratio of the rate of chain transfer to the rate of propagation (k_{tr}/k_p).[113-115] Usually, C_s is also a good indicator for the catalyst purity of a given system. Conventional chain transfer agents such as mercaptans (thiols) have C_s values on the order magnitude of 1-10 for methacrylates. Whereas, cobaloximes such as CoBF, which are not consumed within the reaction, will typically have C_s values in the region 10^4 for methyl methacrylate. This results in cobaloximes being highly efficient at forming low molecular weight macromonomers, hence only ppm amounts are often required to achieve significant reductions in molecular weight.[29, 87, 90, 116]

C_s values can be measured using the Mayo equation from construction of a Mayo plot, *equation 1*: a series of polymerisations are undertaken with various ratios of CTA to monomer, including one with no CTA present, and stopped at low conversion (generally < 5-10 %), so as to avoid changes in monomer concentration such as reduced monomer concentration and to minimise termination. From this a linear Mayo plot of $1/DP_n$ vs. [S]/[M] can be constructed, with a slope equal to C_s for that polymerisation system, whereas DP_n^0 will be given by the intercept.[29, 87, 99, 116]

Mayo equation

$$\frac{1}{DP_n} = \frac{1}{DP_n^0} + C_S\left(\frac{[S]}{[M]}\right)$$

Equation 1.1: Mayo equation, where DP_n is the number average degree of polymerisation in the presence of CTA, DP_n^0 is the number average degree of polymerisation without CTA, C_s is the chain transfer constant, [S] and [M] are the concentration of CTA and monomer respectively.

This system is very effective for all but very low DP_n *(< 20)* when a revised form of Mayo equation (*equation 1.2*) must be utilised due to the significant effects of the formation of monomeric product.[115, 117-119]

Mayo equation low DP_n

$$\frac{1}{DP_n - 2} = \frac{1}{DP_n^0} + C_S\left(\frac{[S]}{[M]}\right)$$

Equation 1.2: Modified Mayo equation for low DP, where DP_n is the number average degree of polymerisation in the presence of CTA, DP_n^0 is the number average degree of polymerisation without CTA, Cs is the chain transfer constant, [S] and [M] are the concentration of CTA and monomer respectively.

The number average DP can be calculated either from M_n SEC, or by division of M_w SEC by two times the monomer mass. M_w is only acquired for systems where the $Đ$ is approximately 2 due to a high rate of chain transfer – as is the case with CCTP. M_w is typically used as the more accurate method of measurement for CCTP, as Mn has high susceptibility to baseline deviation. [115, 117-119]

1.4.5 Mechanism of CCTP

Three distinct mechanisms have been proposed for catalytic chain transfer polymerisation to date, a system that has been found to be justly catalytic through the recovery of the regenerated cobalt complex.[48, 99, 101, 103, 104] Two of the three techniques are characterised by activation of a substrate by the cobalt complex prior to attack by the monomer; the third involves a sequential reaction of two species with the metal centre as depicted in the (*scheme 1*).

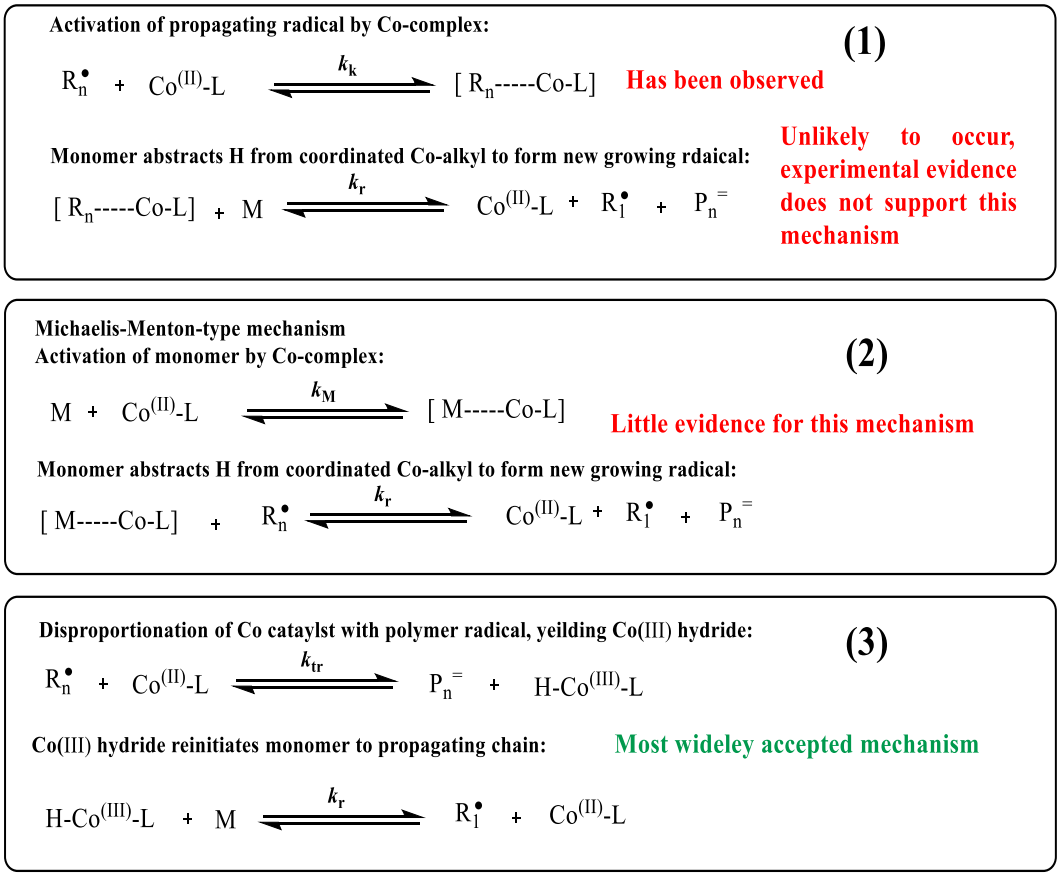

Scheme 1.1: Proposed mechanisms for catalytic chain transfer polymerization. Where R_n and R_1 are the polymeric and monomeric radicals, M is the monomer, Co(II)-L is the cobalt chelate CCTA and Pn = is a polymer with an unsaturated chain end.[82]

The first proposed mechanism (**1**) involves the formation of an intermediate Co complex by the reaction of the propagating radical followed by the subsequent abstraction of hydrogen from a monomeric unit followed by facilitation of a new propagating radical chain.[116, 120] The initial part of this mechanism has been observed experimentally; however, the mechanism is unlikely to occur due to the monomer not being able to be directly involved in the abstraction of the hydrogen atom from the monomeric unit.[116, 120] The second mechanism (**2**) acquires Michaelis-Menton-type mechanism affiliated to enzymatic comportment. This mechanism suggest that CCT is dependent upon the concentration of monomer, which has also been disapproved. [29, 97, 99, 101, 103, 104, 121]

The third mechanism (**3**): is the most acknowledged mechanism for CCTP is by means of a two-step radical reaction: Initially a hydrogen radical is abstracted by the Co(II) complex from a growing polymer chain, which results in an extremely reactive

Co(III)H intermediate and a macromonomer.[29, 87, 90, 99, 101, 103, 104] The subsequent reduction of Co(III)H back to Co(II) yields a monomeric radical, capable of propagation. The mechanism of CCTP can be outlined as the abstraction of a hydrogen radical from a growing polymer chain, and transfer of this radical to a monomer unit.

Therefore for monomers containing a α-methyl group (such as MMA), hydrogen abstraction takes place from the α-methyl group, whereas for monomers without a α-methyl group (such as styrene), abstraction takes place from the backbone. The resulting species for monomers containing a α-methyl group, are a terminated polymeric species with the hydrogen atoms as α and a vinyl group as ω-unsaturated end group (a 'macromonomer') and a new propagating centre in the form of a monomeric radical is also formed. The overall effect of the catalyst, is the formation of low molecular weight macromonomer without affecting the kinetic chain length or rate of polymerisation, much like conventional catalytic chain transfer polymerisation.[29, 87, 90, 99, 101, 103, 104]

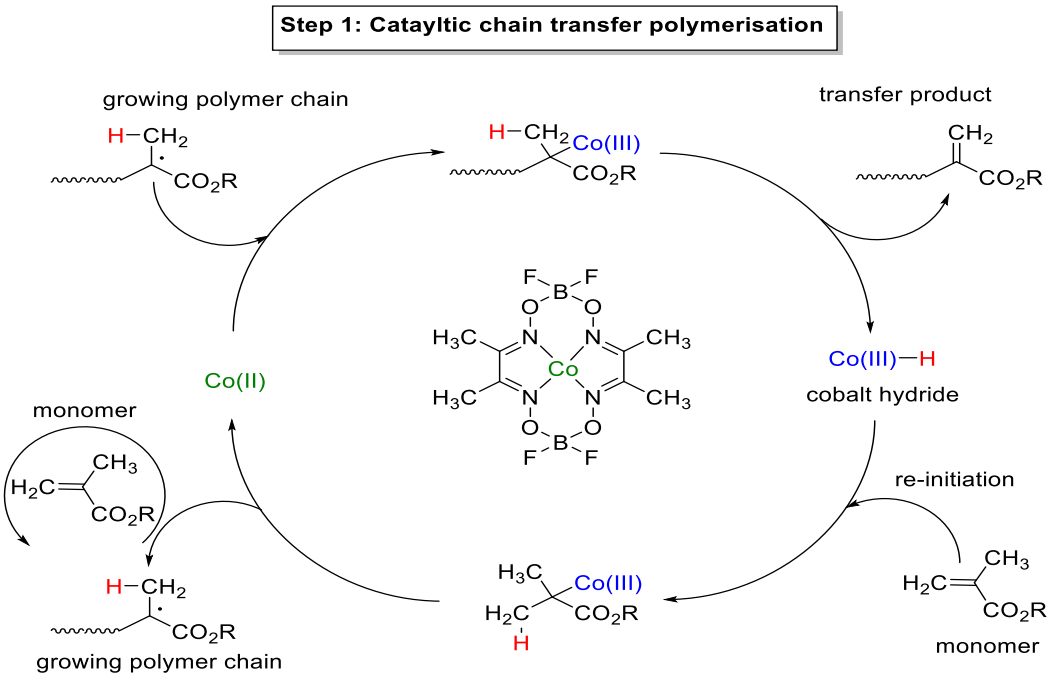

Scheme 1.2: Proposed mechanism for catalytic cycle for CoBF-mediated CCTP [28]

Even though, the third proposed mechanism CCTP is widely accepted it still acquires some discrepancy from the scientific community due to difficulties and lack of

analytical methods capable at elucidating the active species during polymerisation: the catalyst is paramagnetic therefore ^{1}H-NMR is problematic– hindering the NMR analysis of the complex.[23, 92, 122] Nevertheless, DuPont have investigated the possible polymer end group (which are identical to those produced in chain transfer and bimolecular termination in FRP) have been exploited using ^{1}H and ^{13}C NMR to measure the amount of vinylidene groups per polymer chain.[122] The authors determined that > 82 % of polymer chains possess vinyl functionality.[122] However, the number of groups terminated by disproportionation or combination were not evaluated (yet the values obtained are coherent with the values expected with the percentage for termination by disproportionation for methacrylates).[92-94, 122, 123]

Matrix assisted laser desorption time-of-flight mass spectrometry (MALDI-ToF-MS) has allowed mass spectra of PMMAs synthesised via emulsion polymerisation with molecular weight 1400 gmol^{-1} recorded with high resolution, and work by Haddleton *et al.* has found that > 99 % of polymer chains detected by MALDI-TOF analysis were terminated with vinyl functionality[92-94, 122, 124].

As with all typical free radical polymerisation; radicals are consumed throughout the polymerisation process by standard chain termination events, and thus a constant supply of radicals is required for successful polymerisation.[27] Usually, reactions are carried out in the presence of azo or peroxide initiators which are thermally degradable at timescales which roughly ensures a constant stream of radical flux is maintained. However, CCTP is limited to the types of initiators acquired for polymerisation compared to conventional free radical polymerisation, since peroxide and persulfates initiators, oxygen centred radicals have been shown to often result in poisoning of the catalyst, preventing CCT and in turn preventing formation of low molecular weight macromonomer[29, 87, 90].

1.4.6 Monomer selection:

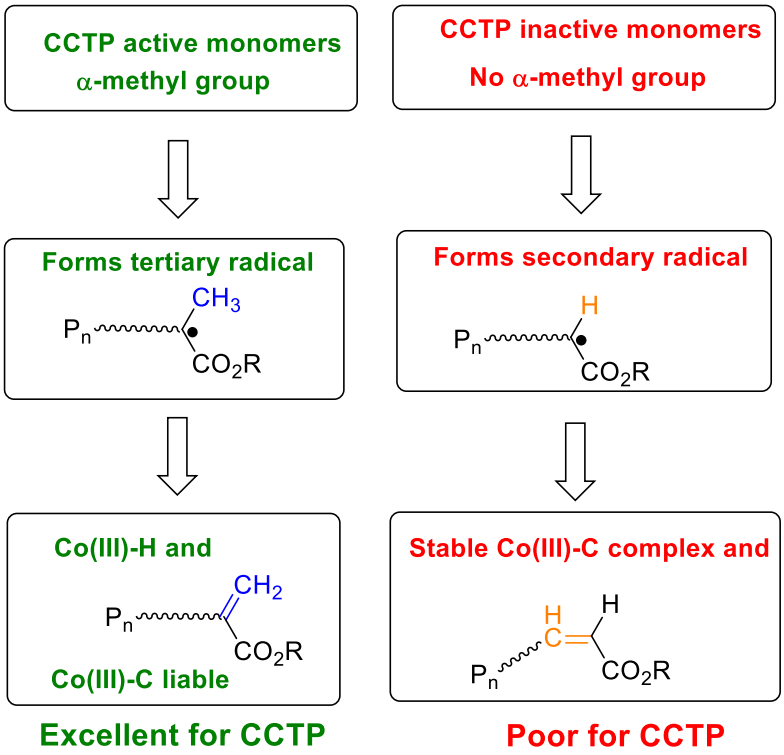

Scheme 1.3: General monomer properties for CCT active and less active monomers

1.4.7 Monomers

Even though, CCTP is extremely effective for forming very low molecular weight polymers/oligomers based on methacrylic monomers via (*scheme 1.2*); acrylic type monomers possess a more significant problem. Therefore, it is important to categorise the monomers into two different categories; active and in active species. Active species, would inherently possesses an α-methyl group (the exception being styrene), and an H-atom that is easily abstracted by the CCTA complex. This results in formation of liable Co(III)-C bond and facilities the subsequent formation of Co(III)-H and ω-vinyl terminated polymer chain[29, 87, 108, 125].

Therefore, methacrylates are usually utilised in CCTP due to the presence of tertiary propagating radicals and they provide high chain transfer efficiency due to the ability of being recyclable during polymerisation. On the contrary, monomers that are classified as inactive (lacking α-methyl group and are secondary propagating radicals), such as such as acrylates, there is no easily abstractable H-atom. This results in formation of extremely stable Co(III)-C bond; which essentially removes the

catalyst from the catalytic cycle, resulting in decrease concentration of catalyst available for chain transfer reactions (reducing chain transfer efficiency). The H-atom in these systems are abstracted from the backbone, vinyl bond, which is usually less desirable for post polymerisation and modification. The active and non-active monomers for CCTP is depicted and summarized in (*scheme 1.3)*[29, 87, 88, 102]. Furthermore, it is important to note that styrene monomer is classified as an exception, since having moderate activity despite the absence of an abstractable H-atom[29, 87, 102].

Moreover, another very interesting fact about styrene is that rate of CCT in styrene polymerisation has been demonstrated to be UV-light dependent. The rate of CCT in dark were less than 100 but increases to a maximum of C_s 5000 under UV irradiation.[29, 87] This is due to the fact that UV irradiation homolyzes the Co(III)-C bond formed by addition of styrene radical to the Co(II). In addition, C_s is also found to be initiator concentration dependent, decreasing with higher initiator concentration.[29]

1.4.7.1 CCTP of reactive monomers

A significantly large number of vinylene monomers such as methacrylates, α-methyl styrene, and methacrylonitrile in addition to styrene have been utilised in CCTP; with MMA and other alkyl derivatives of methacrylate's extensively exploited and utilised.[29, 87, 126] The CCT rate constants of these monomers classified as CCT-active monomers are about 10^5 –10^7 L/mol s. In congestion, to these monomers, other monomers with more diverse and complex architecture have also shown to polymerise efficiently under CCT conditions. [29, 87, 88]

These monomers include wide range of functionalities capable of post-polymerisation modification, for example highly reactive species of glycidyl methacrylates, 2-isocyanatoethyl methacrylates, and even tolerant of carboxylic acid functionalities (methacrylic acids), and biologically derived materials for example 2-methacryloxyethyl phosphoryl choline, glycerol monomethyl methacrylate, or 3-O-methacryloyl-1, 2:5,6-di-*O*-isopropylidene-D-glucofuranose (sugar-monomers).[90, 126-132]

The ability of these polymers exhibiting reactive and tolerant functional groups, combined with terminal vinyl groups have been exploited both as a macromonomers and for post-polymerisation modifications. The macromonomers can be used further in polymerisation involving the synthesis of graft, hyper-branched polymers and other unique polymeric morphologies. In the case of hyper-branched polymers synthesised from di or multifunctional methacrylate monomers, significant number of vinyl end group functionality remains which can be exploited for further polymerisation.[29, 87, 90, 131, 133] The most common form of post polymerisation functionalisation technique in CCTP involves the addition of functional thiols to the olefinic bonds, commonly termed thiol-ene additions.[127-131, 133, 134]

Thiol-ene type reactions are more prevalent in comparison to other Michael type additions is due to its tolerance to a range of reaction conditions, functionalities and solvents. Furthermore, thiol-ene orthogonal nature has led to widespread application in dendrimer synthesis, where high selectivity is essential and required. Usually, thiol-ene or "thiol-ene click" addition reaction is either performed by anti-Markovnikov radical addition pathways or by using nucleophilic catalysis, mild base which is commonly referred to thiol-Michael addition. [127-131, 133, 134]

Michael addition reactions is usually favoured over anti-Markovnikov radical addition reaction since it requires much milder conditions the end-functionalised polymer obtained has high yield with minimal by product formation.[29, 87, 90, 98] In contrast to conventional thiolene reactions, the utilisation of activated vinyl groups is essential for thiol-Michael addition, common examples of these activated-enes include (meth)acrylate, fumarate esters and maleimide derivatives. [29, 98, 127-131, 133, 134]

1.4.7.2 CCT copolymerisation with less active monomers

The second group of monomers as discussed before involves significantly more types of monomers, for example acrylates, vinyl acetate, tetrafluoroethylene (TFE), acrylonitrile, vinyl chloride, and other crucial commercial vinyl monomers. These groups of monomers exhibits significantly lower rate constants in CCT, at least several magnitude lower than the comparison, first group (active monomers)[29, 87, 98, 121, 126, 128]. Therefore, these polymers can be classified as CCT inactive polymers. These

monomers as stated before, exhibit secondary propagating radicals which in turn results in low rate constant in CCT, due to the increased stability of the Co(III)-C bond to the polymer chain end and the requirement for the formation of an internal vinyl bone in the product. MALDI-ToF have been utilised and have shown Co-C complex with the propagating radical in the case of acrylates.[92, 93, 121, 135, 136]

Several methods have been devised and utilised to weaken Co-C bond with the inactive monomer, in order to increase rate constant of CCT, including irradiating the reaction mixture with ultraviolet light or increasing the temperature.[137] However, such approaches have proven unsuccessful as it leads to increase back-biting, resulting to a mixture of vinyl-terminated polymers. As a result, the internal double bonds formed will exhibit limited synthetic application, either for modification or post-polymerisation reactions.[29, 87, 88, 90] Therefore, homopolymerisation of such reaction is hardly attempted by CCTP, as the amount of CCTA required would be impractical and costly procedure.[29, 87, 98, 138]

Nevertheless, copolymerisation of inactive and active monomers, for example acrylates with more active CCT monomers (methacrylates) have been extensively studied. For example, copolymerisation of smaller monomers such as acrylates with olefinically unsaturated macromonomers leads to graft copolymers.[29, 87, 110, 131, 133] However, if larger macromonomers are copolymerised with small amount of commoner, the resulting product resembles a more star like architecture, however incorporating macromonomers into other macromonomers leads to branched and hyperbranched systems discussed previously.[29, 87, 88, 131, 133, 139]

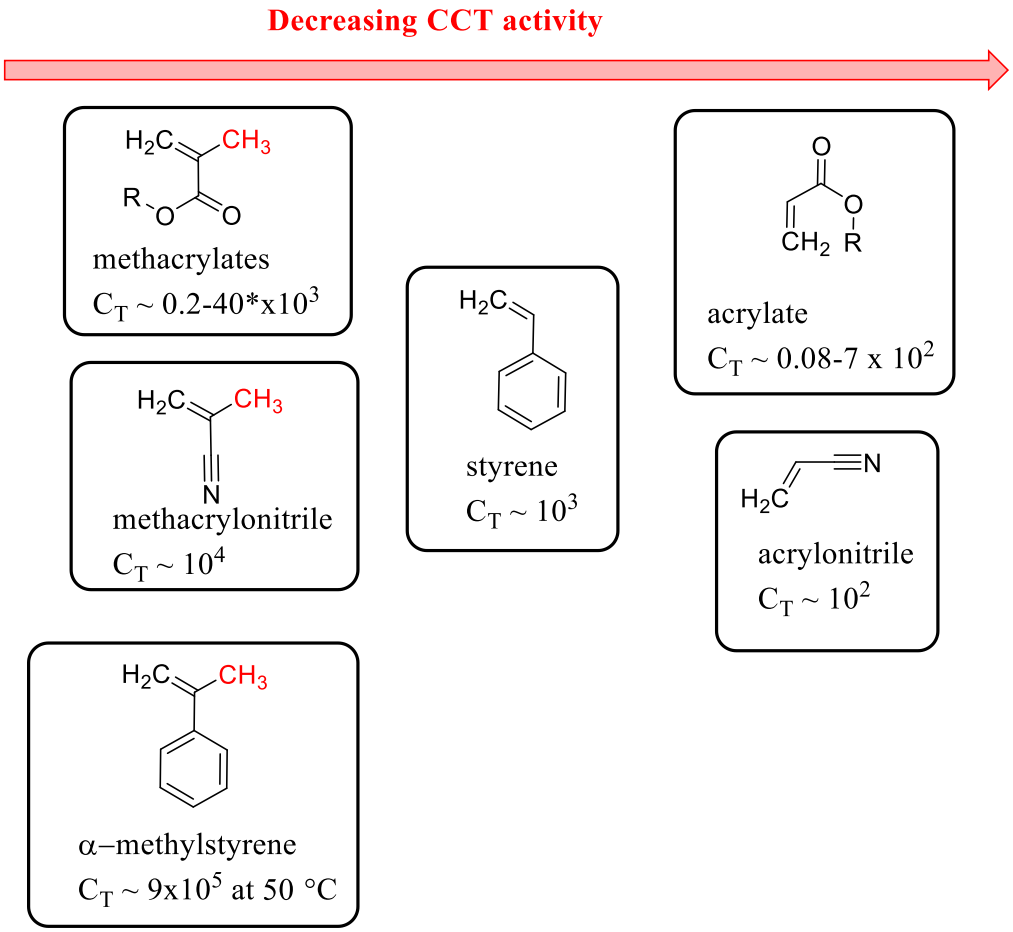

Figure 1.15: Structures and CCT activities of monomers commonly used in CCTP [29].

1.4.8 Uses and applications of CCTP macro- monomer

Besides CCTP's industrial application of controlling MW of polymers in FRP systems, the bulk products prepared by CCT have varied applications especially into products where aesthetics are important such as automotive industry. Generally, products derived from CCT are utilised in further chemistry, however there are some applications where they are deployed directly.[140]

For example, in electrophotographic toners the catalyst from CCT is directly utilised in an emulsion systems to combine with suspensions of black or coloured pigments which are in turn precipitated to obtain toners with narrow particle size and emulsions that are significantly more stable than those attained with thiol chain-transfer reagents[29, 87]. Other common examples, where CCTP derived macromonomers are utilised directly are casting composition for thermoformable sheet compositions, lowering viscosities and improving robustness of the final sheet goods.[29, 98]

In automotive industry functional monomers are utilised in production of low volatile organic compounds (VOC) with high solids coating, such has hydroxyethyl methacrylate (HEMA).[23, 141] The monomers are copolymerised as the multiple hydroxyl group on the macromonomer enables the polymers to cross link with of trimethyl orthoformate and hexamethylene diisocyanate trimer, in the presence of sulfonate catalyst, this forms a product with excellent flow ability, cures to enable good weatherability and adhesion after the application of coating.[29, 141-145]

Other useful applications of CCTP derived oligomers are in the application of dimers, for example the use of hydroxyethyl methacrylate dimer as a CTA in MMA polymerisation, results in α,ω–telechelic polymer.[23] Telechelic polymers are, normally, classified as low molecular weight macromolecules possessing a reactive functional group at both α and ω terminal ends. The viable conventional route for the formation of telechelic polymers is an addition fragmentation reaction whereby the macromonomer dimer splits in half: with one half consists of ω-terminal end of each macromolecule whereas the other half is released as a functional initiating radical[23, 98, 146]. Telechelic polymers from radical chain polymerisation have broad range methodologies in polymer chemistry, such as functional initiators, iniferters, functional chain transfer agents (telomers) and are utilised in incorporation of cleavable weak link along polymer chains[23, 146, 147].

Other commonly used dimers for similar applications are methacrylic acid, ethyl methacrylate, methacrylonitrile, and α-methylstyrene[29, 113, 148, 149]. With α-methylstyrene used must predominantly since it is extremely effective in controlling molecular weight in polystyrene manufacturing and malodorous sulphur containing compounds for the application of spray-up moulding and room-temperature curable hand lay-up moulding[29, 148, 149]. Furthermore, the dimers of α-methylstyrene is also extensively used in dental adhesiveness which is cured by UV-radiation, presence of the α-methylstyrene dimer controls the hardening time and heat of polymerisation[29, 87, 148].

An further common application of CCTP polymers is utilising macro-monomers to give grafted architecture by combining the polymerisation technique with (reversible

addition-fragmentation transfer) RAFT.[150] This ensures that the polymers obtain would acquire narrow dispersity and are structured before terminating with CCT to give unsaturated vinyl end-group macro-monomers. The polymers obtained are subsequently copolymerised with acrylic monomers to obtain comb-like or less frequently star like structures. Macromonomers synthesised via CCTP ranging in molecular weight from 4 – 20 kg mol^{-1}, have also been copolymerised but with a difunctional acrylic monomer, so that it can form a cross linked core which will enable it to bind to the macromonomer "arms" together.[150] For rheological modifiers butanediol diacrylate have been copolymerised with the monomers aforementioned previously to form star like structures with range of hydrophobicity (depending on ratio of monomers used to make the arms).[38, 150-152]

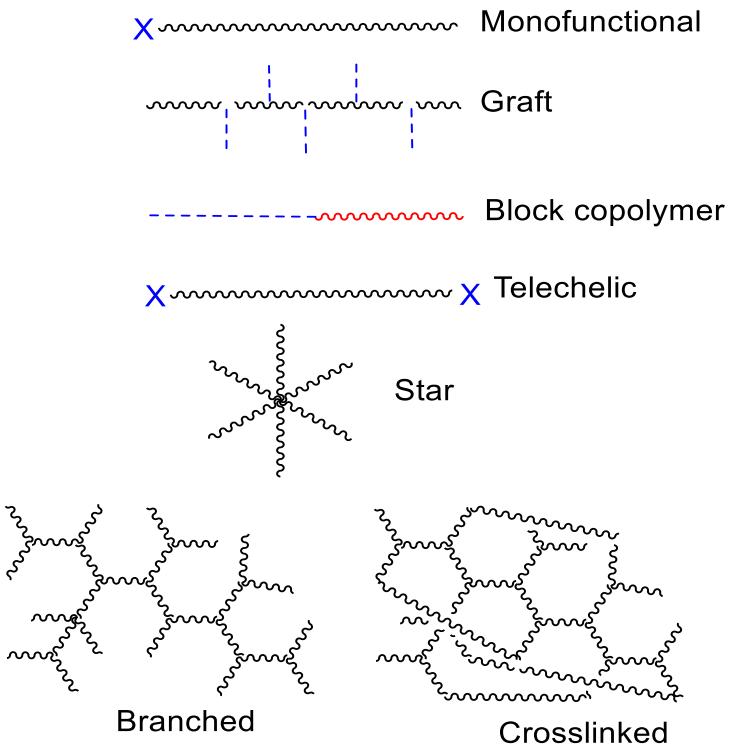

Figure 1.16: Polymer structures attainable from CCT

1.5 Controlled radical polymerisation

Polymers derived from free radical polymerisation rarely exhibit well defined architectures, and will often form polymers with dispersities *(Đ)* > 2.[24, 25, 32, 153] The higher *Đ* could be attributed to many undesirable side reaction such termination and

chain transfer which is commonly encountered in radical polymerisation but could be supressed by maintaining low radical concentration.[32] However, in order to synthesise well defined macromolecules with predetermined molecular weights, low *Đ*, precisely controlled end-group functionalities, and chain topologies we need to utilise living/ controlled polymerisation techniques with respect to:

- Topology (e.g., linear, star shaped, comb shaped, dendrite, cyclic etc.)
- Terminal functionalities
- Composition and arrangement of comonomers (e.g., statistical, periodic, block, graft, gradient)
- Molecular weight predetermined by the ratio of concentration of reacted monomer to introduced initiator ($DP_n = \Delta[M]/[I_o]$)
- Narrow *Đ* (M_w/M_n)

A living polymerisation is a chain polymerisation which proceeds in the absence of the kinetic steps of termination or chain transfer.[154] The following experimental criteria have been proposed by Quirk and Lee and utilized as diagnostic characteristics for living polymerisation:

1. Polymerisation proceeds until all of the monomer has been consumed. Further addition of the monomer results in continued polymerisation.
2. The number-average molecular weight M_n (or X_n, the number-average degree of polymerisation) is the linear function of conversion.
3. The number of polymer molecules (and active centers) is a constant, which is sensibly independent of conversion.
4. The molecular weight can be controlled by the stoichiometry of the reaction.
5. Narrow molecular weight polymers are produced. The polymer must have a Poisson distribution of molecular weight.
6. Block copolymers can be prepared by sequential monomer addition.
7. Chain-end-functionalised polymers can be prepared with quantitative yield

Quirk and Lee emphasised that completion of any single criterion is not adequate enough for a polymerisation to be considered to be living or not; since chain transfer and chain termination reactions can have different outcomes and various criteria have different sensitivities to these side-reactions.[32, 154] Therefore, a modified definition of

living polymerisation was established proposing that the terms living polymerisation with reversible termination and living polymerisation with reversible chain transfer shall be utilised to describe those living polymerisations that proceed in the absence of the kinetic steps of irreversible chain transfer and irreversible chain termination, respectively.[26, 32, 154]

Further, requirements for obtaining polymers with controlled molecular weights and low $Đ$ in living polymerisation are that the rate of initiation should be significantly greater or equal to the rate of propagation, and the exchange between species of various reactivities and lifetime must be fast in comparison to propagation.[24-26, 154] Although, side reaction may occur in controlled polymerisation the extent should be in accordance that it does not disturb the control of the molecular structure of the polymer chain.[32] In some instances living polymerisation can include, slow initiation, reversible formation of species with range of activities and lifetimes, and reversible formation of inactive (dormant) species (reversible deactivation). However, living polymerisation may not include irreversible deactivation (i.e. termination) and irreversible transfer.[32, 154]

Therefore a number of methods have developed especially at the start of 1990s, which enabled an adaptions of living ionic polymerisation to living radical polymerisation (LRP), also commonly referred to as controlled radical polymerisation (CRP) explain in *section 1.5*. However, the must established CRP techniques have been branched into three fundamental methodologies: stable free radical polymerisation (SFRP), most frequently referred to as nitroxide mediated polymerisation (NMP)[155, 156], transition-metal-catalysed atom transfer radical polymerisation (ATRP, Cu-RDRP, SET LRP)[157, 158 159-161] and degenerative transfer with alkyl iodides, methacrylate macromonomers, and dithioesters via reversible addition-fragmentation chain transfer (RAFT)[25, 162-164] polymerisation.

The common theme between these three methods of CRP is that in order to extend the lifetime of propagating chains, a dynamic equilibrium needs to be established between the low concentration of active propagating chains and predominant amount of dormant chains which are incapable to propagate or terminate. These techniques will be discussed in more detail in subsequent sections[25].

1.5.1 Nitroxide Mediated Polymerisation (NMP)

Stable free radical polymerisation (SFRP), most frequently referred to as nitroxide mediated polymerisation (NMP), recommended IUPAC term for NMP is ‘‘aminoxyl-mediated radical polymerisation’’ (AMRP). However, keeping with the historical context throughout this chapter will refer to its common terminology[165]. NMP was initially discovered in Australia at CISRO in 1984, at the Division of Applied Organic Chemistry, and was subsequently patented by the Australians under “Alkoxyamines useful as initiators” the same year[24, 165, 166]. The first publication on NMP was by Solomon, Rizzardo and Cacioli in a European patent application, Free radical polymerization and the produced polymers, which was published in 1985[24, 156, 167].

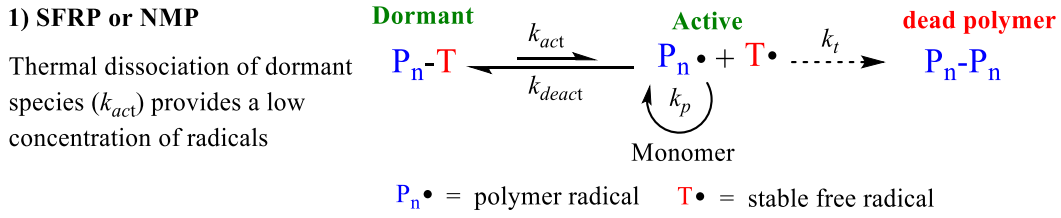

Scheme 1.4: Proposed mechanism for SFRP or NMP[24, 166, 167]

NMP utilises a nitroxide, initially 2,2,6,6-tetramethyl-1-piperidinyloxyl (TEMPO) to reversibly deactivate/trap growing polymer radicals (equilibrium is pushed to the left-hand side) to form excess dormant species of alkoxyamines as a result of radical effect. In all radical polymerisation, bimolecular termination is known to occur at a rate R_t, this is reliant on the concentration of radicals [P•], where $R_t = k_t[P•]$. As a result, at the same polymerisation rate (i.e. the same [P•]), fundamentally the same number of chains terminate regardless of being in conventional or CRP systems. Nevertheless, a major difference between conventional FRP and CRP is that, in CRP since there are greater number of growing chains the number of terminated chains are significantly less and constitutes to a small fraction of total chains (~1-10%)[24, 156, 165-168].

Whereas, in conventional process all the chains known to be terminated. Therefore, the remaining chain in CRP are dormant chains, capable of reactivation, functionalisation, and chain extension to form block copolymers and other unique polymeric architecture depending upon its application and as a result CRP in essence behaves like a living system. Furthermore, the initiation rate are relatively fast at least

equal to or greater than the propagation, which in turn gives control over stereochemistry such molecular weights ($DP_n = \Delta[M]/[I]_0$) and very low and narrow molecular weight distribution (MWDs)[24]. It stands out from other controlled radical polymerisations such as ATRP and RAFT polymerisation as a result of its simplicity: the polymerisation is thermally initiated in the absence of an external radical source or a metal catalyst[24, 156, 165, 167, 168].

1.5.2 Atom Transfer Radical Polymerisation (ATRP)/Transition metal mediated living radical polymerisation (TMM LRP)

In 1995, two independent groups led by Sawamoto[157] and Matyjaszewski[158] synthesised new class of controlled living radical polymers via ATRP. Sawamoto utilised a ruthenium(II) catalyst to yield a controlled polymerisation of methyl methacrylate, whereas Matyjaszewski in comparison utilised a copper based system (a reversible redox reaction between Cu(I)Cl and Cu(II)Cl_2) to synthesise well-defined polystyrene polymers. Many different transition elements have been utilised in the polymerisation of ATRP including copper, iron, cobalt, ruthenium and nickel (typically in the form of salts with chlorine, bromine or iodine).[24, 25]

Nevertheless, the most commonly utilised transition metal is copper, mostly due to its low cost and versatility. Whereas, the common complexing ligands include nitrogen and phosphine based structures. The function of the ligand is to solubilise the metal ion complex, which as well affects the reduction potential of the transition metal ion. While the alkyl bromides and chlorides are frequently utilised as initiators, alkyl iodides have also been known to be utilised but significantly less than the other counterparts.[169]

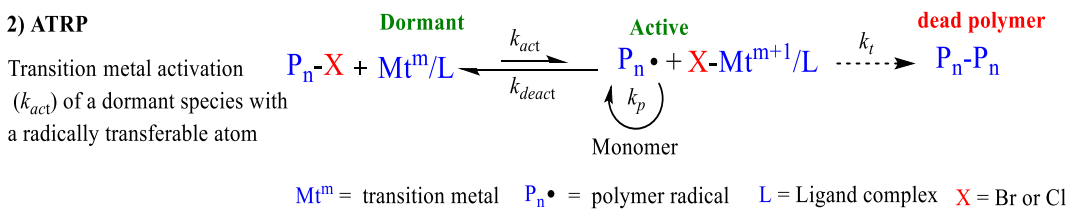

Scheme 1.5: Proposed mechanism for ATRP

The generic mechanism of ATRP involves; a dynamic equilibrium being established between usually an alkyl halide (or halogen end-capped polymer chain, P_nX referred to as a macromolecule) and the corresponding radical ($P_n\cdot$) by means of a transition metal complex (Mt^m/ligand – X-Mt^{m+1}/ligand), where Mt^m represents the transition metal species in oxidation state m, L is a ligand, and X-Mt^{m+1} refers to the deactivators-transition metal complexes in their higher oxidation state, coordinated with halide ligands.

The equilibrium in ATRP has some similarity to NMP/SFRP; since the equilibrium is shifted towards the dormant species (left hand side), so that the radical concentration is kept to a minimum. Therefore limiting radical termination reactions and allowing control over molecular weight and polymer architecture. Nevertheless, terminations cannot be fully avoided in ATRP and consequently terminations in the initial stages of the polymerisation will lead to a build-up of the deactivator (i.e. X-Mt^{m+1}/ligand) concentration.[169] As a result, due to persistent radical effect, the equilibrium will be shifted towards the dormant species (left hand side) and the radical concentration will be reduced. The polymerisation, therefore could be described as in a sense self-regulating.[170, 171]

Electron paramagnetic resonance (EPR) has been used in determining the concentration of deactivators throughout ATRP reaction. The results demonstrated that the deactivator concentration reaches about 5-10 % of the initial activator concentration during the polymerisation.[172] Therefore, in order to improve the control of the reaction in ATRP a small amount of deactivators is added to the system in order to shift the equilibrium towards the dormant species (typically 10 % deactivator relative to the activator concentration is added, this corresponds to the amount of deactivator formed during the polymerisation due to irreversible terminations).[24, 25, 169, 171, 173]

Finally, in a conventional living polymerisation (e.g. anionic polymerisation), the chain end must be living and as result should not be irreversibly terminated, though it should be able to be utilised as macroinitiators for further polymerisations. In ATRP systems, this is acknowledged by the reversible halogen end-capping.[158] Therefore, upon the completion of the polymerisation, all the chains should (ideally) acquire a

halogen atom at the chain end in order to mimic the criteria's for a living system. Therefore the presence of end-capping enables the utilisation of macroinitiators (corresponding to the initial alkyl halide initiator) for formation block copolymers, post polymerisation/ functionalisation (or other advanced polymer architectures).[24, 169, 171]

1.5.3 Reversible addition-fragmentation chain transfer (RAFT)

RAFT is another successful form of living radical polymerisation. RAFT polymerisation using thiocarbonylthio compounds, including dithioesters and trithiocarbonates was discovered by a team of serval researchers at CSIRO in Melbourne, Australia in 1998.[162] Subsequently, another research group from France reported a process with an analogous mechanism but using xanthate RAFT agents (MADIX) in late 1998.[174] The RAFT process has proved to be the most effective and versatile in polymerising a variety of monomers since the method allows synthetic tailoring of macromolecules with complex architectures including block, graft, comb, and star structures with predetermined molecular weights, low $Đ$ and with relative ease.[163]

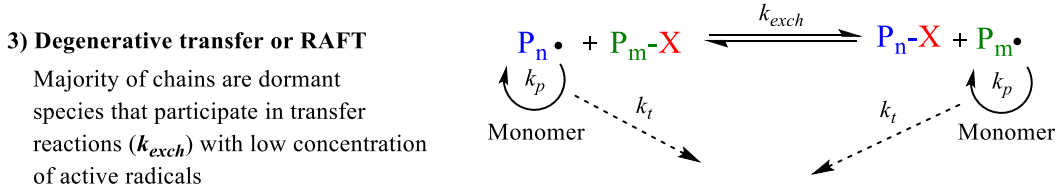

Scheme 1.6: Proposed simplified mechanism for RAFT[25]

The mechanism of RAFT polymerisation is illustrated in *scheme 1.7*. Succeeding activation (step 1), the radical species add to the RAFT agent (CTA) to enter equilibrium between active and dormant species (steps 3 and 5). The chain transfers steps that form the foundation of the RAFT mechanism is degenerate since it involve a reversible transfer of the functional chain end-group (normally a thiocarbonylthio group, Z−C(=S)S−R) between the dormant chains (macroRAFT agent or macroCTA) and the propagating radicals.[163, 174] In an efficient process, the rate of addition/fragmentation equilibrium will be higher than that of the propagation, so in essence there would be less than one monomer unit added per activation cycle; consequently, all chains will have a similar (DP) at a given time. The overall process

is comprised of the insertion of monomers between the R- and Z−C(=S)S-groups of a RAFT agent, which form the α and ω end-group of the majority of the resulting polymeric chains.[25, 162-164]

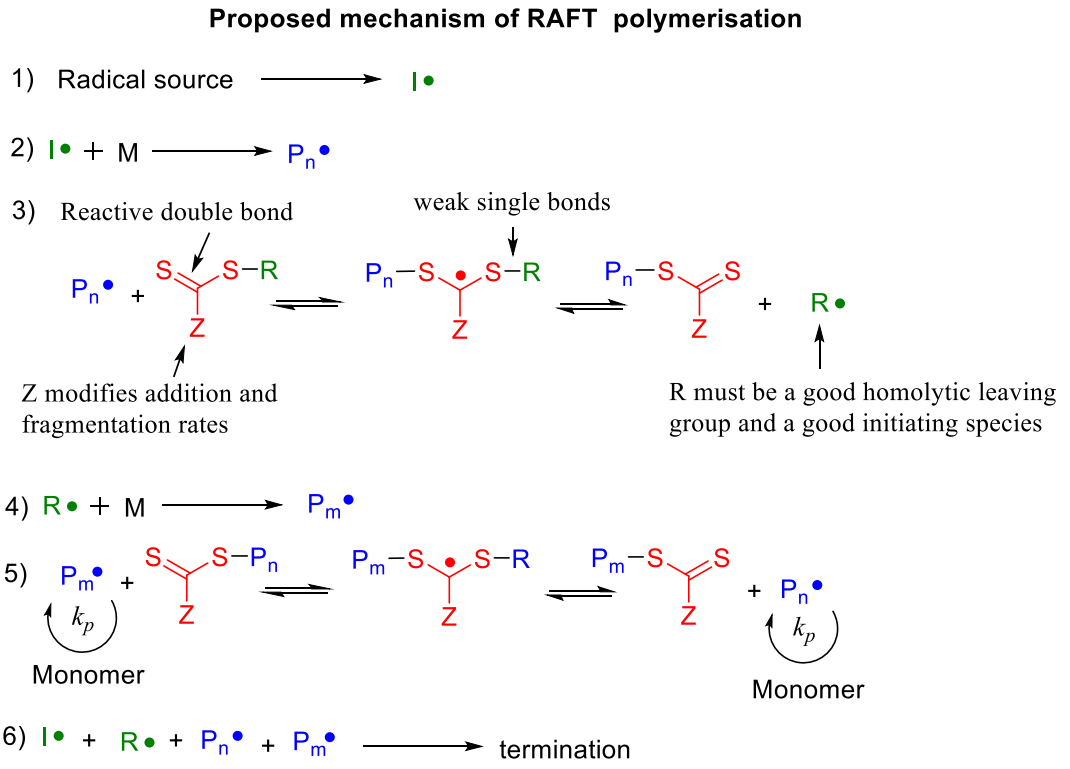

Scheme 1.7: Proposed expanded mechanism of RAFT

Compared to other common CRP polymerisation such as NMP and ATRP, RAFT polymerisation has some significant differences when achieving control over polymerisation. In NMP and ATRP polymerisation techniques involve reversible deactivation of propagating radicals by radical-radical reaction. Therefore the dormant species (alkoxyamine in NMP and halo-compound in ATRP) is as well the source of radicals. As a result, the position of the deactivation-activation equilibria and the 'persistent radical effect' governs the rate of polymerisation.[163, 174] Whereas, in RAFT polymerisation the deactivation- activation equilibria is the chain transfer reactions. External source of radicals is required in order to initiate and maintain polymerisation; radicals are neither formed nor destroyed in those steps. The polymerisation kinetics is similar to conventional radical polymerisation. Therefore, the rate of polymerisation should be half order with respect to the initiator and independent of the macroRAFT agent or macroCTA.[163, 174]

1.5.4 Sulphur free –RAFT (SF-RAFT)

The utilisation of either transition metals or sulphur comprising catalysts/chain transfer agents often requires purification methods such as precipitation or dialysis to isolate a pure usable products. In addition, the halide (as used in transition-metal-mediated approaches) and reversible addition fragmentation chain-transfer (RAFT) agents are typically attached to the polymer backbone even after purification, and may be undesirable in certain applications. Furthermore, RAFT or copper mediated techniques are often most suited to acrylic and acrylamide monomers and are often less effective with methacrylates, due to lower rates of propagation.[4, 113, 175-184]

Whereas, SF-RAFT utilises the macromonomer formed via CCTP in emulsion polymerisation as macroCTAs. The monomers utilised have very low rates of k_p, such as methacrylates and α-methyl styrene, which in turn makes them very effective at forming low M_n macromonomers which in turn acts as macroCTAs in the subsequent steps for the formation of diblock and multi-block copolymers. SF-RAFT can be utilised to form well-defined, sequence-controlled multiblock copolymers in a facile, rapid, quantitative and scalable manner by development of a novel 'transition metal' and 'sulfur' free polymerisation approach combined with an emulsion biomimetic segregation strategy in a similar manner to nature. Furthermore, in SF-RAFT a wide range of methacrylic monomers can be utilised regardless of the low rate of propagation, it has good tolerance of various functionalities, and is stable at elevated temperatures and low pH.[4, 30, 111, 185]

The mechanism of SF-RAFT has been described previously; and it follows similar reaction pathways and kinetics to normal RAFT polymersiation.[4, 30, 120, 186] Initiation, in a typical way, produces propagating radicals constituting of monomer (**2**), subsequently transfer to macromonomer (**1**) forms new propagating radicals (**3**) composed of monomer (**2**). These chains add to monomer (**2**) to form block copolymer radicals (**6**) and a new macromonomer (**5**) based on monomer (**2**). Upon the transfer of the block copolymers to macromonomers, a block copolymer (**4**) is formed with the vinyl terminated ω-chain end. The methodology can utilised to synthesis of multi-block and other more complex architectures with narrow *Đ*.

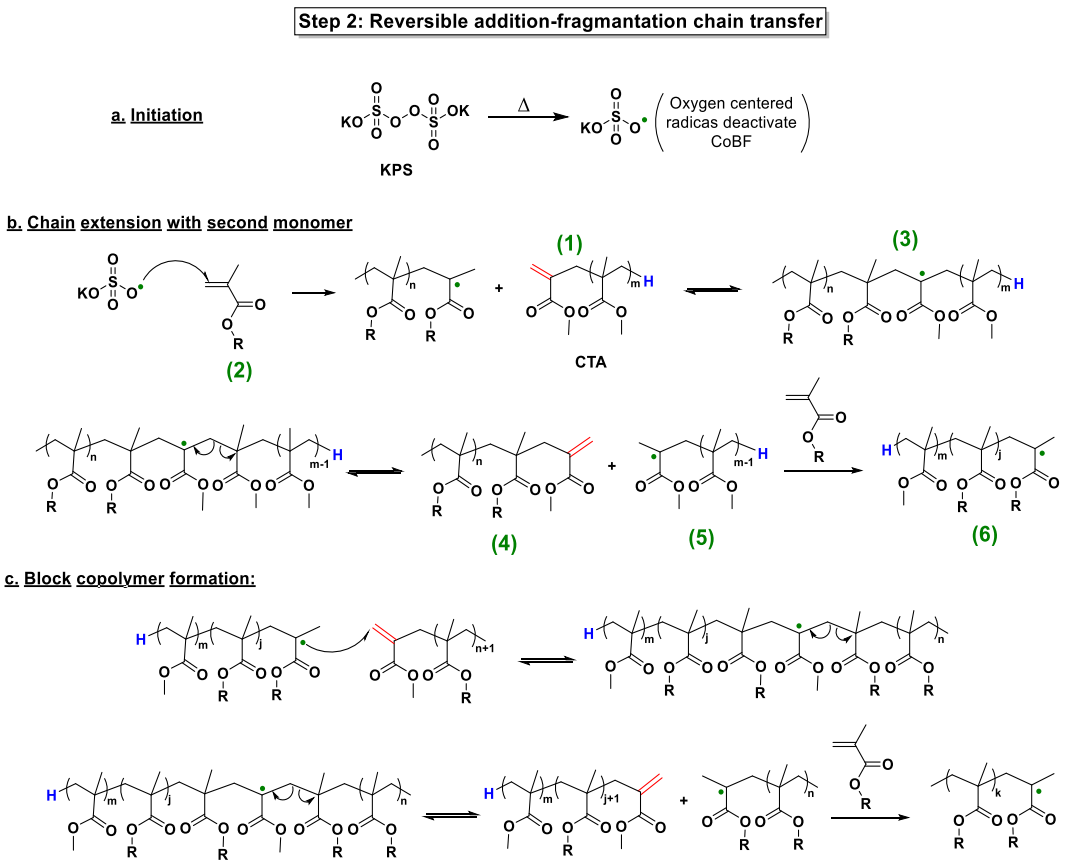

Scheme 1.8: SF-RAFT mechanism[4, 120]

Furthermore, the macromonomer utilised as CTAs can be stored and used at later date. The block copolymers were performed under monomer starved conditions, this means that the polymer particles are not saturated with monomer, but are being polymerised at an instantaneous conversion of 90% or greater. This ensures control of the monomer concentration within the polymer particles.[4, 30, 111, 120, 185] If the reaction were to operate under monomer-flooded conditions, the control over the copolymer composition would be lost. A high [macromonomer]:[monomer] ratio maximises transfer events and is crucial for narrow *Đ*. Low initiation rates are required in block synthesis as the initiator radical-derived chains could give rise to a homopolymer impurity. Radical-radical termination produces non-macromonomer (dead) chains (i.e. long kinetic chain lengths are critical for block purity).[30, 120]

1.6 References

1. T. Soejima, K. Satoh and M. Kamigaito, in *Sequence-Controlled Polymers: Synthesis, Self-Assembly, and Properties*, American Chemical Society, 2014, vol. 1170, ch. 12, pp. 189-200.
2. J. De Neve, J. J. Haven, L. Maes and T. Junkers, *Polymer Chemistry*, 2018, **9**, 4692-4705.
3. J.-F. Lutz, M. Ouchi, D. R. Liu and M. Sawamoto, 2013, **341**, 1238149.
4. N. G. Engelis, A. Anastasaki, G. Nurumbetov, N. P. Truong, V. Nikolaou, A. Shegiwal, M. R. Whittaker, T. P. Davis and D. M. Haddleton, *Nature Chemistry*, 2016, **9**, 171.
5. C. S. Mahon and D. A. Fulton, *Nature Chemistry*, 2014, **6**, 665.
6. T. Terashima and M. Sawamoto, in *Sequence-Controlled Polymers: Synthesis, Self-Assembly, and Properties*, American Chemical Society, 2014, vol. 1170, ch. 17, pp. 255-267.
7. E. Brulé, C. Robert and C. M. Thomas, in *Sequence-Controlled Polymers: Synthesis, Self-Assembly, and Properties*, American Chemical Society, 2014, vol. 1170, ch. 23, pp. 349-368.
8. A. B. Chang, G. M. Miyake and R. H. Grubbs, in *Sequence-Controlled Polymers: Synthesis, Self-Assembly, and Properties*, American Chemical Society, 2014, vol. 1170, ch. 11, pp. 161-188.
9. J.-F. Lutz, in *Sequence-Controlled Polymers*, 2017, DOI: 10.1002/9783527806096.ch1, ch. 1, pp. 1-26.
10. D. Chan-Seng and J.-F. Lutz, in *Sequence-Controlled Polymers: Synthesis, Self-Assembly, and Properties*, American Chemical Society, 2014, vol. 1170, ch. 7, pp. 103-116.
11. J.-F. Lutz, *Polymer Chemistry*, 2010, **1**, 55-62.
12. J. Sun, C. Proulx and R. N. Zuckermann, in *Sequence-Controlled Polymers: Synthesis, Self-Assembly, and Properties*, American Chemical Society, 2014, vol. 1170, ch. 3, pp. 35-53.
13. P. J. Milnes and R. K. O'Reilly, in *Sequence-Controlled Polymers: Synthesis, Self-Assembly, and Properties*, American Chemical Society, 2014, vol. 1170, ch. 5, pp. 71-84.
14. C. Boyer, M. R. Whittaker and P. B. Zetterlund, in *Sequence-Controlled Polymers: Synthesis, Self-Assembly, and Properties*, American Chemical Society, 2014, vol. 1170, ch. 13, pp. 201-212.
15. F. Wojcik, D. Ponader, S. Mosca and L. Hartmann, in *Sequence-Controlled Polymers: Synthesis, Self-Assembly, and Properties*, American Chemical Society, 2014, vol. 1170, ch. 6, pp. 85-101.
16. W. R. Gutekunst and C. J. Hawker, *Journal of the American Chemical Society*, 2015, **137**, 8038-8041.
17. G. Moad, C. Guerrero-Sanchez, J. J. Haven, D. J. Keddie, A. Postma, E. Rizzardo and S. H. Thang, in *Sequence-Controlled Polymers: Synthesis, Self-Assembly, and Properties*, American Chemical Society, 2014, vol. 1170, ch. 9, pp. 133-147.
18. Q. Zhang, J. Collins, A. Anastasaki, R. Wallis, D. A. Mitchell, C. R. Becer, P. Wilson and D. M. Haddleton, in *Sequence-Controlled Polymers: Synthesis, Self-Assembly, and Properties*, American Chemical Society, 2014, vol. 1170, ch. 22, pp. 327-348.
19. Zhang. Q., Collins, J., Anastasaki, A., Wallis, R., Becer, C.R. and Haddleton, D.M., *Angewandte Chemie International Edition*, 2013, **52**, 4435-4439.
20. G. Gody, T. Maschmeyer, P. B. Zetterlund and S. Perrier, *Nature Communications*, 2013, **4**, 2505.

21. G. Moad, in *Controlled Radical Polymerization: Mechanisms*, American Chemical Society, 2015, vol. 1187, ch. 12, pp. 211-246.
22. G. Moad, E. Rizzardo and S. H. Thang, *Polymer*, 2008, **49**, 1079-1131.
23. D. M. Haddleton, C. Topping, J. J. Hastings and K. G. Suddaby, 1996, **197**, 3027-3042.
24. W. A. Braunecker and K. Matyjaszewski, *Progress in Polymer Science*, 2007, **32**, 93-146.
25. K. Matyjaszewski and J. Spanswick, *Materials Today*, 2005, **8**, 26-33.
26. K. Matyjaszewski, *Current Opinion in Solid State and Materials Science*, 1996, **1**, 769-776.
27. K. Matyjaszewski and T. P. Davis*, in *Handbook of Radical Polymerization*, 2002, DOI: 10.1002/0471220450.ch3, ch. 3, pp. 117-186.
28. O. George, in *Principles of Polymerization*, 2004, DOI: 10.1002/047147875X.ch1, pp. 1-38.
29. A. A. Gridnev and S. D. Ittel, *Chemical Reviews*, 2001, **101**, 3611-3660.
30. J. Krstina, C. L. Moad, G. Moad, E. Rizzardo, C. T. Berge and M. Fryd, *Macromolecular Symposia*, 1996, **111**, 13-23.
31. T. R. Darling, T. P. Davis, M. Fryd, A. A. Gridnev, D. M. Haddleton, S. D. Ittel, R. R. Matheson Jr., G. Moad and E. Rizzardo, 2000, **38**, 1706-1708.
32. H. S. Bisht and A. K. Chatterjee, *Journal of Macromolecular Science, Part C*, 2001, **41**, 139-173.
33. F. Isaure, P. A. G. Cormack and D. C. Sherrington, *Macromolecules*, 2004, **37**, 2096-2105.
34. N. O'Brien, A. McKee, D. C. Sherrington, A. T. Slark and A. Titterton, *Polymer*, 2000, **41**, 6027-6031.
35. F. Isaure, P. A. G. Cormack and D. C. Sherrington, *Journal of Materials Chemistry*, 2003, **13**, 2701-2710.
36. P. A. Costello, I. K. Martin, A. T. Slark, D. C. Sherrington and A. Titterton, *Polymer*, 2002, **43**, 245-254.
37. A. T. Slark, D. C. Sherrington, A. Titterton and I. K. Martin, *Journal of Materials Chemistry*, 2003, **13**, 2711-2720.
38. M. Destarac, *Macromolecular Reaction Engineering,* 2010, **4**, 165-179.
39. A. Rudin and P. Choi, in *The Elements of Polymer Science & Engineering (Third Edition)*, eds. A. Rudin and P. Choi, Academic Press, Boston, 2013, DOI: https://doi.org/10.1016/B978-0-12-382178-2.00008-0, pp. 341-389.
40. F. K. Hansen and J. Ugelstad, *Journal of Polymer Science: Polymer Chemistry Edition*, 1979, **17**, 3033-3045.
41. G. A. O'neil, M. B. Wisnudel and J. M. Torkelson, *AIChE J,* 1998, **44**, 1226-1231.
42. K. L. Gardner and G. McNally, *J. Polym. Sci. B Polym. Lett. Ed,* 1978, **16**, 267-270.
43. J. W. Gooch, in *Encyclopedic Dictionary of Polymers*, ed. J. W. Gooch, Springer New York, New York, NY, 2011, DOI: 10.1007/978-1-4419-6247-8_903, pp. 55-56.
44. A. Ravve, in *Principles of Polymer Chemistry*, Springer New York, New York, NY, 2012, DOI: 10.1007/978-1-4614-2212-9_3, pp. 69-150.
45. N. P. Cheremisinoff, in *Condensed Encyclopedia of Polymer Engineering Terms*, ed. N. P. Cheremisinoff, Butterworth-Heinemann, Boston, 2001, DOI: https://doi.org/10.1016/B978-0-08-050282-3.50007-X, pp. 32-38.
46. W.-F. Su, in *Principles of Polymer Design and Synthesis*, Springer Berlin Heidelberg, Berlin, Heidelberg, 2013, DOI: 10.1007/978-3-642-38730-2_7, pp. 137-183.
47. N. S. Serkhacheva, O. I. Smirnov, A. V. Tolkachev, N. I. Prokopov, A. V. Plutalova, E. V. Chernikova, E. Y. Kozhunova and A. R. Khokhlov, *RSC Advances*, 2017, **7**, 24522-24536.

48. D. R. Bassett and A. E. Hamielec, *Emulsion Polymers and Emulsion Polymerization*, AMERICAN CHEMICAL SOCIETY, 1981.
49. S. C. Thickett and R. G. Gilbert, *Polymer*, 2007, **48**, 6965-6991.
50. J. M. Asua, 2004, **42**, 1025-1041.
51. C. S. Chern, *Progress in Polymer Science*, 2006, **31**, 443-486.
52. A. van Herk and H. Heuts, in *Encyclopedia of Polymer Science and Technology*, John Wiley & Sons, Inc., 2002, DOI: 10.1002/0471440264.pst112.
53. F. K. Hansen and J. Ugelstad, *Journal of Polymer Science: Polymer Chemistry Edition*, 1978, **16**, 1953-1979.
54. C.-S. Chern and H.-T. Chang, *Polymer International*, 2002, **51**, 1428-1438.
55. I. A. Maxwell, B. R. Morrison, D. H. Napper and R. G. Gilbert, *Macromolecules*, 1991, **24**, 1629-1640.
56. I.-W. Cheong and J.-H. Kim, *Colloids and Surfaces A: Physicochemical and Engineering Aspects*, 1999, **153**, 137-142.
57. E. M. Coen, R. A. Lyons and R. G. Gilbert, *Macromolecules*, 1996, **29**, 5128-5135.
58. L. Vorwerg and R. G. Gilbert, *Macromolecules*, 2000, **33**, 6693-6703.
59. J. M. Asua, E. D. Sudol and M. S. El-Aasser, *Journal of Polymer Science Part A: Polymer Chemistry,* 1989, **27**, 3903-3913.
60. J. M. Asua, *Macromolecules*, 2003, **36**, 6245-6251.
61. B. S. Hawkett, D. H. Napper and R. G. Gilbert, *Journal of the Chemical Society, Faraday Transactions 1: Physical Chemistry in Condensed Phases*, 1980, **76**, 1323-1343.
62. I. A. Penboss, R. G. Gilbert and D. H. Napper, *Journal of the Chemical Society, Faraday Transactions 1: Physical Chemistry in Condensed Phases*, 1986, **82**, 2247-2268.
63. J. M. Asua and J. C. De La Cal, 1991, **42**, 1869-1877.
64. L. L. de Arbina, M. J. Barandiaran, L. M. Gugliotta and J. Asuat, *Polymer*, 1996, **37**, 5907-5916.
65. M. Abdollahi, *Polymer Journal*, 2007, **39**, 802.
66. H. Baharvand, A. Rabiee and H. J. C. J. Jamshidi, 2013, **75**, 241-246.
67. R. M. Fitch and C. H. Tsai, *Polymer Colloids*, 1971, 73-102.
68. I. Kuehn and K. Tauer, *Macromolecules*, 1995, **28**, 8122-8128.
69. P. Nazaran and K. Tauer, *Macromolecular Symposia*, 2007, **259**, 264-273.
70. T. Tanrisever, O. Okay and I. Ç. Sönmezoğlu, *Journal of Applied Polymer Science*, 1996, **61**, 485-493.
71. F. K. Hansen, in *Polymer Latexes*, American Chemical Society, 1992, vol. 492, ch. 2, pp. 12-27.
72. A. R. Goodall, M. C. Wilkinson and J. Hearn, *Journal of Polymer Science: Polymer Chemistry Edition*, 1977, **15**, 2193-2218.
73. Z. Song and G. W. Poehlein, *Journal of Colloid and Interface Science*, 1989, **128**, 486-500.
74. G. Lichti, R. G. Gilbert and D. H. Napper, *Journal of Polymer Science: Polymer Chemistry Edition*, 1983, **21**, 269-291.
75. S. Beyaz, T. Tanrisever and H. Kockar, *Macromolecular Research*, 2010, **18**, 1154-1159.
76. G. W. Ceska, *Journal of Applied Polymer Science*, 1974, **18**, 427-437.
77. C. e. Yan, S. Cheng and L. Feng, *Journal of Polymer Science Part A: Polymer Chemistry*, 1999, **37**, 2649-2656.
78. D. I. Christie, R. G. Gilbert, J. P. Congalidis, J. R. Richards and J. H. McMinn, *Macromolecules*, 2001, **34**, 5158-5168.
79. *Polymer Dispersions and Their Industrial Applications*, 2002, DOI: 10.1002/3527600582.ch1, pp. 1-14.
80. H. Warson, *Polymer International,* 1996, **41**, 352-352.

81. J. L. Reimers and F. J. Schork, 1996, *Journal of Applied Polymer Science.*, **60**, 251-262.
82. D. Kukulj, T. P. Davis, K. G. Suddaby, D. M. Haddleton and R. G. Gilbert, *Journal of Polymer Science Part A: Polymer Chemistry,* 1997, **35**, 859-878.
83. K. G. Suddaby, D. M. Haddleton, J. J. Hastings, S. N. Richards and J. P. O'Donnell, *Macromolecules*, 1996, **29**, 8083-8091.
84. N. M. B. Smeets, J. P. A. Heuts, J. Meuldijk and A. M. van Herk, *Journal of Polymer Science Part A: Polymer Chemistry*, 2008, **46**, 5839-5849.
85. N. M. B. Smeets, T. G. T. Jansen, A. M. van Herk, J. Meuldijk and J. P. A. Heuts, *Polymer Chemistry*, 2011, **2**, 1830-1836.
86. N. M. B. Smeets, U. S. Meda, J. P. A. Heuts, J. T. F. Keurentjes, A. M. van Herk and J. Meuldijk, *Macromolecular Symposia*, 2007, **259**, 406-415.
87. J. P. A. Heuts and N. M. B. Smeets, *Polymer Chemistry*, 2011, **2**, 2407-2423.
88. T. P. Davis, D. Kukulj, D. M. Haddleton and D. R. Maloney, *Trends in Polymer Science*, 1995, **3**, 365-373.
89. J. P. A. Heuts, G. E. Roberts and J. D. Biasutti, *Australian Journal of Chemistry,* 2002, **55**, 381-398.
90. S. Slavin, K. McEwan and D. M. Haddleton, in *Polymer Science: A Comprehensive Reference*, eds. K. Matyjaszewski and M. Möller, Elsevier, Amsterdam, 2012, DOI: https://doi.org/10.1016/B978-0-444-53349-4.00068-6, pp. 249-275.
91. J. Jennings, G. He, S. M. Howdle and P. B. Zetterlund, *Chemical Society Reviews*, 2016, **45**, 5055-5084.
92. A. Anastasaki, C. Waldron, V. Nikolaou, P. Wilson, R. McHale, T. Smith and D. M. Haddleton, *Polymer Chemistry*, 2013, **4**, 4113-4119.
93. D. R. Maloney, K. H. Hunt, P. M. Lloyd, A. V. G. Muir, S. N. Richards, P. J. Derrick and D. M. Haddleton, *Journal of the Chemical Society, Chemical Communications*, 1995, DOI: 10.1039/C39950000561, 561-562.
94. J. S. Town, G. R. Jones, E. Hancox, A. Shegiwal and D. M. Haddleton, 2019, **0**, 1900088.
95. in *Progress in Inorganic Chemistry*, DOI: 10.1002/9780470166321.ch2, pp. 105-204.
96. A. Bakac, M. E. Brynildson and J. H. Espenson, *Inorganic Chemistry*, 1986, **25**, 4108-4114.
97. S. V. Kolesov, A. M. Steklova, M. Ge, G. Y. Zaikov and K. S. Minsker, *Polymer Science U.S.S.R.*, 1986, **28**, 2096-2103.
98. A. Gridnev, *Journal of Polymer Science Part A: Polymer Chemistry*, 2000, **38**, 1753-1766.
99. N. S. Enikolopyan, B. R. Smirnov, G. V. Ponomarev and I. M. Belgovskii, *J. Polym. Sci. Polym. Chem. Ed,* 1981, **19**, 879-889.
100. A. E. Childress and M. Elimelech, *Journal of Membrane Science*, 1996, **119**, 253-268.
101. B. R. Smirnov, V. D. Plotnikov, B. V. Ozerkovskii, V. P. Roshchupkin and N. S. Yenikolopyan, *Polymer Science U.S.S.R.*, 1981, **23**, 2807-2816.
102. B. Smirnov, I. Morozova, L. Pushchaeva, A. Marchenko and N. J. D. A. N. S. Enikolopian, 1980, **255**, 609-612.
103. B. R. Smirnov, A. P. Marchenko, G. V. Korolev, I. M. Bel'govskii and N. S. Yenikolopyan, *Polymer Science U.S.S.R.*, 1981, **23**, 1158-1168.
104. B. R. Smirnov, A. P. Marchenko, V. D. Plotnikov, A. I. Kuzayev and N. S. Yenikolopyan, *Polymer Science U.S.S.R.*, 1981, **23**, 1169-1178.
105. K. J. Abbey, D. L. Trumbo, G. M. Carlson, M. J. Masola and R. A. Zander, *Journal of Polymer Science Part A: Polymer Chemistry*, 1993, **31**, 3417-3424.
106. A. F. Burczyk, K. F. O'Driscoll and G. L. Rempel, *J. Polym. Sci. Polym. Chem. Ed.,* 1984, **22**, 3255-3262.
107. K. A. Lance, K. A. Goldsby and D. H. Busch, *Inorganic Chemistry*, 1990, **29**, 4537-4544.
108. A. A. Gridnev, *Polymer Science U.S.S.R.*, 1989, **31**, 2369-2376.

109. Erbe, M, Van Dyck-Erbe, R.L. & Schmitz, H.J., *J Mater Sci: Mater Med,* 1996, **7**, 517-522.
110. U. Ali, K. J. B. A. Karim and N. A. Buang, *Polymer Reviews*, 2015, **55**, 678-705.
111. A. Shegiwal, A. M. Wemyss, M. A. J. Schellekens, J. de Bont, J. Town, E. Liarou, G. Patias, C. J. Atkins and D. M. Haddleton, *Journal of Polymer Science Part A: Polymer Chemistry*, 2019, **57**, E1-E9.
112. A. A. Gridnev, S. D. Ittel, M. Fryd and B. B. Wayland, *Organometallics*, 1993, **12**, 4871-4880.
113. C. L. Moad, G. Moad, E. Rizzardo and S. H. Thang, *Macromolecules*, 1996, **29**, 7717-7726.
114. F. R. Mayo, *Journal of the American Chemical Society*, 1943, **65**, 2324-2329.
115. T. P. Davis, M. D. Zammit, J. P.A. Heuts and K. Moody, *Chemical Communications*, 1998, DOI: 10.1039/A807177B, 2383-2384.
116. J. P. A. Heuts, D. J. Forster and T. P. Davis, *Macromol. Rapid Commun.*, 1999, **20**, 299-302.
117. K. G. Suddaby, D. R. Maloney and D. M. Haddleton, *Macromolecules*, 1997, **30**, 702-713.
118. J. P. A. Heuts, T. P. Davis and G. T. Russell, *Macromolecules*, 1999, **32**, 6019-6030.
119. J. P. A. Heuts, D. J. Forster, T. P. Davis, B. Yamada, H. Yamazoe and M. Azukizawa, *Macromolecules*, 1999, **32**, 2511-2519.
120. J. Krstina, G. Moad, E. Rizzardo, C. L. Winzor, C. T. Berge and M. Fryd, *Macromolecules*, 1995, **28**, 5381-5385.
121. A. A. Gridnev, *Polymer Journal*, 1992, **24**, 613-623.
122. E. F. Mccord, W. L. Anton, L. Wilczek, S. D. Ittel, L. T. J. Nelson, K. D. Raffell, J. E. Hansen and C. Berge, *Macromol. Symp.,* 1994, **86**, 47-64.
123. D. M. Haddleton, E. Feeney, A. Buzy, C. B. Jasieczek and K. R. Jennings, *Chemical Communications*, 1996, **10**, 1157-1158.
124. J. S. Town, Y. Gao, E. Hancox, E. Liarou, A. Shegiwal, C. J. Atkins and D. Haddleton, *Rapid Commun Mass Spectrom*, 2020; 34(S2):e8654.
125. D. A. Morrison, T. P. Davis, J. P. A. Heuts, B. Messerle and A. A. Gridnev, *Polymer Science Part A: Polymer Chemistry*, 1996, **44**, 6171-6189.
126. Nurmi, L., Lindqvist, J., Randev, R., Syrett, J., and D. M. Haddleton, *Chemical Communications*, 2009, **19** ,2727-2729.
127. S. Slavin, E. Khoshdel and D. M. Haddleton, *Polymer Chemistry*, 2012, **3**, 1461-1466.
128. Q. Zhang, S. Slavin, M. W. Jones, A. J. Haddleton and D. M. Haddleton, *Polymer Chemistry*, 2012, **3**, 1016-1023.
129. K. A. McEwan, S. Slavin, E. Tunnah and D. M. Haddleton, *Polymer Chemistry*, 2013, **4**, 2608-2614.
130. Haddleton, D.M., Depaquis, E., Kelly, E.J., Kukulj, D., Morsley, S.R., Bon, S.A.F., Eason, M.D. and Steward, A.G., *Journal of Polymer Science Part A: Polymer Chemistry*, 2001, **39**, 2378-2384.
131. N. M. B. Smeets, *European Polymer Journal*, 2013, **49**, 2528-2544.
132. A. H. Soeriyadi, G.-Z. Li, S. Slavin, M. W. Jones, C. M. Amos, C. R. Becer, M. R. Whittaker, D. M. Haddleton, C. Boyer and T. P. Davis, *Polymer Chemistry*, 2011, **2**, 815-822.
133. K. A. McEwan and D. M. Haddleton, *Polymer Chemistry*, 2011, **2**, 1992-1999.
134. G.-Z. Li, R. K. Randev, A. H. Soeriyadi, G. Rees, C. Boyer, Z. Tong, T. P. Davis, C. R. Becer and D. M. Haddleton, *Polymer Chemistry*, 2010, **1**, 1196-1204.
135. D. M. Haddleton, D. R. Maloney, K. G. Suddaby Adam Clarke and S. N. Richards, *Polymer*, 1997, **38**, 6207-6217.
136. H. C. M. Byrd and C. N. McEwen, *Analytical Chemistry*, 2000, **72**, 4568-4576.

137. Pierik, S.C.J. and van Herk, *A.M, Macromol. Chem. Phys.*, 2003, **204**, 1406-1418.
138. G. Patias, A. M. Wemyss, S. Efstathiou, J. S. Town, C. J. Atkins, A. Shegiwal, R. Whitfield and D. M. Haddleton, *Polymer Chemistry*, 2019, **10**, 6447-6455.
139. C. J. Atkins, G. Patias, J. S. Town, A. M. Wemyss, A. M. Eissa, A. Shegiwal and D. M. Haddleton, *Polymer Chemistry*, 2019, **10**, 646-655.
140. P. Cacioli, D. G. Hawthorne, R. L. Laslett, E. Rizzardo and D. H. Solomon, *Journal of Macromolecular Science: Part A - Chemistry*, 1986, **23**, 839-852.
141. K. Adamsons, G. Blackman, B. Gregorovich, L. Lin and R. Matheson, *Progress in Organic Coatings*, 1998, **34**, 64-74.
142. A. Ravve, in *Principles of Polymer Chemistry*, Springer New York, New York, NY, 2012, DOI: 10.1007/978-1-4614-2212-9_2, pp. 17-67.
143. D. Fukuhara and D. Sundberg, *JCT Research*, 2005, **2**, 509-516.
144. Z. Guan, *Journal of the American Chemical Society*, 2002, **124**, 5616-5617.
145. Z. Guan, 2003, **41**, 3680-3692.
146. D. M. Haddleton, C. Topping, D. Kukulj and D. Irvine, *Polymer*, 1998, **39**, 3119-3128.
147. D. M. Haddleton, D. R. Maloney and K. G. Suddaby, *Macromolecules*, 1996, **29**, 481-483.
148. B. Yamada, S. Tagashira and S. Aoki, *Journal of Polymer Science Part A: Polymer Chemistry,* 1994, **32**, 2745-2754.
149. D. L. Trumbo, K. J. Abbey and G. M. Carlson, *J. Polym. Sci. C Polym. Lett.*, 1987, **25**, 229-232.
150. A. H. Soeriyadi, C. Boyer, J. Burns, C. R. Becer, M. R. Whittaker, D. M. Haddleton and T. P. Davis, *Chemical Communications*, 2010, **46**, 6338-6340.
151. C. Barthet, J. Wilson, A. Cadix, M. Destarac, C. Chassenieux and S. Harrisson, *ACS Macro Letters*, 2017, **6**, 1342-1346.
152. B. Wenn, A. C. Martens, Y. M. Chuang, J. Gruber and T. Junkers, *Polymer Chemistry*, 2016, **7**, 2720-2727.
153. G. Moad and D. H. Solomon, in *The Chemistry of Radical Polymerization (Second Edition)*, eds. G. Moad and D. H. Solomon, Elsevier Science Ltd, Amsterdam, 2005, DOI: https://doi.org/10.1016/B978-008044288-4/50028-5, pp. 451-585.
154. R. P. Quirk and B. Lee, 1992, **27**, 359-367.
155. M. K. Georges, R. P. N. Veregin, P. M. Kazmaier and G. K. Hamer, *Macromolecules*, 1993, **26**, 2987-2988.
156. C. J. Hawker, A. W. Bosman and E. Harth, *Chemical Reviews*, 2001, **101**, 3661-3688.
157. M. Kato, M. Kamigaito, M. Sawamoto and T. Higashimura, *Macromolecules*, 1995, **28**, 1721-1723.
158. J.-S. Wang and K. Matyjaszewski, *Journal of the American Chemical Society*, 1995, **117**, 5614-5615.
159. G. R. Jones, A. Anastasaki, R. Whitfield, N. Engelis, E. Liarou and D. M. Haddleton, 2018, **57**, 10468-10482.
160. C. Boyer, N. A. Corrigan, K. Jung, D. Nguyen, T.-K. Nguyen, N. N. M. Adnan, S. Oliver, S. Shanmugam and J. Yeow, *Chemical Reviews*, 2016, **116**, 1803-1949.
161. S. Perrier and P. Takolpuckdee, 2005, **43**, 5347-5393.
162. J. Chiefari, Y. K. Chong, F. Ercole, J. Krstina, J. Jeffery, T. P. T. Le, R. T. A. Mayadunne, G. F. Meijs, C. L. Moad, G. Moad, E. Rizzardo and S. H. Thang, *Macromolecules*, 1998, **31**, 5559-5562.
163. S. Perrier, *Macromolecules*, 2017, **50**, 7433-7447.
164. G. Moad, E. Rizzardo and S. H. Thang, *Chem. Asian J.*, 2013, **8**, 1634-1644.
165. G. Moad and E. Rizzardo, in *Nitroxide Mediated Polymerization: From Fundamentals to Applications in Materials Science*, The Royal Society of Chemistry, 2016, DOI: 10.1039/9781782622635-00001, pp. 1-44.

166. J. W. Ma, M. F. Cunningham, K. B. McAuley, B. Keoshkerian and M. Georges, *Chemical Engineering Science*, 2003, **58**, 1177-1190.
167. R. B. Grubbs, *Polymer Reviews*, 2011, **51**, 104-137.
168. E. G. Bagryanskaya and S. R. A. Marque, in *Nitroxide Mediated Polymerization: From Fundamentals to Applications in Materials Science*, The Royal Society of Chemistry, 2016, DOI: 10.1039/9781782622635-00045, pp. 45-113.
169. K. Matyjaszewski, *Macromolecules*, 2012, **45**, 4015-4039.
170. H. Fischer, *Chemical Reviews*, 2001, **101**, 3581-3610.
171. K. Matyjaszewski and J. Spanswick, in *Reference Module in Materials Science and Materials Engineering*, Elsevier, 2016, DOI: https://doi.org/10.1016/B978-0-12-803581-8.01354-0.
172. T. G. Ribelli, F. Lorandi, M. Fantin and K. Matyjaszewski, *Macromol. Rapid Commun.*, 2019, **40**, 1800616.
173. A. Kajiwara and K. Matyjaszewski, *Polymer Journal*, 1999, **31**, 70-75.
174. G. Moad, E. Rizzardo and S. H. Thang, *Accounts of Chemical Research*, 2008, **41**, 1133-1142.
175. H. Willcock and R. K. O'Reilly, *Polymer Chemistry*, 2010, **1**, 149-157.
176. C.-W. Chang, E. Bays, L. Tao, S. N. S. Alconcel and H. D. Maynard, *Chemical Communications*, 2009, DOI: 10.1039/B904456F, 3580-3582.
177. D. Pissuwan, C. Boyer, K. Gunasekaran, T. P. Davis and V. Bulmus, *Biomacromolecules*, 2010, **11**, 412-420.
178. C. Boyer, A. H. Soeriyadi, P. B. Zetterlund and M. R. Whittaker, *Macromolecules*, 2011, **44**, 8028-8033.
179. I. Schreur-Piet and J. P. A. Heuts, *Polymer Chemistry*, 2017, **8**, 6654-6664.
180. J. Zhou, H. Yao and J. Ma, *Polymer Chemistry*, 2018, **9**, 2532-2561.
181. A. Anastasaki, C. Waldron, P. Wilson, C. Boyer, P. B. Zetterlund, M. R. Whittaker and D. Haddleton, *ACS Macro Letters*, 2013, **2**, 896-900.
182. S. P. S. Koo, T. Junkers and C. Barner-Kowollik, *Macromolecules*, 2009, **42**, 62-69.
183. Y. Zhao, X. Liu, Y. Liu, Z. Wu, X. Zhao and X. Fu, *Chemical Communications*, 2016, **52**, 12092-12095.
184. L. Martin, G. Gody and S. Perrier, *Polymer Chemistry*, 2015, **6**, 4875-4886.
185. A. Shegiwal, A. M. Wemyss, E. Liarou, J. Town, G. Patias, C. J. Atkins, A. Marathianos, D. W. Lester, S. Efstathiou and D. M. Haddleton, *European Polymer Journal*, 2020, DOI: https://doi.org/10.1016/j.eurpolymj.2020.109491, 109491.
186. G. Nurumbetov, N. Engelis, J. Godfrey, R. Hand, A. Anastasaki, A. Simula, V. Nikolaou and D. M. Haddleton, *Polymer Chemistry*, 2017, **8**, 1084-1094.

Chapter 2

Optimising conditions for preparation of statistical carboxylated polymethacrylate co-oligomers using emulsion polymerisation

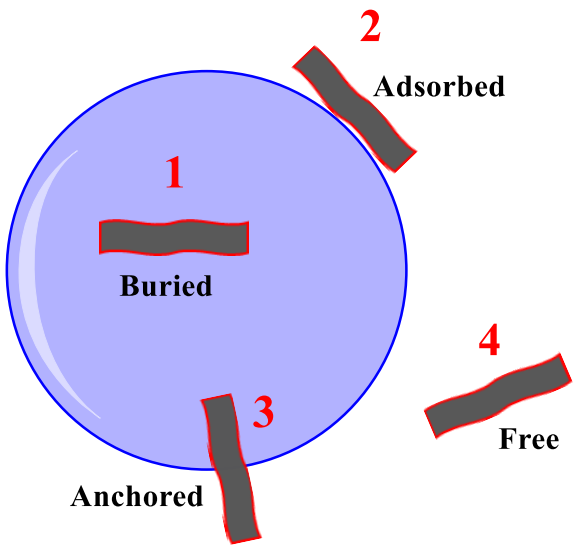

Possible locations of poly(methacrylic acid) in a latex

2.1 Introduction

Processes for controlling the physical properties of composite polymer systems and the morphology of latex particles are well established in industry.[1-4] Structural latex particles bearing carboxylic functional groups, either at their surface or internally, are used in paper coatings, textile coatings, impact modifiers, medical diagnostics and adhesives to various substrates.[1, 2, 5-7] Water-soluble carboxylic acid monomers such as fumaric acid (FA), itaconic acid (IA), acrylic acid (AA) and methacrylic acid (MAA), listed in order of increasing hydrophobicity, are widely used in emulsion polymerisation for the manufacture of carboxylated latexes. They are usually incorporated into the latex particle surface, and even in small quantities have been shown to improve colloidal stability, freeze-thaw stability, mechanical properties, and rheological and adhesive properties.[1-3, 6, 7]

Conventional emulsion polymerisation does not favour the addition of very hydrophilic monomers as they remain in the aqueous phase instead of entering the polymer particles. Therefore, in order to partially solve this problem we utilise carboxylic monomers with other more hydrophobic monomers to give statistical copolymers in various ratios with respect to carboxylic monomers to tune the polymers according to their application. A second method of partially solving the problem is by lowering the pH with carboxylic acids (i.e. more acidic), which takes the acids from the dissociated carboxylate ions state to the fully protonated acid, which in turn should make the acid less hydrophilic and partition into the hydrophobic monomer phase/ particle more readily. Furthermore, the tuning of the pH of the reaction mixture affects the location of the acid within the latex particle which will be exploited throughout this *chapter 2*.

The location of the carboxyl groups in polymer latex particles, and in the aqueous phase surrounding them, has been extensively studied.[1, 2, 4, 6, 7] It has been established that there are four possible positions that the acid can adopt within the latex (illustrated in *figure 2.1*):

1. The acid can be co-polymerised and buried within the polymer particles;

2. The acid can co-polymerise but reside in the outer shell of the particles (i.e. at the surface). However, this is dependent on the chain mobility (e.g. if the latex core is highly cross-linked it may not be possible to migrate to the surface);
3. The acid may be adsorbed onto the surface as a surface-active copolymer chain (*i.e. acting as a surfactant*);
4. The acid may not be associated with the particle, and remain free in the aqueous phase, either as homo-polymer or water-soluble copolymer chain[1, 2, 5-9]. In the latter, there remains the probability that the free chain enters and exits the particle depending on the surface activity.[1, 2, 7, 9]

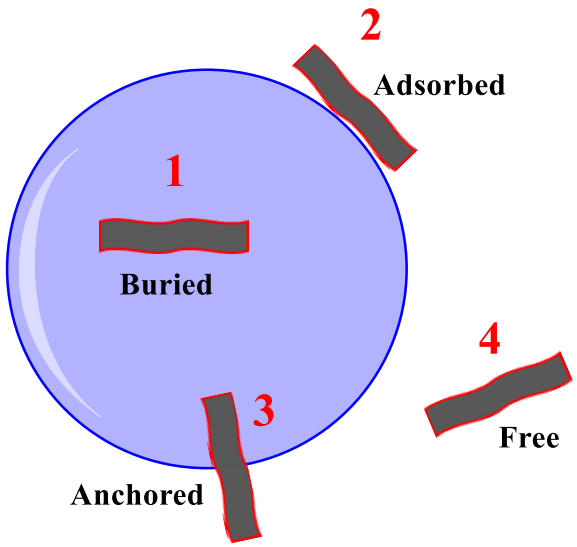

Figure 2.1: Possible locations of poly(methacrylic acid) in a latex

The location of the acid is important as it governs the structure of polymer molecule and, in turn, the stability of the latex molecule formed. The final distribution of the acid is determined by a number of factors, such as the reactivity ratio of the monomers, or the partitioning behaviour of the carboxylic acid over the pH range of the reaction mixtures.[2] The partitioning of the acidic monomers between the aqueous and particle phases during polymerisation has important implications for the final latex formed.

Carboxylic acid containing monomers are often highly soluble in water. Nevertheless, they will still partition to varying degrees into the organic phase, subject to their relative hydrophobicity[1, 2, 6, 10.] Monomers AA, IA, and FA are greatly partitioned to

the water phase even at pH levels below their pKa's, while MAA is more balanced between the two phases[1, 3, 7, 10].

The utilisation of AA tends to produce significant amounts of water-soluble polymer, and the amount of the acidic copolymer that is in the particles is usually situated near the outer surface of the latex particles.[1-3, 10] With MAA, there is significantly less water-soluble polymer formed, and the MAA copolymer in the particle is to some extent more evenly dispersed.[1, 2, 10] The differences between AA and MAA, and their pH behaviour, were reported in a study by *Dos Santos et al.*,[2, 10] where they compared the results of two copolymers in the formation of poly(styrene-co-*n*-butyl acrylate) latexes. It was reported that at pH 2.2 the interior portion of the particles contained 88% of the MAA, with the outer regions containing 10%, and the water phase containing only 2% of the MAA introduced.

Conversely, with AA an even distribution of the carboxyl groups were found among all three locations at pH 2.2. When the pH level of the reaction medium was adjusted to 4, the results of MAA remain very similar to those at that of pH 2.2, whereas for AA around 80% of the carboxyl group were located within the water phase and only 5% within the interior of the particles. When the pH of the reaction medium was further increased to 6, it was found that the partitioning of both MAA and AA to the water phase had significantly increased with practically no incorporation in the particles[2, 10].

For the purpose of our research, we have chosen to work with MAA at low pH's to ensure that the carboxylic acid functionality is predominately located within the particles. In this chapter we utilise CCTP which has been shown to be an effective way for forming low M_n macromonomers with methacrylates, with vinyl-end group functionality (i.e. ω-unsaturated end group). This technique was exploited in the statistical co-polymerisation of poly (MAA_n-*co*-MMA_m) in various ratio, to determine the chemical and mechanical stability of the latex with a large percentage of acid monomer.

The characterisation of emulsion polymerisation products, can be divided into two domains: one constituting of the particle and the other of the molecule. In turn this leads to separating the properties into two categories; the first consisting of features such as particle size, particle number, surface charge and zeta potential which corresponds to the mechanistic aspects of emulsion polymerisation process. These characterisations have significant effect on the final latex properties including colloidal stability, mechanical properties, latex viscosity and film formation being some examples.

Whereas the second group deals with the polymer molecule and is more concerned with chemical composition (monomer sequence and tacticity), molar mass distribution, glass transition temperature (T_g) and utilises an completely different selection of techniques to investigate those properties. Nevertheless, the two domains are interlinked and changes in one domain affects the counterpart domains, therefore usually studies in emulsion polymerisation either undertakes purely kinetic considerations or the synthetic. In this chapter we investigate both mechanism and properties, swell as covering both domains aforementioned.

2.2 Synthesis of bis[(difluoroboryl)dimethylglyoximato]cobalt(II), (COBF)

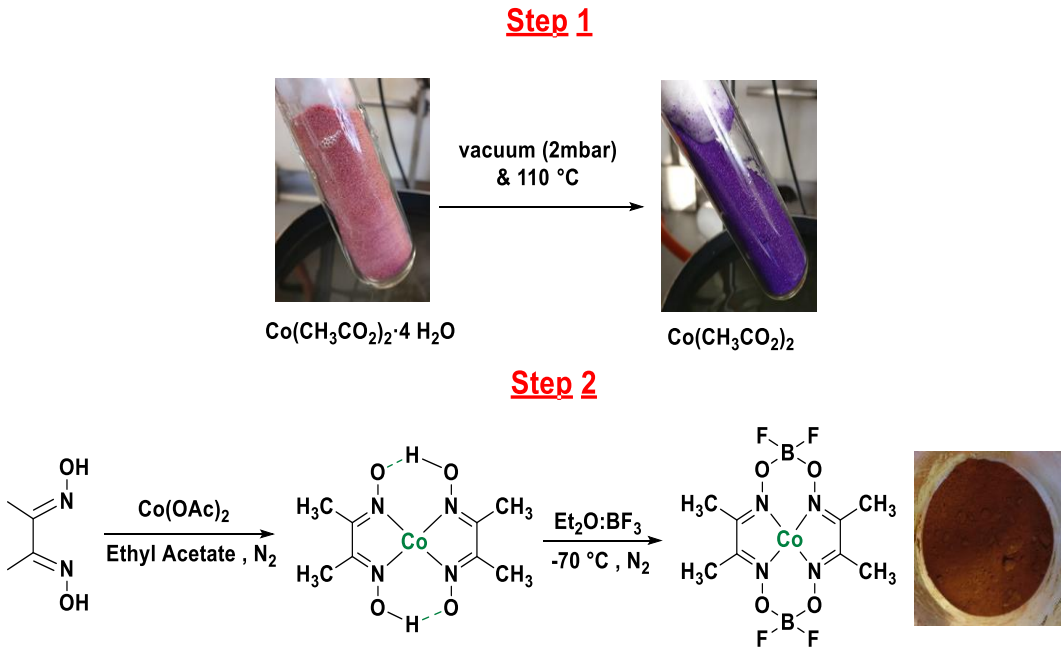

Scheme 2.1: Synthesis of bis[(difluoroboryl)dimethylglyoximato]cobalt(II), (CoBF)

Throughout these chapters, we will demonstrate the utilisation of bis[(difluoroboryl)dimethylglyoximato]cobalt(II) denoted CoBF, as CTA's under emulsion polymerisation conditions suited for methacrylic monomers. Nevertheless, it is quite trivial to substitute the methyl group at the equatorial position (R-group) of the cobaloximes (up to hexyl groups) in order to acquire catalyst suited for the hydrophobicity of the monomers and therefore ensuring the solubility of the catalyst within the monomer. In our system since, we are dealing with relatively hydrophilic monomers in the formation of statistical co-oligomers, CoBF is highly desired catalyst to utilise. By changing the equatorial ligands (R-groups) on the cobaloximes this would result in two possible effects in emulsion polymerisation:

1. It may affect the transfer activity of the catalyst either by steric or electronic effects.
2. Or it may affect the solubility of the catalyst in the aqueous and organic phases or both phases in the emulsion polymerisation process which in turn can affects the concentration of the catalyst at the locus of the polymerisation and hence the observed CTA.

As a rule of thumb, as the hydrophobicity of the equatorial ligand (R-group) increases on the cobaloximes catalysts or the hydrophilicity of the monomer increases the partition coefficient also increases. COBF, was synthesised by a modified published procedure;[11, 12] the macrocyclic ring that formed by having two dimethyl glyoxime molecules attached to a cobalt atom and the subsequent capping by BF_3.OEt, (*scheme 2.1).*

Table 2.1: Infrared stretching frequencies of CoBF

Type of bonds	Infrared stretching frequencies (cm^{-1})
O-H, non-bonded (wm)	3596
O-H, non-bonded (wm)	3527
Asym CH_3 (w)	2926
C=N	1618
B-O	1210
N-O	1165
N-O	1091
B-F	942
B-O	824
Co-N	501

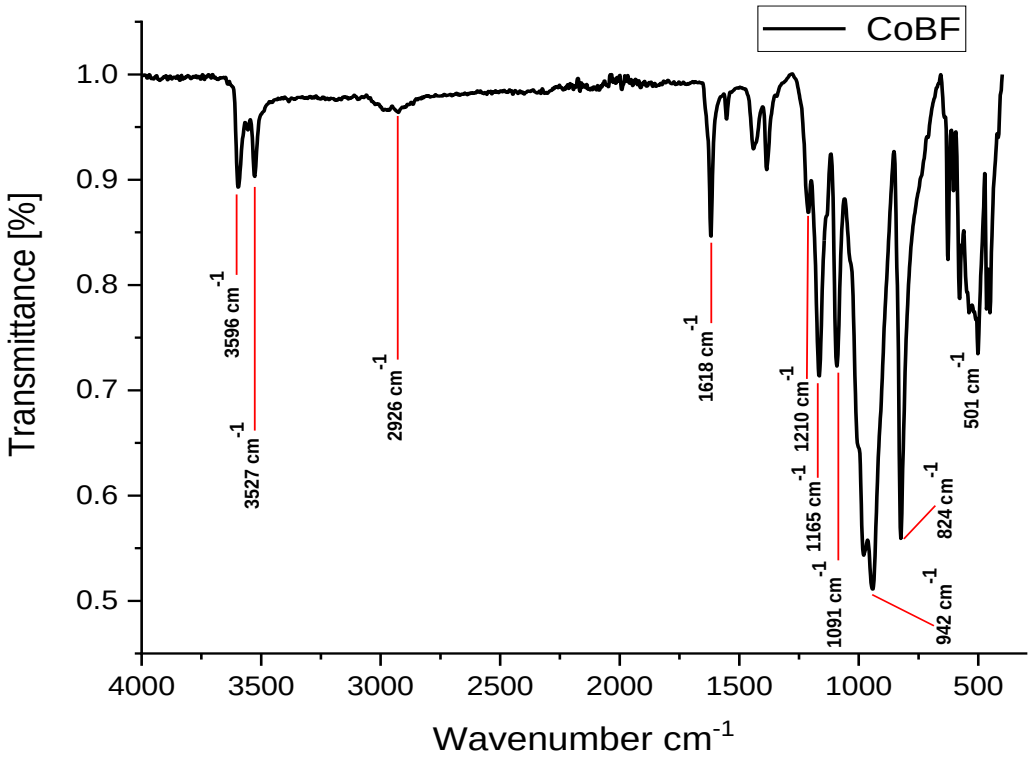

Figure 2.2: Infrared spectrum of CoBF

As the carbon chain length of the equatorial group increases, the C=N stretching frequency increases, whilst for the N-O stretching frequency no effect was observed according to the Haddleton group. The effects are highly probable to be due to the electron withdrawing nature of the C=O group on the ethyl acetate (i.e. which is utilised in the synthesis as the solvent and during recrystallization period), and its interaction with the cobalt atom and respective back donation and interaction with C=N and N-O groups.

Electrospray ionization technique (ESI) is a soft ionization; commonly utilised to determine the molecular weights of proteins, peptides, catalyst, synthetic and biological macromolecules. The technique offers the advantage of not fragmenting the macromolecules into smaller charged particles, rather it turns the macromolecule solution into small droplets. Those droplets in turn are further desolvated into smaller droplets resulting in molecules with attached protons as macromolecular ions. The desolvated protonated molecular ions are subsequently passed through a mass analyser to the detector and finally the mass of the sample can be determined.

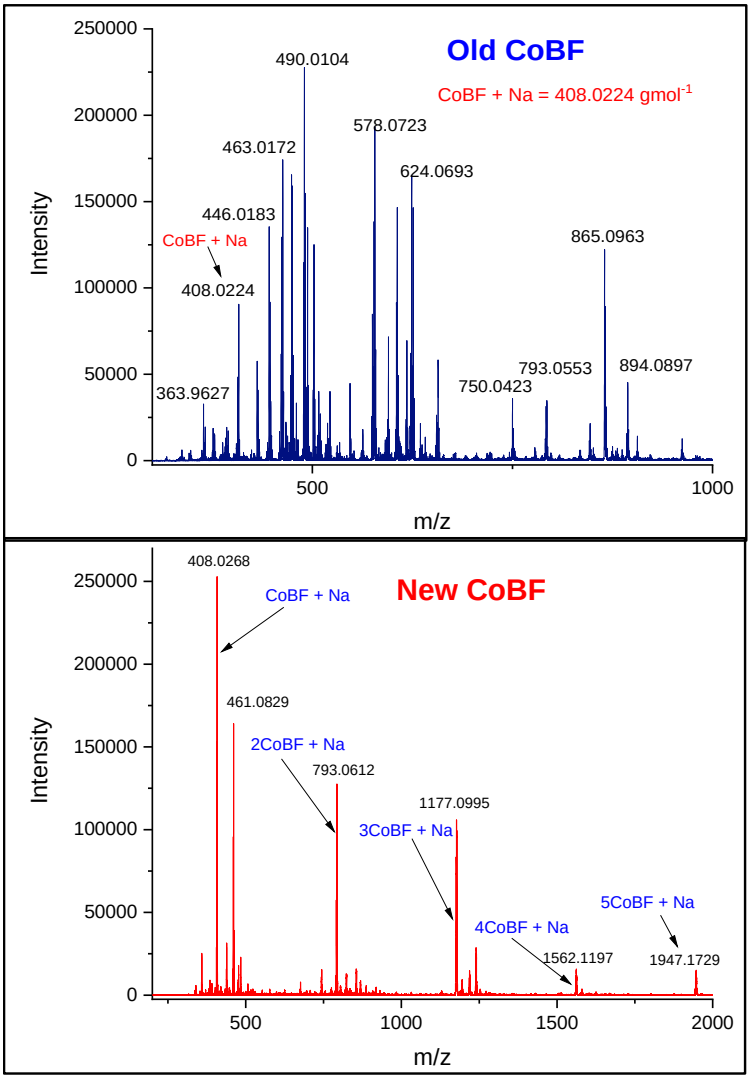

Figure 2.3: ESI of old CoBF top and new CoBF bottom

The theoretical molecular weight of the new batch of CoBF; was 384.75 gmol^{-1} + 22.98 gmol^{-1} = 407.73 gmol^{-1}.

Actual molecular weight of newly synthesised CoBF according to ESI: 408.026 gmol^{-1}

Actual molecular weight of old CoBF according to ESI: 408.022 gmol^{-1}

$$Percentage\ error = \left|\frac{((E+m(Na^+))-(T+m(Na^+)))}{(T+m(Na^+))}\right| \times 100 \quad (1)$$

Where $\boldsymbol{E}$ is the experimental CoBF value, $\boldsymbol{m(Na^+)}$ is the mass of a sodium ion and T is the theoretical CoBF value. The error for the new CoBF is: 0.0726 % (Da) and each subsequent major peak in the ESI are the multiples of CoBF with sodium ion

abduct which is a further indication that CoBF was successfully synthesized. Whereas, the error for the old CoBF is: 0.0716 % (Da), with significantly more peaks occurring on the spectra for the old CoBF compared to the new CoBF, suggesting slight contamination and possibly degradation of old CoBF (old CoBF is 17 years old), since from (*table 2.2 and figure 2.4*), higher amounts of the old CoBF (133 ppm) were required, compared to the new CoBF 113 ppm to obtain the same molecular weight (1600 g mol^{-1}), co-oligomer for the formation of poly($MAA_{15wt\%}$-*co*-$MMA85_{wt\%}$) according to SEC.

Both the new and old CoBF forms dimers, trimers, tetramers and pentamers of CoBF with sodium abduct, with the intensity of each peak decreasing with each additional addition of the CoBF molecule. This occurs due to the fact that the sample concentration in the solvent is very high and upon ionization the organometallic complex (*CoBF*) induces molecular stacking. The molecular stacking of CoBF, is more apparent with the new CoBF than the old CoBF as depicted from (*figure 2.3).*

Table 2.2: Old and New CoBF co-oligomer formation

CoBF / ppm	$M_{n,SEC}$ **/ g mol^{-1} (THF)**	M_w **/ gmol^{-1}**	$Đ$
114 (*New*)	1600	2700	1.65
133 (*Old*)	1600	2700	1.73

Furthermore, the SEC data also shows that not only less of the new CoBF were required to obtain low M_n statistical co-oligomers of poly($MAA_{15wt\%}$-*co*-$MMA8_{5wt\%}$) but all co-oligomers formed had monomodal Gaussian distribution compared to the old CoBF. Furthermore, the Đ of all the co-oligomers were in the range between 1.6-2.0, which is in the region expected for free radical reactions and if $Đ$ of greater than 2.0 were acquired. This would usually be attributed to many undesirable side reaction such termination and chain transfer which is commonly encountered in radical polymerisation but could be supressed by maintaining low radical concentration[13].

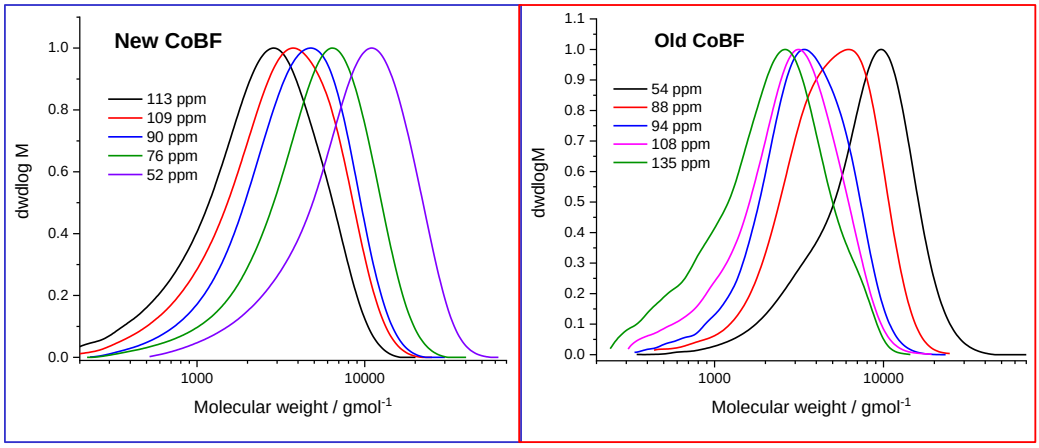

Figure 2.4: New CoBF (Right) and Old CoBF (Left) comparisons for the formation of co-oligomers pol(MAA$_m$-co-MMA$_n$) by CCTP

Finally, compared with the CCT of statistical co-oligomers of the old CoBF for the formation pol(MAA$_{15wt\%}$-*co*-MMA$_{85wt\%}$), the apparent chain transfer constant (C_S^E) increased from 592 ± 81 to 700 ± 87, when the new CoBF was utilised, reflecting the higher apparent chain transfer activity of new CoBF towards the co-oligomers which is related to its higher purity.

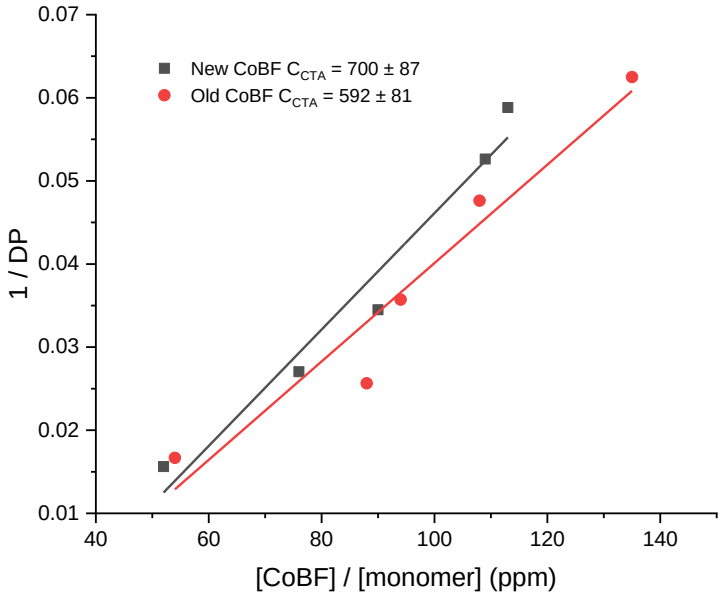

Figure 2.5: CTA constant between new and old CoBF for formation of pol(MAA$_m$-co-MMA$_n$)

Whereas, the apparent CTA constant C_S^E for the formation of poly(MMA) in bulk polymerisation for the new CoBF was 18400 ± 685. In solution polymerisation of toluene the C_S^E for poly(MMA) was 32000 ± 226, which is significantly higher than

bulk polymerisation as the solution of toluene is a good medium for the polymer chain to have good chain mobility, especially when the conversion of the reaction increases the intrinsic viscosity also increases (i.e. mayo plot the reaction is stopped at 10-15% conversion). In the presence of toluene heat can also be discharged more easily as polymerisations are an exothermic process (*table 2.3 & figure 2.6*). For GMA, the CTA constant C_S^E was 7700 ± 721, which is in line with the values obtained in literature[14, 15].

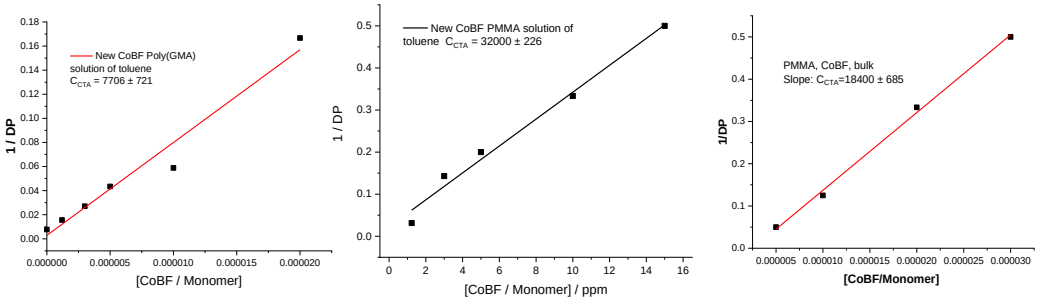

Figure 2.6: Mayo plot of the apparent CTA constant (C_S^E) of new CoBF catalyst in solution of toluene and bulk polymerisation for MMA and GMA monomers

Table 2.3: Apparent CTA constant (C_S^E) of new CoBF catalyst in solution of toluene and bulk polymerisation for MMA and GMA monomers

Catalyst	Monomer	Solvent	C_s
CoBF	MMA	Toluene	32000 ± 226
CoBF	MMA	Bulk	18400 ± 685
CoBF	GMA	Toluene	7700 ± 721

2.3 Synthesis of a range of statistical co-oligomer (35wt% MAA & 65wt% MMA→ 100wt %MMA)

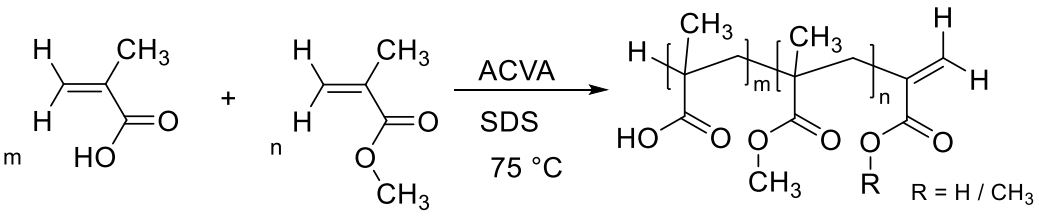

Scheme 2.2: Statistical polymerisation of co-oligomers pol(MAA_m-co-MMA_n) by CCTP

The formation of statistical co-oligomers of methacrylate's were carried out in a 500 ml double-jacketed reactor and purged with nitrogen. The CoBF catalyst was

dissolved in 112 mL of monomer (ratio of monomer were changed starting from 35 wt% MAA & 65 wt% MMA and leading to 100 wt% MMA by sequent reduction of MAA by 5wt% and subsequent increase in MMA by 5 wt%) and fed semi-continuously into 250 mL of water with poly(styrene) seed at 5.28 wt% with respect to total monomer over a period of 60 min (*scheme 2.1*). The initiator used was the water soluble 4,4' azobis (4-cyanovaleric acid) (ACVA) and the polymer particles were stabilised using an sodium dodecyl sulfate *(*SDS) as surfactant. The surfactant controls the latex particle size and provides colloidal stability. Adding more surfactant to a reaction mixture can improve stability, but adding significant amounts could nucleate additional, unwanted particles (secondary nucleation). The use of azo initiators is important since peroxides or redox systems are usually incompatible with catalytic chain transfer agents due to poisoning of the CoBF catalyst.

The feed strategy used was semi-continuous: in order to sustain control of the monomer concentration in the polymer particles, the polymerisation was performed under monomer-starved conditions. This means that the polymer particles are not saturated with monomer, but are being polymerised at an instantaneous conversion of 90% or greater. If the reaction was operating under flooded conditions, the control over the copolymer composition would be lost.

Furthermore, the incorporation of seed within these co-oligomers were in order to reduce the particle size and increase the shelve life of the polymer latex seeded reaction were undertaken, usually the smaller the particle size the longer the shelve life of the latex. Seed latexes are frequently used in preparing several batches of product with a strictly controlled, consistent particle diameter. During seeded emulsion polymerisations a common batch of seed latex particles are swollen with monomer until the swelling equilibrium is attained. The swelling process is followed by the monomer diffusion through the continuous phase from monomer droplets.

Since the monomer absorption rate of every seed particle from the aqueous phase is identical due to the uniformed size of the seed, this enables the seed swollen with monomer to be grown to a specified size with uniformed distribution of particles. Surfactants are added in order to stabile the growing particle surface, however as stated

before excessive surfactant to the reaction mixture must be avoided as it leads to secondary nucleation. Meanwhile, no new particles are formed during the polymerisation, the number of particles is set by the original number in the well characterised seed latex.

The seeds were prepared in a 500 mL double-jacketed reactor and purged with nitrogen. The monomer (styrene, 60 mL) was deoxygenated under nitrogen and fed semi-continuously into 240 mL of water over the period of 90 mins. The initiator used was 4,4' azobis (4-cyanovaleric acid) (ACVA) and the polymer particles stabilised using 8.25 wt% of sodium dodecyl sulfate (SDS) as surfactant. The seed (5.28 wt %) was utilised and the next subsequent step of forming the co-oligomers. The particle size of the seed utilised was 36 nm, molecular weight M_n = 33600, polydispersity $Đ$ = 2.4.

Table 2.4: SEC data for co-oligomers with various concentrations of MAA to MMA

Reaction	$M_{n,SEC}$ / gmol^{-1} (DMF)	M_w / g mol^{-1}	$Đ$	pH	Z-average/ (d.nm)	PDi
S1-seed	33600	80600	2.4		36	0.225
S2-35wt%MAA-65wt%MMA	18100	30200	1.67	3.12	182	0.104
S3-30wt%MAA-70wt%MMA	17100	30700	1.80	3.17	164	0.091
S4-25wt%MAA-85wt%MMA	17300	30300	1.75	3.12	144	0.096
S5-20wt%MAA-80wt%MMA	14500	23500	1.62	3.17	146	0.104
S6-15wt%MAA-85wt%MMA	12400	29200	2.35	3.06	129	0.089
S7-10wt%MAA-90wt%MMA	11100	25600	2.31	3.05	122	0.112
S8-5wt%MAA-95wt%MMA	10300	24800	2.43	2.95	118	0.109
S9-100wt%MMA	10300	26500	2.58	3.17	109	0.116

Facile synthesis of co-oligomers using CCT in emulsion polymerisation showed that methacrylate monomers underwent very efficient chain transfer with CoBF catalyst. Extremely small amounts of the CoBF (24 ppm for all reactions in *table 2.4*) were

added to a polymerisation to achieve large reductions in molecular weight due to the catalytic nature of the transfer process. However, there is a general decrease in M_n (i.e. reaction S2-S9) according to GPC, the reduction in M_n is generally more significant from reaction S2-S7 and less significant from S7-S9, as the acid concentration decreases the M_n of the co-oligomers decrease. This could be attributed to a few factors; firstly, even though CoBF is stable at elevated temperatures and pH, the combination of MAA and ACVA (making the pH of the system extremely acidic) and the factor of high temperature could destroy the catalyst, which in turn results in less catalyst available to act as CTA, in order to reduce the M_n of the polymers.

Another factor to consider is that at higher MAA concentration reaction S2 (which is hydrophilic) as opposed to MMA, the partitioning of the catalyst towards the relatively hydrophilic monomer will not be favoured. Therefore, as the concentration of the acid decreases reaction S2-S9, we get a general reduction in M_n, due to the system becoming more hydrophobic and since CoBF is relatively hydrophobic, the catalyst would favour partitioning towards the hydrophobic monomer/ particles.

Furthermore, the more hydrophilic co-oligomer in essence would have higher critical chain length, in order for it to enter the particle, whereas the co-oligomers with higher concentration of MMA as opposed MAA in them, will have lower critical chain compared to the other co-oligomers. Therefore, at a given time, higher concentration of catalyst and monomers would be present in the particles for the co-oligomers that are relatively hydrophobic resulting in lower M_n, *table 2.4*.

Table 2.5: DMA data for co-oligomers with various concentrations of MAA to MMA

Reaction	Onset T_g / °C	Mid T_g / °C	End T_g / °C	Tan delta /°C
S2-35wt%MAA-65wt%MMA	172	177	190	187
S3-30wt%MAA-70wt%MMA	164	176	183	176
S4-25wt%MAA-85wt%MMA	165	169	175	175
S5-20wt%MAA-80wt%MMA	152	158	167	162
S6-15wt%MAA-85wt%MMA	140	142	145	142
S7-10wt%MAA-90wt%MMA	126	132	139	140
S8-5wt%MAA-95wt%MMA	118	124	131	136
S9-100wt%MMA	113	124	130	127

The final factor to be considered is the glass transition temperature T_g obtained via Dynamic Mechanical Analysis (DMA) testing, which in turn affects the chain mobility of these polymers. The T_g is defined as the point at which amorphous polymer (or in amorphous regions within semi-crystalline materials) upon heating undergoes structural change from a hard brittle state to a soft rubbery or viscous liquid state.

Furthermore, the T_g is also defined as a temperature at which amorphous polymer takes on characteristic glassy-state properties like brittleness, stiffness and rigidity (upon cooling), a process defined as vitrification. It is important to note that amorphous polymers only exhibits a T_g and crystalline polymers exhibits a T_m (melt temperature), whereas if a polymer is semi-crystalline it will acquire regions of amorphous portion which in turn results in acquiring a T_g.

There are many factors that are listed below that determine polymers T_g:

1. Molecular weights: in a linear homopolymer chain, an increase in molecular weight results in a decrease in chain end concentration, which in turn results in decrease in free volume at the end region, resulting in an increase in T_g.
2. Molecular structure: the presence of bulky, inflexible side group decreases chain mobility which results in an increases in T_g of polymeric materials.
3. Chemical cross linking: increasing cross- linkers' results in decease in chain mobility which decreases free volume and which also increases the T_g of the polymeric materials.

4. Polar groups: the insertion of polar group increases the intermolecular forces between polymeric chains and the inter chain interaction and cohesion leads to decrease in free volume which increases the T_g.

The determination of T_g is fundamental to understating material's properties since the T_g is very sensitive to chemical and physical structure of the polymers, and therefore is used as a tool to characterize materials. There are three common techniques for measuring T_g:

1. Differential Scanning Calorimetry (DSC) – which is the most conventional and commonly used technique for most polymeric materials. DSC uses a heat flow technique where a small sample is heated while measuring the amount energy required to the test sample compared to the inert reference material. This in turn forms an inflection curve, since the T_g creates changes in properties of materials, the polymeric chain reorient, needing a change in energy to heat. Three points most commonly selected and reported points on the inflection curve are: the onset, which is the lowest value, the mid-point and end point[16, 17].

2. Thermal Mechanical analysis (TMA) – TMA uses a mechanical approach for measuring T_g by characteristically using to measure the Coefficient of Thermal Expansion (CTE) of polymeric materials. A small sample is heated on a quartz stage with a sensitive probe measuring the expansion of the test sample upon heating. This creates an expansion curve, where a CTE can be calculated over a range of temperature. When a material undergoes a T_g during a TMA test there is as significant change within the curve and the onset method can be utilised to calculate its T_g.

   There is also another method to obtain T_g via TMA, called the penetration probe technique in which a known amount of force is placed on a test sample using a penetration probe. Upon heating up the sample, the probe slowly starts to penetrate the test sample and at the point which the probe penetrates into the sample a certain distance is regarded as the “softening point”. The T_g again is

calculated, when a significant change is observed on the curve shape and is an indication that the test sample can no longer support the probe[17, 18].

3. Dynamic Mechanical Analysis (DMA) – DMA is most likely the most sensitive technique of the aforementioned methods above for measuring T_g. DMA measures the response of a material to an applied oscillatory strain (or stress), and how that response varies with temperature, frequency, or a combination of the two. DMA has the capacity to measure elastic and viscous components of polymers separately. DMA versatility allows us to measure behaviours such as elastics modulus, shear modulus, mechanical damping and viscoelastic behaviours.

   Compared to DSC, DMA is regarded as a highly sensitive technique and can be 10 to 100 times more sensitive to the changes occurring at the T_g compared to DSC. DMA can recognize small transitional regions that are beyond the resolution of DSC. DMA is very useful technique for analysing challenging polymers such as epoxies, polymers with T_g's well below ambient temperature and highly cross-linked polymers[17, 19, 20].

For our co-oligomers it was challenging to acquire reliable results with DSC and as result DMA was utilised due to its higher sensitivity (10 to 100 times more sensitive to the changes occurring at the T_g compared to DSC), which showed promising results. Nevertheless DSC requires significantly less sample 15 mg compared to DMA, which requires 1800 mg (i.e. DMA requires 120 times more sample in comparison to DSC for reliable measurements).

The homopolymer of poly(MAA) has a T_g = 228 °C and the homopolymer of poly(MMA) is 105 °C, by tuning the ratio of MAA to MMA composition, we notice from *table 2.5*, that as we increase the concentration of acid in the copolymer the T_g of the polymers increases, at higher T_g the chain mobility of the polymers and the catalyst are hindered and therefore, there is insufficient amount of catalyst available to reduce the M_n of the co-oligomers. Therefore, we can compensate for these problem by using slightly higher concentration of the catalyst with respect to the monomers or plasticizers, when compared to conventional monomers used in CCTP. In

conventional CCTP monomers, the co-polymer usually has T_g below the reaction temperature and therefore the chain mobility is not hindered (discussed *in chapter 3*).

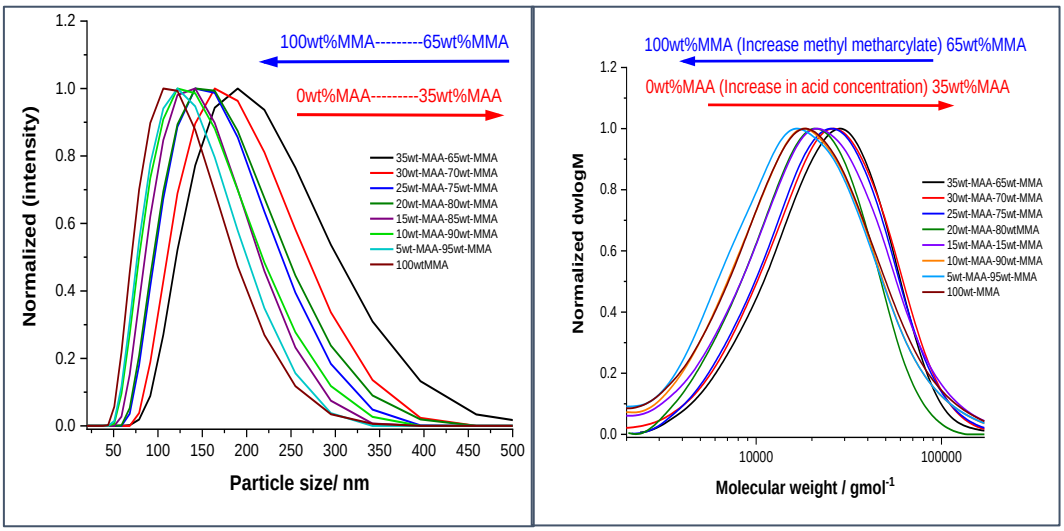

Figure 2.7: SEC and DLS data for data for co-oligomers with various concentrations of MAA to MMA

In addition increasing the acid concentration of the co-oligomers resulted in an increase in particle size, according to DLS (*table 2.4 and figure 2.7*), without the use of seed, increasing the acid resulted in phase separation ascribed to the particles becoming very hydrophilic and in turn causing water to enter the particles over time giving rise to latex destabilisation, whereas when $MAA_{15\%}$-*co*-$MMA_{85\%}$ was used particle sizes <310 nm were obtained giving stable latex's with long shelf life (stable after 15 months). Whereas, the polymers synthesised (*table 2.4*), had polystyrene seed present to reduce particle size and increase shelf life of the polymer, even the co-oligomer with highest composition of acid ($MAA_{35\%}$-$MMA_{65\%}$) was still stable after 21 months and the particle size for all the co-oligomers were below <190 nm.

Table 2.6: End properties of poly(MAA-co-MMA) emulsion co-oligomer B1 is reaction with the seed and C4 reaction without the seed

Reaction	CoBF / ppm	M_n, SEC / g mol^{-1} (THF)	M_w / g mol^{-1}	Đ	*Z-average* / (d.nm)	PDi	pH
B1	108	2000	3400	1.70	179	0.091	2.45
C4	108	2100	3300	1.58	396	0.087	2.56

Table 2.5, shows that at the same concentration of catalyst (108 ppm), with incorporation of seed reaction B1, the particle size decreases significantly from reaction C4, from 396 nm to 179 nm. The molecular weight of the polymers are similar

and the *Đ*, is in the range expected for free radical reaction. The pH remained below 3, swell indicating that must of the acid is incorporated within the particles.

Moreover, as the M_n of the polymers increases, generally the T_g increases, *table 2.4*, we can see that as we decrease the concentration of MAA from reaction S2, M_n = *18100* (35 wt% MAA-65 wt% MMA) all the way down to S9, M_n = *10300* (100 wt% MMA) in 5 wt% MAA sequence and increase in 5 wt% MMA. There is a general decrease in M_n of the polymers which could result in reduction in T_g. Therefore, a combination of higher M_n and higher T_g of MAA in the co-polymer composition causes a general increase in T_g as the MAA concentration increases.

Furthermore, the co-oligomers with very high concentration of acid reaction S2 (35 wt% MAA and 65 wt% MMA), had a small amount of observed coagulation (5-8 wt %) with respect to the total monomer. As the concentration of the acid decreased in the co-oligomers the coagulation decreased, with reaction S5 (20 wt% MAA and 80 wt% MMA) having approximately (1 wt% with respect to the total monomer), and reaction S6-S9 had no observed coagulation. All of the reactions formed a very stable latex with no phase separation occurring, even after 2 years.

The conversion for these co-oligomers were greater than >98% by ^{1}H NMR. The presence of the ω-end group vinyl protons was confirmed by both ^{1}H NMR and MALDI-ToF-MS (*figures 2.8 & 3.3*), the latter showing a major statistical co-oligomer peak distribution identified as poly(MAA_n-co-MMA_m) chains with a proton at the α-chain end, thus confirming that initiation via H-transfer from Co(III) complex is the dominant mode of initiation, as suggested by the mechanism of CCTP.

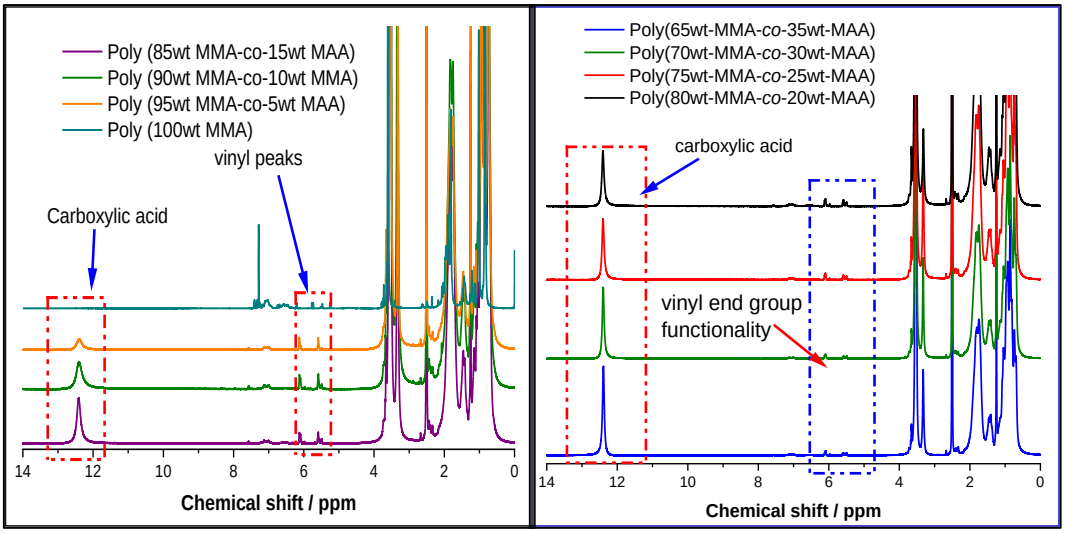

Figure 2.8: NMR of carboxylated latexes with various composition of MMA with respect to MAA.

For all of the reactions the singlet (broad) acid proton peak at 12.40 ppm, and the singlet vinyl protons at 6.10 ppm and 5.56 ppm were present. These peaks are the most crucial peaks since they determine the polymers post-polymerisation / functionalisation. However, as the acid concentration increased the intensity of the singlet (broad) acid proton peak at 12.40 ppm increased with respect to the integral.

Furthermore, as the molecular weight of the polymers increased (due to increase in the acid concentration of the co-oligomers) the vinyl end group functionality becomes less predominant (as since on *figure 2.8*). Furthermore, for a typical co-oligomer of poly (MAA_n-*co*-MMA_m), the NMR assignment peaks are as follows:

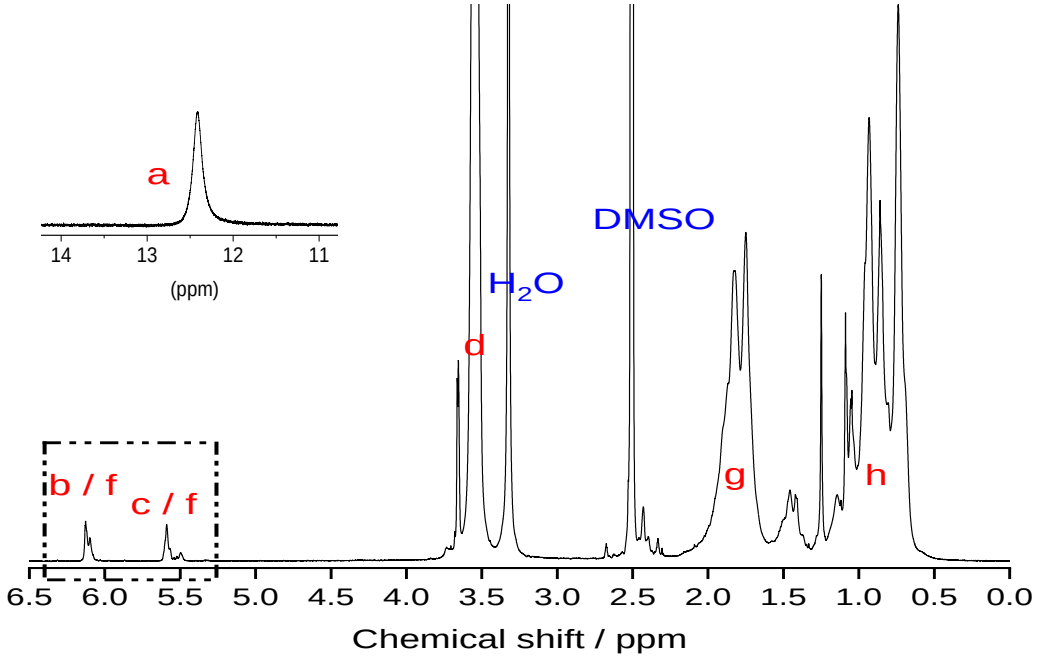

Figure 2.9: ^{1}H NMR spectrum of co-oligomer (reaction C4) with 15 wt% MAA & 85 wt% MMA by composition

Table 2.7: Assignments of peaks for NMR spectrum in figure 5

Peak / (ppm)	Integral	Multiplet type	Assignment
12.40	4.22	Broad singlet	Acid proton [a]
6.12-6.09	1.00	Singlet	Vinyl protons [b] and [e]
5.58-5.49	1.00	Singlet	Vinyl protons [c] and [f]
3.55	64.75	Singlet	Methoxy proton [d]
3.32	16.68	Singlet	Residual water protons
2.50	32.36	Quintet	DMSO (solvent) protons
2.5-0.5	42.48	Broad multiplet	In chain methylene and methyl protons [g] and [h]

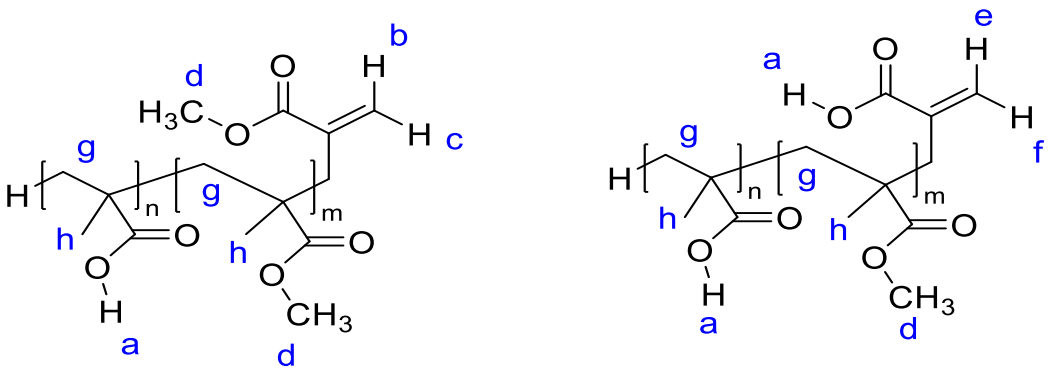

Figure 2.10: Structure of co-oligomer of Poly(MMA-co-MAA) (15 wt% MAA & 85 wt% MMA by composition) with protons labelled for NMR analysis

In addition, titration experiments were carried out with the co-oligomers, with all the latex's diluted with deionised water (pH of deionised water 5.99) so that the average solid content were all 10 wt % prior to the start of the titration. This raised the pH's of the co-oligomers slightly by around ~ 3.0 (more alkaline) for each latex. Subsequently once the pH of the latex had stabilised, ammonium hydroxide (25 % NH_4OH (aq)), was added dropwise until the solution went from white latex to colourless (i.e. transparent). The average of each co-oligomer was taken three times; reaction S2-S4, the amount of NH_4OH (aq) with respect to the acid (MAA) added to the co-oligomer was around ~ 0.5 mol dm^{-3}.

Whereas, for reaction S5 with composition 20 wt% MAA-80 wt% MMA, the concentration of NH_4OH (aq) with respect to the acid (MAA) had increased 0.68 $moldm^{-3}$ and reaction S6 with composition 15 wt % MAA-85 wt% MMA, further increased to 0.96 $moldm^{-3}$ and with reaction S7 with 10 wt% MAA-90 wt% MMA requiring the highest concentration of NH_4OH (aq) 3.61 $moldm^{-3}$ with respect to MAA. Whereas, the co-oligomers with composition below 10 wt% MAA did not dissolve in NH_4OH (aq) as demonstrated in *table 2.8*. Furthermore, from the ^1H NMR in *figure 2.11*, we can see that upon addition of NH_4OH (aq) to the co-oligomers, the vinyl peaks still remain but the carboxylic acid peak at 12.40 ppm disappears for the sample with added NH_4OH (aq).

Table 2.8: Titration of the co-oligomers (carboxylated latexes) with NH_4OH(aq)

Reaction	pH	Initial pH Diluted (10 wt. %)	Final pH	NH_4OH equivalence COOH
S2-35 wt% MAA-65 wt% MMA	3.12	3.32	6.89	0.48
S3-30 wt% MAA-70 wt% MMA	3.17	3.43	8.06	0.49
S4-25 wt% MAA-85 wt% MMA	3.12	3.44	7.37	0.51
S5-20 wt% MAA-80 wt% MMA	3.17	3.38	7.72	0.66
S6-15 wt% MAA-85 wt% MMA	3.06	3.26	9.29	0.96
S7-10 wt% MAA-90 wt% MMA	3.05	3.4	10.88	3.61
S8-5 wt%MAA-95 wt% MMA	2.95	3.35	-	-
S9-100 wt% MMA	3.17	3.41	-	-

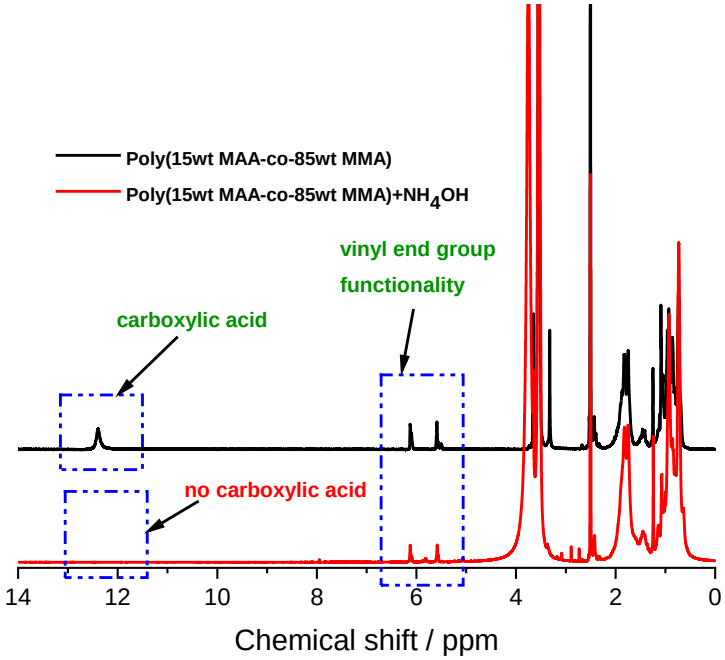

Figure 2.11: ^1H of NMR of poly($MAA_{15wt\%}$ -co-$MMA_{85wt\%}$) prior to and after addition NH_4OH

2.4 Zeta potential analysis of poly (MAA_m-*co*-MMA_n) with different amounts of methacrylic acid

It has been proposed that the addition of carboxylic acids monomer to co-polymers affects the charge on the particle, and hence will affect the particles colloidal stability. Since, the particle size of the co-oligomers were seen to generally decrease with decrease in concentration of MAA (5 wt% MMA decrease for each subsequent reaction) and increase in MMA (5 wt% MMA increase) as shown in (*table 2.4*). There are many well established techniques at determining the surface charge of a nanoparticle in solution.

One such commonly utilised technique is zeta-potential measurements, in which the nanoparticles are known to have surface charge which attracts a thin layer of counter ions to the particle surface known as the stern layer [21-24]. This double layer of ions travels with the nanoparticle as it diffuses throughout the solution. The electric potential at the boundary of the double layer is known as the zeta potential of the particles (depicted in *figure 2.12*) and has values that typically range from +100 to -100 mV[21-24]. The value of zeta potential is indicative of the colloidal stability of the particles.

Therefore, as a rule of thumb if the zeta potential value is greater than +30 mV or less - 30 mV, the particles will have high degrees of stability and subsequently will lead to particles acquiring monodispersity[21-24]. Whereas, with dispersion that have zeta potential less than +25 mV or greater than -25 mV zeta potential value will eventually form agglomerate as a result of interparticle interactions, including van der Waals and hydrophobic interactions, and hydrogen bonding[21-24]. In these cases, it is advisable to add more surfactants to the system in order to increase colloidal stability by providing more electrostatic interactions[21-24]. Lastly zeta potential is not just affected by the properties of nanoparticles, but also the conditions of the solution, such as pH and ionic strength[24].

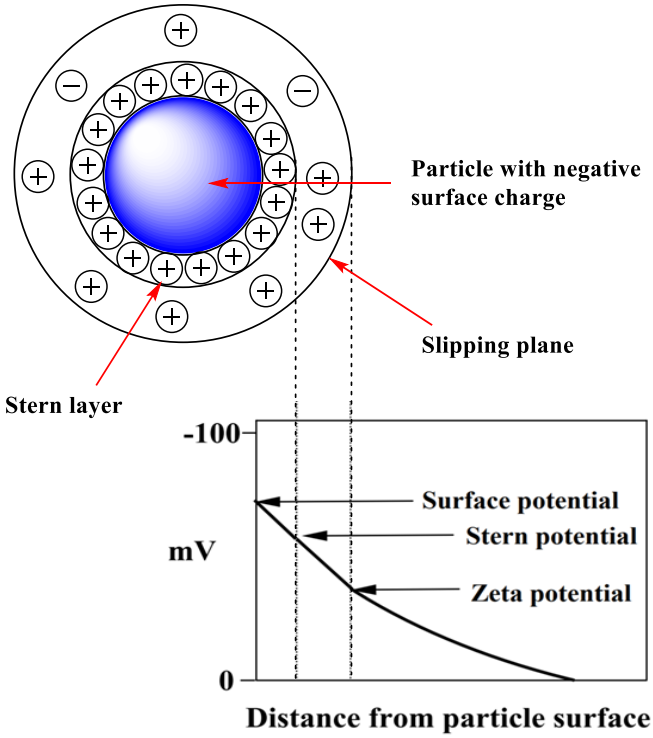

Figure 2.12: Pictorial representation of the double layer of a charged latex particle

The samples for zeta potential were prepared by diluting the co-oligomers to 10wt% solid content and then subsequently using 4µl of the latex in 2ml of filtered deionised water. The particle as stated before is charged and upon application of an electric field, the particle will begin to move. The measurement of the velocity of charged particles relative to the liquid it is suspended in under the influence of an applied electric field (electrophoresis) can be utilised to determine the zeta potential. This is acquired from the velocity of a particle in a unit electric field, which is commonly referred to as the electrophoretic mobility.

Table 2.9: Zeta potential of co-oligomers

Reaction	Zeta potential / mV	Standard deviation / mV	Electrophoretic mobility (µm/s.cm/V)
S2-35 wt%MAA-65wt%MMA	-44.1	5.2	-.3.44
S3-30 wt% MAA-70 wt% MMA	-44.4	3.7	-3.46
S4-25 wt% MAA-85 wt% MMA	-42.8	3.3	-3.33
S5-20 wt% MAA-80 wt% MMA	-42.2	4.5	-3.29
S6-15 wt% MAA-85 wt% MMA	-39.6	5.0	-3.09
S7-10 wt% MAA-90 wt% MMA	-35.6	4.2	-2.77
S8-5 wt% MAA-95 wt% MMA	-35.1	2.9	-2.74
S9-100 wt% MMA	-24.5	2.6	-1.91

From *table 2.9*, we observe that decreasing the acid concentration from reaction S2-S8, we see a general decrease in zeta potential and with reaction S9 with no MAA (homopolymer of poly (MMA)), the co-oligomers have the lowest zeta potential. Since, the zeta potential for the co-oligomers S7-S8 are above are above -35 eV the particles are relatively stable. Whereas, the co-oligomers reaction S2-S7, with zeta potential of equal to and greater the -40 eV, are incredibly stable, as the acid concentration of the particles increase the zeta potential generally increases, which in turn results in more stable latex particles.

Furthermore, the electrophoretic mobility of the particles increases with increase in acid concentration S2-S8, whereas the reaction without any acid (i.e. homopolymer of poly (MMA)) has significantly lower electrophoretic mobility compared to the reactions with acids incorporated within the co-oligomers. The pH of these acids are around ~3, due to the utilisation of ACVA initiator, this has been stated before, ensures that the acids are incorporated within particle. Therefore, the pH with respect to the zeta potential is controlled.

2.5 Different feeding rate for co-oligomer with composition poly ($MAA_{15wt\%}$-*co*-$MMA_{85wt\%}$)

The co-oligomer with composition poly ($MAA_{15wt\%}$-*co*-$MMA_{85wt\%}$), was selected with 133 ppm of CoBF for all the different feed rates, 5.28 wt% of polystyrene seed with respect to the total monomer was utilised, to ensure optimum feeding conditions in order to obtain co-oligomers with desired properties for utilisation as CTA's, in the formation of block copolymers and pseudo tri-block copolymers which will be exploited in (*chapter 3).*

Table 2.10: Different feed rates of the co-oligomers with acid composition poly(MAA 15 wt%-co-MMA 85 wt%)

Reaction	$M_{n,SEC}$ / gmol^{-1} (THF)	M_w / g mol^{-1}	*Đ*	*Z-average* / (d.nm)	PDi
F1-30 min	1100	2400	2.15	218	0.217
F2-60 min	1500	3500	2.41	201	0.107
F3-90 min	3200	4900	1.52	164	0.091
F4-120 min	1200	5400	4.52	136	0.104

From the SEC data *table 2.10,* the M_n shows a general increase from F1-F3 and then a sudden decrease for reaction F4, whereas the M_w, on other hand shows a general increase from reaction F1-F4, which in turn results in reaction F4 having significantly higher *Đ*, then the other reactions (F1-F3). This could be postulated to a few factors such as T_g of the polymers, the number of CTA present at given time and partitioning of the catalyst.

Feeding the polymers fast causes the T_g of the polymers to become lower in essence forming soft polymers, likewise feeding the polymers fast causes the T_g to increase which in turn could form hard polymers. The reactions with fast feed times have smaller M_w, since at any given time fasts reactions have greater concentration of CTA's (CoBF), at a given time which in turn causes the formation of smaller M_w co-oligomers. Furthermore, for the fast reactions F1, since the polymer particles that have formed can be considered soft with respect to reaction F4 (slow feed rate).

The chain mobility of polymers for the fast feed rate are higher for reaction F1 and the CTA's can move into particles more readily, whereas for the slow feed reaction (F4) the contrary is observed.

In addition, since the T_g of homopolymer of poly(MAA) = 228 °C and poly(MMA) = 105 °C. The co-oligomer with 15 wt% MAA-85 wt% MMA composition should have T_g of approximately 124 °C, for free radical polymerisation, which is higher than the reaction temperature which is around 76 °C. Feeding in the polymers at fast rate (i.e. reaction F1 -30 min), causes the particles to be flooded with monomer and the copolymer composition can be lost as suggested by DLS PDi. In addition, a general trend is observed with the particles size as the feed rate decreases the particle size of the polymers decreases F1-F4, which is also indicative of MWt since the MWt increases with increase in feed rate.

Finally, it is expected if the feed rate is fast at a given time there will be more CoBF present, in the reaction mixture with the monomer and since as rule of thumb, when the hydrophobicity of the equatorial ligand (R-group) increases on the cobaloximes catalysts or the hydrophilicity of the monomer increases the partition coefficient also increases. Therefore, for fast reaction times there should be more catalyst concentrations in the dispersed phase (i.e. monomer droplets, monomer swollen micelles and/or polymer particles) as opposed to the concentration of catalyst in the aqueous phase $[Co]_{aq}$. Therefore, due to the zeta potential, particle size, molecular weight, feed rate and the glass transition temperature which in turn determined the stability and shelf life of the latex it was postulated to use poly($MAA_{15wt\%}$-*co*-$MMA_{85wt\%}$) at feed rate 60 min for the formation of the co-oligomers for CTA's.

2.5.1 Flory-fox equation

The Flory fox equation is the most commonly utilised empirical formula that relates the number average molecular weight (M_n), to the glass transition temperature, (T_g) with respect to free volume:

$$T_g = T_{g\infty} - \frac{K}{M_n}$$

Where K is a constant for a given polymer which is related to the free volume present in a polymer and $T_{g,\infty}$ is the limiting value of the glass transition temperature at theoretical infinite (i.e. very high) molecular weight (K = 83604 for the co-oligomers, with $T_{g,\infty}$ = 131 °C). The dependence of K upon the free volume, could be explained with free volume theory of T_g: as a result of greater mobility of chain ends, the free volume increases with the number of chain ends in a given volume (i.e. increases with decreasing molecular weight)[25-27]. After around M_n ~ 10, 000 gmol^{-1} the T_g becomes much less sensitive to changes in molecular weights.

Whereas if we were to utilise a miscible blend of two polymers, a copolymer or a plasticized polymer, then the Fox approach would be more suitable:

$$\frac{1}{T_g} = \frac{m_1}{T_{g,1}} + \frac{m_2}{T_{g,2}}$$

In this case varying the composition of polymer $T_{g,1}$ with respect to polymer with $T_{g,2}$, we can alter the final T_g of the polymer. The effect is calculated by using the weight fractions of the two components, w_1 and w_2, respectively as shown above. The Fox equation should only be applied to systems that utilise components with similar structure and / or solubility parameter (cohesive energy density), (i.e. two mixtures of components that have very weak or no specific intermolecular interaction).

These systems will display optimum mixing by acquiring a single T_g (i.e. according to DSC or DMA), if the systems are not compatible and two different T_g's are obtained the system will deviate from the Fox equation and are considered to be poorly mixed, which in turn will result in the two components have high tendency of phase separating. In our system we utilise the Flory-Fox equation despite the fact that we are using co-oligomers, since the Fox equation alone deviates from the actual T_g by around 10 °C [27, 28].

Table 2.11: SEC date, for the co-oligomers with acid composition (poly(MAA15wt%-co-MMA85wt%) with different concentrations of COBF

Reaction	CoBF /ppm	$M_{n,SEC}$ / g mol^{-1} (THF)	M_w / g mol^{-1}	$Đ$	M_n (NMR) / g mol^{-1}	T_g / °C Actual	T_g / °C Flory fox
C1	0	57500	221000	3.84		**135**	**130**
C2	54	5900	9100	1.56	5600	**116**	**116**
C3	88	3800	5600	1.47	3600	**112**	**109**
C4	94	2700	3900	1.45	2300	**101**	**100**
C5	108	2100	3300	1.58	1900	**92**	**87**
C6	133	1600	2700	1.73	1600	**79**	**79**

The SEC analysis, (*table 2.11*) shows the general expected trend of using CoBF catalyst as CTA. Increasing the CoBF concentration shows a significant decrease in molecular weight between reactions C1 and C2 indicating exceptional catalytic activity as only very small amounts of CoBF (ppm) amount is required for significant reduction in molecular weight. The $Đ$ values obtained for each set of reaction were in the region expected for free radical reaction, and the molecular weights according to GPC complimented by the molecular weights of the polymers obtained by ^{1}H NMR.

Furthermore, the predicted molecular weight obtained from Flory-Fox equation follows the actual T_g obtained by DMA from reaction C2 to C6, whereas for reaction C1 with no catalyst it deviates by just 5 °C, this could be due to significantly higher $Đ$ of the reaction without CoBF due to the polymer's high viscosity, which has previously been postulated with other similar monomers to generate regional differences in monomer concentration due to poor diffusion. Furthermore, all of the reactions C2-C6 were soluble with addition of NH_4OH (aq), *figure 2.13* (before and after addition of NH_4OH (aq)). These polymer will be further analysed in *chapter 3*, prior to being used as CTA's for sulphur free RAFT polymerisation.

Figure 2.13: Co-oligomers with acid composition (poly($MAA_{15wt\%}$-co-$MMA_{85wt\%}$) on left and right (poly($MAA_{15wt\%}$-co-$MMA_{85wt\%}$) with NH_4OH

2.6 Conclusions

Co-oligomers with various concentration of MAA with respect to MMA monomers were synthesised successfully and the conditions were optimized subsequently for eventual utilisation as CTA's for formations of diblock and pseudo- triblock copolymers in sulphur free RAFT polymerisation.

We found that increasing the MAA concentration within the co-oligomers with the same ppm of CoBF, caused the M_n to increase according to SEC and the particle size to increase according to DLS. This could be attributed to a few factors; firstly, even though CoBF is extremely stable at elevated temperatures and pH, the combination of MAA and ACVA (making the pH of the system extremely acidic) and the factor of high temperature could potentially destroy the catalyst, which in turn results in less catalyst available to act as CTA, in order to reduce the M_n of the co-oligomers.

Furthermore, increasing the concentration of the MAA within the co-oligomers increases the T_g of the polymers, since homopolymer of poly(MAA) has a T_g of 228 °C and the homopolymer of poly(MMA) is 105 °C, by tuning the ratio of MAA to MMA composition, we notice that the increase in the MAA concentration causes an increase in the T_g of the co-oligomers, at higher T_g the chain mobility of the polymers and the catalyst are hindered and therefore, there is insufficient amount of catalyst are available to reduce the M_n of the co-oligomers. In addition we found out that the zeta potential of the co-oligomer were generally equal to or greater the -40 eV, which in turn results in incredibly stable latexes, as the acid concentration of the particles increase the zeta potential generally was observed to increase, which in turn results in more stable latex particles.

As a result, we devised that the co-oligomers with the following composition poly($MAA_{15wt\%}$-*co*-$MMA_{85wt\%}$) at feed rate 60 min, to be the most suitable co-oligomer, since it required least amount of CoBF catalyst to form low M_n co-oligomers, had zeta potential of -40 eV, which in turn increases its colloidal stability and latex shelf life, solubilised incredibly well with NH_4OH (aq), which in turn improves the polymers post-polymerisation / functionalisation and application properties (i.e. investigated in *chapter 4*).

2.7 Experimental details

2.7.1 Instruments and analysis

Size Exclusion Chromatography (SEC)

SEC analyses in THF were carried out on an Agilent 390-LC MDS instrument equipped with differential refractive index (DRI) and a dual wavelength UV detector. The system was equipped with 2 x PLgel Mixed D columns (300 x 7.5 mm) and a PLgel 5 µm guard column. The eluent was THF with 2 % TEA (triethylamine) and 0.01 % BHT (butylated hydroxytoluene) additives. Samples were run at 1 ml/min at 30°C. Poly(methyl methacrylate) (PMMA) standards (12) in range of 500-1.5 x 10^6 g mol^{-1} and polystyrene (PS) (13) standards in the range 200-3.6 x 10^6 g mol^{-1} were used to calibrate the system and fitted with a third order polynomial Agilent EasyVials) were used for calibration. Analyte samples were filtered through a GVHP membrane with 0.22 μm pore size before injection. Respectively, experimental molar mass ($M_{n,SEC}$) and dispersity ($Đ$) values of synthesized polymers were determined by conventional calibration using Agilent GPC/SEC software.

Nuclear Magnetic Resonance (^{1}H NMR)

^{1}H NMR spectra were recorded on Bruker DPX-300 and HD-400 spectrometers using deuterated dimethyl sulfoxide, obtained from Aldrich. Chemical shifts are given in ppm downfield from the internal standard tetramethylsilane and data was analysed using ACD/NMR data software.

Dynamic Light Scattering DLS

DLS measurements were performed on a Malvern instrument Zetasizer Nano Series instrument with a detection angle of 173°, where the intensity weighted mean hydrodynamic size (Z-average) and the width of the particle size distribution (PSD) were obtained from analysis of the autocorrelation function. 1 µL of latex was diluted with 1 mL of deionized water previously filtered with 0.20 µm membrane to ensure the minimization of dust and other particulates. At least 3 measurements at 25 °C were made for each sample with an equilibrium time of 2 min before starting measurement.

2.7.2 Materials and general polymerisation procedure

All materials were purchased from Sigma Aldrich or Fisher at highest possible purity. Monomers were used as brought from supplier. Sigma products: 4,4′-Azobis(4-cyanovaleric acid) ≥98.0% (T); ammonia hydroxide solution 25 v/v%, Methyl methacrylate contains ≤30 ppm MEHQ as inhibitor; Methacrylic acid contains 250 ppm MEHQ as inhibitor, 99%; Potassium persulfate, ACS reagent, ≥99.0%; styrene, contains 4-tert-butylcatechol as stabilizer, <15 ppm, ≥99% and Sodium dodecyl sulfate, ACS reagent, ≥99.0%. CoBF old (17 years old) and new batch were synthesised in our group and has been reported previously in literature.[29]

Process for the synthesis of co-oligomer (PMMA/MAA) by CCTP in emulsion.

In a typical CCTP emulsion polymerisation, CoBF (0.02243 g, 0.0583 mmol) was placed in a 250 mL round bottom flask together with a stirring bar. Nitrogen was purged in the flask for at least 1h. Subsequently, MMA (96.3 mL, 90.14 g, 900.29 mmol) and MAA (15.7 mL, 15.94 g, 185.10 mmol) previously deoxygenated for 30 min was added to the flask via a deoxygenated syringe. The mixture was vigorously stirred under inert atmosphere until total dissolution of the catalyst. Meanwhile, 4,4'-azobis(4-cyanovaleric acid) (ACVA) (1.357 g, 4.842 mmol), SDS (2.143 g, 7.434 mmol) and 250 mL of water were charged into a three-neck, 500mL double jacketed reactor, equipped with a RTD temperature probe and an overhead stirrer. The mixture was purged with nitrogen and stirred at 325 rpm for at least 30 min. Subsequently, the mixture was heated under inert atmosphere. When the temperature in the reactor reached 70 °C, the addition of the MMA/MAA-CoBF solution started using a deoxygenated syringe and a syringe pump (feeding rate=1.866 mL/min, feeding time = 60 min). When the addition was over, stirring continued for a further 60 min under the same conditions. The number average molecular weight of the co-oligomers was calculated by analysing the ^{1}H NMR spectra.

Process for the synthesis of bis[(difluoroboryl)dimethylglyoximato] cobalt(II), (CoBF).

Cobalt (II) acetate tetrahydrate was heated under vacuum at 110 °C with pressure off 2 mbar for 5-6 hours (the pink powder turns purple upon becoming anhydrous). Under nitrogen atmosphere equipped with magnetic stirrer anhydrous cobalt (II) acetate (3.14

g, 0.0126 mol) and dimethyl glyoxime (4.47 g, 0.0344 mol) were added and purged with N_2 for 1 hour. Subsequently, ethyl acetate (77.12 ml, 0.87 mol) was dried with $MgSO_4$ and decanted and isolated (filtered with gravity filtration using filter paper). The ethyl acetate was deoxygenated for 30 minutes prior to addition to the mixture. The mixture was stirred vigorously for 30 min. Boron trifluoride etherate (BF_3EtO) (13.03 mL, 0.09 mol) was deoxygenated with nitrogen and added via syringe pump over a period of 10 minutes with continues vigorous stirring. The resulting solution was heated to 55 °C and held at that temperature for 30 minutes to complete the reaction. Sodium bicarbonate (3.57 g, 0.042 mol) was added in portions to avoid excessive frothing. When the bicarbonate addition was complete the reaction mixture was cooled to 5 °C and stirred for an hour to allow product to recrystallize. Filtration was carried out in (2 x 70 mL) H_20 and (2 x 20 mL) MeOH.

2.8 References

1. M. Abdollahi, *Polymer Journal*, 2007, **39**, 802.
2. D. Fukuhara and D. Sundberg, *JCT Research*, 2005, **2**, 509-516.
3. C.-F. Lee, T.-H. Young, Y.-H. Huang and W.-Y. Chiu, *Polymer*, 2000, **41**, 8565-8571.
4. I. Schreur-Piet and J. P. A. Heuts, *Polymer Chemistry*, 2017, **8**, 6654-6664.
5. G. W. Ceska, *Journal of Applied Polymer Science*, 1974, **18**, 427-437.
6. G. W. Ceska, *Journal of Applied Polymer Science*, 1974, **18**, 2493-2499.
7. A. K. Tripathi and D. C. Sundberg, *Industrial & Engineering Chemistry Research*, 2013, **52**, 3306-3314.
8. D. R. Bassett and A. E. Hamielec, *Emulsion Polymers and Emulsion Polymerization*, American Chemical Society, 1981.
9. A. van Herk and H. Heuts, in *Encyclopedia of Polymer Science and Technology*, John Wiley & Sons, Inc., 2002, DOI: 10.1002/0471440264.pst112.
10. A. M. dos Santos, T. F. McKenna and J. Guillot, *Journal of Applied Polymer Science*, 1997, **65**, 2343-2355.
11. A. F. Burczyk, K. F. O'Driscoll and G. L. Rempel, 1984, **22**, 3255-3262.
12. A. Bakac and J. H. Espenson, *Journal of the American Chemical Society*, 1984, **106**, 5197-5202.
13. H. S. Bisht and A. K. Chatterjee, *Journal of Macromolecular Science, Part C*, 2001, **41**, 139-173.
14. J. P. A. Heuts and N. M. B. Smeets, *Polymer Chemistry*, 2011, **2**, 2407-2423.
15. A. A. Gridnev and S. D. Ittel, *Chemical Reviews*, 2001, **101**, 3611-3660.
16. J. D. Menczel, L. Judovits, R. B. Prime, H. E. Bair, M. Reading and S. Swier, in *Thermal Analysis of Polymers*, 2008, DOI: 10.1002/9780470423837.ch2, pp. 7-239.
17. J. D. Menczel, R. B. Prime and P. K. Gallagher, in *Thermal Analysis of Polymers*, 2008, DOI: 10.1002/9780470423837.ch1, pp. 1-6.
18. H. E. Bair, A. E. Akinay, J. D. Menczel, R. B. Prime and M. Jaffe, in *Thermal Analysis of Polymers*, 2008, DOI: 10.1002/9780470423837.ch4, pp. 319-385.

19. K. P. Menard and N. R. Menard, in *Encyclopedia of Polymer Science and Technology*, 2015, DOI: 10.1002/0471440264.pst102.pub2, pp. 1-33.
20. R. P. Chartoff, J. D. Menczel and S. H. Dillman, in *Thermal Analysis of Polymers*, 2008, DOI: 10.1002/9780470423837.ch5, pp. 387-495.
21. G. W. Lu and P. Gao, in *Handbook of Non-Invasive Drug Delivery Systems*, ed. V. S. Kulkarni, William Andrew Publishing, Boston, 2010, DOI: https://doi.org/10.1016/B978-0-8155-2025-2.10003-4, pp. 59-94.
22. V. Selvamani, in *Characterization and Biology of Nanomaterials for Drug Delivery*, eds. S. S. Mohapatra, S. Ranjan, N. Dasgupta, R. K. Mishra and S. Thomas, Elsevier, 2019, DOI: https://doi.org/10.1016/B978-0-12-814031-4.00015-5, pp. 425-444.
23. M. Gumustas, C. T. Sengel-Turk, A. Gumustas, S. A. Ozkan and B. Uslu, in *Multifunctional Systems for Combined Delivery, Biosensing and Diagnostics*, ed. A. M. Grumezescu, Elsevier, 2017, DOI: https://doi.org/10.1016/B978-0-323-52725-5.00005-8, pp. 67-108.
24. A. Kumar and C. K. Dixit, in *Advances in Nanomedicine for the Delivery of Therapeutic Nucleic Acids*, eds. S. Nimesh, R. Chandra and N. Gupta, Woodhead Publishing, 2017, DOI: https://doi.org/10.1016/B978-0-08-100557-6.00003-1, pp. 43-58.
25. T. G. Fox and P. J. Flory, 1954, **14**, 315-319.
26. T. G. F. Jr. and P. J. Flory, 1950, **21**, 581-591.
27. T. G. Fox and S. Loshaek, 1955, **15**, 371-390.
28. J. M. Gordon, G. B. Rouse, J. H. Gibbs and W. M. R. Jr., 1977, **66**, 4971-4976.
29. Q. Zhang, S. Slavin, M. W. Jones, A. J. Haddleton and D. M. Haddleton, *Polymer Chemistry*, 2012, **3**, 1016-1023.

Chapter 3:

Exploiting catalytic chain transfer polymerisation for the synthesis of carboxylated latexes via sulfur-free RAFT

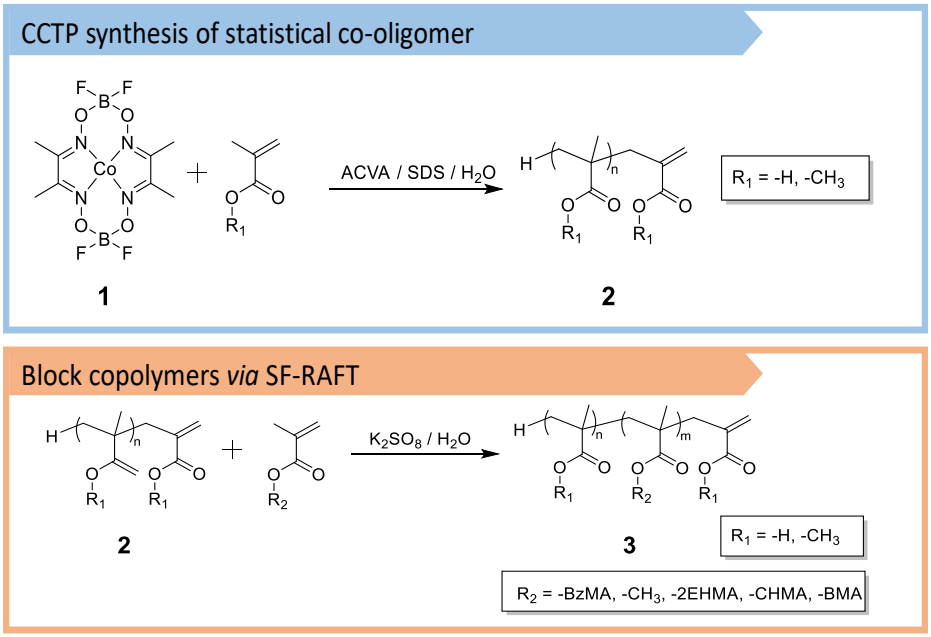

Mechanism of CCTP and SF-RAFT adapted from JPS

This chapter has been published:

1. **A. Shegiwal**, A. M. Wemyss, M. A. J. Schellekens, J. de Bont, J. Town, E. Liarou, G. Patias, C. J. Atkins and D. M. Haddleton, *Journal of Polymer Science Part A: Polymer Chemistry*, 2019, **57**, E1-E9

3.1 Introduction

Techniques for incorporating carboxyl groups into polymer latex particles have attracted attention in recent years.[1-4] Latex particles bearing carboxylic functional groups, either at their surface or internally, have numerous applications in medical diagnostics, adhesives, impact modifiers, as well as paper and textile coatings.[1, 2, 5-8] Water-soluble carboxylic acid containing monomers such as fumaric acid (FA), itaconic acid (IA), acrylic acid (AA) and methacrylic acid (MAA), listed in order of increasing hydrophobicity, are widely used in emulsion polymerization for the synthesis of carboxylated latexes. They are usually incorporated into the latex particle surface, and even in small quantities have been shown to improve colloidal, freeze-thaw stability, and adhesive properties.[1-3, 6, 7, 9, 10]

Traditionally, commercial emulsion polymerisations are prepared via free radical processes. Free radical polymerisation is a robust process, relatively simple to perform, and offers a wide range of monomer compatibility.[11, 12] However, it also suffers from a number of disadvantages, as it is prone to side reactions, which can decrease the reproducibility of reactions, and it is not possible to control the polymer end groups or obtain block copolymers, as it is in living radical polymerisation (LRP).[13-17]

Therefore, supplementary mechanisms for monomer sequence control in polymerisations have been studied and investigated. For instance, the development of living polymerisation methods: such as ionic polymerizations, ring-opening metathesis polymerisation (ROMP), catalytic chain transfer polymerisation (CCTP), and controlled radical polymerisations including nitroxide-mediated radical polymerisation (NMP) and reversible addition-fragmentation chain transfer polymerization/macromolecular design by interchange of xanthates (RAFT/MADIX), has all aided progress in the field of polymer science, and it is now possible to form polymers with complex microstructures in methods that were unconceivable a few decades ago.[11, 17-25 26, 27]

Careful monomer selection in the synthesis of the block copolymer provides additional control over the physical and chemical properties of the final latex and its potential

applications.[28, 29] In particular the glass transition temperature (T_g) is a key physical polymer property which can be controlled by altering the copolymer composition to tailor a product's properties and enhance its film strength, tackiness or film formation ability. For example, many coatings typically use acrylics, polyesters, epoxies and urethanes to produce tough products with relatively high T_g (~ 25 to 65 °C).[1, 2, 4, 13, 15, 30] Conversely, methacrylates, styrene and vinyl acetate are common building blocks to produce polymers of moderate T_g (0 to 25 °C), which are used for latex paints, textile binders, and adhesives. Low T_g (–55 to –25 °C) polymers, composed of hydrophilic monomers, such as acrylic acid, are used for pressure sensitive adhesive (PSA) applications, which are frequently soft.[7, 15, 31, 32]

The location of the carboxyl group in polymer latex particles and in the aqueous phase surrounding them, has been extensively studied.[1, 2, 4, 6, 7] The location of the acid within the chain is important as it governs the structure of the polymer and, in turn, the stability of the latex formed. The distribution of the acid is influenced by a number of factors, such as the reactivity ratio of the monomers or the partitioning behaviour of the carboxylic acid over the pH range of the reactions.[2] Carboxylic acid monomers are often highly water soluble. Nevertheless, they will still partition to varying degrees into the organic phase, subject to their relative hydrophobicity.[1, 2, 6, 33]

Monomers AA, IA, and FA tend to be highly partitioned to the aqueous phase, even at pH levels below their pKa's, and produce significant amounts of water-soluble polymer. With MAA, there is significantly less water-soluble polymer formed, and the MAA containing copolymer is better partitioned towards the particle, especially at low pH.[1, 2, 33]

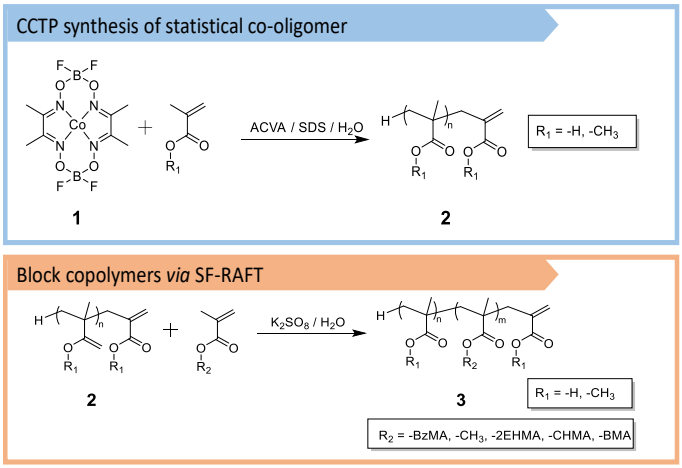

Figure 3.1: Schematic representation of the Co-mediated CCT and sulfur-free RAFT polymerization of methacrylates.[34-36]

In this chapter, CCTP was carried out in a seeded emulsion process, with a polystyrene (PS) core, to synthesise vinyl-terminated statistical co-oligomers of MMA and MAA. These macromonomers were then used *in situ* as chain transfer agents (CTA) for the SF-RAFT polymerisation of various methacrylic monomers, in the formation of di- and pseudo tri-block copolymers. In the synthesis of block copolymers, physical properties such as the glass transition temperature (T_g) of the product can be controlled by the copolymer composition, and so it is possible to tailor a product's properties through the selection of the monomer used to chain extend from the macro-CTA. This chapter investigates how T_g effects the formation of carboxylated latexes by chain extending with MMA, cyclohexyl methacrylate (CHMA), ethyl methacrylate (EMA), benzyl methacrylate (BzMA), butyl methacrylate (BMA) and 2-ethylhexyl methacrylate (2-EHMA).

3.2 Results and discussion

3.2.1 Synthesis of statistical co-oligomers via CCTP

We focused on statistical co-oligomers of MMA (85%) and MAA (15%) as prepared using CCTP in a seeded emulsion. The catalyst used was bis[(difluoroboryl)dimethylglyoximato] cobalt(II), (CoBF) (**1**), which has been previously reported as an effective CTA in the emulsion CCTP of methacrylates.[19, 37] This is due to its relative hydrophilicity, which allows it to distribute throughout the continuous phase and diffuse into the polymer particles. The additional consideration

in this work was the partitioning of the MAA towards the particles, which are the intended loci of polymerisation. To help this, we used 4,4'-azobis(4-cyanovaleric acid) as the initiator, which acted to lower the pH of the reaction mixture to approximately 3, where the MAA is protonated and less hydrophilic. It is noted that the k_p of protonated MAA is also higher than in its ionised form.[38] Under these conditions, we synthesised poly(MMA-*co*-MAA) macromonomers with a range of CoBF concentrations, (*table 3.1).*

Table 3.1: Data of CCTP co-oligomers with varied CoBF concentration under monomer starved condition

Reaction	CoBF / (*ppm*)	M_n^{NMR} (g/mol)	M_n^{SEC} (g/mol)	M_w (g/mol)	*Đ*
C1	0	-	57 500	221 000	3.84
C2	54	5600	5900	9100	1.56
C3	88	3600	3800	5600	1.47
C4	94	2300	2700	3900	1.45
C5	108	1900	2100	3300	1.58
C6	133	1600	1600	2700	1.73

Reaction C2 of *table 3.1*, shows that by adding 54 ppm of CoBF relative to the monomer concentration, the number average molecular weight (M_n) of the product is reduced from 57 500 to 5900 g/mol and dispersity (*Đ*) from 3.84 to 1.56. This higher *Đ* of the reaction without CoBF could be due to the polymer's high viscosity, which has previously been postulated to generate regional differences in monomer concentration due to poor diffusion.[39] Further increases of the CoBF concentration (C2-C6) resulted in lower M_n values for the co-oligomers and comparable *Đ*, (*table 3.1).* Compared with the CCT of homo-polymerisation of MMA, the apparent chain transfer constant (C_S^E) decreased from 820 to 590 in the synthesis of the co-oligomer (*figure 3.2*), reflecting the lower chain transfer activity of CoBF towards MAA.

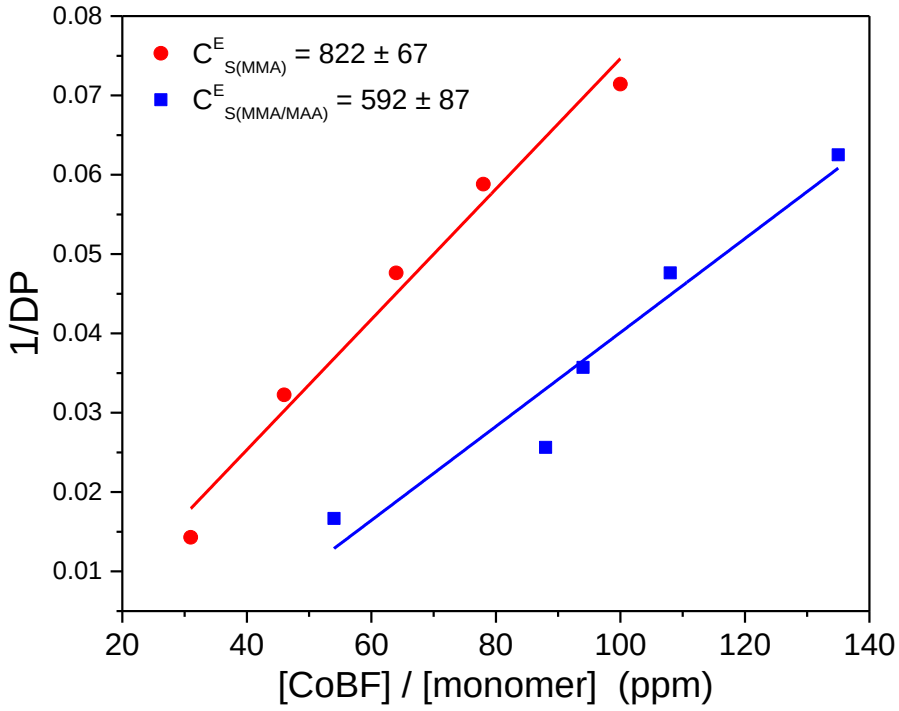

Figure 3.2: Mayo-plot for Poly(MMA) and Poly(85wt% MMA-co-15wt% MAA)

We also see good agreement between the M_n values obtained from SEC and ^{1}H NMR, (*table 3.1 & SI fig S3.1)*. The NMR values are calculated as the ratio of the integrated intensity of a single backbone methyl group proton to the integrated intensity of a proton from the ω-vinyl end group. The similarity between these values demonstrated excellent end group fidelity in the macromonomers.

The distribution of MAA throughout the co-oligomers was investigated using MALDI-ToF. We observe distinct distributions of peaks from each DP of the co-oligomer, which are interlinked by peak separations of 100.05 Da and 86.04 Da, approximately the repeat units of MMA (M_o = 100.05 gmol^{-1}) and MAA (M_o = 86.04 gmol^{-1}), respectively, *figure 3.3A*.

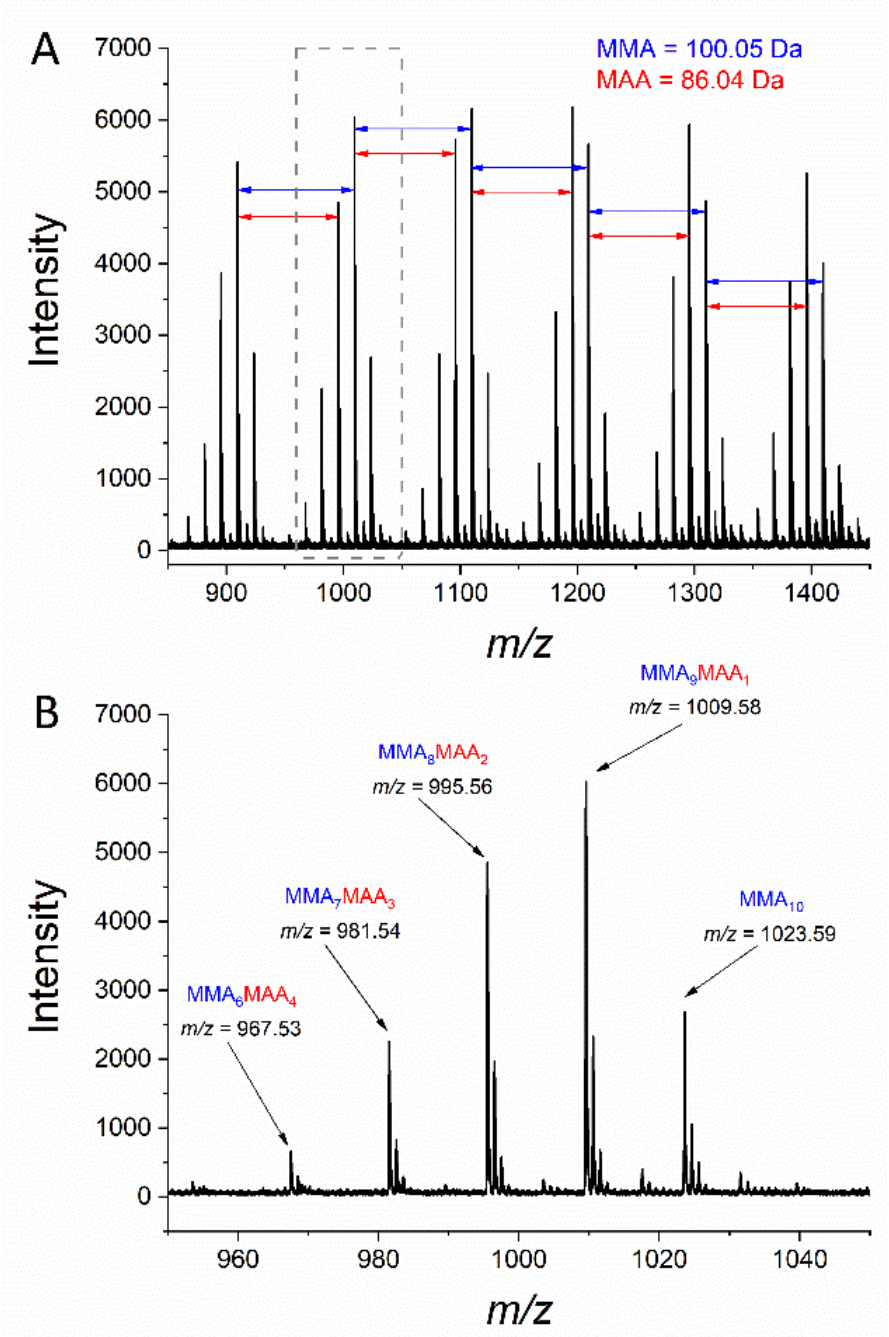

Figure 3.3: MALDI-ToF mass spectrum of the statistical co-oligomers of poly(MMA (85wt%)-co-MAA (15wt%))

The region around DP 10 is expanded in *figure 3.3B*, repeat units are used to determine the make-up of the statistical co-oligomers, with the error being calculated as the difference between the assigned structural mass and the peak mass with minus the cationic mass from the mass spectrum, *(table 3.2).*

Table 3.2: Analysis of MALDI-ToF spectrum DP 10

Peak (m/z)	No. of MMA	No. of MAA	Error (Da)
1023.59	10	0	0.076
1009.58	9	1	0.081
995.56	8	2	0.080
981.54	7	3	0.073
967.53	6	4	0.081

The assignments of all observable peaks confirms the expected product of *figure 3.1*, showing the end group fidelity of the ω-unsaturated macromonomer. The pattern of these peaks is repeated throughout the polymer as DP increases (*figure 3.3*). This shows that at all observable degrees of polymerisation, a large fraction of the polymer chains contain both MMA and MAA. For DP 10 of the sample C6 (*table 3.1*) the largest peak coincided with the $PMMA_9MAA_1$ species with an unsaturated vinyl ω-end group. No evidence of fragmentation was observed for any of the co-oligomers. The error (e_{Da}) in *table 3.2* was calculated using:

$$e_{Da} = \left| {}^{m}/_{z_{th}} - \left({}^{m}/_{z_{obs}} - m(Na^+) \right) \right| \quad (1)$$

where $\frac{m}{z}_{obs}$ is the observed peak position, $m(Na^+)$ is the mass of a sodium ion and $\frac{m}{z}_{th}$ is:

$$\frac{m}{z}_{th} = n(MMA) \cdot m(MMA) + n(MAA) \cdot m(MAA) + m(\omega) \quad (2)$$

where n denotes the number, m is mass and , $m(\omega)$ is the mass of the end groups. The mass of the end groups is functionally 0 due to the vinyl end group, therefore the number of each monomer units is the only unknown for each peak. These were solved iteratively, using only positive whole integers for the number of monomer units, to minimize the error and provide the most accurate assignment possible.

3.2.2 Synthesis of di- and pseudo tri-block copolymers *via* SF-RAFT

The mechanism of SF-RAFT has been described previously.[19, 34, 35, 37] Briefly, with reference to *scheme 3.1*, the reaction involves a propagating species (**4**) reacting with a macromonomer/macro chain transfer agent (**2**) to form adduct **5**. This intermediate

radical may then revert to the starting materials or fragment to produce a new propagating species (**6**) and a new macromonomer (**7**). Reaction of **6** with R_2 monomer produces a block copolymer propagating species, which may then react with a macromonomer (**2**, **3** or **7**) to produce a block copolymer (**3**). The final step produces the vinyl terminated ω-chain end to the block copolymer, and so it is itself a macromonomer that can undergo further reaction.

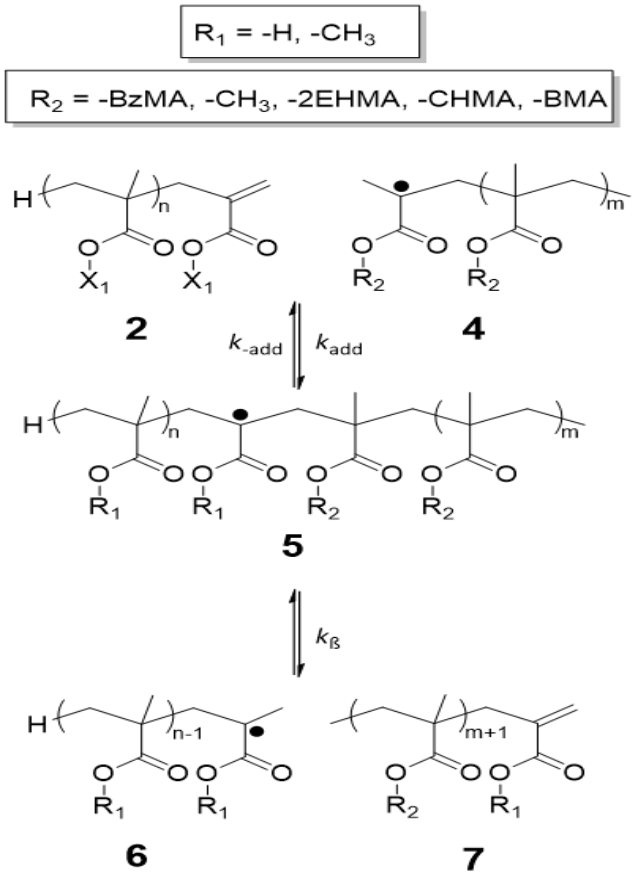

Scheme 3.1: Synthesis of block copolymers by SF-RAFT polymersiation.[34-36, 40, 41]

CCTP co-oligomer with M_n ~ 2500 g mol^{-1} using the data from *table 3.1* was selected for the synthesis of all di- and pseudo tri-block copolymers, with no need for purification steps. Co-oligomer with 15%MAA and 85%MMA composition was utilised for the synthesis of all the di-block co-polymers, since higher concentration of acid incorporated within the latex resulted in small amount of coagulation (3 – 8 wt%). Furthermore, at high acid concentration (35%MAA and 65%MMA) very low molecular weight polymers with replicative results were not possible to achieve. Moreover, increasing the acid concentration within the latex also increases the particle

size of the polymers, whereas 15%MAA-85%MMA composition polymers achieved particle size < 200 nm which ensures a stable latex with long shelf life (stable after 15 months).

All SF-RAFT polymerisations were performed under monomer starved conditions, this means that the polymer particles are not saturated with monomer, but are being polymerised at an instantaneous conversion of 90% or greater.[37, 42] If the monomer feeding rate (i.e. semi-continuous feed) is greater than the polymerisation rate, the reactor will be operating under flooded conditions and control over the copolymer composition would be lost. Starved-feed conditions are preferred from polymerization control perspective as it increases the likelihood that **4** and **6** will interact with a macro-CTA over normal monomer propagation, and also reduces the occurrence of unwanted radical termination events such as disproportionation or recombination. All of the polymers formed showed no visible coagulation.

To be compatible with emulsion polymerisation, all of the monomers used for chain extension are monomers suitable for conventional emulsion polymerisation and thus relatively hydrophobic, and selected to provide a range of T_g values to the final product. Of those selected, 2-EHMA produced the products with the lowest T_g. *Figure 3*, shows the SEC traces of the polymers synthesised here. The di-block of 2-EHMA (*DP=25*) had a T_g of 16°C which can be attributed to the fact that first block consisting of very high T_g polymers MAA T_g (228°C) and MMA (105°C) respectively. Tan delta (δ) for 2-EHMA (*DP = 25*) was 22°C. The co-oligomer of 15 wt% MAA and 85 wt% MMA by composition had a T_g of 127°C, the onset of the T_g was 109°C whereas the end T_g was 142°C according to DMA with the tan δ same as T_g obtained from storage modulus .

For reaction 2-EHMA *(DP = 25)*, the onset T_g was 4°C whereas, the end T_g was 50°C. By addition of the next subsequent block of 2-EHMA (*DP=50*), the T_g increased to 38°C, the onset increased to 17°C, whereas the end T_g remained unchanged. Tan δ for 2EHMA (*DP = 50*), increased to 38°C with a small shoulder peak at 13°C. SEC revealed that with each subsequent addition of the monomer, a complete shift to higher molecular weight occurred, with DLS confirming an increase in the hydrodynamic

diameter of the particles with increasing M_n, (*SI Table S3.3),* for 2-EHMA (*DP = 25 and 50*) respectively.

The low pH of the emulsions suggest that the MAA of the co-oligomer is protonated, and so we would expect it to be well partitioned towards the particle in these reactions. For reaction BMA (*DP = 25 and DP = 50*) with the next two subsequent blocks both consisting of BMA monomers the T_g of the di-block was 55°C, the onset obtained was 44°C and the end point T_g was 71°C. There was a slight decrease in T_g by the addition of the third block (49°C) with the final T_g remaining similar. Tan δ increased by 6°C for both diblock and triblock copolymers of BMA. The SEC and DLS data for copolymerisation of BMA with the macro-CTA (*table 3.3*, DP = 25 and DP = 50) gave similar results to 2-EHMA containing polymers.

With the BzMA and EMA block copolymers products with relatively high T_g's were produced (82°C and 104°C, respectively (*DP = 25*), and by addition of the third block a slight increase in T_g was observed with BzMA (*DP = 50*) T_g~ 86°C, whereas with EMA slight decrease (*DP = 50*) T_g~ 95°C. Furthermore, the onset end-point T_g and tan δ remain relatively the same for BzMA at (*DP = 25 & 50*) polymers but for EMA (*DP=25 & 50*) the onset decreased from 92°C to 79°C. However, the end T_g and tan δ remain similar *(SI table S3.2 & Fig S3.3),* SEC data showed complete shift to a higher molecular weight and increase in particle size was observed with each subsequent addition of the monomer by DLS. In these polymers, we see a less dramatic reduction of *Đ* than in the reactions described above, particularly at higher DPs (*table 3.3*). As the T_g of these polymers is moderately high, the monomers do not partition to the same level of efficiency as with 2-EHMA and BMA, resulting in a higher *Đ* observed compared to the softer polymers.

Finally, we looked at a diblock of CHMA and MMA, which produced polymers with high T_g's (120°C and 118°C, respectively at *DP = 25*). The addition of the third block for CHMA *DP = 50* resulted in the T_g staying constant at 118°C and tan δ staying similar. However, with an MMA pseudo tri-block (*DP = 50*) the T_g increased to 128°C with both onset and end T_g also increasing respectively *(SI Table S3.2 & Fig S3.3).* According to SEC, both (CHMA & MMA derived polymers) exhibit similar behaviours after the formation of the pseudo tri-block. In the di-block formation with

MMA (*table 3.3 & figure 3.4*), a decrease in $Đ$ is observed by SEC data with a complete shift to higher molecular weight. DLS showed an increase in the hydrodynamic diameter of the particles with increasing M_n. The addition of the third block *figure 3.4*, gave an increase in $Đ$ with bimodal peaks appearing. This is attributed to the higher T_g of the monomer reducing the mobility of the macro chain transfer agents, making them less effective in acting as chain transfer agents and thus in controlling chain growth.

Mobility can be improved by plasticizing the high T_g polymers. Plasticizers are often low M_n species relative to their polymeric counterparts, and must be chemically compatible with solvent(s) and polymeric aids. Plasticizers are common reagents added to coating formulations: their typical functionality in coating formulations is to reduce the T_g, and increase coating flexibilities of the end polymer.[43-46] By utilising different plasticizers that are chemically compatible with solvent(s) and polymeric aids, properties can be tailored to specific requirements. Usually, by increasing plasticizer concentration the flexibility of the polymeric material increases, yet a decrease in the tensile strength and hardness is also observed. [43-46]

In this chapter it was found the addition of plasticisers such as o-xylene to MMA diblock and pseudo triblock are very effective at reducing the $Đ$ significantly and achieving monomodal peaks. In synthesis of the MMA pseudo triblock the $Đ$ decreased from 3.21 to 1.39 by addition of 20 wt% o-xylene *(table 3.4)*. Furthermore, o-xylene is a non-polar plasticiser and preferentially plasticises the backbone of the hydrocarbon chains but has less effect on the cluster phase. The low density of o-xylene also makes it desirable to use as plasticiser as it is easily removed from the reaction mixture by rotary evaporation.[47, 48]

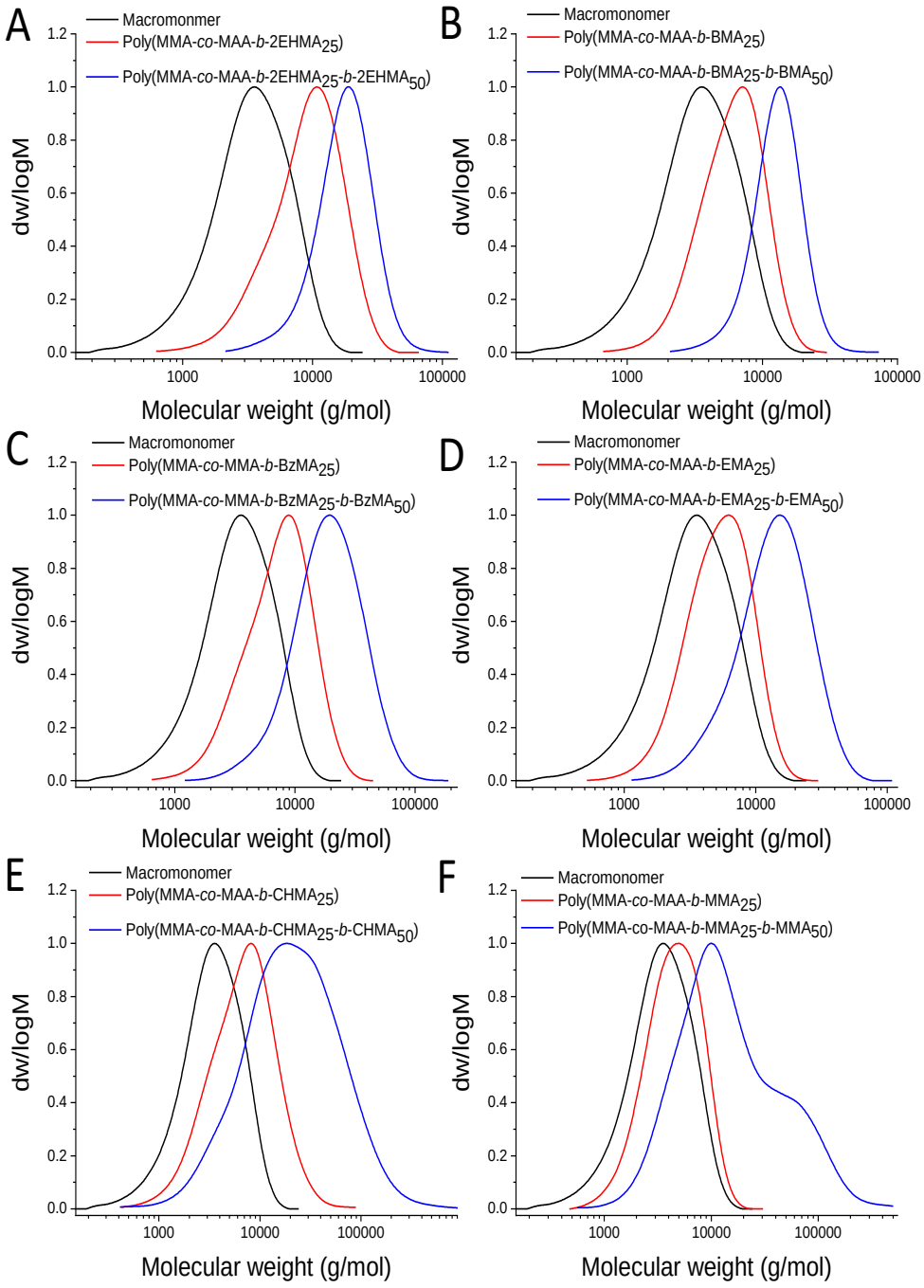

Figure 3.4: SEC of di- and pseudo tri-block copolymers: Red curves are diblock polymers with DP = 25 and blue curves are pseudo tri-blocks, DP = 50 with A representing the SEC data for 2-EHMA , B of BMA , C of BzMA, D of EMA, E of CHMA and F consisting of MMA copolymers

Table 3.3: Properties of di- and pseudo tri-block copolymers of methacrylate derived polymers

Reaction	$M_{n,}^{SEC}$ gmol^{-1} (THF)	M_w (gmol^{-1})	$Đ$	$M_{n,th}$ (gmol^{-1})
p(MMA/MAA)	2500	4000	1.63	-
EHMA (DP=25)	7000	10600	1.51	7400
EHMA (DP=50)	15000	19500	1.30	16900
BMA (DP=25)	5000	6700	1.34	6000
BMA (DP=50)	11500	13900	1.20	12100
BzMA (DP=25)	5700	8600	1.49	6900
BzMA (DP=50)	14600	22700	1.56	14500
EMA (DP=25)	4400	6000	1.37	5400
EMA (DP=50)	10600	15300	1.45	10100
CHMA (DP=25)	4900	8800	1.78	6700
CHMA (DP=50)	12100	34900	2.88	10900
MMA (DP=25)	3700	5200	1.42	5000
MMA (DP=50)	8900	28500	3.22	8700

Table 3.4: Properties of di- and pseudo tri-block copolymers of methacrylate derived polymers with plasticizers.

Reaction	$M_{n,}^{SEC}$ gmol^{-1} (THF)	M_w (gmol^{-1})	$Đ$
CHMA-DP=30	6800	12500	1.84
CHMA-DP=30-20wt%-glycerol	6600	11000	1.67
CHMA-DP=30-20wt%-IPA	6400	10200	1.59
Triblock-MMA-DP=50-o-xylene-10wt%	13800	30400	2.20
Diblock-MMA-DP=30-o-xylene-20wt%	4700	6500	1.39
Triblock-MMA-DP=50-o-xylene-20wt%	7100	9800	1.39

With CHMA a slight increase in *Đ* was initially observed for the formation of diblocks (*DP = 25*) and more significant increase in *Đ* was observed for the formation of pseudo tri-block (*DP = 50*), which is attributed to higher T_g of this polymer *(table 3.3).* The high *Đ* of the higher T_g polymers can be reduced by incorporating plasticisers such as glycerol and isopropanol (IPA) which are effective at plasticising the ionic domains and reducing melt viscosity which in turn reduces the *Đ* from 3.22 to 2.20 by addition of the third block.[47, 48] IPA plasticiser is favoured over glycerol as it has lower density

and easily removed from the reaction mixture by rotary evaporation. However, excess IPA should be avoided as at concentrations greater than >30 wt% IPA with respect to the total polymer, the addition of IPA plasticizers results in bimodal peaks appearing according to SEC data. This is due to the fact that at very higher concentrations the IPA will acts as CTA agents itself.

Nevertheless, when compared with MMA, the addition of the third block for CHMA resulted in a monomodal molecular weight distribution and a complete shift to a higher molecular weight occurred according to SEC. DLS showed an increase in the hydrodynamic diameter of the particles with increasing M_n for the diblock but for the pseudo triblock the particle size decreased suggesting new particles being formed, which is clear from the SEM images *(figure 3.4 & 3.5).*

Furthermore, for all reactions (*SI Table 3.3*) the surface zeta potential at pH ~2.5 was -49 mV ±3 which can be attributed to the presence of carboxylic acid and SDS surfactant which was added initially to the reaction mixture for the formation of the co-oligomer. Furthermore, since the zeta potential is greater than -49 mV the particles have high degree of stability and subsequently, this lead to particles acquiring monodispersity, as seen by DLS and SEC data.

The diblock and pseudo tri-block copolymers contained carboxylic acid functionality monomers and the zeta surface potential are all in the region expected for carboxylated latex.[49, 50] In addition the ^{1}H NMR, shows that with each subsequent addition of the monomer for the diblock and pseudo triblock, vinyl peaks and the carboxylic acid functionality becomes less apparent, (*SI Fig 3.4*).

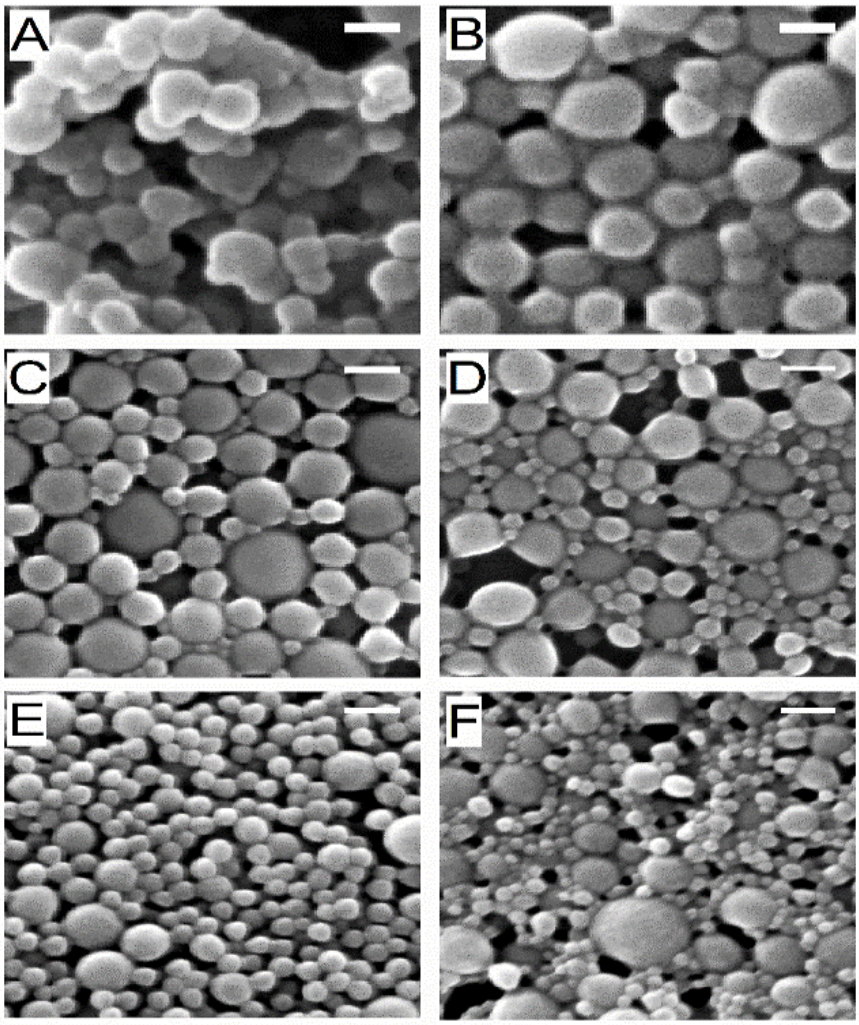

Figure 3.5: SEM micrographs of pseudo tri-block copolymers A representing 2-EHMA, B of BMA, C of BzMA, D of EMA, E of CHMA and F consisting of MMA (scale bar for the SEC data is 200nm)

For each of the latex samples from *table 3.3*, the relative wettability of the polymers on glass was measured through contact angle measurements. SEM images of the pseudo triblock co-polymers were taken and showed a general monomodal distributions. The lower T_g polymers displayed significant number of particles with uniform monomodal peaks. However, SEM images for low T_g polymers were challenging to obtain due to the heat generated by the electron beam which caused the particles to melt if images were not obtain quickly: our observation showed that the size of the particles were uniformed.

SEM images samples D, E and especially F have a broad PSD with many smaller particles, despite the use of the seed. SEM image F of pseudo PMMA triblock copolymer shows many smaller particles. This suggests that new particles are being

formed which in the case of MMA (sample F) explains the bimodal peak according to SEC (*figure 3.4*).The new particles that are being formed are homopolymers of the monomer of the next subsequent block. Multi-block copolymers can be obtain with these monomers and initial decrease in *Đ* is observed with each subsequent addition of the monomer and eventually the *Đ* starts to increase agreement with sulfur free RAFT polymerisation as the block length increases eventually the *Đ* increases.

3.2.3 Contact angel measurement

Drop shape analysis is a convenient way to measure contact angles and thereby surface characterization and wetting properties due to its simplicity and versatility. Contact angle can be measured by forming a drop of liquid or a vapour (but most often a liquid) with a solid surface. The angle that forms between the solid/liquid interface and the liquid/vapour interface is referred to as the contact angle. The most common method for measuring contact angles is using a profile of a drop and measuring the two dimensional angle formed between the solid and drop profile with the vertex at the three-phase line as depicted in *figure 3.6*. Young's equation is commonly utilised to explain the interactions between the forces of cohesion and adhesion and measure the surface free energy.[51-54]

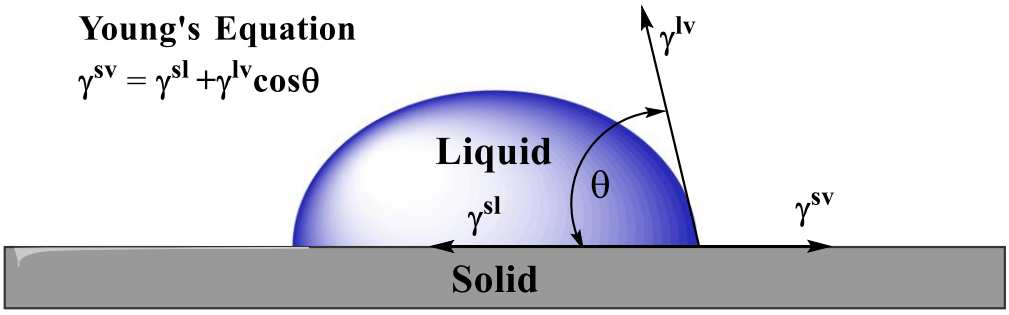

θ = contact angle
γ^{sv} = is the solid surface free energy
γ^{sl} = is the solid/liquid interfacial free energy
γ^{lv} = is the liquid surface free energy

Figure 3.6: Contact angle using Young's equation

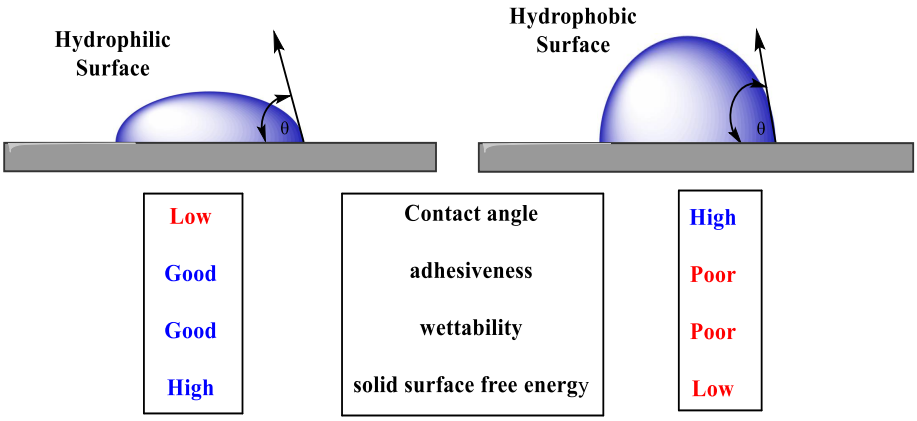

Figure 3.7: Depiction of contact angles of hydrophilic and hydrophobic polymers

Therefore, the contact angle obtained can be used to categorise the different surfaces: a contact angle < 90 ° is considered hydrophilic (θ < 90 °) reflects better wetting, adhesiveness, and higher surface energy. Whereas, a contact angle >90 ° is hydrophobic (θ > 90 °) and has poor wetting, poor adhesiveness and the solid surface free energy would be low. Whiles, surfaces with contact angle above 150 ° is considered superhydrophobic (θ >150 °) and shows tremendous potential in industrial applications such as antifouling, self-cleaning and anti-icing surfaces (depicted in *figure 3.7*).[51-54]

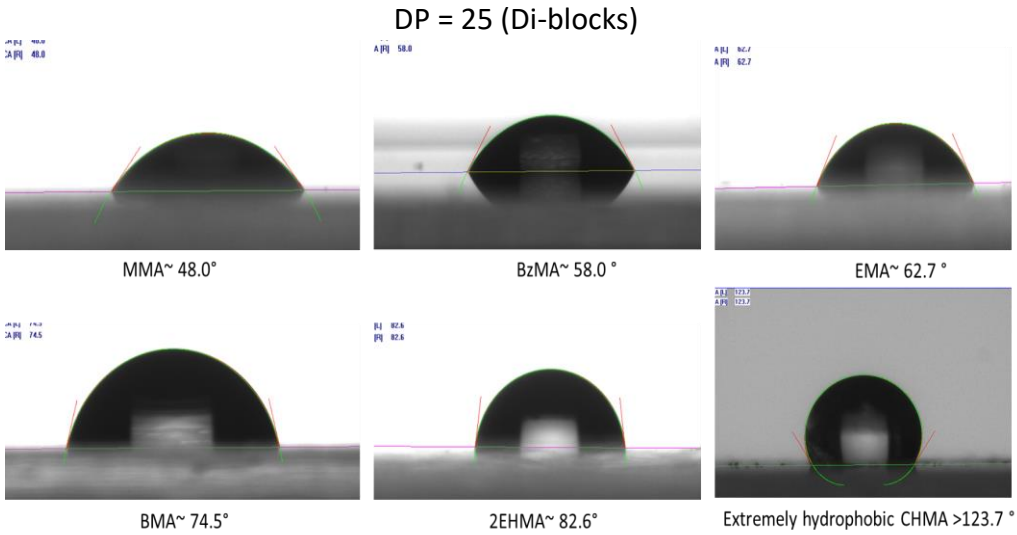

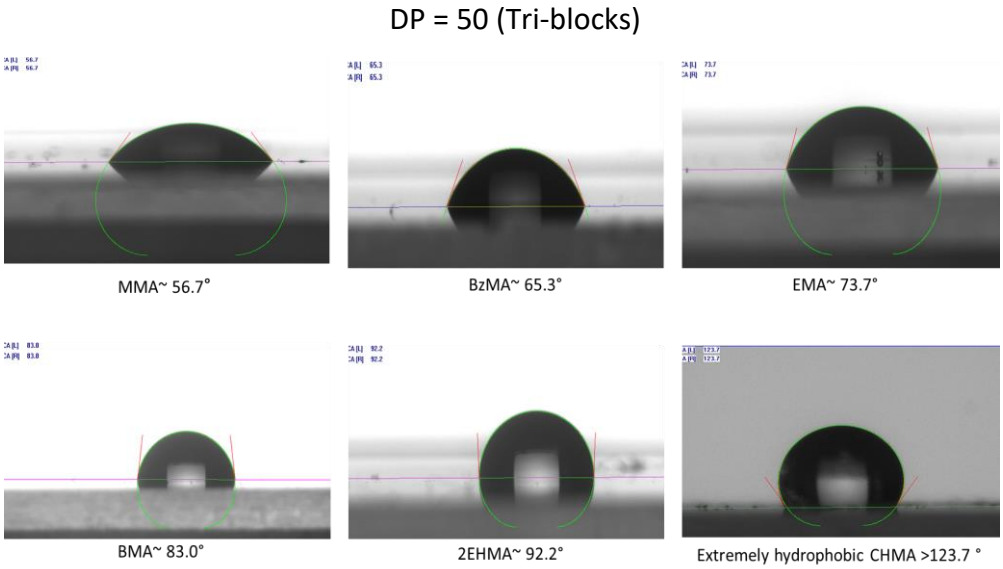

Figure 3.8: Contact angle images DP = 25: with top left reaction G2, top middle D2, top right E2, bottom left reaction C2, bottom middle B2 and bottom right F2 and DP = 50: with top left reaction G3, top middle D3, top right E3, bottom left reaction C3, bottom middle B3 and bottom right F3

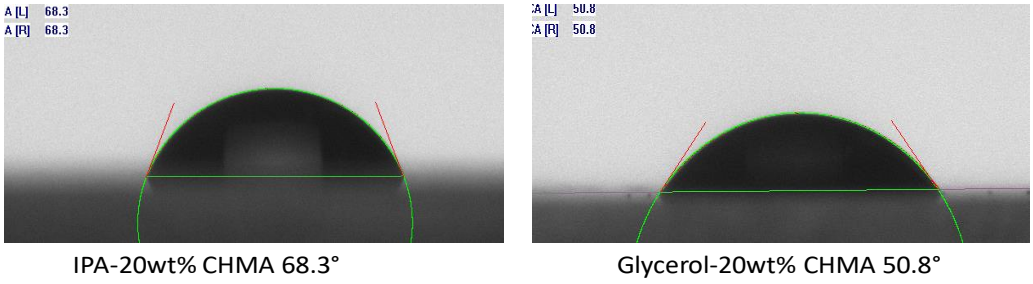

Figure 3.9: Left image CHMA with 20wt% of IPA and right image is glycerol with 20wt%

Starting with MMA di-block co-polymer (*DP = 25)* with contact angle 48.0°, the addition of the next subsequent block *DP = 50* a pseudo tri-block contact angle of 56.7° was obtained, which showed that an increase in the chain length of the polymer resulted in an increase in the hydrophobicity of the polymer by approximately ~10°. Furthermore, relative to the other diblock polymers (*figure 3.8)* CHMA (*DP = 25)* and pseudo tri-block (*DP = 50*) which were the most hydrophobic polymers, according to contact angle measurements, MMA (*DP = 25 & 50*) containing polymers were the most hydrophilic polymers as their surface tension was the lowest of the polymers (*table 3.3*) resulting in a smaller contact angle compared to the other polymers *(figure 3.8).* Therefore, the polymers that were relatively hydrophilic had good adhesiveness and wettability properties to glass with high solid surface free energy.

The next batch of least hydrophobic polymer was BzMA (*DP = 25* contact angle 58.0°) with next subsequent block also consisting of BzMA monomer with *DP = 50* (contact angle 65.3°) the low contact angle could possibly be attributed to the fact that the aromatic ring is delocalised which in turn reduces the surface tension and results in the polymer having similar properties to that of the MMA (*DP = 25*) block copolymer. The other polymers with increasing alkyl chain produced results similar to that of the predicted results based on the hydrophobicity of the alkyl chain *DP = 25*; reaction (EMA 62.7°) < (BMA 74.5°) < (2-EHMA 82.6°) and *DP = 50*; reaction (EMA 73.7°) < (BMA 83.0°) < (2-EHMA 92.2°). As the chain length of the polymers increased by the addition of the third block, the hydrophobicity of the polymers increased by around ~10 degrees.

The other factor governing the contact angle was the length of the alkyl chain on the R group of the methacrylate. With an increase in the alkyl chain length the contact angle increased as expected which in turn resulted in poor adhesiveness and wettability properties of the polymer and low solid surface free energy. The initial co-oligomer which was utilised as CTA agent was very hydrophilic and no contact angle measurements could be taken as the droplets spread instantly onto the surface; this was expected due to 15wt% of MAA in the latex. However, the results for reaction with CHMA at both (*DP = 25 & 50*) were unexpected as the polymers obtained were highly hydrophobic and a ball-like droplet would reside onto the surface of the plate and spread out after within seconds, *(figure 3.8)* illustrates the image after a few seconds which suggested it is highly hydrophobic. To confirm that CHMA both at (*DP = 25 & 50)* were highly hydrophobic, contact angles of the latex with 20wt% of IPA and glycerol which are very hydrophilic plasticizers were taken of polymer at DP = 30. With addition of 20wt% IPA plasticizer the contact angle reduced to 68.3° and with glycerol which is a significantly more hydrophilic plasticizer than IPA the contact angle reduced to 50.8° *(figure 3.8 & 3.9).*

As the chain extension occurred with each subsequent addition of the monomers of different hydrophobicity the contact angle measurements correlated well with the fact that as the alkyl chain length increases the contact angle increased which in turn suggests that the chains are growing of the co-oligomer and the acid is incorporated well within the latex.

3.3 Conclusions

The versatility of CCT combined with sulfur free RAFT polymerisation has been demonstrated by applying it under emulsion polymerization conditions. The formation of various di- and pseudo triblock copolymers containing an acid-based block and a range of different poly(alkyl methacrylate) blocks has been demonstrated. The conditions were optimised for the formation of the co-oligomers with incorporation of carboxylic acid functionality which in turn were utilised for the formation of well-defined di-block and pseudo tri-block copolymers. By changing the composition of the monomers added based on hydrophobicity, and T_g, the latex and the morphology of the polymer latex can be altered based of the desired properties.
Furthermore, control over pH in emulsions is essential, as it determines the location of the acid within the polymer latex.

The pH is also believed to play a role in catalyst activity through the rate of hydrolysis of the CCTA as at very low pH a slightly higher concentration of catalyst is desired. Moreover, seeded polymerizations can be important for eliminating some of the ambiguity associated with the compartmentalization of the organic phase by controlling the particle numbers and particle size. This also allows for better control over the average number of catalyst molecules per particle which in turn allows the latex to have a long shelf-life as the particles are usually smaller with incorporation of the seed.

3.4 Supporting information

3.4.1 Instruments and analysis

Size Exclusion Chromatography (SEC)

SEC analyses in THF were carried out on an Agilent 390-LC MDS instrument equipped with differential refractive index (DRI) and a dual wavelength UV detector. The system was equipped with 2 x PLgel Mixed D columns (300 x 7.5 mm) and a PLgel 5 µm guard column. The eluent was THF with 2 % TEA (triethylamine) and 0.01 % BHT (butylated hydroxytoluene) additives. Samples were run at 1 ml/min at 30°C. Poly(methyl methacrylate) (PMMA) standards (12) in range of 500-1.5 x 10^6 g mol^{-1} and polystyrene (PS) (13) standards in the range 200-3.6 x 10^6 g mol^{-1} were used to calibrate the system and fitted with a third order polynomial Agilent

EasyVials) were used for calibration. Analyte samples were filtered through a GVHP membrane with 0.22 μm pore size before injection. Respectively, experimental molar mass ($M_{n,SEC}$) and dispersity ($Đ$) values of synthesized polymers were determined by conventional calibration using Agilent GPC/SEC software.

Nuclear Magnetic Resonance (^{1}H NMR)

^{1}H NMR spectra were recorded on Bruker DPX-300 and HD-400 spectrometers using deuterated dimethyl sulfoxide, obtained from Aldrich. Chemical shifts are given in ppm downfield from the internal standard tetramethylsilane and data was analysed using ACD/NMR data software.

Dynamic Light Scattering DLS

DLS measurements were performed on a Malvern instrument Zetasizer Nano Series instrument with a detection angle of 173°, where the intensity weighted mean hydrodynamic size (Z-average) and the width of the particle size distribution (PSD) were obtained from analysis of the autocorrelation function. 1 μL of latex was diluted with 1 mL of deionized water previously filtered with 0.20 μm membrane to ensure the minimization of dust and other particulates. At least 3 measurements at 25 °C were made for each sample with an equilibrium time of 2 min before starting measurement.

Contact angle measurements

The contact angle measurements were performed using DSA100 Kruss angle telescope-goniometer. The latex samples were applied onto clear microscope glass slides, 76x26 mm and thickness 1.0-1.2 mm to form films which were than left overnight in an oven at 80 °C. Advancing contact angle, was established by slowly growing the sessile drop to a diameter of approximately 5 mm using a micrometre syringe with a narrow gauge stainless steel needle. Contact angle measurements were taken at multiple points to give an average value that was representative of the entire surface.

MALDI-ToF

Samples were prepared for MALDI-ToF-MS analysis, 1 mg of the sample was dissolved into 1ml of tetrahydrofuran with 15mg of dithranol (Sigma) and 0.1 mg of

sodium iodide salt (sigma). 0.5 µl of this sample mixture was pipetted onto a 328 MTP ground steel target plate (Bruker, Coventry, UK). MALDI-ToF-MS experiments were carried out using an UltrafleXtreme (Bruker, Coventry, UK) operating in reflectron positive mode with an accelerating voltage of 19kV. 500 shots were taken at each measurement of the spot, with ten measurements taken and accumulated into the final spectra (total of 5000 shots).

Scanning Electron Microscopy: Samples preparation

Scanning electron microscopy was performed using a Zeiss SUPRA 55-VP scanning electron microscope (SEM) with a field emission electron gun (FEG). Best results were obtained when using the InLens detector with 3.5 mm working distance, 30 and 20 µm aperture and 4-10 kV acceleration voltage, with respect to sample tolerance. 1 µL of each sample was dissolved in 5 mL of DI water and aliquots of 7 µL were drop casted on silicon wafer chips (5 mm x 7 mm) attached to aluminium specimen stubs. For the improvement of the sample imaging, gold (Au) sputter coating was applied for 15 seconds prior to imaging.

T_g measurements via DMA

The method of analysis used was Pekin Elmer DMA 8000 using single cantilever geometry orientation horizontally with all the polymer latex samples were in powdered form. A sample mass between the mass of 0.06-0.09 g were measured onto material pocket envelopes with length 14.8 mm, width 7.43-7.47 mm and thickness 1.8-2.2 mm. The starting temperature was -60°C and end temperature was 220°C. The strain 0.02 mm and heating rates 2°C/min with frequency of 1 Hz were performed onto the sample. The instrument was calibrated with ulta high molecular weight Poly(MMA) after every run.

3.4.2 General polymerisation procedure

Materials

All materials were purchased from Sigma Aldrich or Fisher at highest possible purity. Monomers were used as brought from supplier. Sigma products: 4,4′-Azobis(4-cyanovaleric acid) ≥98.0% (T); Methyl methacrylate contains ≤30 ppm MEHQ as inhibitor; Methacrylic acid contains 250 ppm MEHQ as inhibitor, 99%; Potassium

persulfate, ACS reagent, ≥99.0%; styrene, contains 4-tert-butylcatechol as stabilizer, <15 ppm, ≥99%; Ethyl methacrylate contains 15-20 ppm monomethyl ether hydroquinone as inhibitor, 99%; Butyl methacrylate 99%, contains ~50 ppm monomethyl ether hydroquinone as inhibitor; 2-Ethylhexyl methacrylate 98%, contains ~50 ppm monomethyl ether hydroquinone as stabilizer; Cyclohexyl methacrylate ≥97%, contains ~60 ppm monomethyl ether hydroquinone as inhibitor and Benzyl methacrylate 96%, contains monomethyl contains ~50 ppm ether hydroquinone as inhibitor; ammonia hydroxide solution 25 v/v% and sodium dodecyl sulfate, ACS reagent, ≥99.0%. CoBF old (i.e. *17 years old*) and new batch was synthesised in our group and has been reported previously in literature.[55]

3.4.3 Polymer synthesis

Process for the synthesis of co-oligomer (PMMA/MAA) by CCTP in emulsion.

In a typical CCTP emulsion polymerisation, CoBF (0.02243 g, 0.0583 mmol) was placed in a 250 mL round bottom flask together with a stirring bar. Nitrogen was purged in the flask for at least 1h. Subsequently, MMA (96.3 mL, 90.14 g, 900.29 mmol) and MAA (15.7 mL, 15.94 g, 185.10 mmol) previously degassed for 30 min was added to the flask via a degassed syringe. The mixture was vigorously stirred under inert atmosphere until total dissolution of the catalyst. Meanwhile, 4,4'-azobis(4-cyanovaleric acid) (ACVA) (1.357 g, 4.842 mmol), SDS (2.143 g, 7.434 mmol), polystyrene seed 5.23 wt% to the total monomer and 250 mL of water were charged into a three-neck, 500 mL double jacketed reactor, equipped with a RTD temperature probe and an overhead stirrer. The mixture was purged with nitrogen and stirred at 325 rpm for at least 30 min. Subsequently, the mixture was heated under inert atmosphere. When the temperature in the reactor reached 70 °C, the addition of the MMA/MAA-CoBF solution started using a degassed syringe and a syringe pump (feeding rate=1.866 mL/min, feeding time = 60 min). When the addition was over, stirring continued for another 60 min under the same conditions. The number average molecular weight of the co-oligomers was calculated by analysing the ^{1}H NMR spectra.

General procedure for the synthesis of block copolymers by Free-Radical polymerisation in emulsion.

The amount of monomer to be subsequently added to the PMMA/MAA co-oligomer latex was calculated according to the desired *DP*. For each addition, the volume of aqueous KPS solution added was equal to the monomer volume. The additions were stopped and dilutions with water were made, when solid content reached values above which coagulation was very likely to occur. After every dilution, the solid content of the latex was measured (in g mL^{-1}) and the value was taken into account for calculating the amounts of reagents of the next addition cycle.

Process for the chain extension of co-oligomer (PMMA/MAA) with BzMA (DP_n = 25) by Free-Radical polymerisation in emulsion.

50 mL of PMMA/MAA co-oligomer latex (0.3286 g/mL) were diluted by adding 40 mL of water to achieve a 28% solids content. The resulting latex was charged in the reactor and purged with nitrogen for 30 min under stirring. Subsequently, the emulsion was heated. When the temperature in the reactor reached 80-82 °C and was stabilised, the simultaneous addition of BzMA (27.84 mL, 28.95 g, 0.164 mol) and potassium persulfate aqueous solution (139 mg potassium persulfate in 27.84 mL of water), both previously degassed for 30 min started by the use of degassed syringes and a syringe pump (feeding rate = 0.16 mL/min, feeding time = 232 min). When the addition was over, stirring continued for another 60 min under the same conditions.

Process for the chain extension of co-oligomer (PMMA/MAA) with BzMA (DP_n = 25) by Free-Radical polymerisation in emulsion with plasticisers.

All of the polymerisation procedures were the same as the process for the chain extension of co-oligomer (PMMA/MAA) with BzMA (DP_n = 25) by free-radical polymerisation in emulsion with the addition of the plactisers at the start of the reaction. The mass of the placticiser added to the reaction medium was calculated with respect to weight percentage of the total monomer with the reaction mixture.

Process for the synthesis of seeds in emulsion.

For the seeded emulsion polymerisation, PS (60 mL, 54.54 g, 523.67 mmol) was placed in a 100 mL round bottom flask, nitrogen was purged in the flask for 30 mins.

Meanwhile, ACVA (0.6 g, 2.141 mmol), SDS (4.5 g, 15.6 mmol) and 240 mL of water were charged into a three-neck, 500 mL double jacketed reactor, equipped with a RTD temperature probe and an overhead stirrer. The mixture was purged with nitrogen and stirred at 325 rpm for at least 30 min. Subsequently, the mixture was heated under inert atmosphere. When the temperature in the reactor reached 70 °C, the addition of the PS solution PS (60 mL, 54.54 g, 523.67 mmol) started using a degassed syringe and a syringe pump (feeding rate = 1.333 mL/min, feeding time = 90 min). When the addition was over the final reaction temperature was at 80°C, stirring continued for another 60 min under the same conditions. The number average molecular weight of the co-oligomers was calculated by analysing the ^{1}H NMR spectra.

Figure S3.1:^{1}H NMR spectrum of co-oligomer (reaction C4) with 15 wt% MAA & 85 wt% MMA by composition

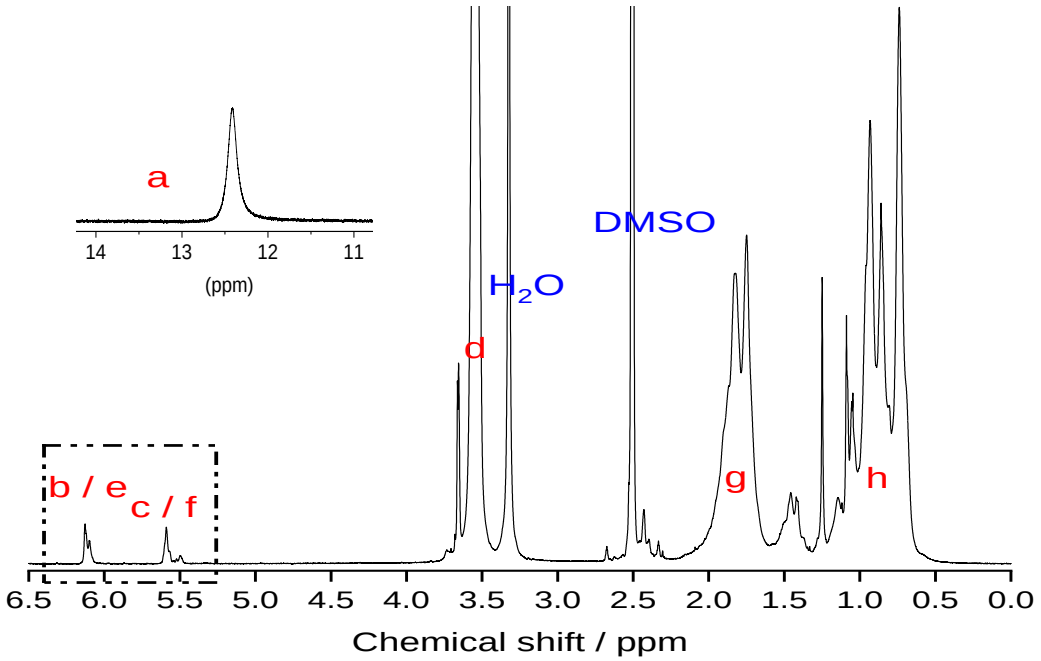

Table S3.1: Assignments of peaks for NMR spectrum in figure S3.1

Peak (ppm)	Integral	Multiplet type	Assignment
12.40	4.22	Broad singlet	Acid proton [a]
6.12-6.09	1.00	Singlet	Vinyl protons [b] and [e]
5.58-5.49	1.00	Singlet	Vinyl protons [c] and [f]
3.55	64.75	Singlet	Methoxy proton [d]
3.32	16.68	Singlet	Residual water protons
2.50	32.36	Quintet	DMSO (solvent) protons
2.5-0.5	42.48	Broad multiplet	In chain methylene and methyl protons [g] and [h]

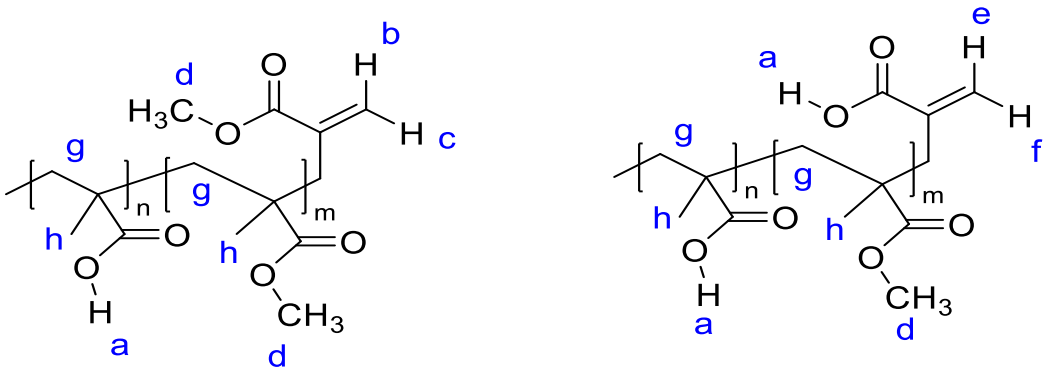

Figure S3.2: Structure of co-oligomer of PMMA/MAA (15 wt% MAA & 85 wt% MMA by composition) with protons labelled for NMR analysis.

Table S3.2:DMA data of the di-block copolymers top and triblock copolymers bottom

DP = 25

Reaction	Onset T_g/ C°	Mid T_g/ C°	End T_g/ C°	Tan δ
15 wt% MAA & 85 wt% MMA	109	127	142	127
B2-2EHMA-DP=25	4	16	50	22
C2-BMA-DP=25	44	55	71	61
D2-BzMA-DP=25	72	82	96	86
E2-EMA-DP=25	92	104	108	101
F2-CHMA-DP=25	108	120	126	121
G2-MMA-DP=25	107	118	124	118

DP = 50

Reaction	Onset T_g/ C°	Mid T_g/ C°	End T_g / C°	Tan δ
15 wt% MAA & 85 wt% MMA	109	127	142	127
B3-2EHMA-DP=50	17	38	51	13/39
C3-BMA-DP=50	38	49	73	55
D3-BzMA-DP=50	77	86	94	86
E3-EMA-DP=50	79	95	106	99
F3-CHMA-DP=50	111	118	125	123
G3-MMA-DP=50	120	128	134	129

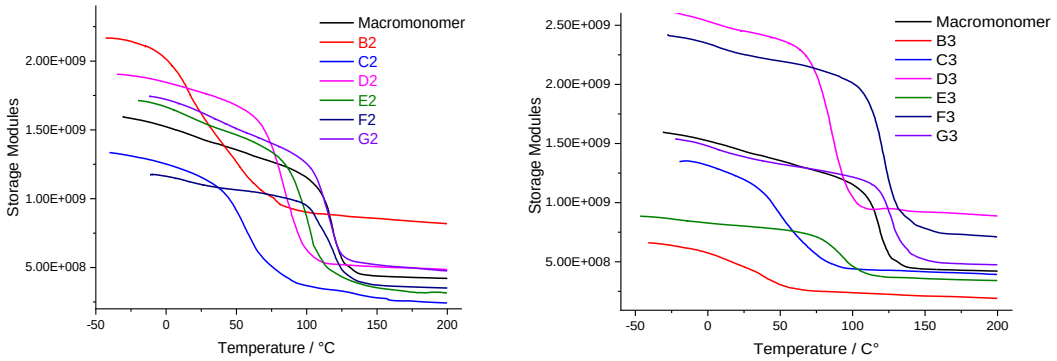

Figure S3.3: DMA data of the di-block copolymers top and triblock copolymers bottom

Surface zeta potential and particle size data for the di-block and tri-block copolymers

Table S3.3:Surface zeta potential data and particle size for the di-block and pseudo tri-block copolymers

Reaction	Zeta potential / mV	Zeta potential S.D. / mV	Particle size/ nm	PDi
15% MAA & 85% MMA	-52.4	7.08	172	0.092
B2-2EHMA-DP=25	-52.2	6.11	202	0.105
B3-2EHMA-DP=50	-48.8	5.72	215	0.166
C2-BMA-DP=25	-49.4	6.06	187	0.080
C3-BMA-DP=50	-49.4	5.72	216	0.106
D2-BzMA-DP=25	-47.1	5.92	190	0.087
D3-BzMA-DP=50	-48.2	5.92	218	0.114
E2-EMA-DP=25	-52.9	7.62	187	0.074
E3-EMA-DP=50	-47.8	6.12	204	0.114
F2-CHMA-DP=25	-45.9	6.10	177	0.115
F3-CHMA-DP=50	-45.3	6.13	158	0.106
G2-MMA-DP=25	-53.8	7.38	183	0.071
G3-MMA-DP=50	-45.9	5.88	191	0.088

^{1}H NMR of di and tri-block copolymers

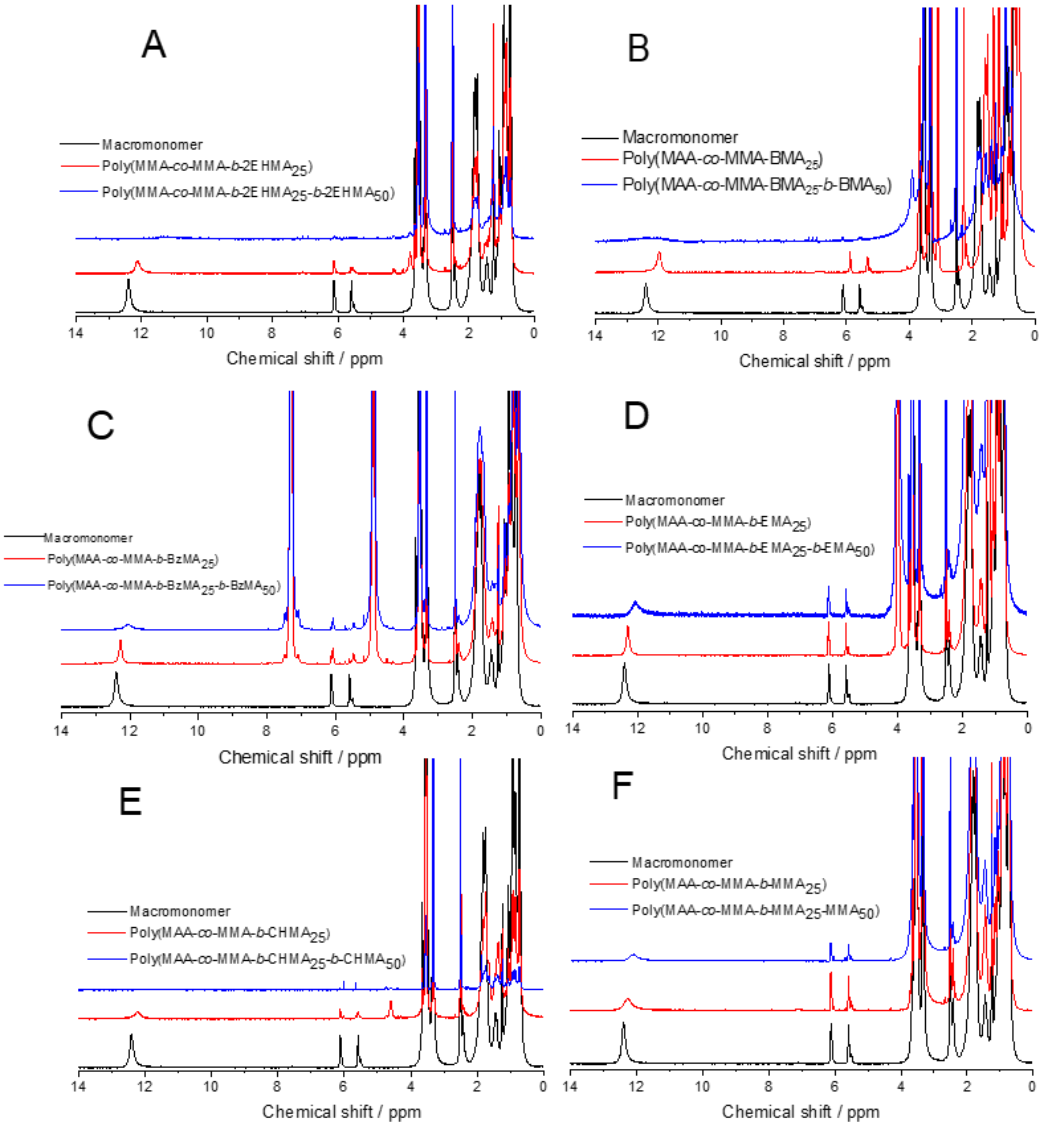

Figure S3.4: ^{1}H NMR of all Di and tri-block copolymers

3.5 References

1. M. Abdollahi, *Polymer Journal*, 2007, **39**, 802.
2. D. Fukuhara and D. Sundberg, *JCT Research*, 2005, **2**, 509-516.
3. C.-F. Lee, T.-H. Young, Y.-H. Huang and W.-Y. Chiu, *Polymer*, 2000, **41**, 8565-8571.
4. I. Schreur-Piet and J. P. A. Heuts, *Polymer Chemistry*, 2017, **8**, 6654-6664.
5. G. W. Ceska, *Journal of Applied Polymer Science*, 1974, **18**, 427-437.
6. G. W. Ceska, *Journal of Applied Polymer Science*, 1974, **18**, 2493-2499.
7. A. K. Tripathi and D. C. Sundberg, *Industrial & Engineering Chemistry Research*, 2013, **52**, 3306-3314.
8. M. Benedetti, T. R. Congdon, S. P. Bassett, M. Alauhdin, S. M. Howdle, D. M. Haddleton, R. Pisano, M. Sangermano and T. L. Schiller, *Polymer Chemistry*, 2017, **8**, 972-975.
9. H. D. M., D. Estelle, K. E. J., K. Dax, M. S. R., B. S. A. F., E. M. D. and S. A. G., *Journal of Polymer Science Part A: Polymer Chemistry*, 2001, **39**, 2378-2384.
10. N. S. Serkhacheva, O. I. Smirnov, A. V. Tolkachev, N. I. Prokopov, A. V. Plutalova, E. V. Chernikova, E. Y. Kozhunova and A. R. Khokhlov, *RSC Advances*, 2017, **7**, 24522-24536.
11. J.-F. Lutz, M. Ouchi, D. R. Liu and M. Sawamoto, *Science*, 2013, **341**.
12. J. J. Vosloo, D. De Wet-Roos, M. P. Tonge and R. D. Sanderson, *Macromolecules*, 2002, **35**, 4894-4902.
13. C. S. Chern, *Progress in Polymer Science*, 2006, **31**, 443-486.
14. S. C. Thickett and R. G. Gilbert, *Polymer*, 2007, **48**, 6965-6991.
15. A. van Herk and H. Heuts, in *Encyclopedia of Polymer Science and Technology*, John Wiley & Sons, Inc., 2002, DOI: 10.1002/0471440264.pst112.
16. K. Matyjaszewski, *Current Opinion in Solid State and Materials Science*, 1996, **1**, 769-776.
17. K. Matyjaszewski and J. Spanswick, *Materials Today*, 2005, **8**, 26-33.
18. C. Barthet, J. Wilson, A. Cadix, M. Destarac, C. Chassenieux and S. Harrisson, *ACS Macro Letters*, 2017, **6**, 1342-1346.
19. N. G. Engelis, A. Anastasaki, G. Nurumbetov, N. P. Truong, V. Nikolaou, A. Shegiwal, M. R. Whittaker, T. P. Davis and D. M. Haddleton, *Nature Chemistry*, 2016, **9**, 171.
20. J. P. A. Heuts and N. M. B. Smeets, *Polymer Chemistry*, 2011, **2**, 2407-2423.
21. D. Kukulj, T. P. Davis and R. G. Gilbert, *Macromolecules*, 1997, **30**, 7661-7666.
22. G. Moad, E. Rizzardo and S. H. Thang, *Polymer*, 2008, **49**, 1079-1131.
23. G. Gody, T. Maschmeyer, P. B. Zetterlund and S. Perrier, *Nature Communications*, 2013, **4**, 2505.
24. R. B. Grubbs, *Polymer Reviews*, 2011, **51**, 104-137.
25. J. Jennings, G. He, S. M. Howdle and P. B. Zetterlund, *Chemical Society Reviews*, 2016, **45**, 5055-5084.
26. N. P. Truong, J. F. Quinn, A. Anastasaki, M. Rolland, M. N. Vu, D. M. Haddleton, M. R. Whittaker and T. P. Davis, *Polymer Chemistry*, 2017, **8**, 1353-1363.
27. K. Jung, C. Boyer and P. B. Zetterlund, *Polymer Chemistry*, 2017, **8**, 3965-3970.
28. S. Pearson, C. St Thomas, R. Guerrero-Santos and F. D'Agosto, *Polymer Chemistry*, 2017, **8**, 4916-4946.
29. N. P. Truong, M. R. Whittaker, A. Anastasaki, D. M. Haddleton, J. F. Quinn and T. P. Davis, *Polymer Chemistry*, 2016, **7**, 430-440.
30. I. Cho and K.-W. Lee, *Journal of Applied Polymer Science*, 1985, **30**, 1903-1926.
31. D. R. Bassett and A. E. Hamielec, *Emulsion Polymers and Emulsion Polymerization*, American Chemical Society, 1981.

32. M. A. Krenceski, J. F. Johnson and S. C. Temin, *Journal of Macromolecular Science, Part C*, 1986, **26**, 143-182.
33. A. M. dos Santos, T. F. McKenna and J. Guillot, *Journal of Applied Polymer Science*, 1997, **65**, 2343-2355.
34. J. Krstina, C. L. Moad, G. Moad, E. Rizzardo, C. T. Berge and M. Fryd, *Macromolecular Symposia*, 1996, **111**, 13-23.
35. J. Krstina, G. Moad, E. Rizzardo, C. L. Winzor, C. T. Berge and M. Fryd, *Macromolecules*, 1995, **28**, 5381-5385.
36. C. L. Moad, G. Moad, E. Rizzardo and S. H. Thang, *Macromolecules*, 1996, **29**, 7717-7726.
37. G. Nurumbetov, N. Engelis, J. Godfrey, R. Hand, A. Anastasaki, A. Simula, V. Nikolaou and D. M. Haddleton, *Polymer Chemistry*, 2017, **8**, 1084-1094.
38. I. Lacík, L. Učňová, S. Kukučková, M. Buback, P. Hesse and S. Beuermann, *Macromolecules*, 2009, **42**, 7753-7761.
39. D. Victoria-Valenzuela, J. Herrera-Ordonez, C. L. A. Ricardo and M. Estévez, *Macromolecular Chemistry and Physics*, 2018, **219**, 1700434.
40. Catherine L. Moad, Graeme Moad, a. Ezio Rizzardo and S. H. Thang, 1996, DOI: S0024-9297(96)00852-2.
41. G. Moad, in *Controlled Radical Polymerization: Mechanisms*, American Chemical Society, 2015, vol. 1187, ch. 12, pp. 211-246.
42. A. Lotierzo, R. M. Schofield and S. A. F. Bon, *ACS Macro Letters*, 2017, **6**, 1438-1443.
43. M. Gilbert, in *Encyclopedia of Materials: Science and Technology*, eds. K. H. J. Buschow, R. W. Cahn, M. C. Flemings, B. Ilschner, E. J. Kramer, S. Mahajan and P. Veyssière, Elsevier, Oxford, 2001, DOI: https://doi.org/10.1016/B0-08-043152-6/01259-6, pp. 1-3.
44. J. A. Lewis, in *Encyclopedia of Materials: Science and Technology*, eds. K. H. J. Buschow, R. W. Cahn, M. C. Flemings, B. Ilschner, E. J. Kramer, S. Mahajan and P. Veyssière, Elsevier, Oxford, 2001, DOI: https://doi.org/10.1016/B0-08-043152-6/01159-1, pp. 6556-6560.
45. S. Porter, G. Sackett and L. Liu, in *Developing Solid Oral Dosage Forms (Second Edition)*, eds. Y. Qiu, Y. Chen, G. G. Z. Zhang, L. Yu and R. V. Mantri, Academic Press, Boston, 2017, DOI: https://doi.org/10.1016/B978-0-12-802447-8.00034-0, pp. 953-996.
46. B. Chen, L. Zhu, F. Zhang and Y. Qiu, in *Developing Solid Oral Dosage Forms (Second Edition)*, eds. Y. Qiu, Y. Chen, G. G. Z. Zhang, L. Yu and R. V. Mantri, Academic Press, Boston, 2017, DOI: https://doi.org/10.1016/B978-0-12-802447-8.00031-5, pp. 821-868.
47. X. Ma, J. A. Sauer and M. Hara, *Polymer*, 1997, **38**, 4425-4431.
48. C. White, B. Pejcic, M. Myers and X. Qi, *Sensors and Actuators B: Chemical*, 2014, **193**, 70-77.
49. R. S. Chow and K. Takamura, *Journal of Colloid and Interface Science*, 1988, **125**, 226-236.
50. A. E. Childress and M. Elimelech, *Journal of Membrane Science*, 1996, **119**, 253-268.
51. Y. Uyama, H. Inoue, K. Ito, A. Kishida and Y. Ikada, *Journal of Colloid and Interface Science*, 1991, **141**, 275-279.
52. Y. Yuan and T. R. Lee, in *Surface Science Techniques*, eds. G. Bracco and B. Holst, Springer Berlin Heidelberg, Berlin, Heidelberg, 2013, DOI: 10.1007/978-3-642-34243-1_1, pp. 3-34.
53. A. Shegiwal, A. M. Wemyss, M. A. J. Schellekens, J. de Bont, J. Town, E. Liarou, G. Patias, C. J. Atkins and D. M. Haddleton, *Journal of Polymer Science Part A: Polymer Chemistry*, 2019, **57**, E1-E9.

54. M. Vuckovac, M. Latikka, K. Liu, T. Huhtamäki and R. H. A. Ras, *Soft Matter*, 2019, **15**, 7089-7096.
55. Q. Zhang, S. Slavin, M. W. Jones, A. J. Haddleton and D. M. Haddleton, *Polymer Chemistry*, 2012, **3**, 1016-1023.

Chapter 4

Polymerisable surfactants for synthesis of polymethacrylates using catalytic chain transfer polymerisation (CCTP) in emulsion combined with sulfur free-RAFT in emulsion polymerisation

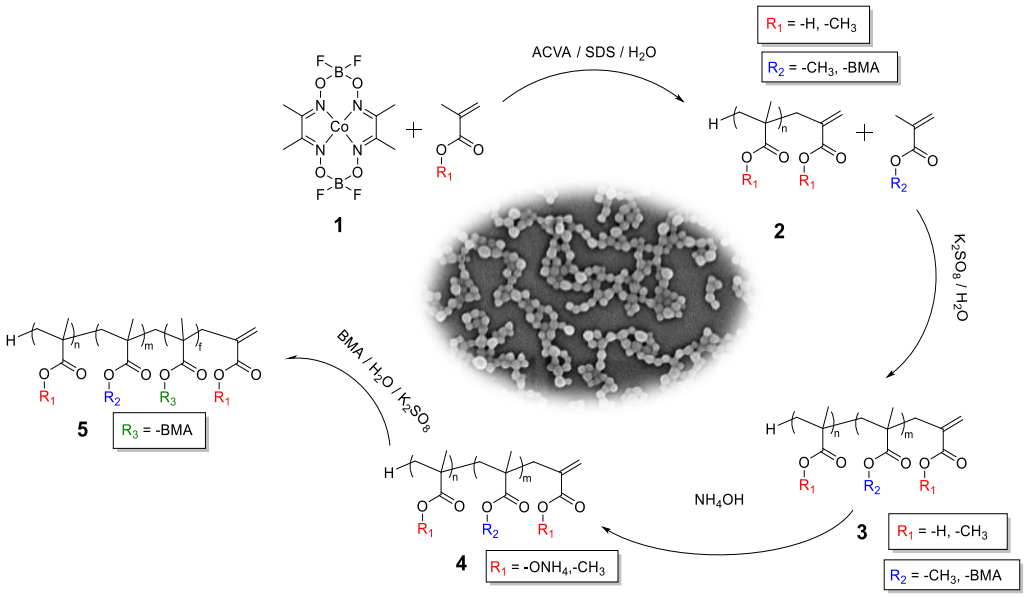

This chapter has been published:

2. A. Shegiwal, A. M. Wemyss, E. Liarou, J. Town, G. Patias, C. J. Atkins, A. Marathianos, D. W. Lester, S. Efstathiou and D. M. Haddleton, European Polymer Journal, 2020, DOI: https://doi.org/10.1016/j.eurpolymj.2020.109491, 109491.

4.1 Introduction

Emulsion polymerisation in the absence of added emulsifier, or surfactant, has received significant attention as a technique for synthesising monodisperse spherical particles and surfactant free clean lattices.[1, 2] Emulsion polymerisation is a complex colloidal phenomena with free radical polymerisation occurring with various external factors affecting nucleation, growth and the stabilization of particles. This has been remarkably successful commercially in many applications including coatings, adhesives and in encapsulation technology.[2-4] Although, the nucleation period is typically very short, the formation of particle nuclei throughout the initial stage of the polymerisation plays a fundamental role in determining the final latex particle size and particle size distribution.[5-12]

Three major mechanisms for particle nucleation in emulsion polymerization have been proposed to date: *Micellar Nucleation Theory*, originally proposed by Harkins[5, 6, 13-15] in 1947 Smith[6, 8] and Ewart[10, 11, 14] and modified by Gardon[5, 7, 8, 10-12, 16], states that micelles are the principal loci of particle formation is usually understood to be the main nucleation mechanism for the monomers with relatively low water solubility ($[M]_{aq} < 15$ mmol dm^{-3}).[5-8, 10, 13-15, 17-19] Homogeneous nucleation models, proposed by Fitch[13-15] and Tsai[5, 8, 15], Priest[5, 8, 10, 12-15] and Roe,[8-11, 13-15] is considered the primary mechanism for formation of particles in systems with surfactant concentration below the critical micelle concentration CMC, surfactant free polymerisation and formation for the monomers with relatively high water solubility's ($[M]_{aq} > 170$ mmol dm^{-3}).[5-8, 10-17, 19-22]

The third nucleation theory which is significantly less common, is called monomer droplets nucleation mechanism as proposed by Hansen[6, 8, 13-15] and, Ugelstad,[6, 13] and Durlin[5-8, 10, 11, 13-15]. However, this third method occurs very rarely: the cases are in some systems such as chlorobutadiene, which have extremely large spontaneous initiation component, the unique systems of mini-emulsion and micro-emulsion polymerisation, and in some controlled radical systems.[7, 12, 23-26] Droplet nucleation is the origin of the high molecular weight products[7, 8, 16, 24, 26].

When reversible deactivation radical polymerisation (RDRP) methods such as atom transfer radical polymerisation (ATRP), nitroxide mediated polymerization (NMP),

single electron transfer living radical polymerisation (SET-LRP) and conventional reversible addition–fragmentation chain transfer polymerisation (RAFT). In comparison to the other techniques, RAFT has been used most successfully under emulsion conditions. There is an excellent review on the use of controlled radical methods in dispersed processes.[27-30] Catalytic chain transfer polymerisation (CCTP) in combination with sulfur-free reversible addition–fragmentation chain transfer polymerisation (SF-RAFT) has been shown to be versatile and simple with relatively mild reactions conditions, requiring only parts per million amounts of bis[(difluoroboryl)dimethylglyoximato] cobalt(II), (CoBF) catalyst in the reaction mixture to obtain low molecular weight co-oligomers with vinyl-end group functionality, a wide range of methacrylic monomers can be utilised regardless of the low rate of propagation, tolerance of various functionalities, and is stable at elevated temperatures and low pH.[31-41]

The utilisation of either transition metals or sulphur comprising catalysts/chain transfer agents often requires purification methods such as precipitation or dialysis to isolate pure usable products. Furthermore, RAFT or copper mediated techniques are often most suited to acrylic and acrylamide monomers and are often less effective with methacrylates, due to lower rates of propagation.[31, 32, 34-36, 39, 42-47]

In this current work we utilise statistical copolymers of methacrylic acid and methyl methacrylate, as synthesised via CCTP, in emulsion, to form the hydrophilic part of an emulsifier. The vinyl-terminated oligomers were in turn successfully utilised as chain transfer agents for the formation of diblock copolymers of butyl and methyl methacrylate, which constitutes to the hydrophobic part of the emulsifier via (SF-RAFT). In turn these polymers were dissolved with various concentrations of ammonium hydroxide and utilised as polymeric polymerisable surfactants in the subsequent emulsion polymerization of butyl methacrylate using potassium persulfate (KPS) as initiator which also stabilizes the polymer particles with no observable coagulation and solid contents as high as 40%.

4.2 Results and Discussion

4.2.1 Synthesis of reactive surfactant *via* SF-RAFT

We focused on statistical co-oligomers of MMA (85 wt%) and MAA (15 wt%) as prepared using CCTP in emulsion polymerisation with bis[(difluoroboryl)dimethylglyoximato] cobalt(II), (CoBF) as the catalyst, which has been previously reported as an effective CTA for the emulsion CCTP of methacrylates.[32, 48] Under these conditions poly($MMA_{85wt\%}$-*co*-$MAA_{15wt\%}$) macromonomers with a range of CoBF concentrations were prepared as previously reported (*table 4.1*)[33]. Co-oligomers with 15 wt% MAA and 85 wt% MMA composition were utilised for the synthesis of all di-block co-polymers, since higher ratios of incorporated acid in the composition resulted in a small amount of coagulation during polymerisation (approximately 3 – 8 wt% with respect to the total solid content). At higher acid concentrations (e.g. 35 wt% MAA and 65 wt% MMA) it was not possible to reproducibly achieve very low M_n polymers with CCTP for reasons that are not fully understood, nevertheless 15wt% acid content was found to be sufficient for these purposes.

Moreover, increasing the acid concentration within the co-oligomers also resulted in an increase in the particle size of the polymers resulting in phase separation ascribed to the particles becoming very hydrophilic and in turn causing water to enter the particles over time giving rise to latex destabilisation, whereas when $MAA_{15wt\%}$-$MMA_{85wt\%}$ was used particle sizes <310 nm were obtained giving stable latex's with long shelf life (stable after 15 months).

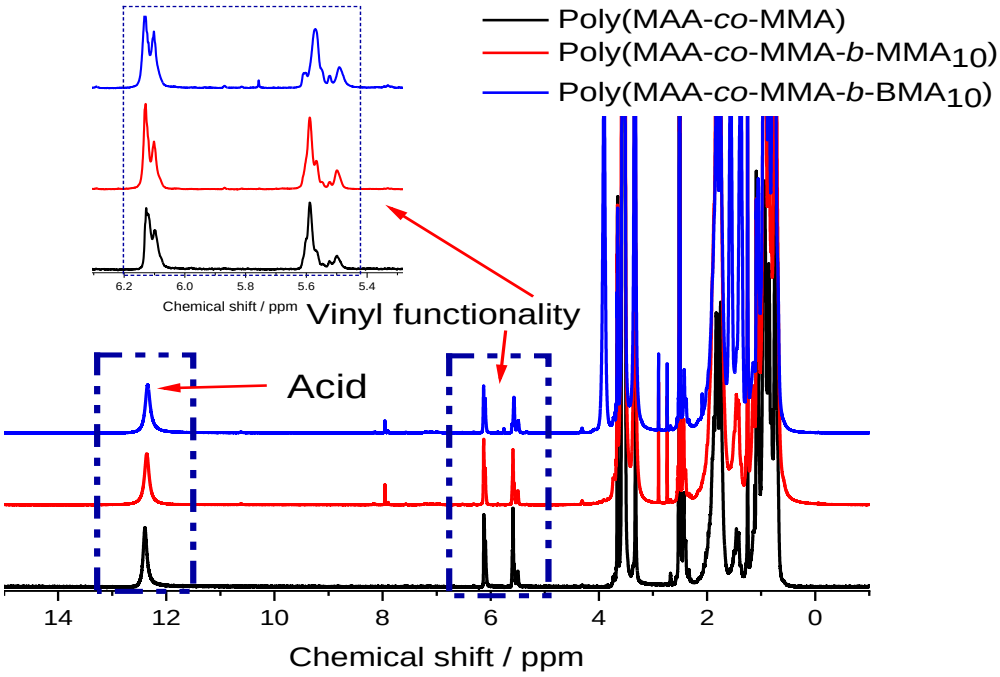

Figure 4.1: 400 MHz ^{1}H NMR in d^6 DMSO of co-oligomer and resulting di-block copolymers.

The CCTP macromonomers **(2),** illustrated in *scheme 4.1*, were used as macro-CTAs for the formation of diblock copolymers **(3)**, with a second block consisting of either butyl methacrylate or methyl methacrylate, with a degree of polymerisation (DP) = 10*)*, both block copolymers contained vinyl end groups and acid (MAA) functionality according to ^{1}H NMR, *figure 4.1*. The second block comprising the hydrophobic part of the emulsifier, with *DP = 10* was selected as a suitable size as when the *DP* was larger (*e.g. DP = 20*) it would not fully solubilise with the addition of ammonium hydroxide solution (NH_4OH), **(4)** leaving a pale white dispersion/solution even upon heating to 60°C. With constant stirring the emulsifier with (*DP = 20*) completely solubilised and whereas with (*DP = 30*) upon addition of (NH_4OH) the latex would remain unchanged (equivalent to the appearance to full fat milk). Upon heating to 60°C it decolourised slightly changing appearance to pale white solution. In turn, polymeric polymerisable surfactants **(4)** were subsequently used in the emulsion polymerization of butyl methacrylate (**5**) using potassium persulfate (KPS) as initiator, which also stabilizes the polymer particles with no observable coagulation and solid contents as high as 40%.

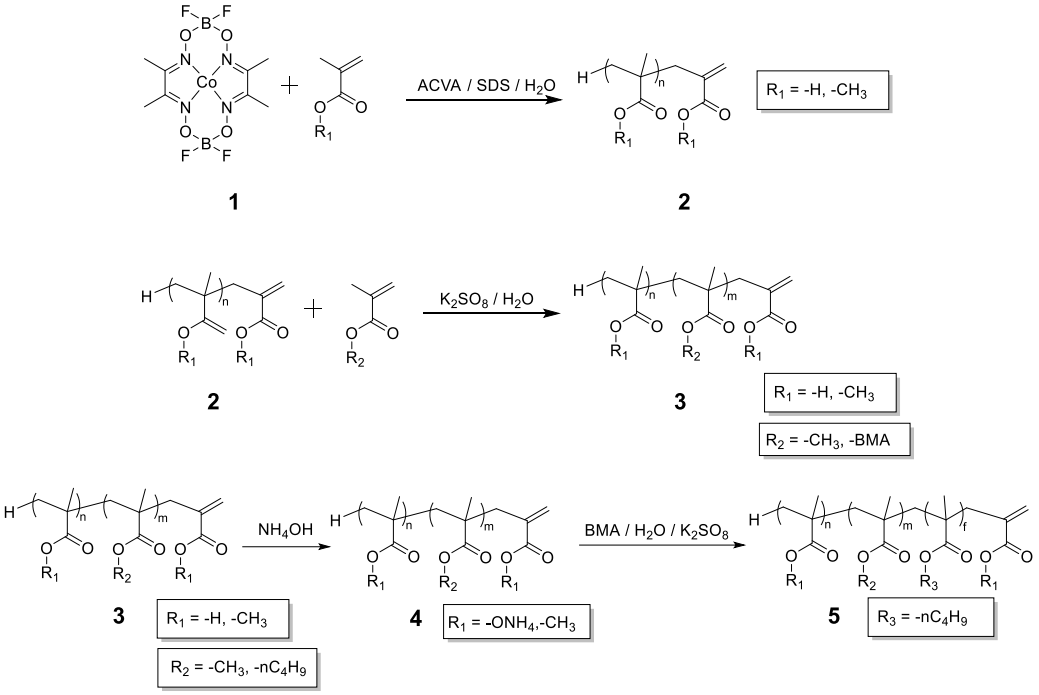

Scheme 4.1: Reaction schemes for CCTP and SF-RAFT polymerisation

4.2.2 Emulsion polymerisation stabilised by polymethacrylate polymerisable surfactants

The polymethacrylate-derived surfactants, as described above, were subsequently used as stabilisers for the emulsion polymerisation of butyl methacrylate. All SF-RAFT polymerisations were performed under monomer-starved conditions, such that the polymer particles were not saturated with monomer, but are being polymerised at an instantaneous conversion of 90% or greater.[32-34, 49, 50] This ensures control of the monomer concentration within the polymer particles. If the reaction were to operate under monomer-flooded conditions, the control over the copolymer composition would be lost.[32, 33, 51]

For all reactions, the [monomer], [initiator] and temperature were kept constant. The temperature was kept >75 °C, as temperatures <70°C are known to reduce the monomer conversion below 100%. This is predominantly due the formation of macroscopic agglomerates on the reactor wall and on the surface of the overhead stirrer, which in turn reduces the latex yield.[11] Furthermore, it has been previously reported that increasing the temperature decreases the particle size due to increasing decomposition rate of the initiator and increasing monomer solubility in the aqueous

phase.[11] Thus, the concentration of the growing chains increases which in turn reduces particle size. However, in these reactions the opposite effect is expected since BMA solubility increases with increase in temperature as a result, the critical chain length increases for the polymer precipitation which may lead larger particles. This was observed for emulsifiers with the hydrophobic moiety consisting of MMA *(DP = 10)* but not for the series of surfactants containing BMA (*DP = 10*) as the hydrophobic moiety, which suggests that the second effect of temperature is also important in determining the particle size as well as to the principal effect of initiated chain concentration in determining the particle size.

Table 4.1: Data for the formation of poly(MMA-co-MAA-b-BMA$_{10}$) diblock with varied concentration of ammonium hydroxide with post free radical polymerisation of poly(BMA) with varied concentration of ammonium hydroxide.

Reaction	$M_{n,SEC}$ / g mol^{-1} (THF)	M_w / g mol^{-1}	Đ	Particle size/ nm	PDi	Prior pH	Post pH
15% MAA & 85% MMA	2200	3700	1.67	-	-	-	2.38
DP-BMA-10	3100	4700	1.50	314	0.099	-	2.23
NH_4OH (0 equiv.)-A'	18000	22400	1.25	644	0.053	2.23	2.19
NH_4OH (0.59 equiv.)-B'	16600	25600	1.54	132	0.283	7.92	4.89
NH_4OH (1.18 equiv.)-C'	18500	26900	1.46	564	0.221	9.19	7.26
NH_4OH (1.77equiv.)-D'	19900	27400	1.38	586	0.088	10.32	7.65

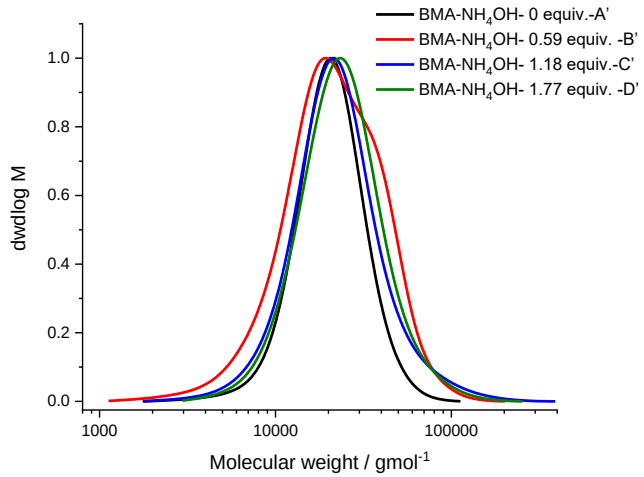

Figure 4.2: : SEC data for the formation of poly(MMA-co-MAA-b-BMA10) diblock with varied concentration of ammonium hydroxide and then post free radical polymerisation of poly (BMA) with varied concentration of ammonium hydroxide.

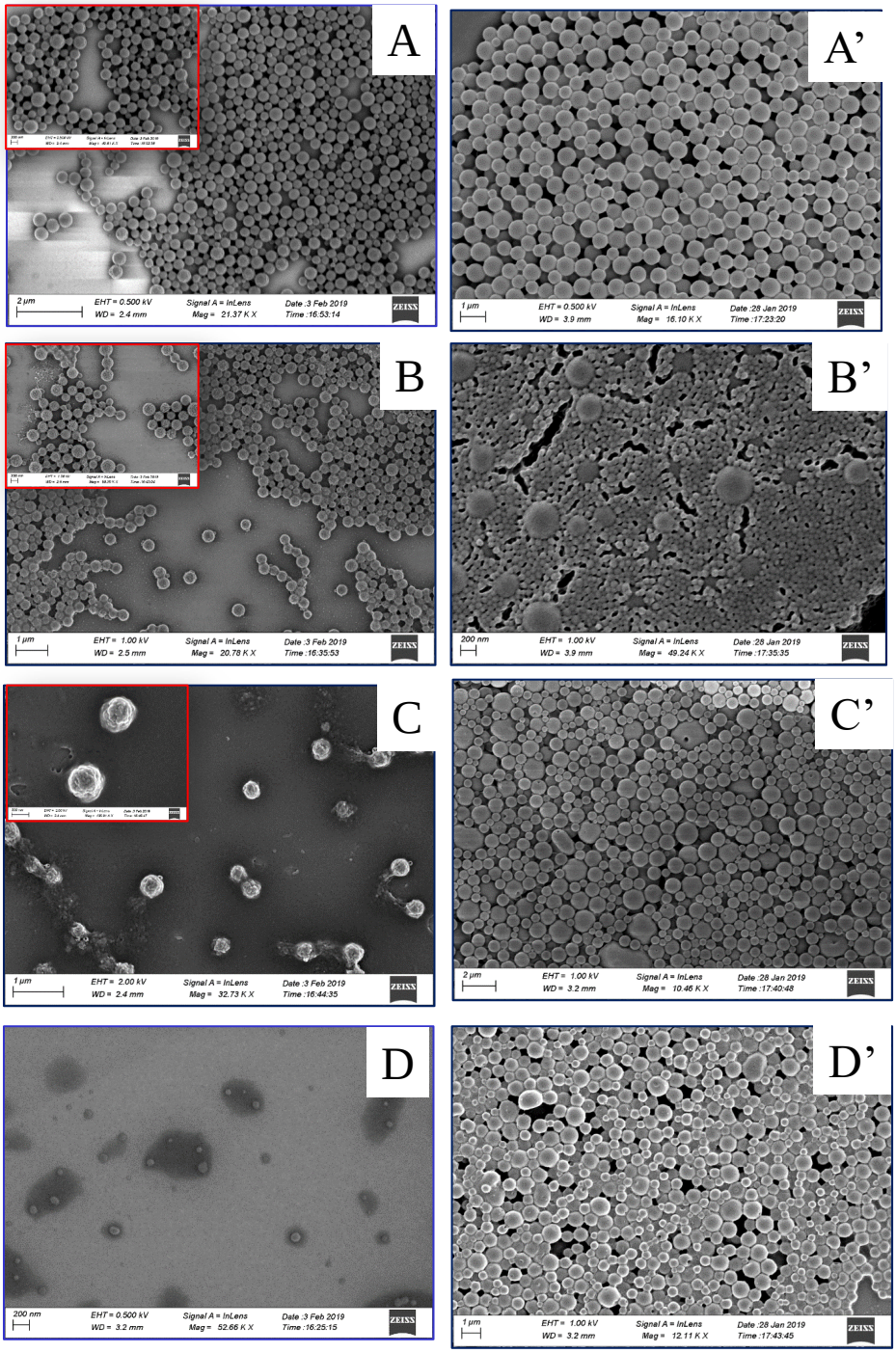

Figure 4.3: Latex particles with A being poly(MMA-co-MAA-b-BMA$_{10}$) diblock, B, C and D are poly(MMA-co-MAA-b-BMA$_{10}$) with 0.59, 1.18 and 1,77 molar equivalence of NH_4OH prior to free radical polymerisation with BMA and A', B' C' and D' post polymerisation with BMA monomer to form poly (BMA).

The diblock copolymers of poly(MMA-*co*-MAA-*b*-BMA$_{10}$) were dissolved in various concentrations of NH_4OH, referred to with respect to molar equivalence with respect to MAA concentration, and utilised as polymerisable surfactants in place of a conventional surfactant such as SDS. For reaction ***A'*** *(figure 4.3)* post polymerisation

with BMA monomer with 0 equivalents of NH_4OH, both the diblock poly(MMA-*co*-MAA-*b*-BMA_{10}) and subsequent *pseudo* tri-block copolymers resulted in monomodal particles of 614 nm, according to DLS and SEM. Upon dropwise addition, of NH_4OH solution to the diblock dispersion of poly(MMA-*co*-MAA-*b*-BMA_{10}) with constant stirring the particle size reduced according to both DLS and SEM. At 0.59 molar equivalence of NH_4OH with respect to MAA reaction ***B*** prior to polymerisation with BMA, the latex appeared slightly soluble with the particle size decreasing from 314 nm to 251 nm.

SEM, images showed reduction particle size upon 0.59 molar equivalence of NH_4OH and the latex particle went from uniform monomodal particles depicted *(figure 4.3: **A**)* to *spongy* less uniform particles *(figure 4.3: **B**)* and most of the particles dissolved with NH_4OH addition and raising of the pH. Upon, free radical polymerization with BMA of the sample with 0.59 molar equivalence of NH_4OH react*ion: **B'** post polymerisation),* new particles were formed with small particle size (*84 nm*) and small number of large particles appeared according to both DLS and SEM. The larger particles (*565 nm*) are due to the initial particles not completely dissolving in NH_4OH such that the BMA polymer grows from the dispersed particles.

For the reaction with 1.18 molar equivalence of NH_4OH reaction *(figure 4.3: **C'** post polymerisation),* prior to the free radical polymerisation with BMA the polymer latex poly(MMA-*co*-MAA-*b*-BMA_{10}) was visually completely soluble with 1.18 molar equivalence of NH_4OH. However, from SEM we observed a small amount of spongy like particles remained prior to the BMA polymerisation (*figure 4.3: **C***). Upon polymerisation with BMA, the SEM showed a few large particles and a majority of the particles uniform in size and the *Đ and* PDi both decreased according to SEM and SEC.

For the reaction with 1.77 molar equivalence of NH_4OH all poly(MMA-*co*-MAA-*b*-BMA_{10}) was visually completely solubilised prior to the polymerisation with BMA. SEM showed the absence of particles upon addition of NH_4OH (*figure 4.3: **D***). Upon polymerisation with BMA, the particles appeared uniform in size according to SEM (*figure 2: **D'** post polymerisation*) and DLS showed a significant reduction in PDi *(table 4.1 & figure 4.2).* Whereas, SEM also showed reduction in *Đ.*

Furthermore, upon each increase in concentration of NH_4OH and associated increase in the pH results in increasing the half-life of the KPS initiator with the molecular weight of the final polymers increasing, the *Đ* decreased suggesting more radicals' present ensuring sufficient propagation and uniformed particle sizes. For all of the reactions, ***A'*** to ***D'*** according to ^1H NMR the ω-vinyl end group functionality remained, 6.12-6.09 ppm and 5.58-5.49 ppm respectively (*table 4.1 and SI figure 4.1 & 4.4*).

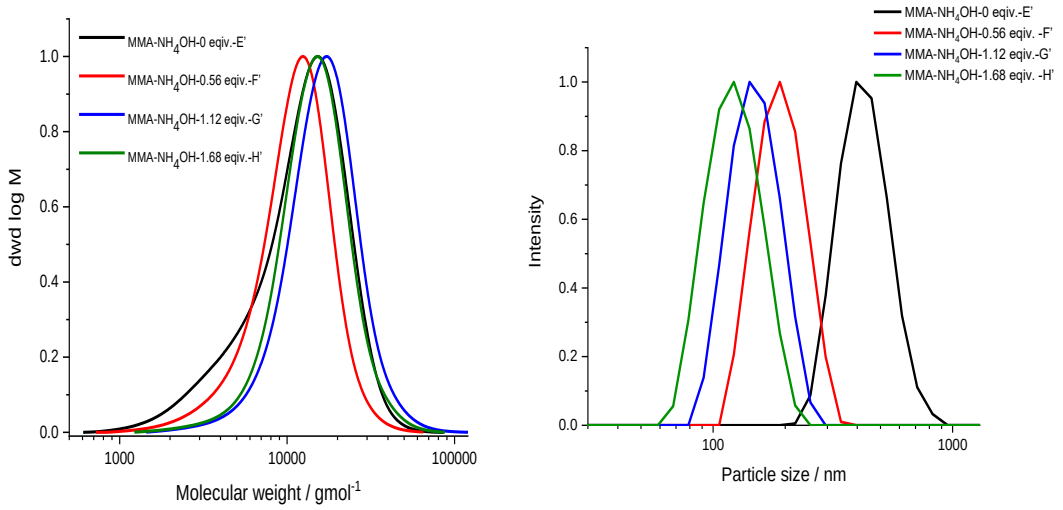

Figure 4.4: SEC and DLS data of formation of poly(MMA-co-MAA-b-MMA10) diblock with varied concentration of ammonium hydroxide and then post free radical polymerisation of poly (BMA) with varied concentration of ammonium hydroxide.

Table 4.2: Data for the formation of poly(MMA-co-MAA-b-MMA_{10}) diblock copolymer with varied concentration of ammonium hydroxide followed by free radical polymerisation of BMA with varied concentration of ammonium hydroxide.

Reaction	$M_{n,SEC}$ / g mol^{-1} (THF)	M_w / g mol^{-1}	*Đ*	Particle size/ nm	PDi	Prior pH	Post pH
15% MAA & 85% MMA	1900	3400	1.75	-	-	-	3.08
DP-MMA-10	3100	4500	1.46	234	0.033	-	2.82
NH_4OH-(0 equiv.)-E'	8900	14000	1.58	415	0.069	2.82	1.89
NH_4OH-(0.56 equiv.)-F'	9200	12300	1.33	186	0.033	6.95	2.95
NH_4OH-(1.12 equiv.)-G'	13900	18100	1.30	144	0.023	7.66	4.37
NH_4OH-(1.68 equiv.)-H'	12400	16000	1.29	118	0.044	9.89	4.85

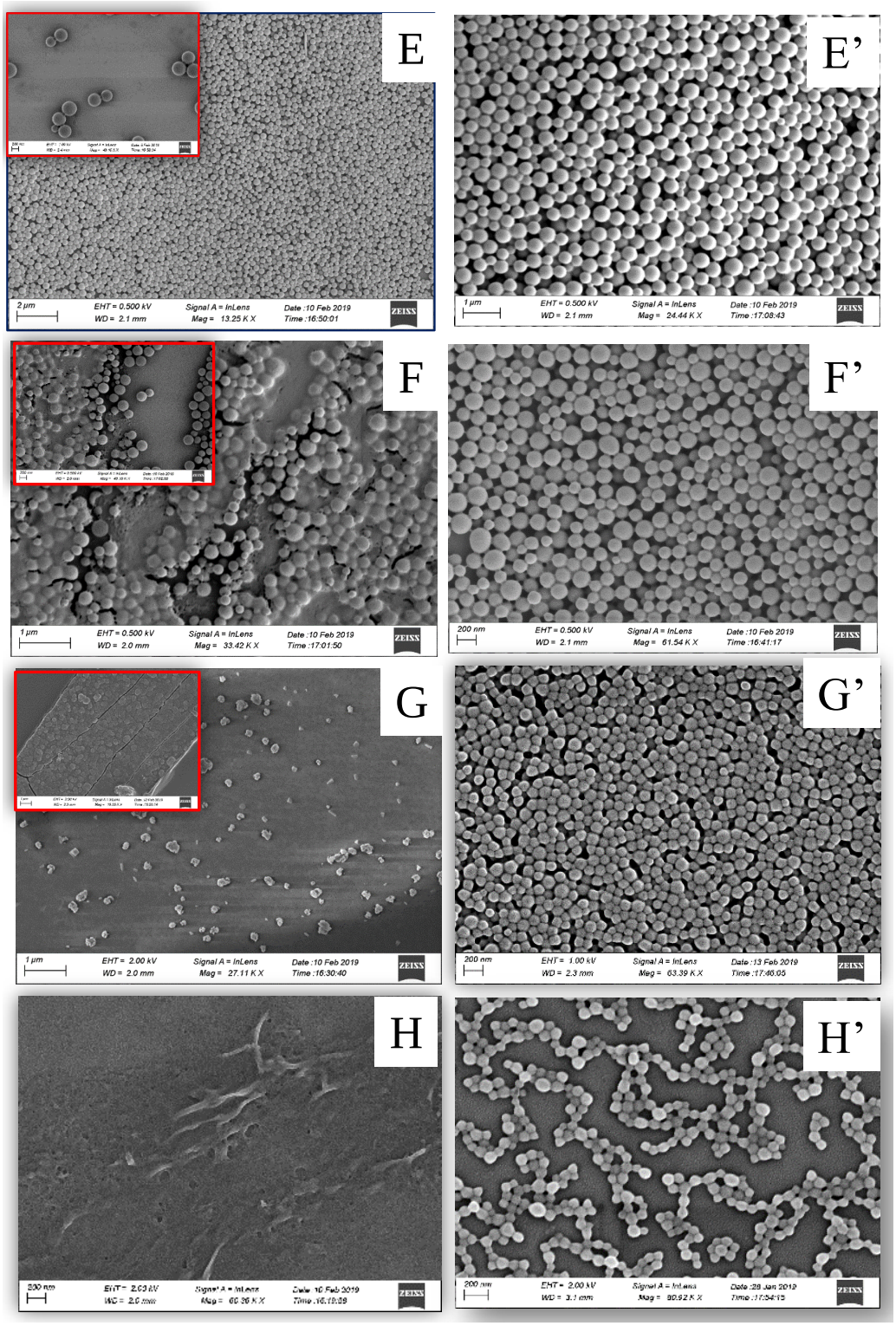

Figure 4.5: Formation of poly(MMA-co-MAA-b-MMA$_{10}$) diblock copolymers with varied concentration of ammonium hydroxide with post free radical polymerisation of poly(BMA) with varied concentration of ammonium hydroxide (inserts are zoomed micrographs from 1 µm to 200 nm).

The diblock copolymers, poly(MMA-*co*-MAA-*b*-MMA_{10}), were dissolved with various amounts of NH_4OH : 0, 0.56, 1.12 and 1.68 molar equivalents with respect to MAA and utilized as polymeric substitutes for standard surfactants. All of the latex, prior to any addition of any NH_4OH, appeared as the SEM image ***E***, with particles of uniform size. With no addition of NH_4OH, reaction ***E'*** both the SEM and DLS showed a large particle 415 nm compared to the reactions where NH_4OH was added. Furthermore, a general trend was observed that larger particles were formed at lower pH (*table 4.2*).

For the reaction with 0.56 molar equivalence of NH_4OH the SEM images prior to reaction showed most of the particles dissolved and some spongy looking particles remained, upon heating it is believed that all the particles dissolved in the NH_4OH, since the solubility of methacrylic containing polymers tends to increase with an increase in temperature and upon post polymerisation with BMA (*figure 4.5:* ***F'***) all of the particles obtained were monomodal in contrast to the surfactant with the hydrophobic moiety consisting of BMA (*table 4.1*). Since BMA is more hydrophobic than MMA it is these polymers are less soluble than the MMA containing analogues at higher temperatures, thus some small particles were observed with SEM at low concentrations of NH_4OH (*figure 4.3*).

Furthermore, the SEC data for 0.56 molar equivalence showed a general decrease in *Đ* and particle size reduced to more than half (186 nm) compared to the reaction with no added NH_4OH. For the reaction with 1.12 and 1.68 molar equivalence of NH_4OH with respect to MAA reaction ***G'*** and ***H'***, showed that prior to the polymerisation SEM images **G** and **H**, showed no presence of any particles and all latex was visually also completely soluble in NH_4OH. Upon completion of the reaction, ***G'*** with 1.12 molar equivalence NH_4OH had particle size of 144 nm according to SEC and ***H'*** with 1.68 molar equivalence of NH_4OH had particle size = 118 nm and the molecular weights showed a general increase in M_n with higher concentrations of NH_4OH.

SEM, images of products from 1.12 and 1.68 molar equivalents of NH_4OH showed that the particles were uniform in size (*figure 4.5:* ***G'***) and ***H'***). Furthermore 1.68 molar equivalents of *NH_4OH,* reaction **H'**, showed particles arranged in worm or necklace

like aggregates yet maintaining a uniformed particle size. For all of the reactions, **E'** to **G'** the vinyl end group functionality was present at reduced amounts according to ^{1}H NMR (*table 4.2 and SI figure 4.3*).

Table 4.3: Formation of poly(MMA-co-MAA-b-MMA$_{10}$) diblock copolymers with 1.68 equivalents of ammonium hydroxide with respect to the MAA with post free radical polymerisation of poly(BMA) at varied temperatures and reaction with latex and KPS dissolved in water having the same pH.

Reaction	$M_{n,SEC}$ / g mol^{-1} (THF)	M_w / g mol^{-1}	*Đ*	Particle size/ nm	PDi	Prior pH	Post pH
15% MAA & 85% MMA	1900	3400	1.75	-	-	3.08	-
DP-MMA-10	3100	4500	1.46	234	0.033	2.82	-
50°C-NH_4OH-1.68 equiv.	15400	25600	1.66	60	0.254	9.57	7.04
65°C-NH_4OH-1.68 equiv.	13700	19700	1.44	43	0.048	9.62	6.44
76°C-NH_4OH-1.68 equiv.	12400	16000	1.29	118	0.044	9.53	4.85
84°C-NH_4OH-1.68 equiv.	8200	11300	1.38	195	0.061	9.64	3.44
76°C-NH_4OH-1.68 equiv.	12900	18400	1.43	58	0.015	9.53	5.99

SEC data (*table 4.3*), shows that the average molecular weights decreases with temperature and the ***Đ*** also decreases with increase in temperature at 50°C with ***Đ*** is 1.66, reducing down to 1.44 at 65°C, and further decreases to 1.29 at 76°C and then at 84°C a slight increase in ***Đ*** is observed to 1.38. Furthermore, at low temperatures some macroscopic coagulum or agglomerates occurred on the reactor wall and on the surface of the overhead stirrer, which in turn reduced the latex yield.[11]

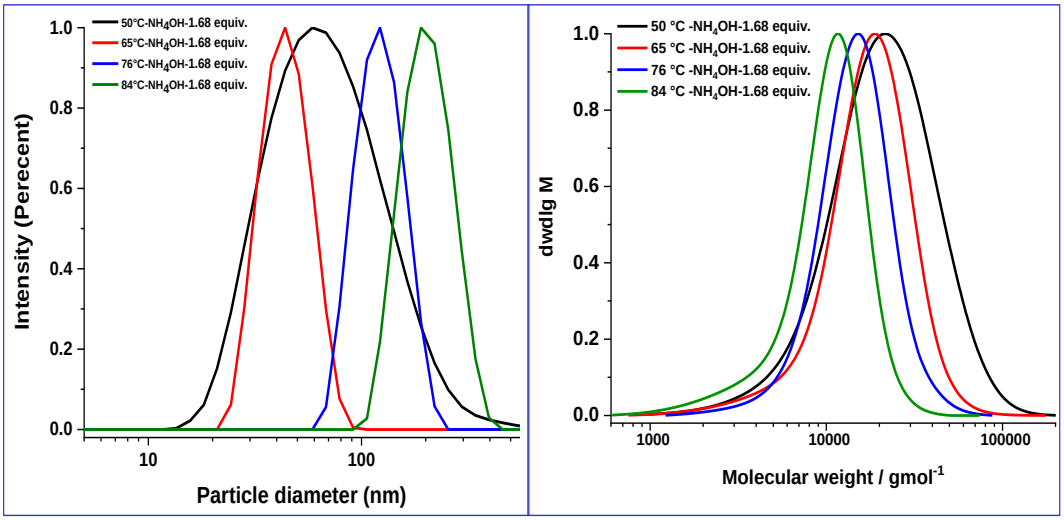

Figure 4.6: DLS and GPC data of formation of poly(MMA-co-MAA-b-MMA10) diblock with 1.68 equivalence of ammonium hydroxide with respect to the MAA with post free radical polymerisation of poly(BMA) at varied temperatures.

From all of the reactions *(table 4.1 & 4.2*), the final pH of the latex dropped from the initial pH; this was initially thought to be due to ammonia from ammonia evaporating at higher temperature or/and KPS producing sulphuric acid at higher temperatures. All of the latexes were dissolved in equal molar equivalence (1.68) of ammonium hydroxide solution with respect to MAA, *(table 4.3*). At lower temperatures there is less significant drop from the initial pH of 9.89 at 50°C the drop in pH was 7.04 whereas as the temperature increases further a more significant drop in pH was seen: 65°C , 6.44, 76°C, 4.85 and finally at 84°C, 3.44.

In order to factor in the significance of temperature on the amount of ammonium hydroxide remaining in solution and [KPS] in aqueous solution the poly(MMA-*co*-MAA-*b*-MMA_{10}) was dissolved with 1.68 equivalents of ammonium hydroxide and heated for 14 hours under nitrogen at 85°C, the initial pH was 9.89 and the final pH after 14 hours was 9.53. Suggesting that the ammonium salt formed from the ammonium hydroxide reacting with poly(MMA-*co*-MAA-*b*-MMA_{10}) remains as the salt and that KPS may play a more important role on pH. The KPS was dissolved in water the initial pH of the deionized water was 5.88 and upon addition of KPS the pH decreased to 3.63, upon heating to 85°C the pH further decreased to 1.87 after 3 hours.

Decomposition of persulfates occurs under moist conditions or at higher temperatures, and once heated to decomposition (120 °C) toxic fumes of SO_x are produced. Throughout use oxygen may be formed. Degradation produces sulfates and at higher temperatures pyrosulfate. In alkaline and neutral solutions persulfate decomposes according to reaction (1) while at higher temperatures and in acidic solutions reactions (2) and (3) occur:

1) $S_2O_8^{(-)} + H_2O \dashrightarrow 2HSO_4^{(-)} + 1/2O_2$
2) $S_2O_8 + H_2O \dashrightarrow H_2SO_5 + H_2SO_4$
3) $H_2SO_5 + H_2O \dashrightarrow H_2O_2 + H_2SO_4$

The foremost kinetic mechanism commences with homolytic cleavage of persulfate to form sulfate ion radicals. These radicals in turn initiate a sequence of propagating reactions producing hydroxyl radicals, which ultimately produce hydrogen peroxide

and a solution of acid sulfate. The net reaction is: $(S_2O_8)^{2-} + H_2O$ gives $1/2O_2 + 2(SO_4)^{2-} + 2H^+$

The final reaction *(table 4.3 & figure 4.6)* was carried out with 1.68 equivalents of ammonium hydroxide with respect to MAA: the pH of the KPS dissolved in water was raised to the same pH as the latex (9.53): post polymerisation the pH dropped to 5.99 and *Đ* according to SEC increased from 1.29 *(table 4.3 & figure 4.6)* to 1.43 with the particle size decreasing from 118 nm to 58 nm (DLS and SEM). This suggests that at higher temperatures KPS still produces some sulphuric acid lowering the pH of the overall reaction. Furthermore, for the reaction of poly(MMA-*co*-MAA-*b*-MMA_{10}) diblock copolymer with 1.68 equivalents of ammonium hydroxide with respect to MAA followed by post free radical polymerisation with BMA at varied temperatures gave polymers with relatively low M_n, SEC, with ^{1}H NMR showing the ω-vinyl end group remaining (*table 4.3 and SI figure 4.2*) (*figure 4.6*). The concentration of initiator has two effects on the particle size.

Firstly, Increasing the KPS concentration increases the concentration of sulfate ions which in turn leads to the stabilisation of particles by achieving smaller particles. Secondly, increasing the concentration of KPS initiator also increases the ionic strength of the aqueous phase, which should result in larger particles. As a result the two opposite effect in theory should compensate each other under the experimental conditions. In (*table 4. 3*) the temperatures were varied and the KPS concentration were kept constant. As the temperature increased the particle size's increased *(table 43 & figure 4.6).*

These reactions (*SI table: 4.2)* demonstrate that for poly(MMA-*co*-MAA-*b*-BMA_{10}) dissolved at various concentrations of NH_4OH followed by post free radical polymerisation of with BMA that the onset of the glass transition temperature, remains relatively the same for all the polymers: $T_{g,\ onset}$ varied between 36 °C ± 3 °C, the $T_{g\ mid}$ = 48 °C ± 1 °C and the $T_{g\ end}$ = 61 °C ± 4 °C. For the reaction with poly(MMA-*co*-MAA-*b*-MMA_{10}) dissolved in varies concentration of NH_4OH and then post free radical polymerisation of with BMA monomer we also observed T_g's that are similar for all the polymers: $T_{g\ onset}$ varied between 38 °C ± 5 °C, $T_{g\ mid}$ = 50 °C ± 2 °C and $T_{g\ end}$ = 64 °C ± 4 °C.

The surface zeta potential (*SI table: 4.3)* for poly(MMA-*co*-MAA-*b*-BMA_{10}) the initial surface zeta potential of the block copolymer was -43 mV, once dissolved at various concentrations of NH_4OH and with post free radical polymerisation of BMA showed: that for reaction with generally large particle size reaction ***A', C' and D'*** including reaction ***B'*** which had combination of large and small particles both according to DLS and SEM has very negative zeta potential -63 ± 8mV compared to the polymers poly(MMA-*co*-MAA-*b*-MMA_{10}). For the reactions with poly(MMA-*co*-MAA-*b*-MMA_{10}) the starting zeta potential of the block copolymer was -52 mV: once dissolved post free radical polymerisation with BMA monomer were undertaken. The zeta potential for the smaller particles reaction ***F', G' H'*** were less negative -38 ± 8mV, whiles for the reaction ***E'*** with large particle according to DLS and SEM, had zeta potential -70 ± 7mV which is in similar region to the particles utilising poly(MMA-*co*-MAA-*b*-BMA_{10}) as polymer surfactant substitute.

Furthermore, since the zeta potential for all the polymers is >-38 ± 8mV the particles have high degree of stability and subsequently, this lead to particles acquiring monodispersity, as seen by DLS and SEC data. The polymers contain carboxylic acid functionality monomers and the zeta surface potential are all in the region expected for carboxylated latex.[33, 52, 53]

4.3 Conclusion

Lowering of the pH with addition of ammonium hydroxide solution and formation of ammonium salts of poly(MMA-*co*-MAA-*b*-BMA_{10}) and poly(MMA-*co*-MAA-*b*-MMA_{10}) resulted in solubilisation to quite low viscosity solutions which could be used as a polymerisable surfactants in emulsion polymerisation. Subsequent emulsion polymerisation of BMA provided latex's with high solid contents (40%), stable, long shelf lives and generally monodisperse particles. This is especially true for higher concentrations of NH_4OH, higher pH, with poly(MMA-*co*-MAA-*b*-BMA_{10}) utilised as the surfactant. Whereas, with poly(MMA-*co*-MAA-*b*-MMA_{10}) we achieved monodisperse particles at varies concentration of ammonium hydroxide and was an effective way to control the average particle sizes. We find out that at lower pH's (acidic) the final latex occurred had larger particle size's. This is due to the ionic initiator utilised (KPS) which at higher temperature and acidic pH produces H_2SO_4 (aq) which lowers the final pH further (more acidic) resulting in larger particle sizes

at lower pH's. Furthermore, these latex particles derived from polymerisable surfactants for polymethacrylate; opens the possibility for numerous applications in medical diagnostics, adhesives, impact modifiers, as well as paper and textile coatings.

4.4 Supporting information

4.4.1 Instruments and analysis

Size Exclusion Chromatography (SEC)

SEC analyses in THF were carried out on an Agilent 390-LC MDS instrument equipped with differential refractive index (DRI) and a dual wavelength UV detector. The system was equipped with 2 x PLgel Mixed D columns (300 x 7.5 mm) and a PLgel 5 µm guard column. The eluent was THF with 2 % TEA (triethylamine) and 0.01 % BHT (butylated hydroxytoluene) additives. Samples were run at 1 ml/min at 30°C. Poly(methyl methacrylate) (PMMA) standards (12) in range of 500-1.5 x 10^6 g mol^{-1} and polystyrene (PS) (13) standards in the range 200-3.6 x 10^6 g mol^{-1} were used to calibrate the system and fitted with a third order polynomial Agilent EasyVials) were used for calibration. Analyte samples were filtered through a GVHP membrane with 0.22 μm pore size before injection. Respectively, experimental molar mass ($M_{n,SEC}$) and dispersity ($Đ$) values of synthesized polymers were determined by conventional calibration using Agilent GPC/SEC software.

Nuclear Magnetic Resonance (^{1}H NMR)

^{1}H NMR spectra were recorded on Bruker DPX-300 and HD-400 spectrometers using deuterated dimethyl sulfoxide, obtained from Aldrich. Chemical shifts are given in ppm downfield from the internal standard tetramethylsilane and data was analysed using ACD/NMR data software.

Dynamic Light Scattering DLS

DLS measurements were performed on a Malvern instrument Zetasizer Nano Series instrument with a detection angle of 173°, where the intensity weighted mean hydrodynamic size (Z-average) and the width of the particle size distribution (PSD) were obtained from analysis of the autocorrelation function. 1 µL of latex was diluted with 1 mL of deionized water previously filtered with 0.20 µm membrane to ensure

the minimization of dust and other particulates. At least 3 measurements at 25 °C were made for each sample with an equilibrium time of 2 min before starting measurement.

Scanning Electron Microscopy: Samples preparation

Scanning electron microscopy was performed using a Zeiss SUPRA 55-VP scanning electron microscope (SEM) with a field emission electron gun (FEG). Best results were obtained when using the InLens detector with 3.5 mm working distance, 30 and 20 µm aperture and 0.5-3 kV acceleration voltage, with respect to sample tolerance. 1 µL of each sample was dissolved in 5 mL of DI water and aliquots of 7 µL were drop casted on silicon wafer chips (5 mm x 7 mm) attached to aluminium specimen stubs. For the improvement of the sample imaging, gold (Au) sputter coating was applied for 15 seconds prior to imaging.

T_g measurements via DMA

The method of analysis used was Pekin Elmer DMA 8000 using single cantilever geometry orientation horizontally with all the polymer latex samples were in powdered form. A sample mass between the mass of 0.06-0.09 g were measured onto material pocket envelopes with length 14.8 mm, width 7.43-7.47 mm and thickness 1.8-2.2 mm. The starting temperature was 0°C and end temperature was 180°C. The strain 0.02 mm and heating rates 2°C/min with frequency of 1 Hz were performed onto the sample. The instrument was calibrated with ultra-high molecular weight Poly(MMA) after every run.

4.4.2 General polymerisation procedure

Materials

All materials were purchased from Sigma Aldrich or Fisher at highest possible purity. Monomers were used as brought from supplier. Sigma products: 4,4′-Azobis(4-cyanovaleric acid) ≥98.0% (T); Methyl methacrylate contains ≤30 ppm MEHQ as inhibitor; Methacrylic acid contains 250 ppm MEHQ as inhibitor, 99%; Potassium persulfate, ACS reagent, ≥99.0%; Butyl methacrylate 99%, contains ~50 ppm monomethyl ether hydroquinone as inhibitor, ammonia hydroxide solution 25 v/v% and sodium dodecyl sulfate, ACS reagent, ≥99.0%. CoBF old (i.e. *17 years old*) and

new batch was synthesised in our group and has been reported previously in literature.[55]

Process for the synthesis of co-oligomer (PMMA/MAA) by CCTP in emulsion.

In a typical CCTP emulsion polymerisation, CoBF (0.02243 g, 0.0583 mmol) was placed in a 250 mL round bottom flask together with a stirring bar. Nitrogen was purged in the flask for at least 1h. Subsequently, MMA (96.3 mL, 90.14 g, 900.29 mmol) and MAA (15.7 mL, 15.94 g, 185.10 mmol) previously deoxygenated for 30 min was added to the flask via a deoxygenated syringe. The mixture was vigorously stirred under inert atmosphere until total dissolution of the catalyst. Meanwhile, 4,4'-azobis(4-cyanovaleric acid) (ACVA) (1.357 g, 4.842 mmol), SDS (2.143 g, 7.434 mmol) and 250 mL of water were charged into a three-neck, 500 mL double jacketed reactor, equipped with a RTD temperature probe and an overhead stirrer. The mixture was purged with nitrogen and stirred at 325 rpm for at least 30 min. Subsequently, the mixture was heated under inert atmosphere. When the temperature in the reactor reached 70 °C, the addition of the MMA/MAA-CoBF solution started using a deoxygenated syringe and a syringe pump (feeding rate=1.866mL/min, feeding time = 60 min). When the addition was over, stirring continued for another 60 min under the same conditions. The number average molecular weight of the co-oligomers was calculated by analysing the ^{1}H NMR spectra.

Process for the synthesis of bis[(difluoroboryl)dimethylglyoximato] cobalt(II), (CoBF).

Cobalt (II) acetate tetrahydrate was heated under vacuum at 110 °C with a pressure of 2 mbar for 5-6 hours with magnetic stirring (the pink powder turns purple upon becoming anhydrous). Under a nitrogen atmosphere equipped with magnetic stirrer anhydrous cobalt(II) acetate (3.14 g, 0.0126 mol) and dimethyl glyoxime (4.47 g, 0.0344 mol) were added and purged with N_2 for 1 hour. Subsequently, ethyl acetate (77.12 ml, 0.87 mol) was dried with $MgSO_4$ and decanted and isolated (filtered with gravity filtration using filter paper). The ethyl acetate was deoxygenated for 30 minutes prior to addition to the mixture. The mixture was stirred vigorously for 30 min. Boron trifluoride etherate (BF_3EtO) (13.03 mL, 0.09 mol) was deoxygenated with nitrogen and added via syringe pump over a period of 10 minutes with continues

vigorous stirring. The resulting solution was heated to 55 °C and held at that temperature for 30 minutes to complete the reaction. Sodium bicarbonate (3.57 g, 0.042 mol) was added in portions to avoid excessive frothing. When the bicarbonate addition was complete the reaction mixture was cooled to 5 °C and stirred for an hour to allow product to recrystallize. Filtration was carried out in (2 x 70 mL) H_20 and (2 x 20 mL) MeOH.

General procedure for the synthesis of block copolymers by Free-Radical polymerisation in emulsion.

The amount of monomer to be subsequently added to the PMMA/MAA co-oligomer latex was calculated according to the desired *DP*. For each addition, the volume of aqueous KPS solution added was equal to the monomer volume. The additions were stopped and dilutions with water were made, when solid content reached values above which coagulation was very likely to occur. After every dilution, the solid content of the latex was measured (in g mL^{-1}) and the value was taken into account for calculating the amounts of reagents of the next addition cycle.

Process for the chain extension of co-oligomer (PMMA/MAA) with MMA (DP_n = 10) by Free-Radical polymerisation in emulsion.

50 mL of PMMA/MAA co-oligomer latex (0.35 g/mL) were diluted by adding 147 mL of water to achieve a 15% solids content. The resulting latex was charged in the reactor and purged with nitrogen for 30 min under stirring. Subsequently, the emulsion was heated. When the temperature in the reactor reached 80-82 °C and was stabilised, the simultaneous addition of MMA (10.399 mL, 9.734 g, 0.0972 mol) and potassium persulfate aqueous solution (52 mg potassium persulfate in 10.399 mL of water), both previously deoxygenated for 30 min started by the use of deoxygenated syringes and a syringe pump (feeding rate = 0.16 mL/min, feeding time = 65 min). When the addition was over, stirring continued for another 60 min under the same conditions.

Process for utilising poly(MMA-co-MAA-b-BMA_{10}) block copolymer as surfactant substitute for Free-Radical polymerisation of poly(BMA) in emulsion.

57.4 mL of poly(MMA-co-MAA-b-BMA_{10}) latex (total surfactant 7 g) was dissolved in (1.8 ml, 0.4064 g, 11.60 mmol) of ammonia solution 25% NH_4OH were diluted by

adding 80 mL of water to achieve a 40% solids content. The resulting latex was charged in the reactor and purged with nitrogen for 30 min under stirring. Subsequently, the emulsion was heated. When the temperature in the reactor reached 76 °C and was stabilised, the simultaneous addition of BMA (60 mL, 53.64 g, 0.3772 mol) and potassium persulfate aqueous solution (0.9 g, 3.329 mmol potassium persulfate in 60 mL of water), both previously deoxygenated for 30 min started by the use of deoxygenated syringes and a syringe pump (feeding rate = 0.16 mL/min, feeding time = 375 min). When the addition was over, stirring continued for another 60 min under the same conditions.

Process for utilising poly(MMA-co-MAA-b-MMA_{10}) block copolymer as surfactant substitute for Free-Radical polymerisation of poly(BMA) in emulsion (varied concentration NH_4OH and temperatures).

52 mL of poly(MMA-co-MAA-b-MMA_{10}) latex (total surfactant 7 g) was dissolved in (1.8 ml, 0.4064 g, 11.60 mmol) of ammonia solution 25 vv% NH_4OH were diluted by adding 85.4 mL of water to achieve a 40% solids content. The resulting latex was charged in the reactor and purged with nitrogen for 30 min under stirring. Subsequently, the emulsion was heated. When the temperature in the reactor reached 76 °C and stable, the simultaneous addition of BMA (60 mL, 53.64 g, 0.3772 mol) and potassium persulfate aqueous solution (0.9 g, 3.329 mmol potassium persulfate in 60 mL of water), both previously deoxygenated for 30 min started by the use of deoxygenated syringes and a syringe pump (feeding rate=0.16 mL/min, feeding time = 375 min). When the addition was over, stirring continued for a further 60 min under the same conditions.

CCTP co-oligomers with varied CoBF concentration under monomer starved condition

SI table 4.1: CCTP co-oligomers with varied CoBF concentration under monomer starved condition.

Reaction	CoBF / (*ppm*)	M_n^{NMR} (g/mol)	M_n^{SEC} (g/mol)	M_w (g/mol)	$Đ$
C1	0	-	57500	221000	3.84
C2	54	5600	5900	9100	1.56
C3	88	3600	3800	5600	1.47
C4	94	2300	2700	3900	1.45
C5	108	1900	2100	3300	1.58
C6	133	1600	1600	2700	1.73

Glass transition temperature (T_g)

SI table 4.2: T_g temperature data of formation of poly(MMA-co-MAA-b-BMA10) and poly(MMA-co-MAA-b-MMA10) diblock with varied concentration of ammonium hydroxide and then post free radical polymerisation of poly (BMA) with varied concentration of ammonium hydroxide.

15wt%MAA-85wt%MMA-BMA_{10}

Reaction	Onset / T_g	Mid / T_g	End / T_g
DP-BMA-10	74	100	110
NH_4OH-0 equiv.-A’	34	49	56
NH_4OH-0.59 equiv.-B’	36	49	64
NH_4OH-1.18 equiv.-C’	39	47	65
NH_4OH-1.77equiv.-D’	35	48	62

15wt%MAA-85wt%MMA-MMA_{10}

Reaction	Onset / T_g	Mid / T_g	End / T_g
DP-MMA-10	109	117	122
NH_4OH-0 equiv.-E’	37	52	68
NH_4OH-0.56 equiv.-F’	43	50	67
NH_4OH-1.12 equiv.-G’	33	48	60
NH_4OH-1.68 equiv.-H’	40	51	64

Surface zeta potential and particle size data for the di-block and tri-block copolymers

SI table 4.3: Zeta potential data of formation of poly(MMA-co-MAA-b-BMA10) and poly(MMA-co-MAA-b-MMA10) diblock with varied concentration of ammonium hydroxide and then post free radical polymerisation of poly (BMA) with varied concentration of ammonium hydroxide

Reaction	Zeta potential/ mV	Zeta potential S.D. / mV	Particle size/ nm	PDi
DP-BMA-10	-43	7	314	0.099
NH_4OH-0mL-A'	-56	8	644	0.053
NH_4OH-0.6Ml-B'	-61	7	132	0.283
NH_4OH-1.2Ml-C'	-62	8	564	0.221
NH_4OH-1.8mL-D'	-69	6	586	0.088
DP-MMA-10	-52	7	234	0.033
NH_4OH-0mL-E'	-70	7	415	0.069
NH_4OH-0.6mL-F'	-40	8	186	0.033
NH_4OH-1.2mL-G'	-39	6	144	0.023
NH_4OH-1.8mL-H'	-37	6	118	0.044

^{1}H NMR of block copolymers and free radical BMA reaction with 1.68 and 1.78 equiv. of NH_4OH.

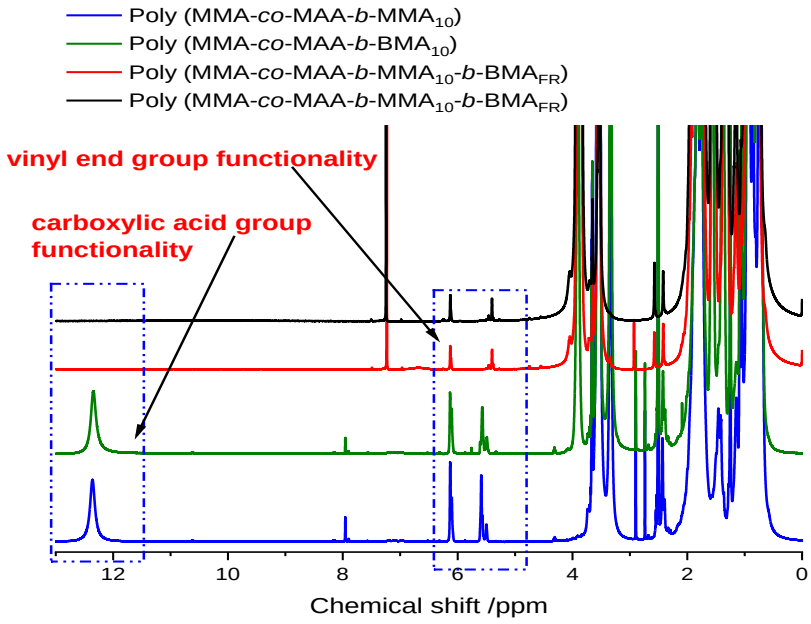

SI Figure 4.1: ^{1}H NMR of block copolymers and free radical BMA reaction

^{1}H Poly(MMA-*co*-MAA-b-MMA$_{10}$) diblock with 1.68 equivalence of ammonium hydroxide with respect to the MAA and then post free radical polymerisation of poly (BMA) at varied temperatures.

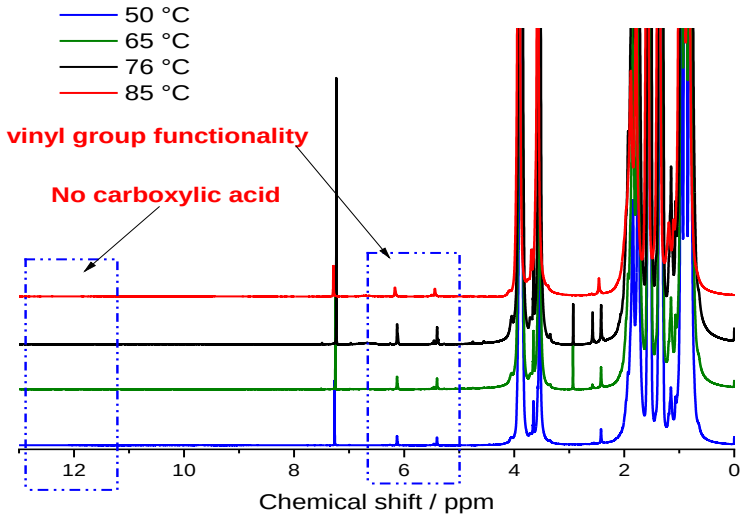

SI Figure 4.2: ^{1}H of poly(MMA-co-MAA-b-MMA10) diblock with 1.68 equivalence of ammonium hydroxide with respect to the MAA and then post free radical polymerisation of poly (BMA) at varied temperatures.

^{1}H Data of formation of poly(MMA-co-MAA-b-BMA$_{10}$) diblock with varied concentration of ammonium hydroxide and then post free radical polymerisation of poly (BMA) with varied concentration of ammonium hydroxide.

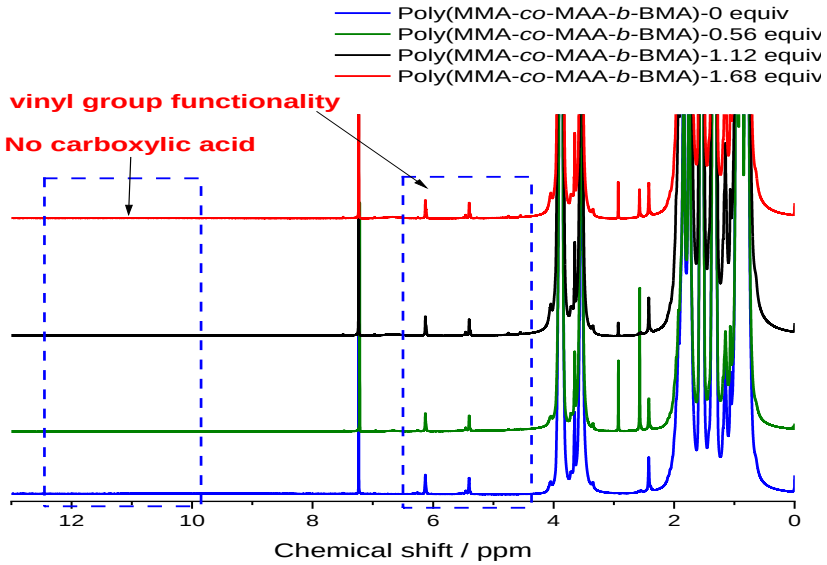

SI Figure 4.3: ^{1}H Data of formation of poly(MMA-co-MAA-b-MMA$_{10}$) diblock with varied concentration of ammonium hydroxide and then post free radical polymerisation of poly (BMA) with varied concentration of ammonium hydroxide

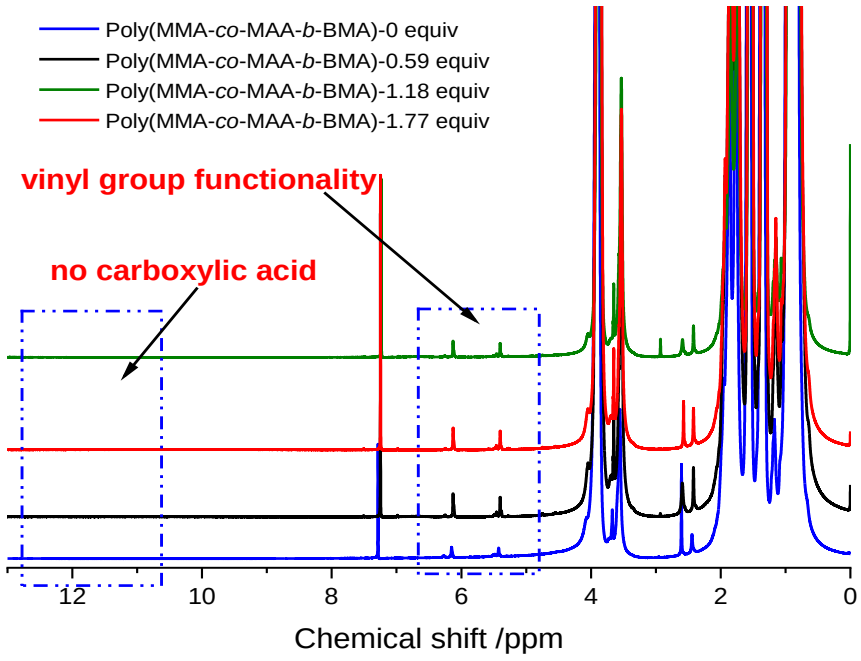

SI Figure 4.4: ^{1}H Data of formation of poly(MMA-co-MAA-b-BMA$_{10}$) diblock with varied concentration of ammonium hydroxide and then post free radical polymerisation of poly (BMA) with varied concentration of ammonium hydroxide

4.5 References

1. I. Martín-Fabiani, J. Lesage de la Haye, M. Schulz, Y. Liu, M. Lee, B. Duffy, F. D'Agosto, M. Lansalot and J. L. Keddie, *ACS Applied Materials & Interfaces*, 2018, **10**, 11221-11232.
2. J. Lesage de la Haye, I. Martin-Fabiani, M. Schulz, J. L. Keddie, F. D'Agosto and M. Lansalot, *Macromolecules*, 2017, **50**, 9315-9328.
3. B. T. T. Pham, D. Nguyen, V. T. Huynh, E. H. Pan, B. Shirodkar-Robinson, M. Carey, A. K. Serelis, G. G. Warr, T. Davey, C. H. Such and B. S. Hawkett, *Langmuir*, 2018, **34**, 4255-4263.
4. D. Nguyen, B. T. T. Pham, V. Huynh, B. J. Kim, N. T. H. Pham, S. A. Bickley, S. K. Jones, A. Serelis, T. Davey, C. Such and B. S. Hawkett, *Polymer*, 2016, **106**, 238-248.
5. M. Abdollahi, *Polymer Journal*, 2007, **39**, 802.
6. H. Baharvand, A. Rabiee and H. J. C. J. Jamshidi, 2013, **75**, 241-246.
7. C. S. Chern, *Progress in Polymer Science*, 2006, **31**, 443-486.
8. I. Kuehn and K. Tauer, *Macromolecules*, 1995, **28**, 8122-8128.
9. G. Lichti, R. G. Gilbert and D. H. Napper, *Journal of Polymer Science: Polymer Chemistry Edition*, 1983, **21**, 269-291.
10. P. Nazaran and K. Tauer, *Macromolecular Symposia*, 2007, **259**, 264-273.
11. T. Tanrisever, O. Okay and I. Ç. Sönmezoğlu, *Journal of Applied Polymer Science*, 1996, **61**, 485-493.
12. S. C. Thickett and R. G. Gilbert, *Polymer*, 2007, **48**, 6965-6991.
13. R. M. Fitch and C. H. Tsai, *Polymer Colloids*, 1971, 73-102.
14. F. K. Hansen and J. Ugelstad, *Journal of Polymer Science: Polymer Chemistry Edition*, 1979, **17**, 3033-3045.

15. F. K. Hansen and J. Ugelstad, *Journal of Polymer Science: Polymer Chemistry Edition*, 1978, **16**, 1953-1979.
16. C.-S. Chern and H.-T. Chang, *Polymer International*, 2002, **51**, 1428-1438.
17. F. K. Hansen, in *Polymer Latexes*, American Chemical Society, 1992, vol. 492, ch. 2, pp. 12-27.
18. A. R. Goodall, M. C. Wilkinson and J. Hearn, *Journal of Polymer Science: Polymer Chemistry Edition*, 1977, **15**, 2193-2218.
19. Z. Song and G. W. Poehlein, *Journal of Colloid and Interface Science*, 1989, **128**, 486-500.
20. S. Beyaz, T. Tanrisever and H. Kockar, *Macromolecular Research*, 2010, **18**, 1154-1159.
21. G. W. Ceska, *Journal of Applied Polymer Science*, 1974, **18**, 427-437.
22. C. e. Yan, S. Cheng and L. Feng, *Journal of Polymer Science Part A: Polymer Chemistry*, 1999, **37**, 2649-2656.
23. A. van Herk and H. Heuts, in *Encyclopedia of Polymer Science and Technology*, John Wiley & Sons, Inc., 2002, DOI: 10.1002/0471440264.pst112.
24. J. M. Asua, 2004, **42**, 1025-1041.
25. L. L. de Arbina, M. J. Barandiaran, L. M. Gugliotta and J. Asuat, *Polymer*, 1996, **37**, 5907-5916.
26. D. R. Bassett and A. E. Hamielec, *Emulsion Polymers and Emulsion Polymerization*, AMERICAN CHEMICAL SOCIETY, 1981.
27. W. Zhang, F. D'Agosto, P.-Y. Dugas, J. Rieger and B. Charleux, *Polymer*, 2013, **54**, 2011-2019.
28. I. Chaduc, M. Girod, R. Antoine, B. Charleux, F. D'Agosto and M. Lansalot, *Macromolecules*, 2012, **45**, 5881-5893.
29. W. Zhang, F. D'Agosto, O. Boyron, J. Rieger and B. Charleux, *Macromolecules*, 2012, **45**, 4075-4084.
30. P. B. Zetterlund, S. C. Thickett, S. Perrier, E. Bourgeat-Lami and M. Lansalot, *Chemical Reviews*, 2015, **115**, 9745-9800.
31. H. Willcock and R. K. O'Reilly, *Polymer Chemistry*, 2010, **1**, 149-157.
32. N. G. Engelis, A. Anastasaki, G. Nurumbetov, N. P. Truong, V. Nikolaou, A. Shegiwal, M. R. Whittaker, T. P. Davis and D. M. Haddleton, *Nature Chemistry*, 2016, **9**, 171.
33. A. Shegiwal, A. M. Wemyss, M. A. J. Schellekens, J. de Bont, J. Town, E. Liarou, G. Patias, C. J. Atkins and D. M. Haddleton, *Journal of Polymer Science Part A: Polymer Chemistry*, 2019, **57**, E1-E9.
34. C. L. Moad, G. Moad, E. Rizzardo and S. H. Thang, *Macromolecules*, 1996, **29**, 7717-7726.
35. C.-W. Chang, E. Bays, L. Tao, S. N. S. Alconcel and H. D. Maynard, *Chemical Communications*, 2009, DOI: 10.1039/B904456F, 3580-3582.
36. D. Pissuwan, C. Boyer, K. Gunasekaran, T. P. Davis and V. Bulmus, *Biomacromolecules*, 2010, **11**, 412-420.
37. A. A. Gridnev and S. D. Ittel, *Chemical Reviews*, 2001, **101**, 3611-3660.
38. J. P. A. Heuts and N. M. B. Smeets, *Polymer Chemistry*, 2011, **2**, 2407-2423.
39. J. Zhou, H. Yao and J. Ma, *Polymer Chemistry*, 2018, **9**, 2532-2561.
40. A. Lotierzo, R. M. Schofield and S. A. F. Bon, *ACS Macro Letters*, 2017, **6**, 1438-1443.
41. A. Lotierzo, B. W. Longbottom, W. H. Lee and S. A. F. Bon, *ACS Nano*, 2019, **13**, 399-407.
42. C. Boyer, A. H. Soeriyadi, P. B. Zetterlund and M. R. Whittaker, *Macromolecules*, 2011, **44**, 8028-8033.
43. I. Schreur-Piet and J. P. A. Heuts, *Polymer Chemistry*, 2017, **8**, 6654-6664.

44. A. Anastasaki, C. Waldron, P. Wilson, C. Boyer, P. B. Zetterlund, M. R. Whittaker and D. Haddleton, *ACS Macro Letters*, 2013, **2**, 896-900.
45. S. P. S. Koo, T. Junkers and C. Barner-Kowollik, *Macromolecules*, 2009, **42**, 62-69.
46. Y. Zhao, X. Liu, Y. Liu, Z. Wu, X. Zhao and X. Fu, *Chemical Communications*, 2016, **52**, 12092-12095.
47. L. Martin, G. Gody and S. Perrier, *Polymer Chemistry*, 2015, **6**, 4875-4886.
48. G. Nurumbetov, N. Engelis, J. Godfrey, R. Hand, A. Anastasaki, A. Simula, V. Nikolaou and D. M. Haddleton, *Polymer Chemistry*, 2017, **8**, 1084-1094.
49. J. Krstina, G. Moad, E. Rizzardo, C. L. Winzor, C. T. Berge and M. Fryd, *Macromolecules*, 1995, **28**, 5381-5385.
50. J. Krstina, C. L. Moad, G. Moad, E. Rizzardo, C. T. Berge and M. Fryd, *Macromolecular Symposia*, 1996, **111**, 13-23.
51. C. J. Atkins, G. Patias, J. S. Town, A. M. Wemyss, A. M. Eissa, A. Shegiwal and D. M. Haddleton, *Polymer Chemistry*, 2019, **10**, 646-655.
52. R. S. Chow and K. Takamura, *Journal of Colloid and Interface Science*, 1988, **125**, 226-236.
53. A. E. Childress and M. Elimelech, *Journal of Membrane Science*, 1996, **119**, 253-268.
54. Q. Zhang, S. Slavin, M. W. Jones, A. J. Haddleton and D. M. Haddleton, *Polymer Chemistry*, 2012, **3**, 1016-1023.

Chapter 5

Optimising the conditions and tracing the formation of fluorescence block–copolymers of poly (MMA-*b*-styrene) utilising low *mass* fluorescence macromonomers of poly (MMA) as derived from CCTP

Image showing the block copolymers under UV-light

5.1 Introduction

In this chapter, the formation of block copolymers in solution polymerisation is examined, starting with low mass macromonomers of poly (methyl methacrylate), synthesised via CCTP in emulsion. The macromonomers deployed for the formation of block copolymers contained the covalently bound fluorescent dye Hostasol methacrylate (HMA), a methacrylate derived from the commercial dye Hostasol [1-4].

Materials containing fluorescent tags, have been proven to be beneficial, especially when they have been observed using a fluorescence microscope in particular laser scanning confocal microscopy (LSCM). Laser scanning confocal microscopy allows the observation of fluorescently tagged materials in systems by tracing the location of the material within the system and subsequently determining its effectiveness[1, 4-6]. These tracing mythologies are commonly utilised in biological systems during biomedical assays as the location of the material can be observed. Other applications of fluorescent dyes are: labelling latex particles to study polymer diffusion within latex films and as tracers in order to investigate the location of individual component within a latex blend[1, 3, 5].

In experiments involving energy transfer, it is crucial to have dyes that are incorporated uniformly and randomly along the backbone of the latex polymer. Furthermore, the typical target for incorporation of fluorescent dyes within polymer backbone is around 1 mol % with respect to the total monomer[4]. However, in our systems we have utilised significantly less dyes (0.01 mol %) with respect to the total monomer and the fluorescent signals have still shown to be very intense.

In the initials step, since we perform the polymerisation in an emulsion system it was crucial that we dissolved the dye (HMA) with the COBF in the oil phase (MMA) in order to prevent the Hostasol from crashing out as a precipitate and since the particles eventually becomes the principle loci of polymerisation and can be considered to be relatively hydrophobic. The MMA monomer solubilises both COBF and the reactive HMA dye ensuring uniform incorporation within the polymer latex backbone by diffusing from the monomer reservoir into the particles hence, allowing the formation of low M_n macromonomers with fluorescence tagging.

Furthermore, the monomer was fed under monomer starved conditions, into the reactor consisting of surfactant (SDS) in concentrations above its CMC with ACVA initiator, both dissolved in the aqueous phase at 75 °C. Feeding the monomer under monomer starved conditions ensured that the distribution of dye within the polymer backbone chain were uniform. Polymerisations have been performed were the dye was incorporated under bulk conditions by Jean- Christophe Graciet's group[4], in Toronto.

However, the results were less promising as lowest molecular weight part of the molecular weight distribution was enriched in the dye. The results obtained were consistent with low dye incorporation obtain at the initials stages of the batch polymerisation and significant dye incorporation at the end of the polymerisation[4, 7]. The locus of the dye within the polymer latex was monitored by utilising gel permeation chromatography (GPC), with tandem fluorescence (FL) and refractive index (RI) detectors. If the dye incorporation is uniform the shape of the signal obtained from FL detectors should be identical to the shape of the signal from the RI detectors[4].

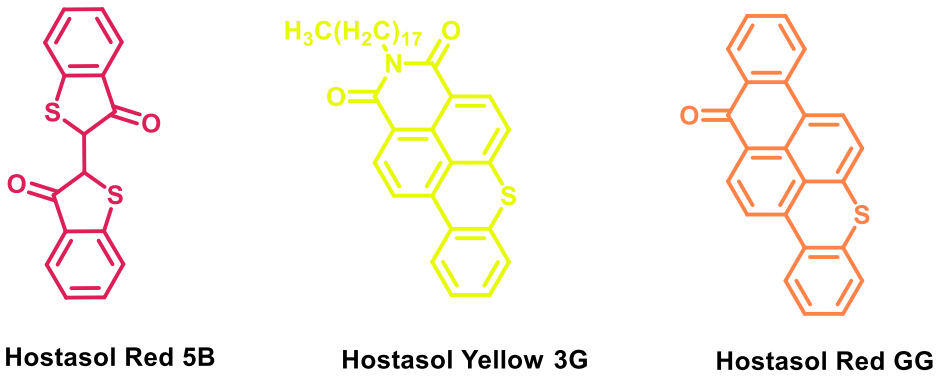

Figure 5.1: Structures of fluorescence dye; HR-5B, HY-3G and HR-GG[4].

In this work, we utilise a derivative similar to the commercial Hostasol yellow 3G™ (HY-3G) (also known as C. I. Solvent yellow 98) which is a yellow fluorescent dye chemically described as Benzo [kl]thioxanthene-3, 4-dicarboximide, *N*-octadecyl (*scheme 5.1*). However, other common forms of the Hostasol derivative dye also exist and have been utilised extensively, such as Hostasol red 5B (HR-5B) and Hostasol red GG (HR-GG), all of which present strong fluorescence properties by absorbing visible light[1, 3-6, 8].

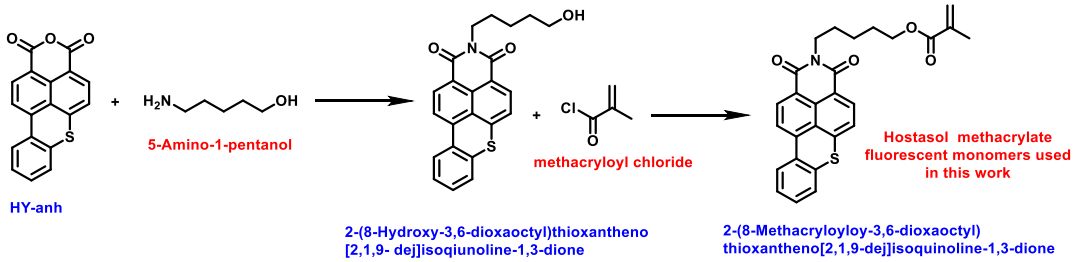

Scheme 5.1: Formation of hostasol methacrylate

An important note to make, is that the covalently bound dyes that are cross-linked within the particles, can be conceptualized as artificial pigments. Since, the substances are pigments due to the fact that the host polymer is insoluble within the substance. Therefore, if the dyes do not aggregate within the particles, the artificial pigments in theory should acquire the same absorption and emission properties as the dye molecules themselves. The objective of these experiments were to synthesis small M_n macromonomers of poly(methyl methacrylate) that contained Hostasol methacrylate (HMA) dye and were synthesised via CCTP in emulsion system. These macromonomers were freeze dried subsequently deployed for the formation of block copolymers. The macromonomers were covalently bound to the fluorescent dyes, namely HMA, a commercial dye. The cross-linked particles and block copolymers were characterized using SEC (RI & FL), ^{1}H and DOSY NMR.

5.2 Results and discussions

5.2.1 Synthesis of low M_n fluorescence poly (MMA) via CCTP

In the initial step, the polymerisation was performed under a monomer starved emulsion polymerisation, it was crucial that the dye was dissolved (HMA) with the COBF in the oil phase (MMA) in order to prevent the Hostasol from precipitating. Furthermore, solubility tests showed that HY-3G had exhibited strong fluorescent and had very good solubility in the monomers (MMA) of the macromonomer and the subsequent monomers of the block copolymers (MAA and styrene). The effectiveness of HY-3G dye's fluorescence, meant that it was not necessary to load any more solvent in order to enhance the fluorescence of the final polymer. This has the advantage, since, we utilise less dye it is less likely for the dye to interfere negatively with the chemical or physical properties of the polymer matrix, since less dye material would be present.

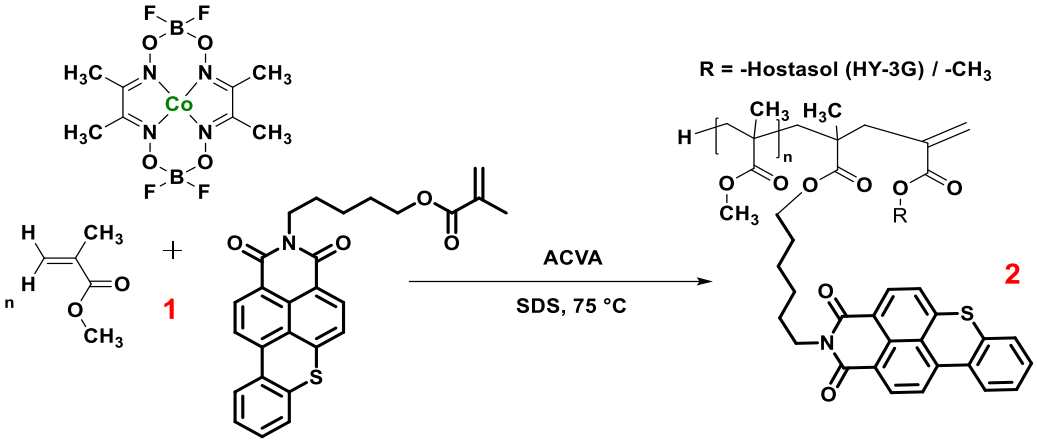

Scheme 5.2: For the formation of fluorescence poly (MMA) in emulsion polymerisation

Table 5.1: SEC data, of poly (MMA) macromonomer tagged with HY-3G dye

Reaction	**$M_{n,SEC}$ / gmol^{-1} (THF)**	**M_w / gmol^{-1}**	***Đ***	***CoBF / ppm***
PMMA	900	1500	1.61	121

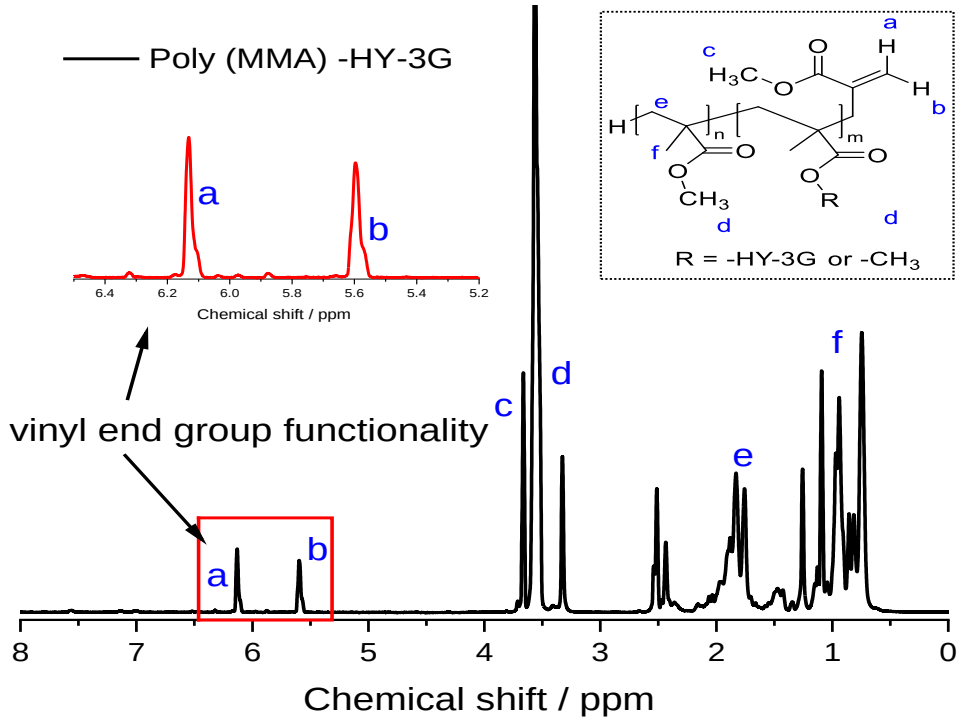

Figure 5.2: Left ^{1}H NMR of poly (MMA) with HY-3G dye and right structure of poly(MMA)

Table 5.2: ^{1}H NMR assignments of poly(MMA) macromonomer

Peak (ppm)	**Integral**	**Multiplet type**	**Assignment**
6.12-6.09	1.00	Singlet	Vinyl protons [a]
5.58-5.49	1.00	Singlet	Vinyl protons [b]
3.66	3.38	Singlet	Terminal methoxy [c]
3.56	21.75	Singlet	First in chain methoxy [d] nearest vinyl
3.33	2.28	Singlet	Residual water protons
2.5-0.5	46.61	Broad multiplet	In chain methylene e and methyl protons [f]

In addition, since the particles of poly(MMA), eventually becomes the principle loci of polymerisation and can be considered to be relatively hydrophobic. The MMA monomer droplet with solubilised COBF and HMA dye are ensured to be incorporated within the polymer latex backbone by diffusing from the monomer reservoir into the particles hence, allowing the formation of low M_n macromonomer with fluorescence tagging. Furthermore, the monomer was fed under monomer starved conditions, into the reactor consisting of surfactant (SDS) in concentrations above its CMC with ACVA initiator, both dissolved in the aqueous phase at 75 °C. Feeding the monomer under monomer starved conditions ensured that the distribution of dye within the polymer backbone chain was uniform.

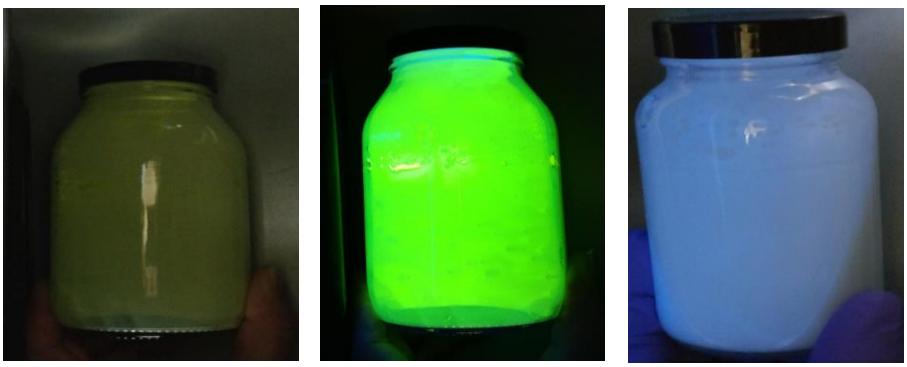

Figure 5.3: The image on the left is the fluorescence poly (MMA) in absence of UV-light, middle image is fluorescence poly (MMA) with HY-3G dye under UV-light and the image on the right is poly (MMA) without HY-3G dye under UV-light.

SEC data, showed very low M_n = 900 gmol^{-1} with $Đ \sim 1.61$ at 121 ppm. Furthermore, since the shape of the molecular weight distributions from the FL detector are very similar in shape to RI detectors this suggests that the incorporation of the dye within

the polymer was uniform (*figure 5.4*). In addition, upon exposure of poly (MMA) with HY-3G dye to UV-light strong fluorescence was observed, whereas when poly (MMA) without HY-3G dye showed no fluorescence as expected under UV-light (*figure 5.3*).

Furthermore, the signal from the FL was 36 times more intense than from RI for the macromonomer of poly(MMA) with HY-3G dye. Subsequently, these fluorescence macromonomers of poly (MMA) were recovered by freeze drying and utilised in block copolymer formations. The ^{1}H NMR & SEC, *figures 5.2 & 5.4*, shows that poly(MMA) was formed with vinyl end group functionality and since extremely low concentrations of HY-3G dye was utilised (less than 30 ppm) in the polymerisation the composition of the poly(MMA) formed was not disturbed as seen by ^{1}H NMR & SEC data.

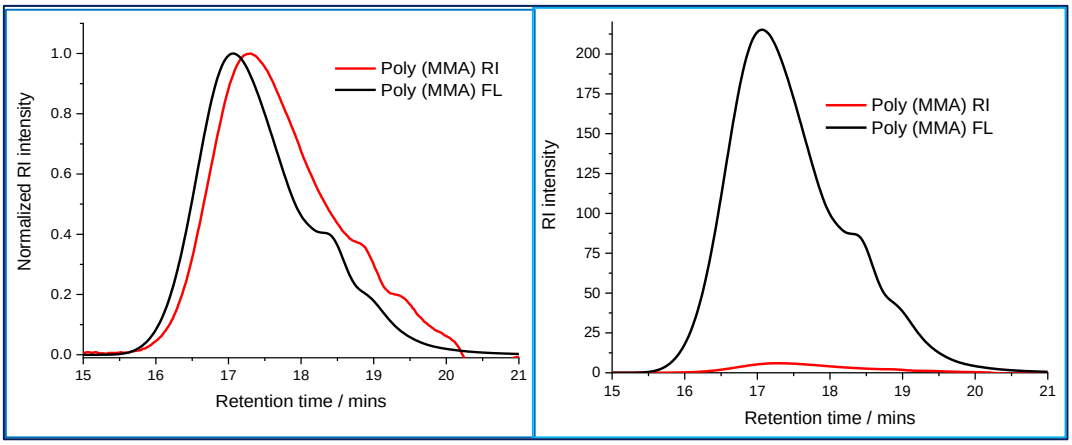

Figure 5.4: SEC (FLD and RI) data of poly (MMA) in emulsion on the left normalized intensity and on the right not normalized RI & FL

5.2.2 Synthesis of block copolymers using low *mass* fluorescent poly(MMA)

Seymour and co-workers have previously reported high level of second monomer incorporation within block copolymers of poly(styrene-*b*-methyl methacrylate) with up 100% shift to higher M_n and up to 88% block copolymer yield[9]. The block copolymers were formed upon conditions where the vinyl monomer was added to a suspension of trapped macro-radicals in a poor solvent, given that the difference in the solubility parameter between the monomer and the macro-radical were not greater than 3.1 Hildebrand units[9, 10].

The objective, being that when the second monomer was injected into the polymerisation vessel, there would be no primary free radicals present from the first initiator. This was ensured by allowing the reaction to proceed at 50 °C for 96 hours, in order for all the initiators from the first stage to decompose before the second monomer could be injected. As observed in most systems, small amount living of macro-radicals of homopolymer remain in the second stage, due to the fact that the viscosity of the reaction medium increases preventing mutual termination[9-12]. Nevertheless, mostly block copolymers are formed upon the addition of the second monomer, with very small amount of homopolymer[9].

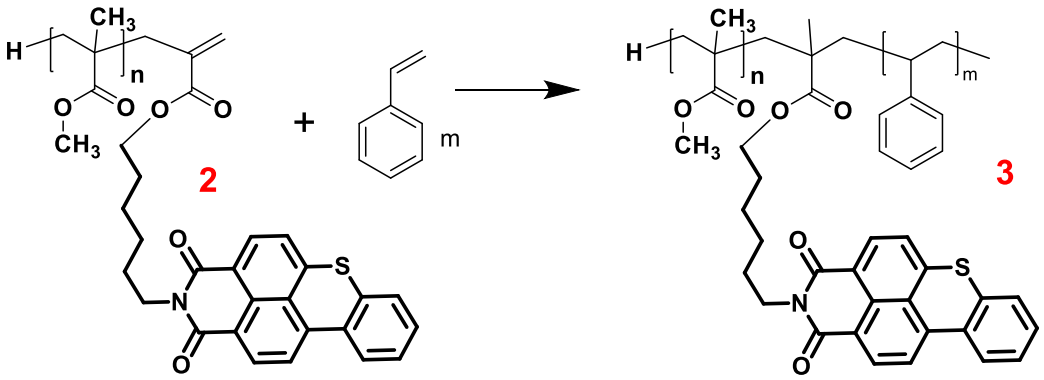

Scheme 5.3: Poly (MMA-b-styrene) block copolymers with HY-3G dye

In the present system (*scheme 5.3*), subsequent fluorescence macromonomer of poly(MMA) with HY-3G dye methacrylate (2) formed in an emulsion system and recovered via freeze drying was utilised in the formation of block copolymers. The concentration of fluorescent of poly(MMA) macromonomer was varied between 0.1389 mmoles, 0.2778 mmoles, 0.5556 mmoles, 1.111 mmoles and 1.667 moles respectively, with respect to styrene which was kept constant at 0.1740 moles. The reaction was carried out under a nitrogen atmosphere, with toluene as the solvent, under batch solution with AIBN initiator at solid contents of 20wt%. The fluorescence properties and block formation were investigated.

Table 5.3: SEC data for crude poly (MMA-b-styrene) block copolymers with HY-3G dye.

Reaction PMMA/ mmole	$M_{n,SEC}$ / gmol^{-1} (THF) (crude product)	M_w / gmol^{-1}	$Đ$	Conversion / %	Precipitate in cyclohexene / wt%	Precipitate in DCM/ wt%
-	30900	72700	2.35	78	-	-
0.1389	29600	57100	1.93	45	97	3
0.2778	25100	48400	1.93	50	90	10
0.5556	16400	39400	2.41	55	88	12
1.1111	11200	33700	3.01	50	91	9
1.6667	6200	25100	4.08	56	88	12

From the SEC data (*table 5.3*), the concentration of fluorescence poly (MMA) macromonomer increases as the M_n decreases. For the reaction with only 0.1389 mmoles of pol(MMA) macromonomer the reduction in M_n is less significant compared to the control reaction of poly(styrene), from 30900 g mol^{-1} to 29600 g mol^{-1} . However, as the concentration of pol (MMA) macromonomer increases 0.2778- 1.667 mmoles the reduction in M_n is much more significant, 25100 g mol^{-1}, 16400 g mol^{-1}, 11200 g mol^{-1} and 6200 g mol^{-1} respectively.

Furthermore, for the first two reactions with 0.1389 mmoles and 0.2778 moles of fluorescent poly(MMA) with respect to styrene, the $Đ$ is in the region expected for free radical ~2. However, upon increasing the concentration of fluorescent poly(MMA) to 0.5556 mmoles 1.111 mmoles and 1.667 mmoles, with respect to styrene, the $Đ$ of individual block copolymers increased to 2.41, 3.01 and 4.08. This could possibly be attributed to the fact that fluorescent poly(MMA) may be acting as "chain stopper" to give a block copolymer, since as the concentration of fluorescent poly(MMA) increases the chain length of the block copolymers decreases (i.e. M_n decreases).

Copolymerisation of smaller monomers such as acrylates or styrenics monomers with olefinically unsaturated macromonomers could leads to graft copolymers. However, if larger macromonomers are copolymerised with small amount of commoner, the resulting product resembles a more star like architecture, however incorporating

macromonomers into other macromonomers could leads to branched and hyper branched systems.

However, when the propagating polyacrylates radical encounters a macromonomer the resulting radical is sterically hindered. If the rate of H abstraction (chain transfer) to any C-H bond in the system is sufficiently high, then this can occur to give a polyacrylates-methacrylate block copolymer and a resulting radical from the chain transfer which can reinitiate or undergo any reaction possible for small primary radicals resulting in block copolymers.

Furthermore, a small portion of the crude product 1 g was separated by two different solvents using solvent separation technique, initially each individual crude samples of the block copolymer (i.e. 1 g) was dissolved in 300 mL of cyclohexane and the undissolved mixture was subsequently filtered through a funnel end capped with cotton wool and the cotton wool was washed subsequently, with 80 mL of cyclohexane in order to remove any residual soluble product with only insoluble product left. The remaining solid was collected and dissolved in 80 mL of DCM as it was insoluble in cyclohexane and then the solvent were evaporated off via rotatory evaporator and analysed. The amount of material collected in each stage was ~90 wt% cyclohexane from 1 g of the initial crude product of and 10 wt% in DCM solvent. Later on in the thesis, since the solid obtained from DCM contains both poly(MMA) homopolymer M_n ~1,000 gmol^{-1} and the block copolymers of poly (MMA-*b*-styrene) with M_n greater than 6000 gmol^{-1}; were separated via dialysis in DCM using dialysis bag of 3.5k membrane size.

.

Table 5.4: SEC data for purified, poly (MMA-b-styrene) block copolymers with HY-3G dye.

Reaction PMMA/ mmoles	$M_{n,SEC}$ / g mol^{-1} (THF) DCM (CH insoluble)	M_w / g mol^{-1}	$Đ$	$M_{n,SEC}$ / g mol^{-1} (THF) (CH soluble)	M_w / g mol^{-1}	$Đ$
0.1389	66800	100700	1.51	24500	46700	1.91
0.2778	43500	83200	1.91	30000	50100	1.67
0.5556	34100	81100	2.38	19100	39500	2.07
1.1111	18800	43600	2.32	12400	27200	2.20
1.6667	6700	22200	3.32	12800	34000	2.65

The SEC data in *table 5.4* of the purified product, shows a similar generic trend that was observed with the crude product (*table 5.3*), as the concentration of fluorescence poly(MMA) macromonomer increased, a general trend in reduction in M_n was observed for each set of individual block copolymers of poly (MMA-*b*-styrene). After the purification the M_n, acquired from the polymers purified in DCM, showed higher M_n, compared to the crude, especially when low concentration of fluorescence poly (MMA) macromonomer was utilised. At 0.1389 mmoles, 0.2278 mmoles, 0.5556 mmoles and 1.111 mmoles the crude M_n = 29600 g mol^{-1}, 25100 g mol^{-1}, 16400 g mol^{-1} and 11200 g mol^{-1} respectively, whereas when purified in DCM the block polymers of poly (MMA-*b*-styrene) M_n, shifted to M_n of 66800 g mol^{-1}, 45300 g mol^{-1}, 34100 g mol^{-1} and 18800 g mol^{-1} respectively at the same concertation of fluorescence poly (MMA).

For the reaction with 1.667 mmoles of poly (MMA), the M_n increased upon solvent purification with DCM but not as significantly as the reactions with lower concentrations of fluorescence poly(MMA). The higher M_n obtained after precipitation in DCM compared to the crude, could be due to the fact that the polymer did not dissolve in cyclohexane yet dissolved in DCM, which could be potentially due to the polarity of the undissolved residue containing predominately poly (MMA) or mixture of poly (MMA-*b*-styrene), whereas styrene is more compatible with cyclohexane solvent.

Furthermore, the SEC data for all of the crude block copolymers of poly (MMA-*b*-styrene), showed that monomodal peaks were obtained via SEC. However, as the amount of fluorescence poly(MMA) used in the reaction increased from 0.5556 mmoles, 1.1111 mmoles and 1.6667 mmoles, the SEC data showed M_n, tailoring at low M_n. Which upon precipitation into cyclohexane and DCM, showed bimodal peaks with small peak occurring at the same retention that poly (MMA) would occur, suggesting not all the macromonomers were utilised in the block copolymer formation of poly(MMA-*b*-styrene).

In addition, the SEC data with cyclohexane precipitate showed a general decrease in M_n, as the concertation of the fluorescence poly (MMA) increased for each subsequent

reactions. The M_n of the polymer obtained from cyclohexane was significantly lower than the precipitate obtained from DCM for the same concentration of fluorescence poly (MMA). Furthermore, both DCM and cyclohexane precipitation resulted in a general decrease in $Đ$ as when compared to the crude product. Although, there will unavoidably poly(styrene) homopolymer present in the crude product ("raw") block copolymers, the product is mostly block copolymer.

This is due to the fact that temperatures and reaction time during polymerisation plays an important role as demonstrated by Gilbert and co-workers[13]: they found that for the formation of the first block higher temperature and shorter reaction time were more desirable since the higher temperature promotes relatively rapid radical formation. Whereas, for the second block it is important to utilise much lower temperature in order to minimise generation of new free radicals which would lead to homopolymer contaminants derived from homopolymerisation of the second monomer by newly created radicals. Therefore, experimental optimisation is essential in order to fine tone the conditions so that only/predominant product obtained in the reaction is the block copolymers of poly (MMA-*b*-styrene).

It should be taken into account, that the actual amount of poly(styrene) homopolymer by mass (the DRI detector in the SEC gives an indication of the mass/weight component in the product i.e., the RI response is proportional to the wt%) is slightly higher in *figure 5.5* as the d_n/d_c value for PS in THF (d_n/ d_{cPS}) 0.189) is higher than that for PMMA (d_n/d_{cPMMA}) 0.089)[14].

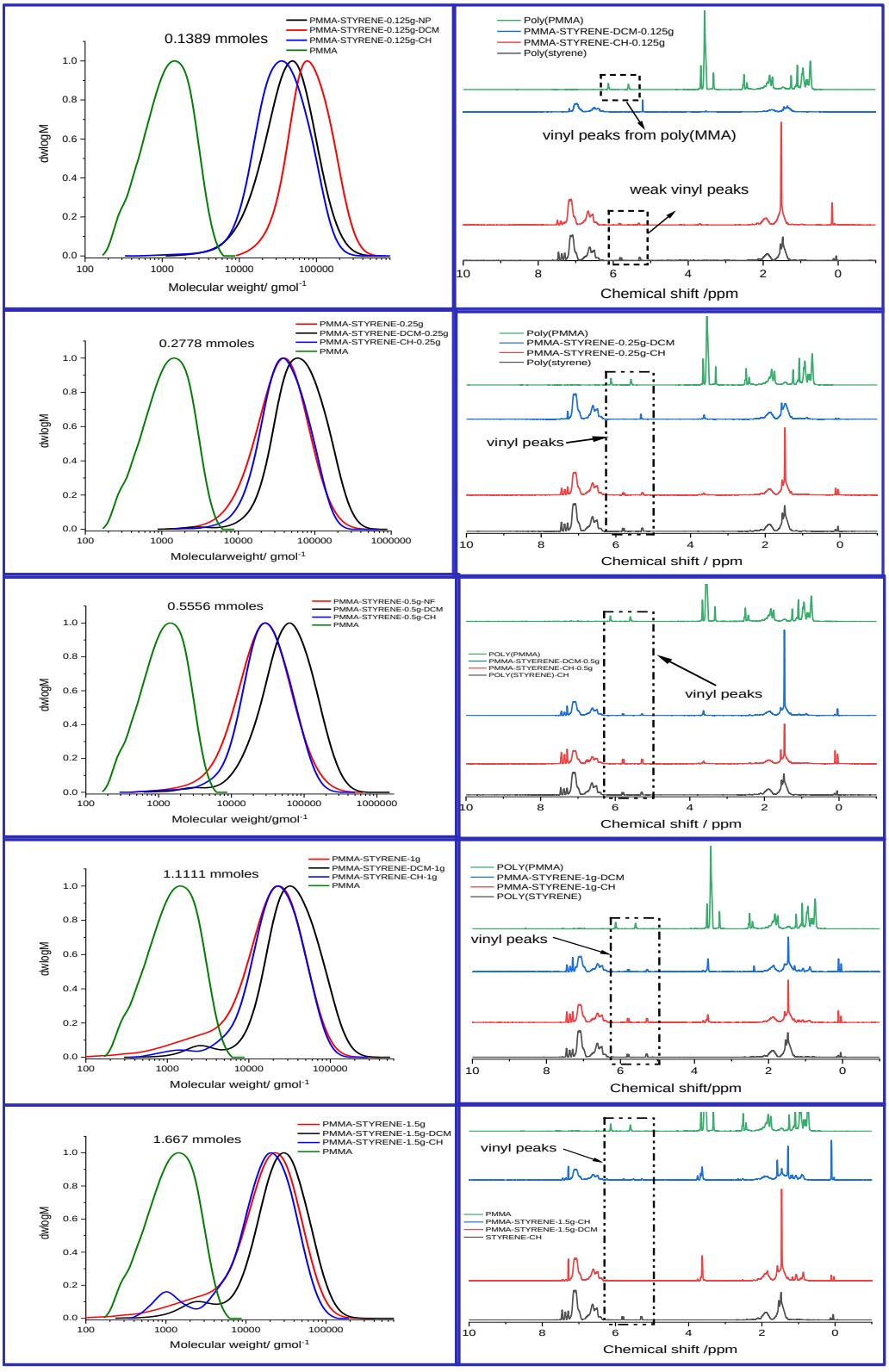

Figure 5.5: Left from top down SEC data shows lowest concentration of poly(MMA) incorporated block copolymers at top 0.1389 mmoles with green GPC representing the initial macromonomer of poly(MMA), red poly(styrene) homopolymer, blue block copolymer obtained from DCM solvent and black representing block copolymers obtained from CH solvent with the highest concentration at the bottom of the figure with 1.6667 moles of poly(MMA) macromonomer with respect to styrene . The ^{1}H NMR data on the right, is of the adjacent SEC data of the fluorescence block polymers of poly(MMA-b-styrene with the same colours representation as that of SEC.

The crude block copolymer polymer of poly (MMA-*b*-styrene) was then extracted with cyclohexane to remove PS and with DCM to remove PMMA homopolymer, therefore upon running ^{1}H NMR, demonstrate that the polymers are not of a random nature since resonances that would indicate a styrene unit next to a methyl methacrylate unit are not detected *figure 5.5*. Furthermore, the crude precipitated in cyclohexane is more predominate with poly (styrene) polymer according to ^{1}H NMR. Whereas, the precipitate obtained from DCM, the peaks due to poly (MMA) in the block copolymer of poly (MMA-*b*-styrene) becomes more predominate, *figure 5.5*.

5.2.3 DOSY NMR analysis of the block copolymer of poly(MMA-b-styrene)

The properties of block copolymers are highly dependent, on the chemical and physical composition of the polymeric structures. Conventionally a block copolymer's composition can be interrogated by a range of analytical techniques including SEC, MALDI and ^{1}H/^{13}C NMR and some limitations of each individual technique which will be discussed. In addition to these more conventional techniques Diffusion Order Spectroscopy (DOSY) has been developed since the early 1990s as technique to obtain polymer composition and molecular weight information[15-17].

SEC is a widely utilised simple technique for determining the number average molecular weight (M_n), the weight average molecular weight (M_w) and the molecular weight distribution (dispersity) of polymeric materials. Since SEC separates molecules based upon their hydrodynamic volume and not molecular weight, a conventional calibration using narrow standards of the same chemical nature and structure as the analyte is required[15-18]. If these criteria cannot be satisfied, standards of a different nature from that of the polymer sample can, to some degree, be utilised, or on the other hand universal calibration can be utilised, in which case it depends on Mark Houwink-Kuhn-Sakurada (MHKS) parameters being known for the standards and the analyte. SEC as with all techniques does encounter some discrepancy, factors such as weak adsorption phenomena can affect polymer mass values determined by SEC. In addition multiple detection methods coupled with SEC are often necessary to reach reliable molecular weight data, due to the fact that the intensity of response obtained in each

detection mode is not only dependent upon the molecular weight but also upon parameters that are functions of the macromolecular compositions[15-18].

Solution state NMR analysis are often performed to determine the M_n of each block for low mass polymers and to determine the relative molar compositions of a sample. However, conventional solution NMR cannot distinguish between a block copolymer sample and a simple mixture. More precisely, the integrals of appropriately selected set of ^{1}H NMR resonances are compared and used to deduce the M_n value of one of the block from the (typically known) M_n value of the other. On condition that the ^{1}H spectrum has been recorded using quantitative experimental parameters (i.e., sufficient time has been permitted for the resonances to relax completely) and no spectral overlap is present, the results therefore acquired from estimation from ^{1}H NMR is rather accurate[15-19].

Mass spectrometry techniques such as matrix-assisted laser desorption/ionization mass spectrometry (MALDI) and ESI MS have proven to be fruitful at determining M_n for narrow molecular weight at low mass but with more success regarding chemical compositions. As oligomers and co-oligomers can be detected as intact molecular adducts with soft ionisation methods, MALDI MS spectra can be used to determine the M_n and M_w molecular weights, as long as polymer dispersity very narrow (less than 1.20). In our group, MS techniques have been exploited extensively for characterization of copolymers including: investigating how labile end groups affect fragmentation patterns, how their fragmentation patterns differ based on their co-monomer arrangement and observed the complexities of copolymer analysis by tandem mass spectrometry[15-18].

In the case of DOSY, a two dimensional NMR technique, diffusion coefficients for individual resonances in a ^{1}H NMR spectrum are investigated. This results in a spectrum recorded in two dimensions: the first dimension (F_2) accounts for the usual chemical shift observed as is familiar to the chemist and secondly (F_1) for self-diffusion coefficients (D). Since the diffusion coefficient is related to hydrodynamic radius and thus molecular weight, DOSY is complementary to other physical techniques utilised in polymer analyses to measure molecular size/shape[15-19]. In the case of a copolymer different repeating units can be assessed by observing copolymer

signals with dissimilar diffusion coefficients, which in turn signifies the presence of monomer impurities or a mixture of homopolymer. Thus any signal arising from the same molecule should have the same diffusion rate and polymers should diffuse at a much slower rate than low molecular weight species such as monomers or solvents. Furthermore, DOSY can also be used sometimes to follow the rate of a polymerization reaction, in case of self-aggregation can be an important tool to exploit the assembly of reversible polymers as well as to measure critical micelle concentrations and micelle size[15-18].

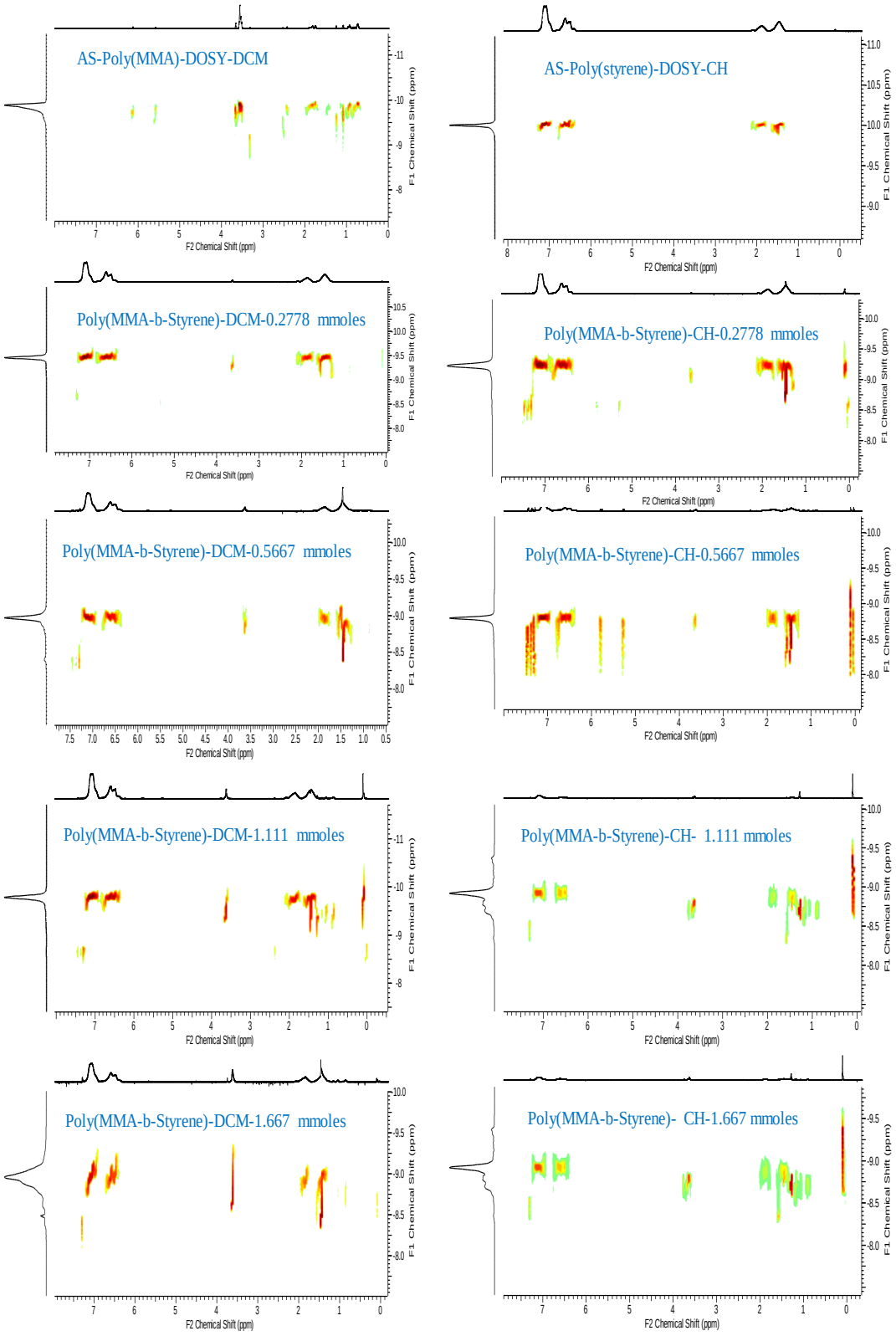

Figure 5.6: DOSY NMR of the block co-polymers of poly (MMA-b-styrene) with DCM extracts on left and cyclohexane extracts on the right with block co-polymers containing lowest concentration of poly(MMA) macromonomer within the block copolymer of poly (MMA-b-styrene) at the top 0.2778 mmoles with respect to styrene and block with the highest concentration of poly(MMA) incorporated within the block copolymers of poly (MMA-b-styrene) at the bottom 1.6667 mmoles.

The DOSY NMR spectra of the poly(styrene) (MWt = 30.9 K) (i.e. controlled reaction) and the small M_n macromonomer of poly(MMA) (MWt = 1 K), top of *figure 5.6*, when compared to the final products of the block copolymer formation with various concentration of low M_n poly(MMA) incorporated within the block of poly(MMA-*b*-styrene), *figure 5.6*, show distinct differences in the diffusion constants of the small M_n macromonomer of poly(MMA), poly(styrene) and the block copolymers of poly (MMA-*b*-styrene). Moreover, all of the protons of the final product are aligned on the same region of the spectrum (same diffusion rate), indicating that they are part of the same molecule.

However, as the concentration of the fluorescence (low M_n = 1K) macromonomer of poly(MMA), increases within the block copolymer from 0.2778 mmoles, 0.5667 mmoles, 1.111 mmoles and eventually to 1.5667 mmoles for each individual reaction, the intensity of the peak for the presence of poly(MMA) protons increases at 6.13 ppm, 5.60 ppm for the vinyl peaks and 3.56 ppm for the methyl group of macromonomer of poly(MMA). In addition, the alignment of all of the protons in the final product are aligned on the same region of the spectrum (indicative of the same diffusion rate), indicating that they are part of the same molecule.

Furthermore, the intensity of the peaks from the poly(MMA) incorporated within the block copolymers of poly(MMA-*b*-styrene), are much more intense in DCM as opposed to cyclohexane, *figure 5.6 & 5.7*. This is due to the fact that the in the DCM phase the homopolymer of poly(MMA) and block copolymers of poly (MMA-*b*-styrene) is present, whereas in cyclohexane predominately the polystyrene homopolymer and styrene monomer is present.

To obtain the block copolymer of poly(MMA-*b*-styrene) each of the reactions in the DCM phase was dialysed in 1 Kd, 2 Kd and eventually in 3.5 Kd dialysis membranes, so that the homopolymer of unreacted poly(MMA) (M_n = 900 g mol^{-1}), could be removed to leave an isolated product as a block copolymer of poly(MMA-*b*-styrene) *figure 5.8*. After dialysis purification with 3.5k membrane, the DOSY NMR peaks are all aligned for the block copolymers of (poly(MMA-*b*-styrene)) with shorter diffusion distance with the same diffusion rate for the samples dialysed in 3.5k dialysis bag when compared to the un-dialysed samples, except for the 0.1389 mmoles where

insufficient material of (poly(MMA-*b*-styrene)) were obtained for analysis and 0.2778 mmoles in which the peaks for pol(MMA) are slightly misaligned with styrene, suggesting that the concentration of pol(MMA) available in the block copolymer is somewhere below the minimum threshold amount.

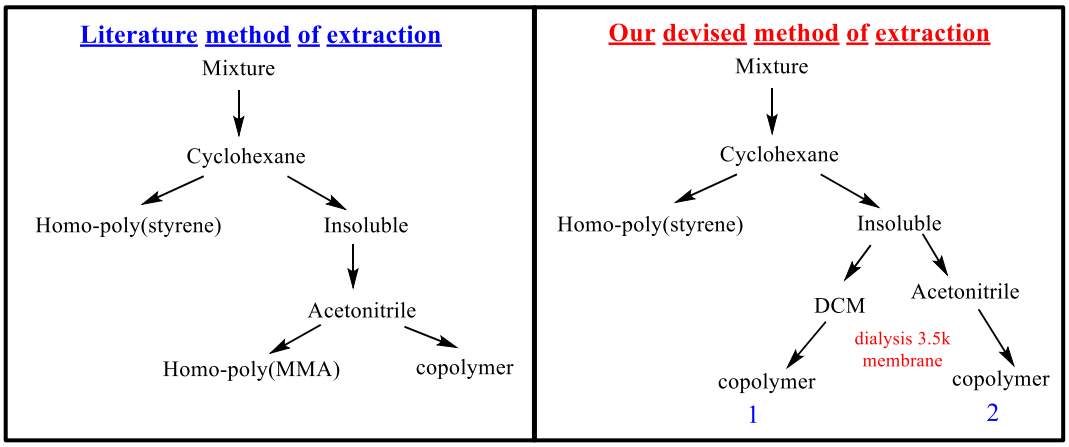

Figure 5.7: Selective extraction scheme for a mixture of poly(MMA-b-styrene) and the final block copolymer[20]

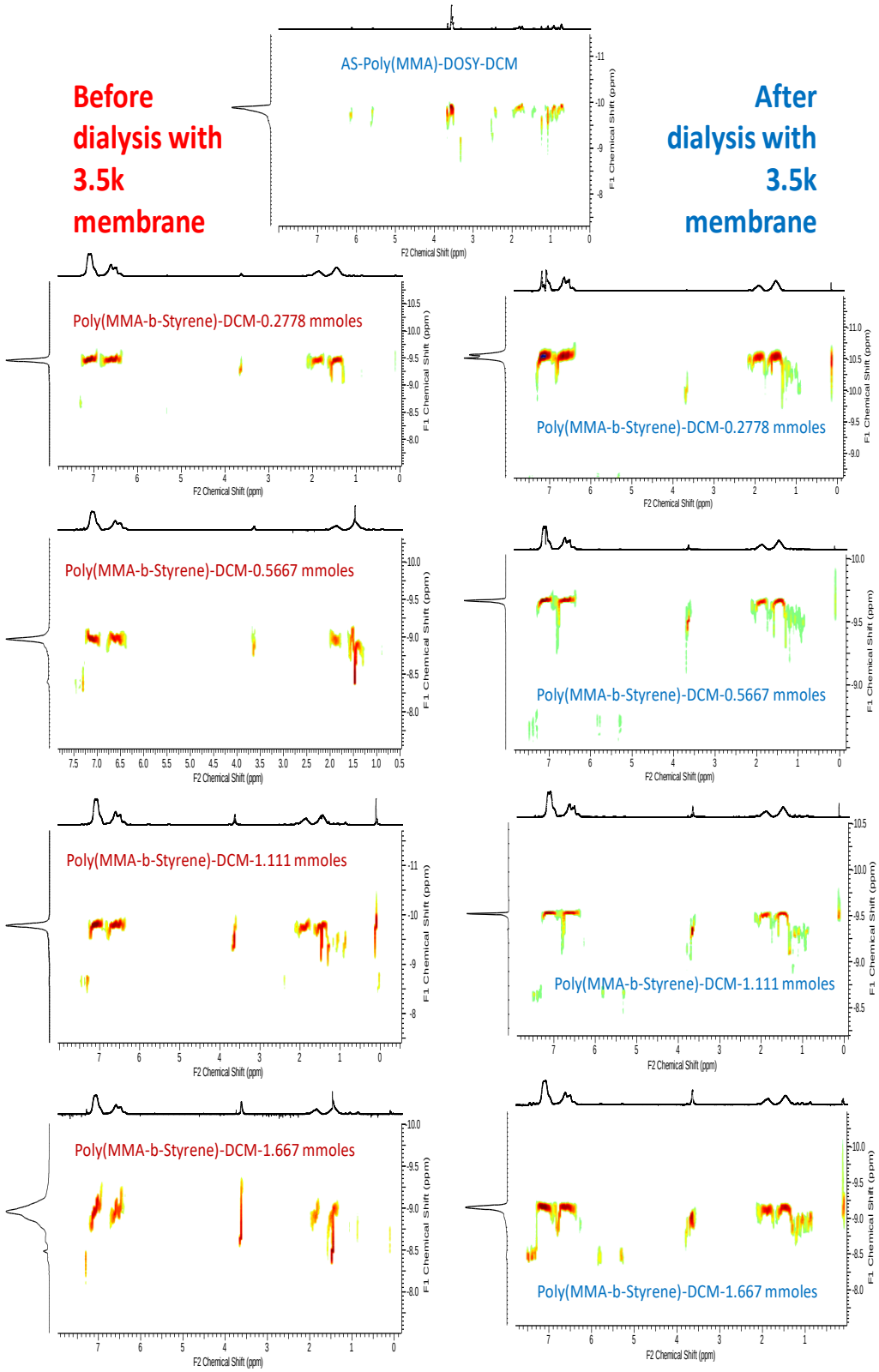

Figure 5.8: Poly(MMA-b-styrene) block co-polymers before and after purification in 3.5k dialysis membrane with block co-polymers containing lowest concentration of poly(MMA) macromonomer within the block copolymer of poly (MMA-b-styrene) at the top 0.2778 mmoles with respect to styrene and the block with the highest concentration of poly(MMA) incorporated within the block copolymers of poly (MMA-b-styrene) at the bottom 1.6667 mmoles.

5.2.4 Fluorescence analysis of the block copolymer of poly(MMA-*b*-styrene) via devised purification method 1 in DCM

Fluorescence detection involves both the selection of suitable excitation and emission wavelengths resulting to higher selectivity and sensitivity[21, 22]. As a result, the technique is useful for analyses requiring low detection limits, particularly in complex matrices, and in precious or limited quantity materials. Fluorescence detectors are very sensitive relative to other modern spectrophotometric detectors such as UV absorption. It is possible to detect even a presence of a single analyte molecule in the flow cell[23]. The sensitivity of fluorescence detection can be 10 -1000 times higher than that of the UV detector for strong UV absorbing materials[21-23]. This sensitivity was observed, with comparisons of RI and FL data obtained via SEC, for the range of block copolymers of poly (MMA-*b*-styrene) synthesised.

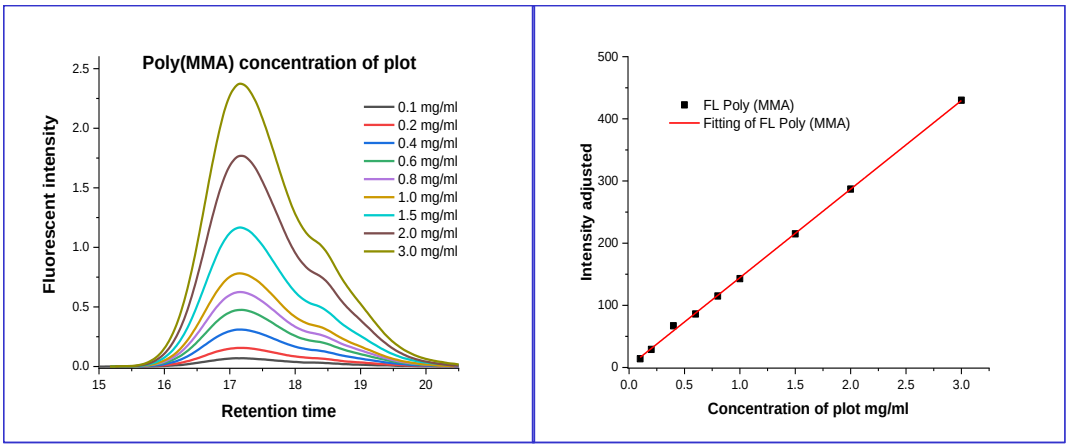

Figure 5.9: Poly(MMA) fluorescence concentration plot

All of the block co-polymers of poly(MMA-*b*-styrene); upon analysis of FL contained some unreacted macromonomer of poly(MMA) even after purification with 1 Kd, 2 Kd and eventually 3.5 Kd dialysis bags, whiles the RI indicated full conversion upon purification with slight tailing towards lower M_n *observed*, especially when higher concentration of poly(MMA) macromonomers were incorporated within the block co-polymers (i.e. 1.111 mmoles and 1.6667 mmoles of poly(MMA)) . As a result, a concentration plot of poly(MMA) macromonomer was constructed, in order to estimate the amount unreacted poly(MMA) within each block co-polymer of poly(MMA-*b*-styrene) with plot fitting of: $\boldsymbol{y = (142.48 \pm 1.24)x + 2.02 \pm 1.73}$ (*figure 5.9)*.

Table 5.5: Intensity and concentration analysis of fluorescence block copolymers of poly (MMA-b-styrene) and determination of unreacted poly(MMA) macromonomer within the block co-polymers in DCM

Reaction PMMA/ mmoles	FL intensity of poly(MMA-b-styrene)	RI intensity of poly(MMA-b-styrene)	FL intensity of (unreacted PMMA) within block copolymer	Concentration mg/ml (unreacted PMMA) poly(MMA-*b*-styrene) / g	Percentage of unreacted PMMA poly(MMA-*b*-styrene) / %
0.1389	2.5	77	5	0.021	1.4
0.2778	5	70	14	0.084	5.6
0.5667	12	73	14	0.084	5.6
1.1111	18	70	43	0.29	19.3
1.6667	28	70	88	0.60	40

Running the SEC at approximately the same concentration for each individual block copolymer (1.5 mg/ml), the RI intensity obtained is approximately 70 irrespective of the concentration of poly(MMA) macromonomer within the block co-polymer of poly(MMA-*b*-styrene), *table 5.5 & figure 10*. However, the FL intensity increases with an increase in concentration of fluorescence poly(MMA) macromonomer within the block co-polymers. For reactions with slight increase in poly(MMA), reaction with 0.1389 mmoles and 0.2778 mmoles, the increase in intensity is less significant from 2.5 to 5 and the unreacted poly(MMA) is roughly at 1.4% and 5.6% respectively. As the concentration of fluorescence poly(MMA) macromonomer within the block co-polymers further increases from 0.5667 mmoles, 1.1111 mmoles and eventually 1.6667 mmoles the increase in fluorescence intensity becomes more significant 12, 18 and 28 respectively. The fluorescence detector used is up 1000 times more sensitive than the refractive index detectors, *table 5.5.*

Nevertheless, the concentration of unreacted poly(MMA) macromonomer also increased for the formation of the block co-polymers of poly (MMA-*b*-styrene); for reaction 0.5667mmoles remain at 5.6%, for the reaction with 1.1111 mmoles of fluorescent poly(MMA) the unreacted macromonomer was 19.3% and for the reaction with highest concentration of fluorescent poly(MMA) 1.6667 mmoles the unreacted macromonomer was 40% (*table 5.5 & figure 5.10*).

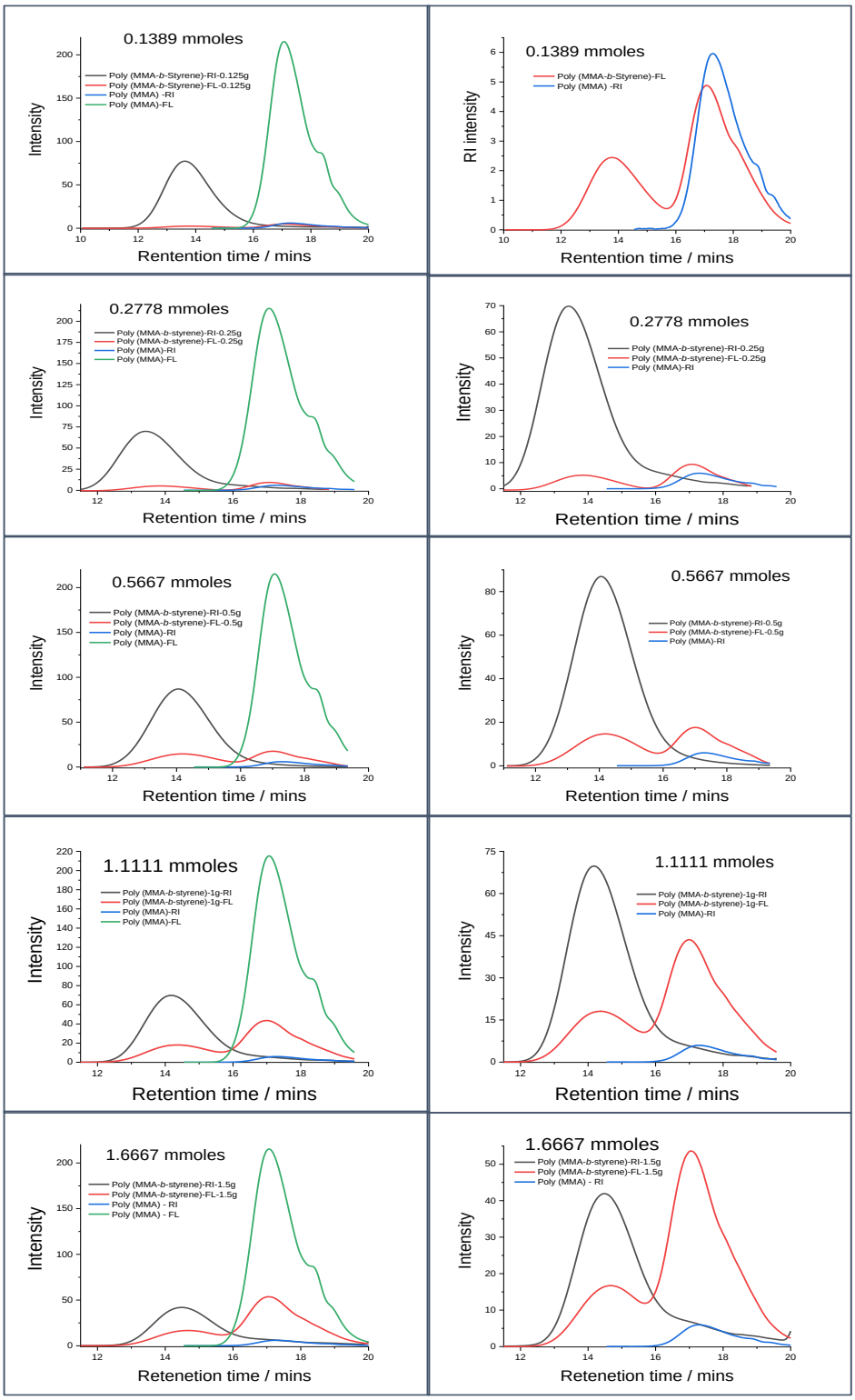

Figure 5.10: Fluorescence analysis of the block copolymer of poly (MMA-b-styrene) with green colour representing poly(MMA) FL, blue colour poly(MMA) RI, red FL of the block copolymer of poly (MMA-b-styrene) and black RI of the block copolymer of poly (MMA-b-styrene) with lowest concentration of incorporated macromonomer within the blocks at the top and highest amount of incorporated macromonomers of poly(MMA) at the bottoms after purification in DCM. Right all SEC data and left zoomed in SEC data

5.2.5 Fluorescence analysis of the block copolymer of poly(MMA-b-styrene) via devised purification method 2 in acetonitrile

Table 5.6: Intensity and concentration analysis of fluorescence block copolymers of poly (MMA-b-styrene) and determination of unreacted poly(MMA) macromonomer within the block co-polymers in acetonitrile

Reaction PMMA/ mmoles	FL intensity of poly(MMA-b-styrene)	RI intensity of poly(MMA-b-styrene)	FL intensity of (unreacted PMMA) within block copolymer	Concentration mg/ml (unreacted PMMA) poly(MMA-b-styrene) /mg	Percentage of unreacted PMMA poly(MMA-b-styrene) / %
0.1389	2.09	70	0.87	4.07×10^{-5}	4.07×10^{-4}
0.2778	4.36	70	2.19	0.013	0.13
0.5667	12.43	70	4.66	0.030	0.30
1.1111	16.66	70	7.29	0.050	0.50
1.6667	25.11	70	7.36	0.050	0.50

For these sets of polymers the first set of purification was performed under cyclohexane: where the insoluble phase contained the block copolymer and the unreacted poly(MMA) macromonomer. Subsequently, the insoluble phase was dialysed in 3.5k dialysis membrane so that the co-polymer is obtained in an insoluble form within the dialysis bag and the macromonomer with molecular weight of around 1 k, was soluble in acetonitrile and would dialysed out of the dialysis membrane , leaving only the co-polymer within the membrane as shown in *figure 5.7* route 2.

Running the SEC at approximately the same concentration for each individual block copolymer (1.0 mg/ml), the RI intensity obtained was approximately 70 irrespective of the concentration of poly(MMA) macromonomer within the block co-polymer of poly(MMA-*b*-styrene) and in instances that it was slightly above or below 70, it was normalized accordingly, with respect to FL intensity of the macromonomer and block copolymers, *table 5.6 & figure 5.11*.

However, the FL intensity increases with an increase in concentration of fluorescence poly(MMA) macromonomer within the block co-polymers. For reactions with slight increase in poly(MMA), reaction with 0.1389 mmoles and 0.2778 mmoles, the

increase in intensity is less significant. However, the intensity approximately doubles from 2.09 to 4.36 and the unreacted poly(MMA) is roughly at 4.07x 10^{-4} % and 0.13 % respectively. As the concentration of fluorescence poly(MMA) macromonomer within the block co-polymers further increases from 0.5667 mmoles, 1.1111 mmoles and eventually 1.6667 mmoles the increase in fluorescence intensity becomes more significant 12.43, 16.66 and 25.11 respectively.

Furthermore, the concentration of unreacted poly(MMA) macromonomer also increased for the formation of the block co-polymers of poly (MMA-*b*-styrene); for reaction 0.5667 mmoles the unreacted poly(MMA) was 0.3%, for the reaction with 1.1111 mmoles and 1.6667 mmoles of fluorescent poly(MMA) the unreacted macromonomer was both approximately around 0.50% (*table 5.6 & figure 5.11.).* Nevertheless, the results obtained via purification method 2 for the block copolymers of poly (MMA-*b*-styrene), resulted in much greater purity of the block copolymer as oppose to route 1 (*figure 5.7*).

The ^{1}H DOSY NMR, after dialysis purification with 3.5 Kd membrane in acetonitrile using route 2 (*figure 5.7*) , the DOSY NMR protons were all aligned for all the block copolymers of poly(MMA-*b*-styrene) with shorter diffusion distance and the same diffusion rate, when compared to the samples dialysed in DCM solvent and the un-dialysed samples (*figure 5.8 & 5.11*). In the case acetonitrile, all of the protons of the final product are aligned on the same region of the spectrum (same diffusion rate), indicating that they are part of the same molecule. Hence, confirming the block copolymer formation and greater block purity compared to the samples dialysed in DCM solvent.

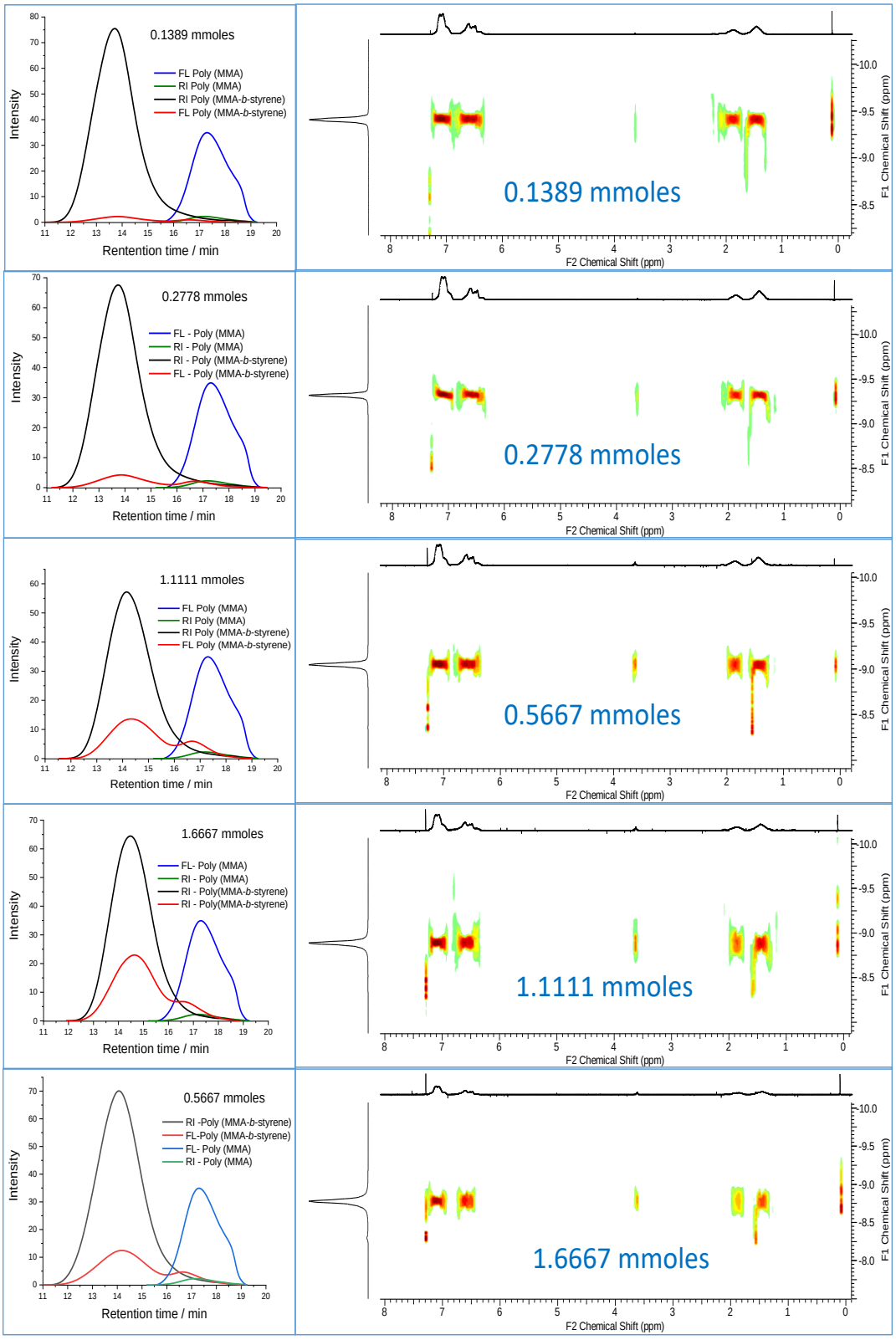

Figure 5.11: Fluorescence analysis of the block copolymer of poly (MMA-b-styrene) with green colour representing poly(MMA) FL, blue colour poly(MMA) RI, red FL of the block copolymer of poly (MMA-b-styrene) and black RI of the block copolymer of poly (MMA-b-styrene) with lowest concentration of incorporated macromonomer within the blocks at the top and highest amount of incorporated macromonomers of poly(MMA) at the bottoms after purification in acetonitrile. Right all SEC data and left zoomed in SEC data.

In the case of DCM solvent, for the reaction with 0.1389 mmoles of poly (MMA) macromonomer within the block copolymer, insufficient material of poly(MMA-*b*-styrene) were obtained for analysis and 0.2778 mmoles the peaks for pol(MMA) were slightly misaligned with styrene, which initially suggested that the concentration of pol(MMA) available in the block copolymer may have been below the minimum threshold amount for formation of efficient block copolymers. However, since the block copolymers obtained using acetonitrile as a purification solvent, all the protons were aligned for all the block copolymers (purified via route 2 using acetonitrile), as a result the hypothesis did not stand. Therefore, we conclude that acetonitrile is a significantly better solvent for purification of block copolymers of poly(MMA-*b*-styrene), as confirm by SEC and ^{1}H DOSY NMR (*table 5.7 & figure 5.11*).

Table 5.7: SEC data for purified, poly (MMA-b-styrene) block copolymers with HY-3G dye in acetonitrile.

Reaction PMMA/ mmoles	M_n, $_{SEC}$ / *g mol^{-1}* (THF) ACN	M_w / *g mol^{-1}*	*Đ*
0.1389	27600	61000	2.21
0.2778	26000	58000	2.23
0.5556	19600	46200	2.36
1.1111	17000	35000	2.06
1.6667	13900	26900	1.93

Furthermore, the SEC data *table 5.7* shows that as we increase the concentration of the poly (MMA) macromonomer within the block co-polymer the molecular weight decreases. In addition, compared to the purification route 1 (*figure 5.7*), route 2 has significantly lower *Đ*, around 2 as expected with free radical polymerisation. The peak at *Mn = 900 g mol^{-1}*, due to the macromonomer of poly (MMA), within the block copolymers of poly(MMA-b-styrene), completely disappears upon purification with acetonitrile. The ^{1}H and DOSY NMR, shows that after purification with acetonitrile, the block copolymer contained no traces of monomer or unreacted macromonomer of poly (MMA) *table 5.7 and figure 5.12.*

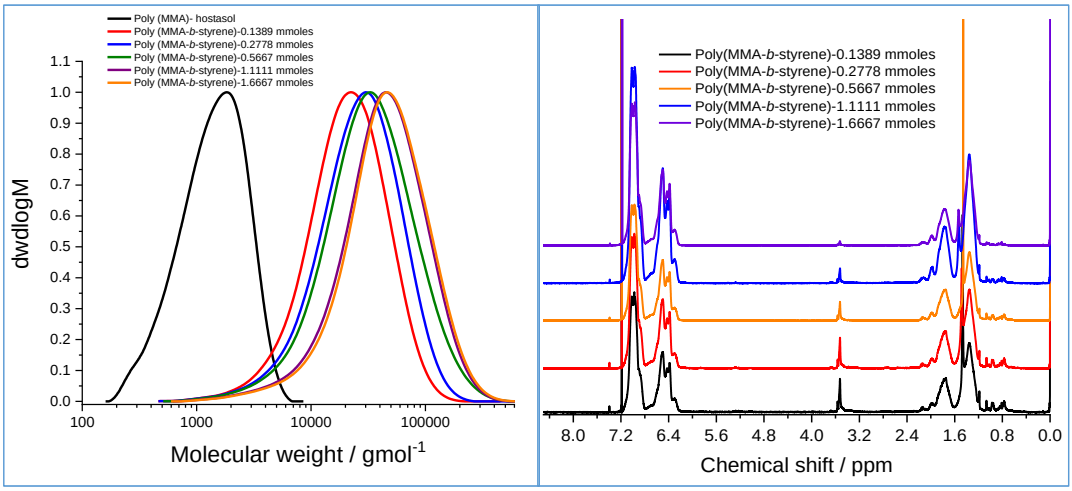

Figure 5.12: After purification with acetonitrile: Left SEC data and right NMR data of all the block co-polymers of poly(MMA-b-styrene).

5.3 Conclusions

Fluorescent block copolymers of poly(MMA-b-styrene) were successfully synthesised with various amounts of poly(MMA) macromonomer within the block copolymers formed via acting as radical chain stoppers. As the concentration of poly(MMA) increased within the block co-polymers of poly(MMA-b-styrene), the M_n decreased supporting them acting as chain stoppers. Furthermore, after purification both SEC and DOSY supported the formation of block copolymers.

The purification with acetonitrile was significantly better solvent for purification of block copolymers of poly(MMA-*b*-styrene) as opposed to DCM solvent, confirmed by SEC (RI & FL) and ^{1}H DOSY NMR. However, fluorescence detection showed the presence of low levels of the fluorescence macromonomer within the block copolymers regardless of the concentration of poly (MMA) incorporated within the block copolymers.

This due to the fact that fluorescence detectors can up to 10-1000 times more sensitive than UV detectors for strong absorbing compounds. The fluorescence detection technique demonstrates that other methodology can be utilised to analyse polymers, especially were specific compositions and full conversions are essential due to its application in medical diagnostics, cosmetics, paints, coating and resins.

5.4 Supporting information

5.4.1 Instruments and analysis

Size Exclusion Chromatography (SEC)

SEC analyses in THF were carried out on an Agilent 390-LC MDS instrument equipped with a differential refractive index (DRI) and a dual wavelength UV detector. The system was equipped with 2 x PLgel Mixed D columns (300 x 7.5 mm) and a PLgel 5 µm guard column. The eluent used was THF with 2 % TEA (triethylamine) and 0.01 % BHT (butylated hydroxytoluene) as an antioxidant additive. Samples were run at 1 ml/min at columns maintained at 30°C. Poly(methyl methacrylate) (PMMA) standards (12) in range of 500-1.5 x 10^6 g mol^{-1} and polystyrene (PS) (13) standards in the range 200-3.6 x 10^6 g mol^{-1} were used as calibrants and the curve fitted with a third order polynomial. Agilent EasyVials) were used for calibration samples. Analyte samples were filtered through a GVHP membrane with 0.22 μm pore size before injection. Respectively, experimental molar mass ($M_{n,SEC}$) and dispersity ($Đ$) values of synthesized polymers were determined by conventional calibration using Agilent GPC/SEC software.

Nuclear Magnetic Resonance (^{1}H NMR)

^{1}H NMR and DOSY NMR spectra were recorded on Bruker DPX-400 and DPX-500 MHz spectrometers using deuterated dimethyl sulfoxide or chloroform ($CDCl_3$), obtained from Aldrich. Chemical shifts are given in ppm downfield from the internal standard tetramethylsilane and data was analysed using ACD/NMR data software.

5.4.2 General polymerisation procedure

Materials

All materials were purchased from Sigma Aldrich or Fisher. Monomers were used as brought from supplier. CoBF was synthesised in our group and has been reported previously in the literature.[24] Monomers were used as brought from supplier. Sigma products: 4,4′-Azobis(4-cyanovaleric acid) ≥98.0% (T); Methyl methacrylate contains ≤30 ppm MEHQ as inhibitor; styrene, contains 4-tert-butylcatechol as stabilizer, <15 ppm, ≥99%; and sodium dodecyl sulfate, ACS reagent, ≥99.0%.

Synthesis of PMMA containing Hostasol

In a typical CCTP emulsion polymerisation, CoBF (0.0485 g, 0.1261 mmol) and Hostasol methacrylate (0.0525 g) was placed in a 250 mL round bottom flask together with a stirring bar. Nitrogen was purged in the flask for at least 1h. Subsequently, MMA (120 mL, 112.32 g, 0.1122 mmol) previously degassed for 30 min was added to the flask via a degassed syringe. The mixture was vigorously stirred under inert atmosphere until total dissolution of the catalyst and Hostasol methacrylate. Meanwhile, 4,4'-azobis(4-cyanovaleric acid) (ACVA) (2.2 g, 7.849 mmol), SDS (1.8 g, 6.242 mmol) 330 mL of water were charged into a three-neck, 500 mL double jacketed reactor, equipped with a RTD temperature probe and an overhead stirrer. Once the reaction temperature reached 75 °C, the mixture of Hostasol and CoBF dissolved in MMA monomer was added over 60 min via syringe pump at 2 mL/min. Upon the completion of the addition of reagents the reaction was left 2 hours to ensure full conversion.

Synthesis of block co-polymers of poly (MMA-*b*-styrene)

In a typical reaction for the formation of poly (MMA-b-styrene), low Mn fluorescent PMMA (1.5 g, 1.6667 mmoles) with AIBN initiator (0.2 g, 0.1218 mmoles), was placed in 100 mL round bottom flask with a stirring bar. Nitrogen was purged in the flask for at least 1h. Subsequently, Styrene (20 mL, 18.12 g, 0.1746 moles) and toluene (60 mL, 51.9 g, 0.5633 moles) previously degassed for 30 min was added to the flask via a degassed syringe. The mixture was vigorously stirred under an inert atmosphere until total dissolution of the fluorescence PMMA and AIBN initiator were acquired. Subsequently the reaction mixture was heated 75 °C and left for 24 hours.

5.5 References

1. G. Chen, L. Tao, G. Mantovani, V. Ladmiral, D. P. Burt, J. V. Macpherson and D. M. Haddleton, *Soft Matter*, 2007, **3**, 732-739.
2. C. Fleming, A. Maldjian, D. Da Costa, A. K. Rullay, D. M. Haddleton, J. St John, P. Penny, R. C. Noble, N. R. Cameron and B. G. Davis, *Nature Chemical Biology*, 2005, **1**, 270-274.
3. A. J. Limer, A. K. Rullay, V. S. Miguel, C. Peinado, S. Keely, E. Fitzpatrick, S. D. Carrington, D. Brayden and D. M. Haddleton, *Reactive and Functional Polymers*, 2006, **66**, 51-64.
4. F. Tronc, M. Li, J. Lu, M. A. Winnik, B. L. Kaul and J.-C. Graciet, 2003, **41**, 766-778.
5. S. Slavin, E. Khoshdel and D. M. Haddleton, *Polymer Chemistry*, 2012, **3**, 1461-1466.
6. J. Nicolas, V. San Miguel, G. Mantovani and D. M. Haddleton, in *Polymers for Biomedical Applications*, American Chemical Society, 2008, vol. 977, ch. 6, pp. 78-94.
7. B. J. Crosby, J. Unsworth and F. W. D. Rost, *Journal of Microscopy,* 1996, **181**, 61-67.
8. J. Nicolas, V. S. Miguel, G. Mantovani and D. M. Haddleton, *Chemical Communications*, 2006, DOI: 10.1039/B609935A, 4697-4699.
9. G. A. Stahl and R. B. Seymour, *The Preparation of Styrene Block Copolymers from Macroradicals Produced in Viscous Media*, Springer US, Boston, MA, 1977.
10. R. B. Seymour and G. A. Stahl, *Journal of Macromolecular Science: Part A - Chemistry*, 1981, **15**, 815-819.
11. R. B. Seymour, P. D. Kincaid and D. R. Owen, in *Polymerization Reactions and New Polymers*, American Chemical Society, 1973, vol. 129, ch. 14, pp. 230-238.
12. R. B. Seymour and G. A. Stahl, *Journal Polymer Science : Polymer Chemistry Edition*, 1976, **14**, 2545-2552.
13. H. Zhang, K. Hong and J. W. Mays, *Macromolecules*, 2002, **35**, 5738-5741.
14. C. J. Knill and J. F. Kennedy, *Polymer handbook (4th Edition): J. Brandrup, E.H. Immergut, E.A. Grulke (Eds.); Wiley, New York, 1999, ISBN 0-471-16628-6* John Wiley & Sons, 2001.
15. W. Li, H. Chung, C. Daeffler, J. A. Johnson and R. H. Grubbs, *Macromolecules*, 2012, **45**, 9595-9603.
16. Y. Bakkour, V. Darcos, S. Li and J. Coudane, *Polymer Chemistry*, 2012, **3**, 2006-2010.
17. W. Hiller, 2019, **220**, 1900255.
18. P. Groves, *Polymer Chemistry*, 2017, **8**, 6700-6708.
19. G. Patias, A. M. Wemyss, S. Efstathiou, J. S. Town, C. J. Atkins, A. Shegiwal, R. Whitfield and D. M. Haddleton, *Polymer Chemistry*, 2019, DOI: 10.1039/C9PY01133A.
20. P. E. J. Louis, R. G. Gilbert, D. H. Napper, P. Teyssie and R. Fayt, *Macromolecules*, 1991, **24**, 5746-5751.
21. T. Kawate and E. Gouaux, *Structure*, 2006, **14**, 673-681.
22. B. Di Bartolo, Dordrecht, 2013.
23. R. A. Keller, W. P. Ambrose, P. M. Goodwin, J. H. Jett, J. C. Martin and M. Wu, 1996, **50**, 12A-32A.
24. Q. Zhang, S. Slavin, M. W. Jones, A. J. Haddleton and D. M. Haddleton, *Polymer Chemistry*, 2012, **3**, 1016-1023.

Chapter 6

Conclusions and Outlooks

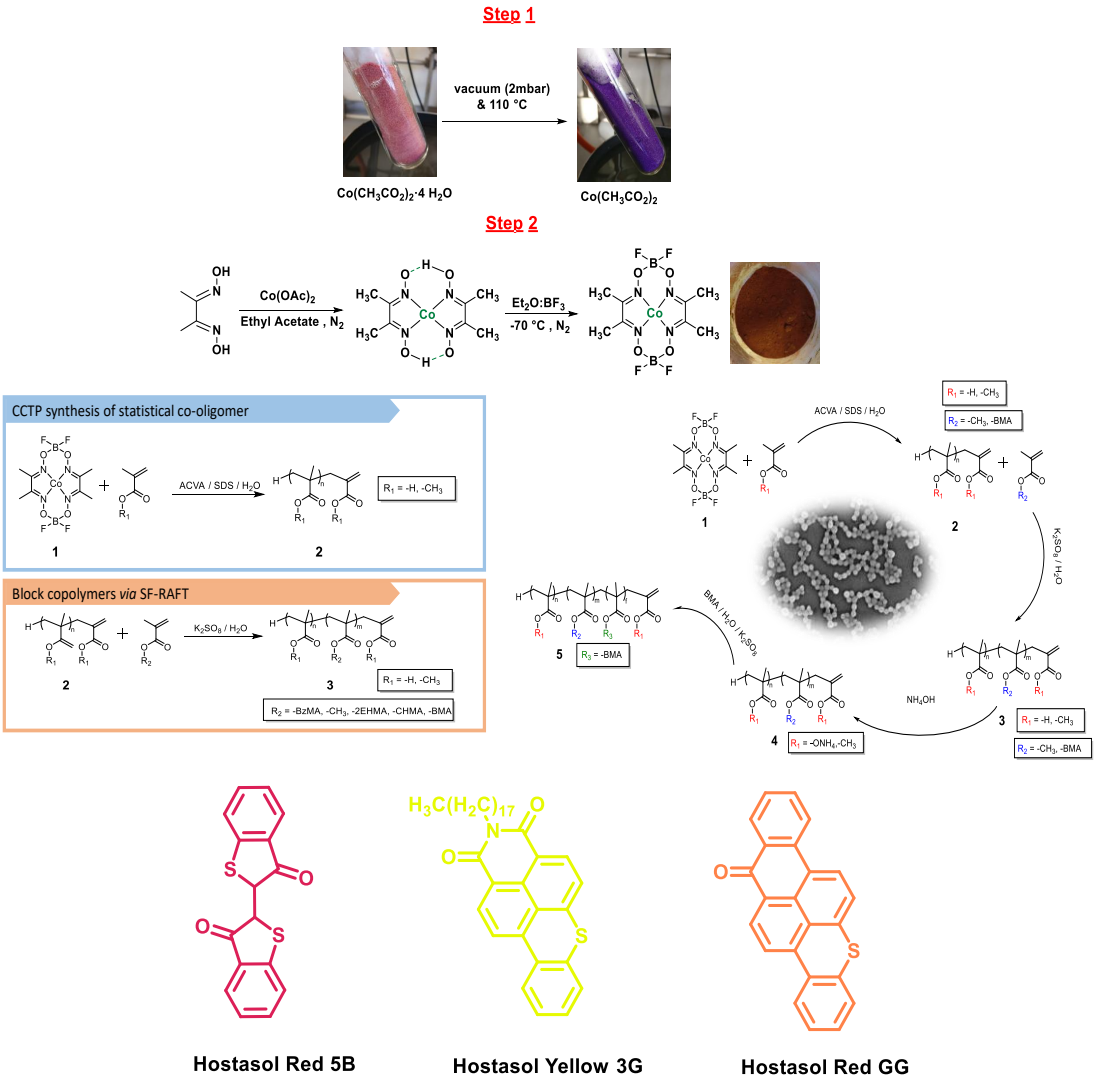

Depiction of graphical abstract of chapters 2-5: future works and outlooks.

6.1 Chapter 2: Conclusions and outlooks

Co-oligomers with various concentration of MAA with respect to MMA monomers were synthesised successfully and the conditions were optimized subsequently for eventual utilisation as CTA's for formations of diblock and pseudo- triblock copolymers in sulphur free RAFT polymerisation.

We found that increasing the MAA concentration within the co-oligomers with the same ppm of CoBF, caused the M_n to increase according to SEC and the particle size to increase according to DLS. This could be attributed to a few factors; firstly, even though CoBF is extremely stable at elevated temperatures and pH, the combination of MAA and ACVA (making the pH of the system extremely acidic) and the factor of high temperature could potentially destroy the catalyst, which in turn results in less catalyst available to act as CTA, in order to reduce the M_n of the co-oligomers.

Furthermore, increasing the concentration of the MAA within the co-oligomers increases the T_g of the polymers, since homopolymer of poly(MAA) has a T_g of 228 °C and the homopolymer of poly(MMA) is 105 °C, by tuning the ratio of MAA to MMA composition, we notice that the increase in the MAA concentration causes an increase in the T_g of the co-oligomers, at higher T_g the chain mobility of the polymers and the catalyst are hindered and therefore, there is insufficient amount of catalyst are available to reduce the M_n of the co-oligomers. In addition we found out that the zeta potential of the co-oligomer were generally equal to or greater the -40 eV, which in turn results in incredibly stable latexes, as the acid concentration of the particles increase the zeta potential generally was observed to increase, which in turn results in more stable latex particles.

As a result, we devised that the co-oligomers with the following composition poly($MAA_{15wt\%}$-*co*-$MMA_{85wt\%}$) at feed rate 60 min, to be the most suitable co-oligomer, since it required least amount of CoBF catalyst to form low M_n co-oligomers, had zeta potential of -40 eV, which in turn increases its colloidal stability and latex shelf life, solubilised incredibly well with NH_4OH (aq), which in turn improves the polymers post-polymerisation / functionalisation and application properties (i.e. investigated in *chapter 4*).

Further analytical methodologies could have be utilised to gain better understanding of the co-oligomers of poly ($MAA_{15wt\%}$-*co*-$MMA_{85wt\%}$) with range of MW from 1500 – 6000 $gmol^{-1}$, using MALDI to obtained understanding of the sequential monomer arrangements with the monomer composition using heat mapping.

Furthermore, an extensive table of CTA constant using mayo plot in various solvents, monomers and polymerisation systems (i.e. bulk and solution polymerisation), would have been devised for the new batch of CoBF synthesised, with conjunction to the old batch of CoBF. Furthermore, would have devised a mythology in investigating the CTA's purify by utilising a range of techniques such as HPLC, ^{1}H NMR, SEC, ESI and MALDI-TOf techniques.

6.2 Chapter 3: Conclusions and outlooks

The versatility of CCT combined with sulfur free RAFT polymerisation has been demonstrated by applying it under emulsion polymerization conditions. The formation of various di- and pseudo triblock copolymers containing an acid-based block and a range of different poly(alkyl methacrylate) blocks has been demonstrated. The conditions were optimised for the formation of the co-oligomers with incorporation of carboxylic acid functionality which in turn were utilised for the formation of well-defined di-block and pseudo tri-block copolymers. By changing the composition of the monomers added based on hydrophobicity, and T_g, the latex and the morphology of the polymer latex can be altered based of the desired properties.

Furthermore, control over pH in emulsions is essential, as it determines the location of the acid within the polymer latex. The pH is also believed to play a role in catalyst activity through the rate of hydrolysis of the CCTA as at very low pH a slightly higher concentration of catalyst is desired. Moreover, seeded polymerizations can be important for eliminating some of the ambiguity associated with the compartmentalization of the organic phase by controlling the particle numbers and particle size. This also allows for better control over the average number of catalyst molecules per particle which in turn allows the latex to have a long shelf-life as the particles are usually smaller with incorporation of the seed.

Further work could be carried out in exploiting synthesise statical co-oligomers with different composition of monomers with range of T_g's as CTA's in formation of block copolymers and investigate the CTA efficiency for the specific co-oligomers, chain mobility, effects of block copolymer composition when utilising the different co-oligomers as CTA's in the formation of diblock and multi-block copolymers using various analytical techniques.

In the case of the block copolymers were the first block consisted of poly ($MAA_{15wt\ \%}$-*co*-$MMA_{85wt\ \%}$) and behaved as the CTA's which has very high T_g's and the B block also had high T_g's (i.e. CHMA and MMA). Other plasticisers could have been investigated to possibly acquire even lower T_g's for the formation of the diblock and pseudo tri-block copolymers.

Furthermore in future works, a mixture of two different CTA's could be utilised in the formation of diblock copolymers. Since a mixtures of macromonomers have not been previously reported to be utilised in formation of block co-polymers via SF-RAFT and there is a strong hypotheses that it could be used to form block co-polymer with properties of changeable dispersity as reported by conventional RAFT in recent literature.

6.3 Chapter 4: Conclusions and outlooks

Lowering of the pH with addition of ammonium hydroxide solution and formation of ammonium salts of poly(MMA-*co*-MAA-*b*-BMA_{10}) and poly(MMA-*co*-MAA-*b*-MMA_{10}) resulted in solubilisation to quite low viscosity solutions which could be used as a polymerisable surfactants in emulsion polymerisation. Subsequent emulsion polymerisation of BMA provided latex's with high solid contents (40%), stable, long shelf lives and generally monodisperse particles. This is especially true for higher concentrations of NH_4OH, higher pH, with poly(MMA-*co*-MAA-*b*-BMA_{10}) utilised as the surfactant.

Whereas, with poly(MMA-*co*-MAA-*b*-MMA_{10}) we achieved monodisperse particles at varies concentration of ammonium hydroxide and was an effective way to control the average particle sizes. We find out that at lower pH's (acidic) the final latex

occurred had larger particle size's. This is due to the ionic initiator utilised (KPS) which at higher temperature and acidic pH produces H_2SO_4 (aq) which lowers the final pH further (more acidic) resulting in larger particle sizes at lower pH's. Furthermore, these latex particles derived from polymerisable surfactants for polymethacrylate; opens the possibility for numerous applications in medical diagnostics, adhesives, impact modifiers, as well as paper and textile coatings.

In future works, the poly(MMA-*co*-MAA-*b*-BMA_{10}) and poly(MMA-*co*-MAA-*b*-MMA_{10}) dissolved in various concentration of ammonia hydroxide with respect to block co-polymers which become polymerisable surfactants in production of other monomer such as acrylates, low and high T_g methacrylates, styrene, alpha methyl styrene, methacrylamide and acrylamides in solution, bulk and emulsion systems depending on the monomers.

Furthermore, we could have utilised the polymerisable surfactants at various concentration with respect to the monomer and see the effect it has on the particle size, molecular weight, T_g, freeze thaw stability, shelve life's of the latex's, hydrophilicity / hydrophobicity and adhesive properties.

In addition initial experiments showed promising results of the co-oligomer poly($MMA_{85wt\%}$-*co*-$MAA_{15wt\%}$) could have been directly utilised in free radical polymerisation with BMA instead of chain extending with MMA_{10} and BMA_{10} as the hydrophobic block for formation of polymerisable surfactants. Furthermore , the co-oligomer poly($MMA_{85wt\%}$-*co*-$MAA_{15wt\%}$) after dissolving in ammonium hydroxide also showed promising results in utilisation of polymerisable surfactants in formations of low M_n macromonomers in CCTP polymersiations.

6.4 Chapter 5: Conclusions and outlooks

Fluorescent block copolymers of poly(MMA-*b*-styrene) were successfully synthesised with various amounts of poly(MMA) macromonomer within the block copolymers formed via acting as radical chain stoppers. As the concentration of poly(MMA) increased within the block co-polymers of poly(MMA-*b*-styrene), the M_n decreased

supporting them acting as chain stoppers. Furthermore, after purification both SEC and DOSY supported the formation of block copolymers.

The purification with acetonitrile was significantly better solvent for purification of block copolymers of poly(MMA-*b*-styrene) as opposed to DCM solvent, confirmed by SEC (RI & FL) and ^{1}H DOSY NMR. However, fluorescence detection showed the presence of low levels of the fluorescence macromonomer within the block copolymers regardless of the concentration of poly (MMA) incorporated within the block copolymers.

This due to the fact that fluorescence detectors can up to 10-1000 times more sensitive than UV detectors for strong absorbing compounds. The fluorescence detection technique demonstrates that other methodology can be utilised to analyse polymers, especially were specific compositions and full conversions are essential due to its application in medical diagnostics, cosmetics, paints, coating and resins.

For the optimising the conditions and tracing the formation of fluorescence block–copolymers of poly (MMA-*b*-styrene) utilising low mass fluorescence macromonomers of poly (MMA) as derived from CCTP. The solvent purification method using cyclohexane, dichloromethane and then dialyses with 3.5 kD membrane bag in dichloromethane solvent to obtain pure poly (MMA-*b*-styrene), could also be investigated using conventional purification which involves cyclohexane and then to obtain the block co-polymer use acetonitrile, which was carried out eventually, however a subsequent further purification of the purified sample could have been dialysed again to try to possibly remove any residual unreacted poly (MMA) macromonomer as FL still showed very small traces of the unreacted macromonomers within the block copolymers.

Furthermore, low mass fluorescence macromonomers of poly (MMA) as derived from CCTP could be used with other monomers such as MAA, MA, BA, MAM, and AM to see the effect that the rate of propagation of the monomer, the reaction solvent and the structure of the monomer has on the final polymer. The initial preliminary experiments demonstrated that we could carry out suspension polymerisation and

some sequential additions of certain monomers resulted in some PISA like characteristic of the block co-polymers.

In addition further investigation could have been carried out at optimising the conditions and tracing the formation of fluorescence block–copolymers of poly (MMA-*b*-styrene) utilising low mass fluorescence macromonomers of poly (MMA) as derived from CCTP. Other fluorescence dye could have been utilised in formation of macromonomer and the subsequent block co-polymer formation and compared with hostasol-3G fluorescent polymers.